Stability Analysis of Thin-Walled Non-Symmetric Steel Beams

Mathiesen, F.

Publication date:
1993

Document Version
Publisher's PDF, also known as Version of record

INSTITUTTET FOR BYGNINGSTEKNIK
DEPT. OF BUILDING TECHNOLOGY AND STRUCTURAL ENGINEERING
AALBORG UNIVERSITETSCENTER • AUC • AALBORG • DANMARK

ENGINEERING MECHANICS
PAPER NO. 19

Ph.D.-Thesis

F. MATHIESEN

STABILITY ANALYSIS OF THIN-WALLED NON-SYMMETRIC STEEL BEAMS

AUGUST 1993

ISSN 0902-7513 R9327

The ENGINEERING MECHANICS papers are issued for early dissemination of research results from the Engineering Mechanics Group at the Department of Building Technology and Structural Engineering, University of Aalborg. These papers are generally submitted to scientific meetings, conferences or journals and should therefore not be widely distributed. Whenever possible, reference should be given to the final publications (proceedings, journals, etc.) and not to the Engineering Mechanics papers.

INSTITUTTET FOR BYGNINGSTEKNIK
DEPT. OF BUILDING TECHNOLOGY AND STRUCTURAL ENGINEERING
AALBORG UNIVERSITETSCENTER • AUC • AALBORG • DANMARK

ENGINEERING MECHANICS
PAPER NO. 19

Ph.D.-Thesis

F. MATHIESEN

STABILITY ANALYSIS OF THIN-WALLED NON-SYMMETRIC STEEL BEAMS

AUGUST 1993 ISSN 0902-7513 R9327

Acknowledgements

The present thesis *Stability Analysis of Thin-Walled Non-Symmetric Steel Beams* has been prepared in the period January, 1990 to December, 1992 at the Department of Building Technology and Structural Engineering, University of Aalborg, Denmark.

Special thanks to my supervisor Professor Dr. Techn. Steen Krenk for encouragement and guidance offered during my study. Furthermore, the assistance from Norma Hornung who prepared the drawings is greatly appreciated.

The work was supported by the Danish Technical Research Council.

Aalborg, January 1993 Frank Mathiesen

Contents

Chapter 1

Introduction

The *beam* has for many years been an important part of civil engineering structures. Successful design of structures involving beam elements requires a well-developed description of the beam behavior. This has been recognized by researchers and during the last century great emphasis has been given towards the establishment of linear as well as nonlinear beam theories. A review of some of the literature connected to beam theories is presented in Section 1.1.

Driven by economic incentivities such as increasing relative cost for materials, by the development of high-strength materials, and by the advancement in structural analysis and design, the trend has been towards the design and construction of increasingly more slender and flexible structures. An important component in this progress is the thin-walled beam. The double symmetric thin-walled beam has been used for many years while the use of thin-walled beams with arbitrary cross-sections is relatively recent.

Using more slender and more flexible structures makes the stability problem essential in the design process. The stability behavior of symmetric beams, such as I- and H-profiles, has been examined for many years and leading to a general solution procedure where the stability failure is determined by considering an ideal structure. Possible precritical deformations are hereby neglected. In case of beam and frame structures with non-symmetric cross-sections the precritical deformations may be significant leading to a more complex behavior of the structure. This implies that the critical behavior is more complicated as for the symmetric structure. A rational utilization of these profiles therefore necessitates a detailed description of the stability problem.

A theory is developed for beams of arbitrary shape, (Chapter 2). The beam is represented by a curve with a local set of base vectors fixed to the cross-section at each point of the curve. The generalized displacements are the translation vector for the curve and the rotation vector for the cross-sections. The equilibrium equations for the beam are reformulated as a virtual work equation, and this defines three strain components and three curvature components. The two shear strain components describe the difference between the tangent vector of the curve and the normal vector to the cross-section. It is important for a systematic derivation of the equations that all three rotation components are preserved as independent displacement parameters. If desired the Bernoulli hypothesis concerning the normality of the cross-sections can be introduced in the final equations. The warping effect, characteristic of thin-walled beams, is treated separately in order to preserve the generality.

The general theory is specialised to stability analysis by considering a prebuckled/initial state, with prebuckling curvatures and stresses, and a neighbouring postbuckled state, (Chapter 3). The effect of prebuckling deformation is considered consistently by using the equilibrium equations of the initial state.
Specialising the theory to thin-walled beams requires the appropriate constitutive equations. This is the subject of Chapter 4. A small strain deformation measure expressed by the generalized deformations is introduced and by energy principles the constitutive equations are developed. A brief discussion of energy principles is presented in Chapter 5 where also the transition from virtual work to potential energy or vice versa for the present formulation is considered.
An example of the possibilities of the present formulation in a numerical context is given by the development of a two node beam element, (Chapter 6). The strain deformations are assumed negligible while the curvature contributions are retained in the formulation. This leads to a formulation in terms of the rotation components only. A link between displacements and rotations is obtained by introducing the zero strain condition via the Lagrange Multiplier method. A mixed formulation is hereby obtained where linear shape functions can be used. This chapter serves as an introduction to the development of the incremental updated element considered in Chapter 8.

Analytical stability analysis can be performed in a manageable way by some minor modifications of the general formulation, (Chapter 7). Neglecting strain deformations leads to a formulation expressed entirely in terms of the three rotation components. An asymptotic buckling- and postbuckling theory is developed by means of a perturbation method. The asymptotic postbuckling behavior of a straight column in axial compression is considered for arbitrary cross-section parameters. The theory is also illustrated by analysing buckling and postbuckling of the beam in pure bending. The format of the results for this case are used to discuss the relation of the present general theory to previously published theories for simply curved beams. Further the governing parameters describing the initial postbuckling behavior are determined.
Finally on the basis of the previous chapters a numerical formulation of the nonlinear stability problem is obtained in Chapter 8. The performance of the incremental updated Lagrangian two node hybrid element developed, is discussed by considering four canonical problems. The results strongly indicate that initial deformations and non-symmetric properties are essential for a proper determination of the critical load.

1.1 Review of Literature - Thin-Walled Beams

In this section a brief overview of the progress in beam analysis during the last thirty years is given with reference to the literature presented in the Bibliography. The references used are only a small part of the literature on this subject but they seem to give a good impression of the developments and current status in beam analysis.

As a consequence of the frequent use of beam components in civil engineering structures research regarding the behavior of the *beam* has been intense for many years. The behavior of a beam structure can be divided into two types of analysis. First the *beam analysis* where the deformation as a direct consequence of the increase in loading is considered. Secondly, the *stability/buckling analysis* where the beam structure at a certain load level suddenly

changes the load-deflection relationship. Both types of analysis can be performed linearly as well as nonlinearly.

Everyday problems are usually considered linear, and for good reasons. Materials and structures are commonly used in their linear elastic, small-deflection range. Slight nonlinearity does not invalidate a linear design basis. In this review only geometric nonlinearity will be considered.
The linear theory for the prismatic member as developed by Vlasov (1961) is well known and has found its way into everyday engineering practice. Analytical analysis of the torsional-flexural buckling have been performed by Vlasov and specialised examples have been investigated by Timoshenko & Gere (1961), Chajes & Winter (1965), Kollbrunner & Hajdin (1972) and others. Even in a linear analysis closed form solutions are only obtainable in a few specialised cases which requires alternative solution methods. Numerical techniques such as the finite difference methods and numerical integration have been used, but these are also limited in scope. There has been, therefore, strong motivation to formulate the finite element method for the stability analysis of thin-walled open beams. The use of the finite element method ensures that a wide range of loading and boundary configurations, and cross-sectional shapes can be analysed. A finite element formulation was developed by Barsoum & Gallagher (1970).
Most of the literature up to this point was mainly concerned with the straight beam. Due to the flexible performance of the beam member the curved beam gained in interest. A detailed analysis of the bending and buckling of the thin-walled open section ring was given by Cheney (1963). Later the single-curved beam was considered by Yoo (1982), Yang & Kuo (1987) and Papangelis & Trahair (1986) regarding the formulation of the linear stability equations. The latter works were all specialised to the single-curved beam from the beginning, whereby the possibility of a general theory with inclusion of initial/prebuckling curvatures is lost. In the classical stability analysis, Timoshenko & Gere (1961) and Vlasov (1961), it is assumed that the prebuckling deformations are small enough to be ignored. Attard (1986) derived a finite element capable of handling the lateral buckling problem where prebuckling deformations in the plane of the loading are present.

In case of a beam structure the deflections and stresses may influence the performance significantly which indicates that a large-displacement (nonlinear) analysis is appropriate. Especially for non-symmetric cross-sections the deformations prior to an eventually stability failure plays an important role. Ghobarah & Tso (1971) formulated a nonlinear theory for the thin-walled beam where special attention was given to twist because of the relatively small torsional rigidity. Using linear displacement fields Connor *et al.* (1968) and Bazant & Nimeiri (1973) obtained some numerical results by use of incremental equations and successively updating. Later Bathe & Bolourchi (1979) presented a more general introduction for the solution of large-displacement problems by means of the finite element method.

During the last twenty years many versions of how to solve the nonlinear behavior of the beam member have been published. In a nonlinear analysis the geometric representation of the beam is essential. In analysis of steel beams a common assumption is that the deformations are small and the rotations are finite. This implies that the beam can be described by a curve through a characteristic point of the cross-section, represented by a position vector, and a set of local base vectors representing the orientation of the cross-section. The local unit vectors are commonly related to a reference configuration by rotation of a set of base vectors in the reference configuration. For the spatial beam the nonlinear analysis is complicated by the

non-commutative nature of the rotation increments. Numerous alternative approaches are available for the proper parametrisation of the rotation fields in the configuration space of the beam model, see e.g. Argyris *et al.* (1978), Simo & VuQuoc (1985), Elias (1986), Cardona & Geradin (1988) and Crisfield (1990). Classically, geometrically-derived measures such as Euler angles were used, see e.g. Rosen & Friedmann (1979), but techniques which are more suitable for finite element computations have been commonly used in recent applications. This includes for example Rodrigues parameters, Kouhia (1991) and Saleeb *et al.* (1992), semi-tangential rotations, Yang & McGuire (1986), and co-rotational formulation, Hsiao (1987) and Crisfield (1990).

In general two approaches are used to develop a nonlinear theory. One type of formulation consists in deriving directly the beam equation from a three-dimensional non-linear theory, with a full account of finite rotations, and afterwards introducing the appropriate beam kinematical assumptions, see e.g. Peterson & Petersson (1985), Yang & McGuire (1986), Surana & Sorem (1989), Hong Chen & Blandford (1991), Kouhia (1991) and Gendy & Saleeb (1992). The work of Peterson & Petersson considers the general three-dimensional continuum, while the work of Surana & Sorem represents the general formulation for the curved rod and finally Yang & McGuire , Hong Chen & Blandford, Kouhia and Gendy & Saleeb specialise to the thin-walled beam.
A second approach is an equilibrium method where the basis is force and moment equilibrium along a characteristic line and then by use of energy principles to derive the weak form of the beam equation, see e.g. Dupuis (1969), Wempner (1973), Rosen & Friedmann (1979), Simo & Vu-Quoc (1985,1991), Elias (1986), Cardona & Geradin (1988) and Reissner (1989). The works of Dupuis, Simo & Vu-Quoc, Elias and Cardona & Geradin represents the general formulation for the rod while Wempner, Rosen & Friedmann and Reissner considers the thin-walled beam. Using a line approach some modifications have to be made in order to obtain a complete formulation. Effects such as warping stiffness, deformations due to cross-sectional forces and non-coincidence of cross-sectional centroid and shear center locations can not be accounted for directly. If these effects are to be considered then the constitutive equations have to be expressed accordingly.

As only a few problems can be solved analytically most of the literature is concerned with the finite element formulation of the nonlinear problem. Finite element formulations typically uses one of three techniques: Co-rotational, updated or total Lagrangian representation. A co-rotational Lagrangian formulation refers to the provision of a reference frame that continuously rotates with the element. Hsiao (1987) and Crisfield (1990), for example, used co-rotational concepts in developing their three-dimensional elements, which include large joint rotations. A total Lagrangian formulation involves using the initial, undeformed element geometry to express the equilibrium equations of the deformed structure. Several investigators, see e.g. Cardona & Geradin (1988) and Surana & Sorem (1989), have used total Lagrangian schemes in their large-deformation analysis of space-frame structures. Recently, updated Lagrangian schemes have been used with succes by for example Yang & McGuire (1986), Meek & Loganathan (1989), Hong Chen & Blandford (1991) and Kouhia (1991). Updated Lagrangian formulations involve expressing the nonlinear equilibrium equations in incremental from, in terms of the geometry at the start of an incremental step. Further the natural mode technique, i.e. a method where the rigid body motions are separated from the displacements that produce strains, has been used by Gattass & Abel (1987) and Conci & Gattass (1990) to examine the nonlinear behavior of beams in an incremental updated

Lagrangian scheme.

In the finite element formulation a major problem has been the moment imbalances at corner nodes for the spatial beam element. Solution strategies have been offered by Argyris *et al.* (1979), Yang & McGuire (1986) and Elias (1986). Especially the strategy proposed by Elias, using a modified rotation vector, seems to be recognized as a solution of the imbalance problem.

In the stability analysis mentioned so far the main concern has been the bifurcation problem and only a few numerical examples of the postbuckling behavior occurs in these works. Postbuckling analysis plays an important role in the understanding of elastic structures as a postbuckling analysis of a perfect system can be used to reveal information about the behavior of real imperfect members, Chajes (1983). Koiter (1945) presented a general theory of stability including postbuckling analysis. A general introduction to the buckling and postbuckling behavior of elastic structures was given by Thompson & Hunt (1973), Budiansky (1974) and Roorda (1980). The postbuckling analyses were performed by use of the perturbation method. An intensive study of the lateral and postbuckling behavior of a number of common thin-walled elastic beams was performed by Trahair & Woolcock (1973) and Woolcock & Trahair (1974,1975). The buckling and initial postbuckling of the thin-walled, simply supported column with arbitrary open cross-section has been examined in a paper by Grimaldi & Pignataro (1979) and later by Szymczak (1980).

Chapter 2

Static Beam Theory

In order to investigate the stability behavior of nonsymmetric steel beams a satisfactory beam theory has to be available. A complete small deformation theory for thin-walled beams has been developed by Vlasov (1961) and it seems that this work is approved by modern researchers as a fundamenthal basis for nonlinear beam theories. From this point though the agreement is not overwhelming in the literature, see e.g. Wempner (1973), Simo & Vu-Quoc (1985), Elias (1986), Cardona & Geradin (1988) and Hong Chen & Blandford (1991). The fundamental ideas seems the same but along the developing process different assumptions influence the final form.

Basically two approaches can be used in order to develop a beam theory. One can consider the beam as a three-dimensional continuum where the beam theory is developed by considering various stress and displacement distributions over the cross-section of the beam. Such a procedure has for example been used by Peterson & Petersson (1985) and Hong Chen & Blandford (1991). In a preliminary fase this procedure was also used by the writer Mathiesen (1990) but an unsatisfactory form was obtained as the beam theory was to be expanded into a stability theory for thin-walled beams.
A beam can be defined as a structural member for which one dimension, the length, is considerably larger than the other dimensions. This makes it natural to separate the description of the deformation and stress in the beam into cross-sectional distribution and lengthwise variation. The second kind of approach is to consider the beam as a one-dimensional structure, where the behavior of the beam is described by generalized displacements and forces. Expressing equilibrium along a characteristic line of the beam cross-section leads to the governing equations. Such an approach has for example been used by Dupuis (1969) and Simo & Vu-Quoc (1985) in the derivation of the nonlinear equilibrium equations for the rod. The general form has been specialized to thin-walled structures by e.g. Wempner (1973) and Rosen & Friedmann (1979).

In this chapter a general nonlinear beam theory is developed in a straight forward way by static considerations along a for the beam characteristic curve.
In Section 2.1 a geometrical description of the beam is introduced and in Section 2.2 the equilibrium equations and virtual work equation are presented. Using the virtual work equation a set of generalized deformations are defined in Section 2.3. Finally the rotation dependency of external loads is considered in Section 2.4.

2.1 Geometrical Description

A slender beam as shown in Fig. 2.1 is described by a curve through a characteristic point of the cross-section. The curve is described by the position vector $\mathbf{r}_a(s_0)$, where the subscript a refers to a characteristic point of the cross-section. The parameter s_0 indicates the arc-length in a reference state and will be used as the independent variable in establishing a stability theory for slender beams.

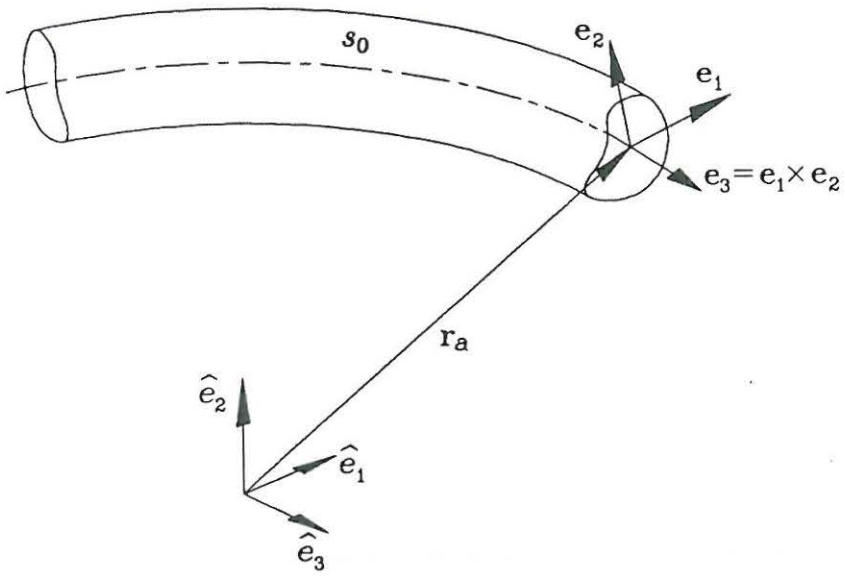

Fig. 2.1: Geometry of the beam.

At each point of the curve the orthogonal unit vectors $\mathbf{e}_\alpha = (\mathbf{e}_1, \mathbf{e}_2)$ describe the plane of the cross-section, while $\mathbf{e}_3 = \mathbf{e}_1 \times \mathbf{e}_2$ is the normal to the cross-section. The local unit vectors are considered as generated by rotation of the base vectors $\hat{\mathbf{e}}_j = (\hat{\mathbf{e}}_1, \hat{\mathbf{e}}_2, \hat{\mathbf{e}}_3)$ of a global rectangular Cartesian x_j coordinate system. The rotation is expressed through the rotation vector $\boldsymbol{\varphi}(s_0)$. This representation is non-singular and degenerates to a simple, intuitive form in the case of infinitesimal rotations, Goldstein (1950).

In the following a beam theory is developed in terms of the two generalized displacement vectors $\mathbf{r}_a(s_0)$ and $\boldsymbol{\varphi}(s_0)$.

2.2 Equilibrium and Virtual Work

Let $\mathbf{N}(s_0)$ be the internal force vector. Force equilibrium of the deformed beam element shown in Fig. 2.2 is then expressed by

$$\frac{d\mathbf{N}}{ds_0} + \mathbf{p} = \mathbf{0} \tag{2.1}$$

where $\mathbf{p}(s_0)$ is the density of the distributed force. $\mathbf{M}(s_0)$ denotes the internal moment vector, and moment equilibrium then takes the form

$$\frac{d\mathbf{M}}{ds_0} + \frac{d\mathbf{r}_a}{ds_0} \times \mathbf{N} + \mathbf{f} \times \mathbf{p} = \mathbf{0} \tag{2.2}$$

where $\mathbf{f}(s_0) = f_\alpha \mathbf{e}_\alpha$ indicates the location of the external force in the cross-section.

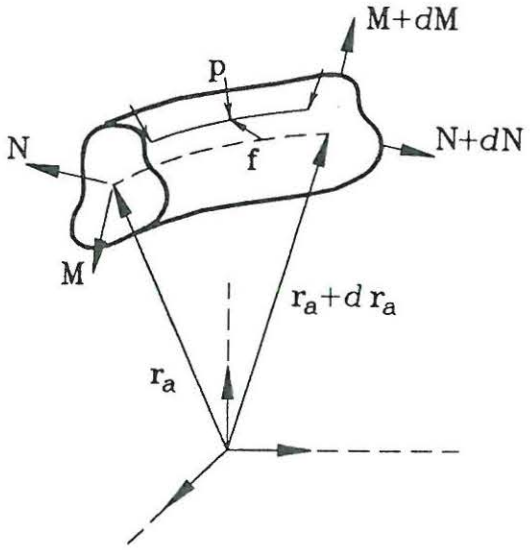

Fig. 2.2: Deformed beam element.

The equilibrium equations (2.1) and (2.2) are now reformulated as a virtual work equation, thereby defining generalized strain measures corresponding to the internal forces and moments. Let $\delta \mathbf{r}_a$ be the virtual translation and $\delta \boldsymbol{\varphi}$ the virtual rotation. The virtual quantities are considered as infinitesimal variations superimposed on the finite displacements. The infinitesimal rigid body motion $\delta \mathbf{e}_j$ of $\mathbf{e}_j$ defines the variation of the rotation vector by (see e.g. Goldstein (1950))

$$\delta \mathbf{e}_j \;=\; \delta \boldsymbol{\varphi} \times \mathbf{e}_j \tag{2.3}$$

In general $\delta \boldsymbol{\varphi}$ is not an exact differential, i.e.

$$\boldsymbol{\varphi} \;\neq\; \int \delta \boldsymbol{\varphi} \tag{2.4}$$

An exception occurs in plane motion.
The virtual work equation corresponding to (2.1) and (2.2) then is

$$\int_0^l \left\{ \delta \mathbf{r}_a \cdot \left(\frac{d\mathbf{N}}{ds_0} + \mathbf{p} \right) \;+\; \delta \boldsymbol{\varphi} \cdot \left(\frac{d\mathbf{M}}{ds_0} + \frac{d\mathbf{r}_a}{ds_0} \times \mathbf{N} + \mathbf{f} \times \mathbf{p} \right) \right\} ds_0 \;=\; 0 \tag{2.5}$$

Integration by parts leads to

$$\int_0^l \left\{ \left(\frac{d\,\delta \mathbf{r}_a}{ds_0} - \delta \boldsymbol{\varphi} \times \frac{d\mathbf{r}_a}{ds_0} \right) \cdot \mathbf{N} \;+\; \frac{d\,\delta \boldsymbol{\varphi}}{ds_0} \cdot \mathbf{M} \right\} ds_0$$

$$= \left[\delta \mathbf{r}_a \cdot \mathbf{N} + \delta \boldsymbol{\varphi} \cdot \mathbf{M} \right]_0^l \;+\; \int_0^l \left(\delta \mathbf{r}_a + \delta \boldsymbol{\varphi} \times \mathbf{f} \right) \cdot \mathbf{p} \; ds_0 \tag{2.6}$$

In equation (2.6) the left side is the internal virtual work δV_{int}, while the right side represents

the external virtual work δV_p. The contents of δV_{int} and δV_p is treated in detail in Sections 2.3 and 2.4 respectively.

2.2.1 Virtual Work Corresponding to Warping

In Section 2.2 the virtual work equation for a beam element identified by a curve is developed. This approach is general and can be used to investigate different kinds of beam structures. The scope of this thesis includes thin-walled beams which necessiates treatment of the warping effect characteristic for thin-walled beams. The contribution from warping is treated separately in this section and is in the following not incorporated in the derivations until the emphasizes are concentrated on thin-walled beams.

The warping contribution is expressed through the bimoment $B(s_0)$ and letting $b(s_0)$ represent the distributed bimoment, equilibrium for the bimoment is given by

$$\frac{dB}{ds_0} + b = 0 \tag{2.7}$$

The warping effect is hereby represented by a scalar equilibrium equation contrary to force and moment equilibrium in Section 2.2. Introducing the scalar function $\theta(s_0)$ as the corresponding generalized displacement the virtual work equation for the bimoment can be established. Multiplication with the virtual displacement $\delta\theta$ and integration along the beam element leads to

$$-\int_0^l \delta\theta \left(\frac{dB}{ds_0} + b\right) ds_0 = \int_0^l \frac{d\delta\theta}{ds_0} B\, ds_0 - \Big[\delta\theta B\Big]_0^l - \int_0^l \delta\theta\, b\, ds_0 = 0 \tag{2.8}$$

Comparing the second statement with (2.6) the resemblance is obvious which indicates that considerations regarding the structure of (2.6) can be transmitted to (2.8).

2.3 Internal Virtual Work - Generalized Deformations

In equation (2.6) the principle of virtual work is written in vectorial form. A component form is obtained by introducing a component representation of $\mathbf{N}(s_0)$ and $\mathbf{M}(s_0)$. Following Dupuis (1969) the internal force and moment vectors are decomposed with respect to the unit vectors $\mathbf{e}_j = (\mathbf{e}_1, \mathbf{e}_2, \mathbf{e}_3)$, locked to the cross-section.

$$\begin{aligned} \mathbf{N}(s_0) &= N_\alpha \mathbf{e}_\alpha + N_3 \mathbf{e}_3 \\ \mathbf{M}(s_0) &= M_\alpha \mathbf{e}_\alpha + M_3 \mathbf{e}_3 \end{aligned} \qquad \alpha = 1,2 \quad ; \quad \text{summation} \tag{2.9}$$

Substitution of this representation reduces the internal virtual work of equation (2.6) to the following form.

$$\delta V_{int} = \int_0^l \Big\{ \delta\varepsilon_\alpha N_\alpha + \delta\varepsilon_3 N_3 + \delta\kappa_\alpha M_\alpha + \delta\kappa_3 M_3 \Big\} ds_0 \tag{2.10}$$

Here $\delta\varepsilon_j$ and $\delta\kappa_j$ are the incremental generalized strain and curvature components, respectively. Their definition follows from the substitution process. The incremental strain components are given by

$$\delta\varepsilon_j = \left(\frac{d\,\delta\mathbf{r}_a}{ds_0} - \delta\boldsymbol{\varphi} \times \frac{d\mathbf{r}_a}{ds_0}\right) \cdot \mathbf{e}_j \quad , \quad j = 1,2,3 \tag{2.11}$$

$\delta\mathbf{r}_a$ and $\delta\boldsymbol{\varphi}$ are considered as variations of the position vector $\mathbf{r}_a$ and the rotation vector $\boldsymbol{\varphi}$, respectively. The unit vectors $\mathbf{e}_j$ follow the cross-section, and their variation is given by the infinitesimal rotation $\delta\mathbf{e}_j = \delta\boldsymbol{\varphi} \times \mathbf{e}_j$, Goldstein (1950). Using this relation the incremental strain formula (2.11) can be integrated to yield the total strain components

$$\varepsilon_j = \left(\frac{d\mathbf{r}_a}{ds_0} - \mathbf{e}_3\right) \cdot \mathbf{e}_j \quad , \quad j = 1,2,3 \tag{2.12}$$

The validity can be confirmed by taking the first variation of (2.12) and making use of the infinitesimal rotation relation (2.3). This definition of the strain components is a local decomposition of the difference between the tangent vector $d\mathbf{r}_a/ds_0$ along the characteristic curve and the current cross-section normal $\mathbf{e}_3$. This is expressed by the alternative form of (2.12)

$$\frac{d\mathbf{r}_a}{ds_0} = \mathbf{e}_3 + \varepsilon_j\,\mathbf{e}_j \tag{2.13}$$

and is illustrated in Fig. 2.3.

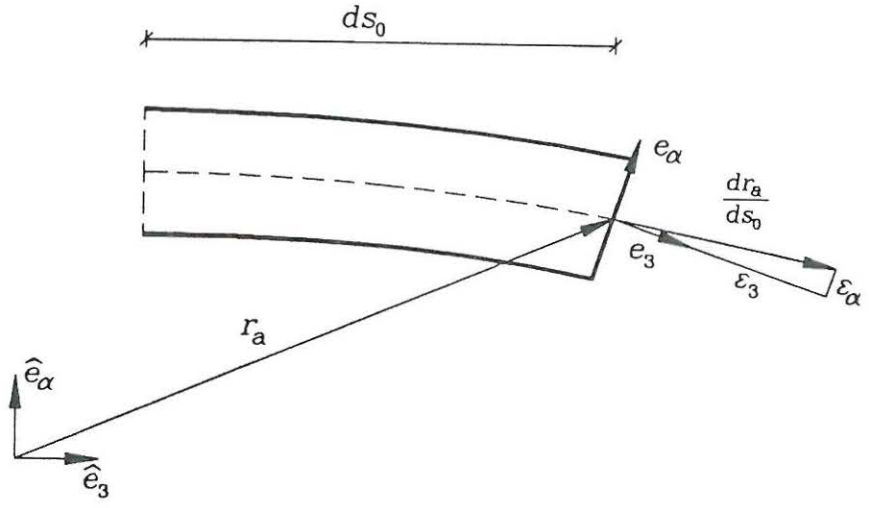

Fig. 2.3: Tangent vector and strain components.

The internal virtual work (2.10) also defines the components $\delta\kappa_j$ of the incremental generalized curvature.

$$\delta\kappa_l = \frac{d\,\delta\boldsymbol{\varphi}}{ds_0} \cdot \mathbf{e}_l \quad , \quad l = 1,2,3 \tag{2.14}$$

$\delta\kappa_j$ is the variation of the total curvature component κ_j, defined by

$$e_{jkl}\,\kappa_l \;=\; \frac{d\mathbf{e}_j}{ds_0}\cdot\mathbf{e}_k \tag{2.15}$$

where e_{jkl} is the permutation symbol. This is demonstrated by substituting the increments $\delta\mathbf{e}_j = \delta\boldsymbol{\varphi}\times\mathbf{e}_j$ into the variation of (2.15). The components κ_j may not be the principal curvatures and twist of the characteristic curve because they refer to the unit vectors $\mathbf{e}_j$ attached to the cross-section. A simple example is a straight pretwisted beam, for which $\delta\kappa_3 \neq 0$. This interpretation of the generalized curvatures κ_j is also found in Wempner (1973). The physical meaning of equation (2.15) is illustrated in Fig. 2.4.

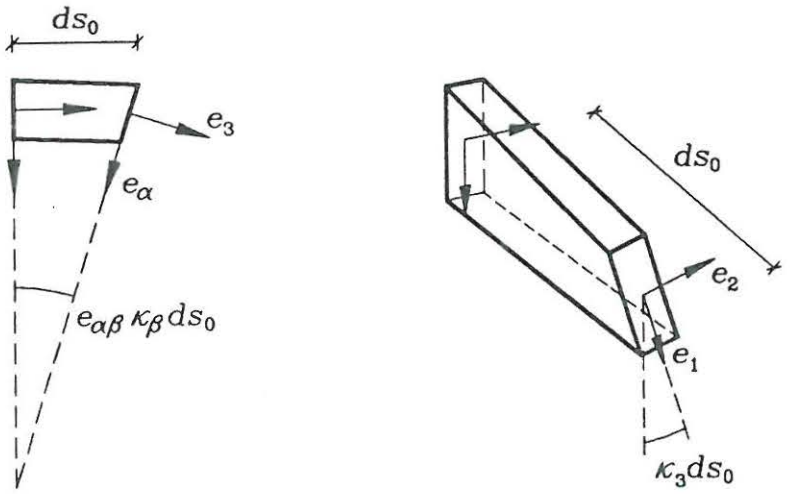

Fig. 2.4: Curvature and twist.

The components ε_j of the strain vector differ from the corresponding components in the Lagrangian strain tensor often used in solid mechanics Malvern (1969). The Lagrangian strain components correspond to the non-orthogonal base vectors $(\mathbf{e}_\alpha, d\mathbf{r}_a/ds_0)$. Decomposition of $\mathbf{N}$ and $\mathbf{M}$ in this non-orthogonal basis would lead to an undesirable coupling between $\mathbf{r}_a$ and $\boldsymbol{\varphi}$ in the corresponding curvature κ_3.

2.4 External Virtual Work

From equation (2.6) it follows that the external virtual work

$$\delta V_p \;=\; \Big[\delta\mathbf{r}_a\cdot\mathbf{N}+\delta\boldsymbol{\varphi}\cdot\mathbf{M}\Big]_0^l \;+\; \int_0^l\Big(\delta\mathbf{r}_a+\delta\boldsymbol{\varphi}\times\mathbf{f}\Big)\cdot\mathbf{p}\;ds_0 \tag{2.16}$$

consists of a boundary contribution, i.e. point loads, and distributed forces along the beam element.

The contents of the integral in (2.16) follows from the definitions of $\mathbf{f}$ and $\mathbf{p}$. It is stated earlier that the point of attack $\mathbf{f}$ follows the rotations of the cross-sections which means that the moment $\mathbf{f}\times\mathbf{p}$ is rotation dependent whether $\mathbf{p}$ is a conservative load or not.

This rotation dependency is obvious in connection with the distributed force which isn't the case for the boundary term. The internal forces in the boundary terms can be associated with external loads at the ends by static considerations. Introducing the external loads at the boundaries as a set of n forces where $\mathbf{P}^i$ is the force vector and $\mathbf{F}^i$ is the point of attack of the corresponding force vector, see e.g. Fig. 2.5. The point of attack $\mathbf{F}^i$ follows the rotation of the cross-section and is related to the corresponding vector $\hat{\mathbf{F}}^i$ in the global coordinate system via a transformation operator $\mathbf{A}(\boldsymbol{\varphi})$ (see e.g. Appendix A) as indicated in Fig. 2.5.

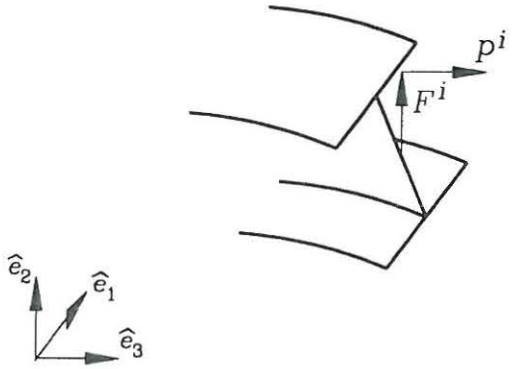

Fig. 2.5: Boundary loads.

Force equilibrium at the boundary then takes the form

$$\mathbf{N} = \sum_{i=1}^{n} \mathbf{P}^i \tag{2.17}$$

and moment equilibrium

$$\mathbf{M} = \sum_{i=1}^{n} \left(\mathbf{F}^i \times \mathbf{P}^i \right) = \sum_{i=1}^{n} \left((\mathbf{A}(\boldsymbol{\varphi}) \cdot \hat{\mathbf{F}}^i) \times \mathbf{P}^i \right) \tag{2.18}$$

One should notice the difference in the way in which the boundary force and moment behave. From (2.18) it follows that the moment contributes through the transformation operator $\mathbf{A}$, which implies that the contribution is rotation dependent.
Substitution of (2.17) and (2.18) into the boundary term of (2.6) leads to

$$\left[\delta \mathbf{r}_a \cdot \mathbf{N} + \delta \boldsymbol{\varphi} \cdot \mathbf{M} \right]_0^l = \left[\delta \mathbf{r}_a \cdot \sum_{i=1}^{n} \mathbf{P}^i + \delta \boldsymbol{\varphi} \cdot \sum_{i=1}^{n} \left(\mathbf{A}(\boldsymbol{\varphi}) \cdot \mathbf{F}^i \right) \times \mathbf{P}^i \right]_0^l \tag{2.19}$$

By this approach external moments can be generated by a pair of equal and opposite forces acting on the ends of an arbitrarily-oriented rigid arm that follows the motion of the cross-section. This representation of moments is commonly used in the literature and can be used in different ways leading to e.g. quasitangential, pseudotangential and semitangential moments, see e.g. Argyris *et al.* (1978) and Yang & McGuire (1985).

2.5 Conclusions

A general nonlinear theory for the beam has been derived by considering the beam as represented by a curve with a local set of base vectors fixed to the cross-section at each point of the curve. The orientation of the local base vectors is related to a set of global base vectors by a rotation vector via an ortogonal transformation operator. The generalized displacements are hereby the translation vector for the curve and the rotation vector for the cross-sections. The equilibrium equations for the beam are reformulated as a virtual work equation, and this defines three strain components and three curvature components. The strain components describe the difference between the tangent vector of the curve and the normal vector to the cross-section. The warping effect, characteristic of thin-walled beams, is treated separately but can easily be added to the virtual work equation as a scalar component.
The rotational dependency of external point loads is incorporated by introducing the external loads as a set of forces with a corresponding rigid arm.

Chapter 3

Static Stability Theory

Instability can occur when other forms of equilibrium, qualitatively different from the fundamental precritical shape (e.g. bifurcation), become possible. In order to obtain a stability formulation one can use different approaches. One can for instance use a pure kinematical approach where the formulation is based entirely on a deformation measure developed from a displacement field. Here the initial stresses have to be identified through the higher order terms. Another possible approach is a statical one, where one through equilibrium considerations establish the governing differential equations.

Using the results from Chapter 2 a static stability theory is presented in this chapter. The governing equations are derived by considering the beam in two adjacent states, an initial state (Section 3.1.1) and a buckled state (Section 3.1.2). A weak formulation of the stability equation is obtained in Section 3.2 by subtracting the virtual work equation for the initial state from that of the buckled state.

3.1 Variational Formulation

The virtual work as expressed in (2.6) is used to derive a weak formulation of the stability

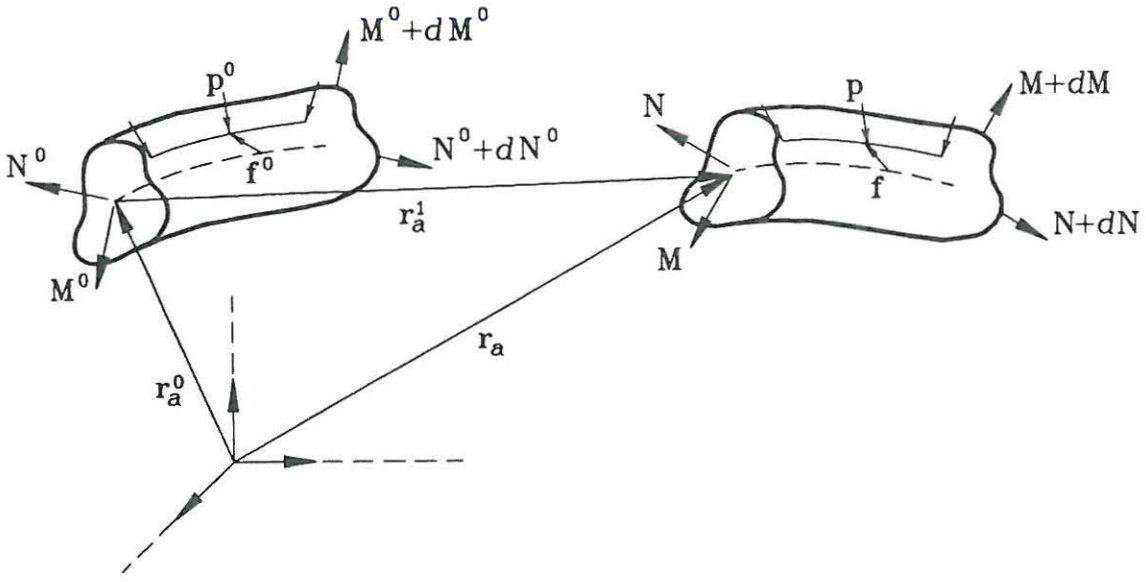

Fig. 3.1: Beam element in initial and buckled state.

equation. This is accomplished by considering the beam in two adjacent states, an initial state (critical), and a buckled state (postcritical).

In the present formulation of the stability equation the initial state may include deformation imposed prior to buckling, so-called initial deformations. These terms are important e.g. in connection with lateral buckling of thin-walled beams with non-symmetric cross-section.

3.1.1 Initial State

In the initial state it is assumed that all parameters describing the beam, including deformation have been determined. No relationship is required between the geometry and statics in this state. The parameters in the initial state are indicated by superscript (^{0}). The characteristic curve of the beam is described by $\mathbf{r}_a^0(s_0)$ and the local unit vectors $\mathbf{e}_j^0$ are obtained from the global base vectors $\hat{\mathbf{e}}_j$ and the finite rotation

$$\mathbf{e}_j^0 \;=\; \mathbf{A}(\boldsymbol{\varphi}^0)\cdot\hat{\mathbf{e}}_j \tag{3.1}$$

where $\mathbf{A}$ is an orthogonal transformation tensor and $\boldsymbol{\varphi}^0(s_0)$ is the corresponding rotation vector. Appendix A gives a detailed description of the finite rotation tensor $\mathbf{A}(\boldsymbol{\varphi})$.

The beam is in equilibrium which means that the virtual work equation according to (2.6) is given by

$$\begin{aligned}\int_0^l \left\{\left(\frac{d\,\delta\mathbf{r}_a}{ds_0} - \delta\boldsymbol{\varphi}\times\frac{d\mathbf{r}_a^0}{ds_0}\right)\cdot\mathbf{N}^0 \;+\; \frac{d\,\delta\boldsymbol{\varphi}}{ds_0}\cdot\mathbf{M}^0\right\} ds_0 \\ = \left[\delta\mathbf{r}_a\cdot\mathbf{N}^0 + \delta\boldsymbol{\varphi}\cdot\mathbf{M}^0\right]_0^l \;+\; \int_0^l \left(\delta\mathbf{r}_a + \delta\boldsymbol{\varphi}\times\mathbf{f}^0\right)\cdot\mathbf{p}^0\; ds_0\end{aligned} \tag{3.2}$$

The strain components in the initial state can be found from (2.12), which leads to

$$\varepsilon_j^0 \;=\; \left(\frac{d\mathbf{r}_a^0}{ds_0} - \mathbf{e}_3^0\right)\cdot\mathbf{e}_j^0 \tag{3.3}$$

A geometric description of the beam is accomplished by introducing the curvatures κ_α^0 and the twist κ_3^0 in the initial state. It follows from (2.15) that

$$e_{jkl}\,\kappa_l^0 \;=\; \frac{d\mathbf{e}_j^0}{ds_0}\cdot\mathbf{e}_k^0 \tag{3.4}$$

The internal forces are decomposed in the basis $\mathbf{e}_j^0$, whereby $\mathbf{N}^0 = N_j^0\mathbf{e}_j^0$ and $\mathbf{M}^0 = M_j^0\mathbf{e}_j^0$.

3.1.2 Buckled State

Equilibrium in the buckled state implies that

$$\int_0^l \left\{\left(\frac{d\,\delta\mathbf{r}_a}{ds_0} - \delta\boldsymbol{\varphi}\times\frac{d\mathbf{r}_a}{ds_0}\right)\cdot\mathbf{N} \;+\; \frac{d\,\delta\boldsymbol{\varphi}}{ds_0}\cdot\mathbf{M}\right\} ds_0$$

$$= \left[\delta \mathbf{r}_a \cdot \mathbf{N} + \delta\boldsymbol{\varphi} \cdot \mathbf{M}\right]_0^l + \int_0^l \left(\delta \mathbf{r}_a + \delta\boldsymbol{\varphi} \times \mathbf{f}\right) \cdot \mathbf{p}\, ds_0 \tag{3.5}$$

The position and rotation vectors are now expressed with reference to their value in the critical state, i.e.

$$\mathbf{r}_a(s_0) = \mathbf{r}_a^0(s_0) + \mathbf{r}_a^1(s_0) \tag{3.6}$$

and

$$\boldsymbol{\varphi}(s_0) = \boldsymbol{\varphi}^0(s_0) + \boldsymbol{\varphi}^1(s_0) \tag{3.7}$$

Thus $\mathbf{r}_a^1$ and $\boldsymbol{\varphi}^1$ are the increments from the critical state.
The current local unit vectors $\mathbf{e}_j$ are related to the global basis $\hat{\mathbf{e}}_j$ similarly to (3.1). Decomposition of the increment of the rotation vector in the initial basis corresponding to $\boldsymbol{\varphi}^1 = \varphi_j^1 \mathbf{e}_j^0$ leads to the following relationship between the initial unit vectors $\mathbf{e}_j^0$ and the current unit vectors $\mathbf{e}_j$

$$\mathbf{e}_j = \mathbf{A}(\boldsymbol{\varphi}^1) \cdot \mathbf{e}_j^0 = A_{lj}\, \mathbf{e}_l^0 \tag{3.8}$$

The generalized deformations in the buckled state can be found directly from (2.12) and (2.15). The total strain components $\varepsilon_j(s_0)$ are simply given by (2.12)

$$\varepsilon_j = \left(\frac{d\mathbf{r}_a}{ds_0} - \mathbf{e}_3\right) \cdot \mathbf{e}_j = \left(\frac{d\mathbf{r}_a^0}{ds_0} - \mathbf{e}_3^0 + \frac{d\mathbf{r}_a^1}{ds_0} - \left(\mathbf{A}(\boldsymbol{\varphi}^1) - \mathbf{I}\right) \cdot \mathbf{e}_3^0\right) \cdot \mathbf{A}(\boldsymbol{\varphi}^1) \cdot \mathbf{e}_j^0 \tag{3.9}$$

Decomposition of $\mathbf{r}_a^1$ in the initial basis, i.e. $\mathbf{r}_a^1 = r_{al}^1\, \mathbf{e}_l^0$, and substitution of (3.4) and (3.8) leads to the component form of the total strain

$$\varepsilon_j = \left(\varepsilon_l^0 + \left(\frac{dr_{al}^1}{ds_0} + r_{ak}^1 e_{kln} \kappa_n^0\right) - \left(A_{l3} - \delta_{l3}\right)\right) A_{lj} \tag{3.10}$$

Investigating (3.10) it follows that the strain components are nonlinear with respect to the rotation components according to the presence of A_{lj}. The influence from the initial state is accounted for by the presence of both the initial strains and curvatures.
The curvatures $\kappa_l(s_0)$ in the buckled state are given by

$$e_{jkl}\, \kappa_l = \frac{d\mathbf{e}_j}{ds_0} \cdot \mathbf{e}_k = \frac{d\, A_{nj}}{ds_0} A_{nk} + e_{nmr}\, \kappa_r^0\, A_{nj} A_{mk} \tag{3.11}$$

where equations (3.4) and (3.8) have been used to obtain the final form. It appears that also the curvature components are nonlinear in the rotation components. Further one should notice that only the initial curvatures represent the influence from the initial state.
The nonlinearity in the rotation components in the strain and curvatures is a consequence of the representation of the cross-section by the orthogonal rotation tensor $\mathbf{A}$.
The internal force and moment components N_j and M_j refer to the current base vectors $\mathbf{e}_j$. Let N_j^1 and M_j^1 be the increments of the components. Since the initial components N_j^0 and

M_j^0 follow the cross-section the decomposition in the buckled state is

$$\begin{aligned} \mathbf{N}(s_0) &= \left(N_j^0 + N_j^1\right)\mathbf{e}_j &&= \mathbf{N}^0 + \left[N_j^1\mathbf{e}_j + (\mathbf{A}(\boldsymbol{\varphi}^1) - \mathbf{I})\cdot\mathbf{N}^0\right] \\ \mathbf{M}(s_0) &= \left(M_j^0 + M_j^1\right)\mathbf{e}_j &&= \mathbf{M}^0 + \left[M_j^1\mathbf{e}_j + (\mathbf{A}(\boldsymbol{\varphi}^1) - \mathbf{I})\cdot\mathbf{M}^0\right] \end{aligned} \tag{3.12}$$

The terms inside the square brackets are the vector increments $\mathbf{N}^1$ and $\mathbf{M}^1$. It is evident that the internal forces $\mathbf{N}^0$ and $\mathbf{M}^0$ from the initial state contribute through products with the tensor

$$\widetilde{\mathbf{A}}(\boldsymbol{\varphi}^1) = \mathbf{A}(\boldsymbol{\varphi}^1) - \mathbf{I} = \tilde{A}_{lj}(\varphi_m^1)\mathbf{e}_l^0\mathbf{e}_j^0 \tag{3.13}$$

The last term in (3.13) is the dyadic form of the tensor $\widetilde{\mathbf{A}}$ when the rotation vector $\boldsymbol{\varphi}^1$ is decomposed in the initial basis. Substitution of (3.13) leads to

$$\begin{aligned} \mathbf{N}^1(s_0) &= \left[N_j^1 + \mathbf{e}_j\cdot\left(\widetilde{\mathbf{A}}(\boldsymbol{\varphi}^1)\cdot\mathbf{N}^0\right)\right]\mathbf{e}_j &&= \left[N_j^1 - \tilde{A}_{lj}N_l^0\right]\mathbf{e}_j \\ \mathbf{M}^1(s_0) &= \left[M_j^1 + \mathbf{e}_j\cdot\left(\widetilde{\mathbf{A}}(\boldsymbol{\varphi}^1)\cdot\mathbf{M}^0\right)\right]\mathbf{e}_j &&= \left[M_j^1 - \tilde{A}_{lj}M_l^0\right]\mathbf{e}_j \end{aligned} \tag{3.14}$$

Thus the vector increment in the internal forces $\mathbf{N}^1(s_0)$ and $\mathbf{M}^1(s_0)$ depends on the increment of the components N_j^1 and M_j^1 as well as a rotation contribution from the initial forces $\mathbf{N}^0$ and $\mathbf{M}^0$. The increments N_j^1 and M_j^1 have to be expressed by constitutive equations while $\mathbf{N}^0$ and $\mathbf{M}^0$ are given by the equilibrium equations for the initial state.

3.2 Weak Formulation of the Stability Equation

In Section 3.1 the initial state is from the beginning introduced as the critical state, i.e. the beam is in equilibrium but different kinds of equlibrium forms exist. These other equilibrium forms are identified as the buckled state. The stability equation which describes this phenomena can be obtained by subtracting the virtual work equation for the initial state from that of the buckled state. If a solution to the hereby developed stability equation exists which is different from the trivial one then the beam structure is in a critical state. This implies that the initial state may not be the critical state at first, but then the initial state can be used as a preliminary state which successively can be updated until it represents the critical state.

The stability equation is found by subtracting the equation for the initial state from that of the buckled state. In order to accomplish this some assumptions regarding the external load has to be taken. Assuming that the beam structure initially is subjected to proportional loading means that a given ratio between the external forces exists in the initial state. The external load can then be represented by a single load parameter λ_0. The initial stress terms are then given by

$$N_j^0 = \lambda_0\,\bar{N}_j^0 \quad , \quad M_j^0 = \lambda_0\,\bar{M}_j^0 \quad , \quad p_j^0 = \lambda_0\,\bar{p}_j^0 \quad , \quad P_j^{0i} = \lambda_0\,\bar{P}_j^{0i} \tag{3.15}$$

where the bar indicates the initial stress distribution.

Then a certain combination of initial forces defines the critical load parameter λ_0 which describes the point at which other forms of equilibrium become possible. When the beam structure has reached the critical point the external load may still be increased, therefore the load vector in the buckled state is expressed as $(1 + \lambda)$ times the value in the initial state i.e. proportional loading. Subtracting (3.2) from (3.5) leads to weak form of the stability equation

$$\int_0^l \Big\{ \left(\frac{d\,\delta\mathbf{r}_a}{ds_0} - \delta\boldsymbol{\varphi} \times \frac{d\mathbf{r}_a}{ds_0} \right) \cdot \mathbf{N}^1 + \frac{d\,\delta\boldsymbol{\varphi}}{ds_0} \cdot \mathbf{M}^1 - \delta\boldsymbol{\varphi} \cdot \frac{d\mathbf{r}_a^1}{ds_0} \times \mathbf{N}^0 - \lambda\,\delta\mathbf{r}_a \cdot \mathbf{p}^0$$

$$- \delta\boldsymbol{\varphi} \cdot \left(\widetilde{\mathbf{A}}(\boldsymbol{\varphi}^1) + \lambda\,\mathbf{A}(\boldsymbol{\varphi}^1) \right) \cdot \mathbf{f}^0 \times \mathbf{p}^0 \Big\}\, ds_0 - \Big[\delta\mathbf{r}_a \cdot \mathbf{N}^1 + \delta\boldsymbol{\varphi} \cdot \mathbf{M}^1 \Big]_0^l = 0 \qquad (3.16)$$

Equation (3.16) represents the vectorial form of the stability equation. Comparing with the virtual work equation (2.6) the resemblance is obvious and ofcourse (2.6) can be obtained from (3.16) by eliminating the initial stress terms. Recalling the definitions of the increments $\mathbf{N}^1(s_0)$ and $\mathbf{M}^1(s_0)$ from (3.14) one will notice that the initial stress terms indeed are represented which makes it possible to perform stability analysis based on (3.16). The transition point from the initial to the buckled state is defined by $\lambda = 0$ and the existence of a nontrivial solution, i.e. $\mathbf{r}_a^1(s_0) \neq \mathbf{0}$ or $\boldsymbol{\varphi}^1 \neq \mathbf{0}$. The vectorial form is not particularly suitable as a method of calculating therefore a component form is introduced in the following.

The products in (3.16) are now expressed in terms of components. The variations of the displacement parameters are decomposed in the initial basis whereby $\delta\boldsymbol{\varphi} = \delta\varphi_j \mathbf{e}_j^0$ and $\delta\mathbf{r}_a = \delta r_{a_j} \mathbf{e}_j^0$. Using (3.8) and (3.14) together with the expressions (2.11) and (2.14) for the variation of the generalized deformation components leads to

$$\int_0^l \Big\{ \delta\varepsilon_j \left(N_j^1 - N_l^0\, \tilde{A}_{lj} \right) + \delta\kappa_j \left(M_j^1 - M_l^0\, \tilde{A}_{lj} \right) - \delta\varphi_l\, e_{lnk} \left(\tilde{A}_{n3} + \varepsilon_j A_{nj} - \varepsilon_n^0 \right) N_k^0$$

$$- \lambda\,\delta r_{a_k}\, p_k^0 - \delta\varphi_l\, e_{lnk} \left(\tilde{A}_{n\alpha} + \lambda\, A_{n\alpha} \right) f_\alpha^0 p_k^0 \Big\}\, ds_0$$

$$- \Big[\delta r_{a_l} \sum_{i=1}^{n} \left(\lambda\, P_l^{0^i} \right) + \delta\varphi_k\, e_{kln} \sum_{i=1}^{n} \left(P_n^{0^i} (\tilde{A}_{l\alpha} + \lambda\, A_{l\alpha})\, F_\alpha^{0^i} \right) \Big]_0^l = 0 \qquad (3.17)$$

The virtual work as expressed in (3.16) and (3.17) is for convenience referred to as δV. The first term in the integrand is the contribution from the axial and shear deformations. The second term arising from the bending and torsion action is often the most significant in beam problems. The next term is the contribution from rotation of $\mathbf{N}^0$ and finally the last terms give the work produced by increasing the distributed force $\mathbf{p}^0$ and the rotation of the point of load application $f_\alpha^0 \mathbf{e}_\alpha^0$. The boundary terms express the increase of the endloads in the buckled state. The endforce contribution may easily be identified as the difference of the buckling load and the initial endforce, but in case of endmoments the contributions is more complex.

The equations in (3.16) and (3.17) represent the general form of the stability equation and can

be used for different kinds of beam problems, since no assumptions regarding the condition of the beam element in the initial state have been made.

3.3 Conclusions

A weak form of the nonlinear stability equation for the beam has been derived. The initial stress terms as well as the initial displacements are incorporated in a general and consistent way. The initial deformations are accounted for indirectly via the generalized strains and curvatures while the initial stress terms appear directly in the stability equation.

The stability equation has been derived by use of a line approach. As a beam possesses a finite extent in the plane of the cross-sections a direct use may suffer in consistens because of effects such as e.g. twisting and initial curvature. This insuffiency can be removed by a proper choice of constitutive equations as it is shown in Chapter 4.

Chapter 4

Constitutive Equations

Whether one uses a kinematical or statical approach in the derivation of a stability theory constitutive equations are required, as stated in Chapter 3. The object of the constitutive equations is to express an unambiguous relation between a deformation measure, *strains*, and a set of internal forces, *stresses*. The deformation measure is commonly developed by kinematical considerations, i.e. a displacement field is used to express a set of strains. The governing parameter in the relation is the deformation measure which is used to derive the internal forces by either direct integration over the cross-section or by an energy approach.

In the present formulation it is the aim to develop the stability equations by mixing the statical line approach with a kinematical derivation of the constitutive equations. This means that part of the influence from the initial state is accounted for by the line approach given in Section 3.2 and the *rest*, which arises when the beam is given a finite extent in the plane of the cross-section, is accounted for through constitutive equations based on a kinematical viewpoint.

In this chapter different ways of establishing constitutive equations for beam structures is discussed with respect to their influence on the stability equations. In addition a strain measure is developed which in a simple but consistent way incorporates effects from initial curvatures. This strain measure is expanded in order to incorporate the warping effect whereby constitutive equations for thin-walled beams are derived.

4.1 Constitutive Equations for Beam Structures

Constitutive equations may be linear as well as nonlinear depending on the choice of displacement field and strain measure. The nonlinear form could, for instance, be developed by use of a linear displacement field in a nonlinear strain field or vice versa. Naturally, these different approaches implies the possibility of deviations in higher order terms.
Depending on the problem to be solved, e.g.

- beam analysis
- stability analysis (bifurcation)
  - buckling
  - postbuckling

the choice may influence the overall result. As the object of this project is to establish a stability theory, it is essential to obtain relations that incorporate initial stresses as well as initial curvatures consistently.
The constitutive equations express the change relative to a previous state of the internal forces due to deformation. Therefore the constitutive equations depend on the condition of the beam element in this previous state, i.e. if initial stresses or initial deformations are present.
A theory for the straight prismatic beam with initial stresses and small deformations has been given a complete treatment by Vlasov (1961) and Timoshenko & Gere (1961). The influence from the initial stresses was there found by equilibrium considerations of the deformed beam element. They found that in the presence of initial stresses only a contribution to the St. Venant torsional stiffness arises, i.e. the uncoupled linear constitutive equations derived through beam analysis need only to be modified for the torsional stiffness in order to be usable in a buckling analysis.
In case of both initial deformations and stresses the agreement in the literature is not overwhelming regarding how to express the constitutive equations and thereby how to develop a stability theory. Especially the single curved beam has been studied intensively see e.g. Yoo (1982) and Yang & Kuo (1987). In the approach of Yang & Kuo it is a main point to account for the initial curvature in a linear displacement field as well as in the derivatives with respect to the axial coordinate. In a nonlinear strain measure these effects of curvature are incorporated in the development of the constitutive equations. By this approach coupling between extension and bending is included not only in the generalized displacements but also in the generalized deformations. Vlasov and Timoshenko & Gere discussed this special case only briefly. Vlasov did only consider the effect of curvature in a set of modified generalized deformations and ended up with constitutive equations analog to those for the straight beam where only the generalized deformations were influenced by the curvature.
The works mentioned above have all been concerned with the buckling problem and in all cases a linear displacement field was used. The approach with a linear displacement field in a nonlinear strain measure was also applied by Grimaldi & Pignataro (1979) who analysed the postbuckling behavior of the simply supported column. Performing a postbuckling analysis, which indicates finite displacements, in such a way seems to lack in consistency when deformations prior to buckling have to be accounted for. This is also pointed out by Kouhia (1991) who used a nonlinear displacement field in a nonlinear strain measure to develop a stability theory.

In the present paper it is the object, along with the line approach and the nonlinear displacement field, to develop a strain measure which in a consistent way at least incorporates the effect of twist on the torsional rigidity in the constitutive equations. The influence from initial curvatures is consistently included via the generalized deformations ε_j and κ_j, neglecting the effect of curvature on the derivatives with respect to the axial coordinate. The accuracy of this assumption is studied in an example in Section 7.5.3 where *the beam in pure bending* is examined.

4.2 Constitutive Equations - Energy Approach

In order to discuss different strain measures with respect to their influence on the constitutive equations a general introduction to the derivation of constitutive equations via an energy approach is given in this section.
If a suitable strain distribution has been determined the internal forces can for example be found directly by integration over the cross-section or indirectly by use of an energy approach. The integration process has its weakness in connection with the torsional moment which has to be found by alternative methods if warping and initial stress effects are to be incorporated. The energy approach on the other hand avoids this problem and leads to a form where the internal work can be integrated to yield the elastic energy. Therefore a method to derive the constitutive equations by an energy approach is presented in this section.

The material is assumed to be linear elastic with an axial modulus of elasticity E and shear modulus G. For elastic materials the elastic energy is a function of the strains. For the elastic beam this means that the elastic energy pr. length is a function of the strain components $\epsilon_j(x_\alpha, s_0)$. The elastic energy pr. length W is defined by

$$\begin{aligned} W(\epsilon_j) &= \int_A u(\epsilon_j)\, dA \\ &= \int_A \frac{1}{2} \left\{ \epsilon_\alpha\, G\, \epsilon_\alpha \;+\; \epsilon_3\, E\, \epsilon_3 \right\} dA \end{aligned} \tag{4.1}$$

where u is the elastic energy pr. volume. In the general case the actual stress components $\sigma_j(x_\gamma, s_0)$ and the actual strain components are related through the elastic energy by

$$\sigma_j = \frac{\partial u}{\partial \epsilon_j} \tag{4.2}$$

The actual stress state $\sigma_j(x_\gamma, s_0)$ may in general consist of an initial stress contribution $\sigma_j^0(x_\gamma, s_0)$ and an increment corresponding to the increments in the strain components. For linear elasticity this leads to

$$\sigma_\alpha(x_\gamma, s_0) = \sigma_\alpha^0 + G\left(\epsilon_\alpha - \epsilon_\alpha^0\right) \quad ; \quad \sigma_3(x_\gamma, s_0) = \sigma_3^0 + E\left(\epsilon_3 - \epsilon_3^0\right) \tag{4.3}$$

By this introduction of the initial stresses, no direct relationship is assumed between statics and geometry in the initial state. The stress components in the initial state σ_j^0 are expressed by the initial internal forces.
The change in elastic energy pr. volume from the initial state to the actual state is given by

$$\begin{aligned} u - u^0 &= \int_{\epsilon_j^0}^{\epsilon_j} \sigma_j\, d\epsilon_j \\ &= \sigma_j^0 \left(\epsilon_j - \epsilon_j^0\right) + \frac{1}{2} G \left(\epsilon_\alpha - \epsilon_\alpha^0\right)^2 + \frac{1}{2} E \left(\epsilon_3 - \epsilon_3^0\right)^2 \end{aligned} \tag{4.4}$$

The strain components ϵ_j may be expressed by a set of generalized deformations, e.g. ε_j and

κ_j, which can be associated with a set of internal forces N_j and M_j. Substituting (4.4) into the expression for the elastic energy pr. length (4.1) and performing the integrations leads to a functional in terms of the generalized deformations.
By standard variational procedures this functional can be used to establish the constitutive equations. In general this implies that

$$N_j = \frac{\partial W\left(\varepsilon_j, \kappa_j\right)}{\partial \varepsilon_j} \quad , \quad M_j = \frac{\partial W\left(\varepsilon_j, \kappa_j\right)}{\partial \kappa_j} \tag{4.5}$$

The internal forces are hereby expressed by the derivatives of the elastic energy with respect to their corresponding deformations.

4.3 Kinematics - Strain Measure

As pointed out a main point in the development of constitutive equations is to define a strain measure. For beam structures the behavior of a beam element is well-described by three strain components, a normal strain and two shear strains. The normal strain can be developed in a satisfactory form by a pure kinematical approach while the shear strain distribution suffers by such an approach. The discussion in this section is therefore mainly concerned with the normal strain while the shear strains are discussed in detail in Section 4.4.

The discussion in this section is concerned with a Lagrangian description of the beam. In the Lagrangian description attention is focused on what is happening at or in the neighbourhood of a particular material point, Malvern (1969). The actual position of a material point is described by the position vector $\mathbf{r}(\mathbf{x})$ in a Cartesian x_j coordinate system. Using the position vector $\mathbf{r}_a(x_3)$ and $\boldsymbol{\varphi}(x_3)$ as generalized displacements, it follows that

$$\mathbf{r}(x_j) = \mathbf{r}_a(x_3) + (x_\alpha - a_\alpha)\, \mathbf{e}_\alpha \tag{4.6}$$

where the unit vectors $\mathbf{e}_\alpha$ are related to the global unit vectors by the rotation tensor $\mathbf{A}(\boldsymbol{\varphi})$. $\mathbf{e}_j$ are the actual unit vectors where $\mathbf{e}_\alpha$ represent the plane of the cross-section in the actual state. The point identified by a_α lies on the axis of rotation. This point, which may be a characteristic point of the cross-section, can be chosen in an arbitrary way. A possible choice of this point is given in Section 4.4.
The position vector in (4.6) is linear in the variable x_α and the translation vector $\mathbf{r}_a$, but it is in general nonlinear in the rotation vector $\boldsymbol{\varphi}$. The dependency on the rotation vector is a consequence of the rotation operator $\mathbf{A}$ which may be the infinitesimal or the finite rotation tensor, see Appendix A.
In a three-dimensional approach the Green-Lagrange strain tensor is the main choice in order to determine the strain components. The Green-Lagrange strain tensor $\mathbf{E}$ is defined by (see e.g. Malvern (1969))

$$\mathbf{E} = \frac{1}{2}\left(\frac{\partial \mathbf{r}}{\partial \mathbf{x}} \cdot \frac{\partial \mathbf{r}}{\partial \mathbf{x}} - \mathbf{I}\right) \tag{4.7}$$

The Green-Lagrange tensor is as it appears in general nonlinear regardless of the choice of

displacement field. The term nonlinear is used according to the distribution over the cross-section as well as in the generalized displacements. In the following the Green-Lagrange tensor is used to develop a suitable strain measure by mixing a finite strain measure with a *small* strain measure.

4.3.1 Normal Strain

The normal strain of the Green-Lagrange tensor is defined by

$$E_{33} = \frac{1}{2}\left(\frac{\partial \mathbf{r}}{\partial x_3} \cdot \frac{\partial \mathbf{r}}{\partial x_3} - \mathbf{e}_3 \cdot \mathbf{e}_3\right) \tag{4.8}$$

Reformulating leads to

$$E_{33} = \frac{1}{2}\left(\frac{\partial \mathbf{r}}{\partial x_3} + \mathbf{e}_3\right) \cdot \left(\frac{\partial \mathbf{r}}{\partial x_3} - \mathbf{e}_3\right) \tag{4.9}$$

It appears that the normal strain depends on the tangent vector $\partial \mathbf{r}/\partial x_3$. Using (4.6) it follows that

$$\frac{\partial \mathbf{r}}{\partial x_3} = \frac{\partial \mathbf{r}_a}{\partial x_3} + (x_\alpha - a_\alpha)\frac{\partial \mathbf{e}_\alpha}{\partial x_3} \tag{4.10}$$

For *small strains* the tangent vector $\partial \mathbf{r}/\partial x_3$ is assumed to be comparable to the normal vector of the cross-section $\mathbf{e}_3$ as indicated by the relation in (2.13), i.e. a small strain measure for the normal strain $\epsilon(x_j)$ is given by

$$\epsilon(x_j) = \left(\frac{\partial \mathbf{r}}{\partial x_3} - \mathbf{e}_3\right) \cdot \mathbf{e}_3 \tag{4.11}$$

Note that this formulation of the normal strain leads to a linear distribution over the cross-section but may include nonlinear terms in the generalized displacements, depending on the definition of the rotation tensor $\mathbf{A}$. Further for $x_3 = s_0$ one notice the resemblance with the strain measure in (2.12) defined by the virtual work approach.

Discussion of Strain Measures

The strain measures may be expressed directly by the generalized displacements $\mathbf{r}_a(s_0)$ and $\boldsymbol{\varphi}(s_0)$ or indirectly through the generalized deformations, ε_j and κ_j defined by (2.12) and (2.15), respectively. This means that a comparison between the two normal strains can be carried out on two levels, corresponding to a discussion with respect to generalized deformations or generalized displacements. Comparing with respect to deformations leads to identification of similarities as well as terms which with confidence may be neglected while comparing with respect to displacements leads to identification of the different possibilities in connection with nonlinear stability analysis.
First the two definitions of the normal strain are reformulated by use of the generalized deformations ε_j and κ_j derived in Section 3.2 which are associated with the internal forces N_j and M_j respectively.

Using the generalized deformations the tangent vector can be expressed by

$$\frac{\partial \mathbf{r}}{\partial x_3} = \mathbf{e}_3 + \varepsilon_j \, \mathbf{e}_j + (x_\alpha - a_\alpha) \, e_{\alpha k l} \kappa_l \, \mathbf{e}_k \tag{4.12}$$

Inserting (4.12) in the expression for the Green-Lagrange normal strain (4.9) leads to

$$\begin{aligned} E_{33} &= \varepsilon_3 - (x_\beta - a_\beta) \, e_{\beta\alpha} \, \kappa_\alpha \\ &\quad + \tfrac{1}{2} \varepsilon_j \, \varepsilon_j + (x_\beta - a_\beta) \, e_{\beta\alpha} \, \varepsilon_\alpha \, \kappa_3 - (x_\beta - a_\beta) \, e_{\beta\alpha} \, \kappa_\alpha \, \varepsilon_3 \\ &\quad - \tfrac{1}{2} \kappa_\gamma e_{\gamma\alpha} (x_\alpha - a_\alpha)(x_\beta - a_\beta) e_{\beta\eta} \kappa_\eta + \tfrac{1}{2} (x_\beta - a_\beta)(x_\beta - a_\beta) \kappa_3 \kappa_3 \end{aligned} \tag{4.13}$$

and for the linearized small strain component (4.11) it follows that

$$\epsilon = \varepsilon_3 - (x_\beta - a_\beta) \, e_{\beta\alpha} \, \kappa_\alpha \tag{4.14}$$

The small strain component is linear while the Green-Lagrange component contains a quadratic distribution over the cross-section as well as a quadratic dependency of the generalized deformations.

Observing expression (4.13) it is evident that it contains coupling between all kinds of deformation modes shear-extension-bending-torsion, even if the point a_α is chosen in a favorable way. The majority of these coupling terms are negligible and may therefore be omitted according to the discussion performed in the following. Strain deformations are in general small compared with curvature deformations for beam problems. This implies that the quadratic term of strain deformations is negligible. Likewise the coupling term between shear and twist in the second line can be neglected. The normalstrain ε_3 is considered as small compared to 1 implying that the linear bending contribution is much greater than coupling between extension and bending. This coupling term can therefore be neglected.

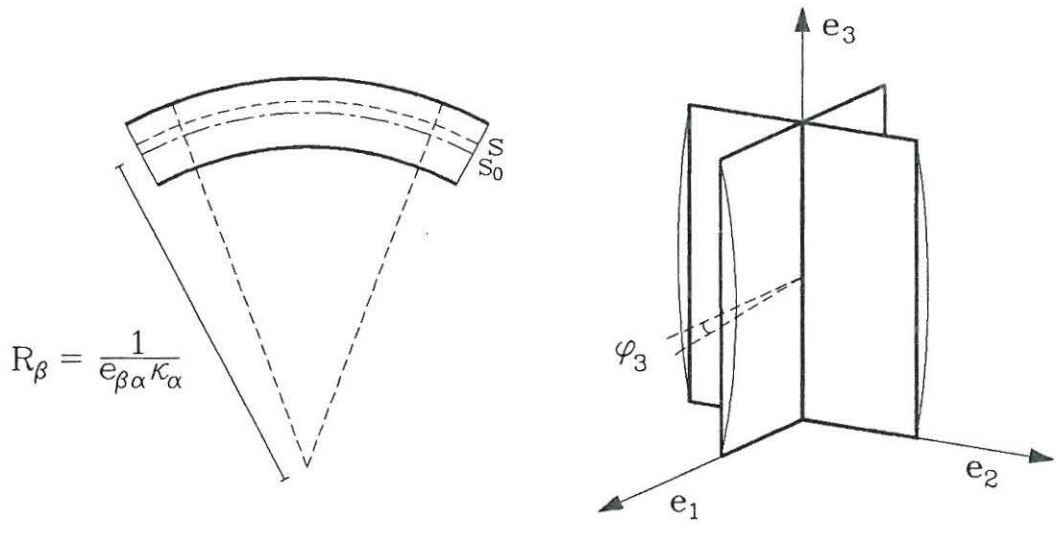

Fig. 4.1: a) Radius of curvature and cross-section dimensions. b) Twist of cruciform column.

The first term in the third line is a nonlinear bending contribution which can be considered as an effect from the radius of curvature. This term does not represent the total effect as it may appear from Fig. 4.1a where it is indicated that the radius of curvature depends on the position in the cross-section plane. In this context it is assumed that the cross-section dimensions are small compared with the radius of curvature. Therefore the effect of curvature is not accounted for in the following. Finally if a beam is twisted a longitudinal strain arises as a second order effect as indicated in Fig. 4.1b. This effect is described by the last term and may be important for the torsional rigidity and can therefore not be ignored, especially not for beams with non-symmetric cross-sections, see e.g. Vlasov (1961) and Timoshenko & Gere (1961).

The small strain component in (4.14) does not contain any of the second order terms, which indicates that the strain measure in this form is uncapable of handling several stability problems. On the other hand the Green-Lagrange strain measure contains many terms which complicates the problem and do not improve the overall result significant. This leads to the idea that mixing the two strain measures would be a good approximation in order to establish a strain measure which in a simple way can incorporate the necessary effects in the constitutive equations.

The previos discussion was concentrated on the generalized deformations. Continuing the discussion with respect to the generalized displacements adds some impressions. The two definitions for the normal strain, (4.9) and (4.11), together with the possibility of chosing a linear or a nonlinear displacement field leaves us with four levels for the normal strain distribution as indicated in Table 4.1.

Table 4.1: Generalized displacements and normal strain distribution.

	Small strain		Green-Lagrange	
Displacement Field	distribution over cross-section	generalized displacements	distribution over cross-section	generalized displacements
linear	linear	linear	quadratic	quadratic
nonlinear	linear	nonlinear	quadratic	nonlinear

It is obvious that the linear displacement field together with the small strain formulation can't be used in a buckling analysis unless the initial stress terms are incorporated via alternative methods, e.g. the statical line approach in Section 3.2. For this kind of analysis the linear strain apart from a few cases is qualified to enter such an analysis because it except for the quadratic distribution over the cross-section contains all the elastic terms to appear in such an analysis. If the linear strain measure should be able to handle any problem the torsional moment has to be modified for an influence from the initial stresses.

The small strain in connection with a nonlinear displacement field may be a good choice for a stability analysis via the principle of virtual work or minimum potential energy. It is

possible to investigate the buckling as well as postbuckling behavior because of the nonlinear terms in the generalized displacements. But still one misses the influence from initial stresses on the torsional stiffness.
The Green-Lagrange strain in connection with the linear displacement field is well-suited for a buckling analysis because it would contain all the possible combinations of second order terms in an energy formulation. On the other hand a postbuckling analysis would suffer because the quadratic terms of the normal strain are not complete.
Finally the fully nonlinear Lagrangian normal strain would be the one to use for a buckling and postbuckling analysis. This strain formulation contains all the terms which can lead to a sufficiently good description of the instability phenomen. A weakness of this normal strain is the amount of terms and thereby adding an undesirable difficulty in the formulation.
According to these observations it would be preferable to develop a strain measure which in a simple but consistent way leads to a stability formulation which is usable for buckling as well as postbuckling analysis.

The preliminary investigations and considerations are now used to establish a strain measure which contains the necessary terms in order to establish a consistent stability theory. The strain measure is formulated by use of a mixing between the two definitions of the normal strain given in (4.13) and (4.14). The small strain definition in (4.14) is extended in order to incorporate the effect of twist, i.e. it is assumed that the normal strain distribution can be expressed by

$$\epsilon(x_\gamma, s) \;=\; \varepsilon_c \;-\; (x_\beta - a_\beta) e_{\beta\alpha}\, \kappa_\alpha \;+\; \frac{1}{2}\,(x_\alpha - a_\alpha)\,(x_\alpha - a_\alpha)\,\kappa_3\,\kappa_3 \tag{4.15}$$

A similar normal strain has also been suggested by Hong Chen & Blandford (1991) who by presuming small strains developed a large-displacement theory for beams.

By use of this normal strain it is the aim to establish the constitutive equations for thin-walled beams where the initial geometrical quantities ε_j^0 and κ_j^0 as well as the initial internal forces N_j^0 and M_j^0 are accounted for in a consistent way.

4.3.2 Shear Strain

In case of a kinematical approach for the shear strain the Green-Lagrange tensor and the small strain lead to identical expressions. The shear strain $\epsilon_\alpha(s_0)$ is defined by

$$\epsilon_\alpha \;=\; E_{\alpha 3} + E_{3\alpha} \;=\; \frac{\partial \mathbf{r}}{\partial x_3} \cdot \frac{\partial \mathbf{r}}{\partial x_\alpha} \;=\; \frac{\partial \mathbf{r}}{\partial x_3} \cdot \mathbf{e}_\alpha \tag{4.16}$$

Using this definition directly would lead to an unsatisfactory distribution. Therefore the shear strain is not discussed further in this section, but instead a detailed discription, where a statical approach is used, is given in the next section.

4.4 Constitutive Equations for Thin-Walled Beams

In this section the constitutive equations for thin-walled beams are formulated by use of the normal strain given by (4.15) and the energy approach described in Section 4.2.

The definition of the normal strain in (4.15) is extended in order to incorporate the warping effect, characteristic of thin-walled beams. Warping of the cross-section is described by the St. Venant warping function $\omega(x_\gamma)$ Vlasov (1961) and leads to both axial and shear strains. The intensity of warping is described by the generalized displacement $\theta(s_0)$ introduced in Section 2.2.1 and the corresponding generalized deformation is $d\theta/ds_0$. In the coupling coefficient between extension and torsion the warping effect is not incorporated. This is in accordance with the literature on this subject where it is found that the warping contribution is negligible for thin-walled cross-sections, Krenk (1983).

According to this it is assumed that the normal strain distribution can be expressed by

$$\epsilon(x_\gamma, s) \;=\; \varepsilon_c \;-\; (x_\beta - c_\beta) e_{\beta\alpha}\, \kappa_\alpha \;-\; \omega\, \frac{d\theta}{ds_0} \;+\; \frac{1}{2}\,(x_\alpha - a_\alpha)\,(x_\alpha - a_\alpha)\,\kappa_3\,\kappa_3 \tag{4.17}$$

where the generalized strain in the elastic center $\varepsilon_c(s_0)$ is given by

$$\varepsilon_c(s_0) \;=\; \varepsilon_3 \;-\; (c_\beta - a_\beta)\, e_{\beta\alpha}\, \kappa_\alpha \tag{4.18}$$

The elastic center is determined by demanding that extension and bending uncouples in energy sense, i.e.

$$\int_A \varepsilon_c\, E\,(x_\beta - c_\beta)\, e_{\beta\alpha}\, \kappa_\alpha \; dA \;=\; 0 \tag{4.19}$$

leading to a condition concerning the weighted static moment

$$\int_A E\,(x_\alpha - c_\alpha)\, dA \;=\; 0 \tag{4.20}$$

Before proceeding with the shear strain $\epsilon_\alpha(x_\alpha, s_0)$, it is important to define the warping function $\omega(x_\gamma)$ precisely. In the straight beam theory the St. Venant problem of uniform torsion defines a unique shear strain distribution $\tilde{\gamma}_\alpha(x_\beta)$ over the cross-section. Setting the warping displacement θ equal to the twist κ_3, i.e

$$\kappa_3 \;-\; \theta \;=\; 0 \tag{4.21}$$

corresponds to homogeneous torsion, see e.g. Vlasov (1961). Within infinitesimal strain theory this is expressed by the normalized St. Venant shear strain by

$$\tilde{\gamma}_\alpha(x_\beta) \;=\; -\frac{\partial \omega}{\partial x_\alpha} \;-\; e_{\alpha\beta}\,(x_\beta - a_\beta) \tag{4.22}$$

It follows that a unique determination of $\tilde{\gamma}_\alpha(x_\beta)$ requires specification of a_α and an additive constant. These constants can be determined by the condition that $\omega(x_\gamma)$ is orthogonal to the two remaining linear terms of (4.17) in energy sense, i.e.

$$\int_A \left(\varepsilon_c \;-\; (x_\beta - c_\beta) e_{\beta\alpha}\, \kappa_\alpha\right) E\, \omega \; dA \;=\; 0 \tag{4.23}$$

leading to the two conditions

$$\int_A E\,\omega\,dA = 0 \quad , \quad \int_A E\,(x_\alpha - a_\alpha)\,\omega\,dA = 0 \tag{4.24}$$

Note that, by these energy approaches, the integrations are weighted with the modulus of elasticity as the integration in (4.20). This means that an nonhomogeneous axial modulus is incorporated in the determination of the characteristic points. These conditions define the point a_α as a characteristic of the cross-section. In the following, a_α will be referred to as the shear center of the cross-section. The reason for this terminology is that the shear stress distribution $G\tilde{\gamma}_\alpha$ from torsion must be supplemented with a shear stress distribution corresponding to a resulting shear force, and their contributions to the strain energy become additive when the shear resultant acts through the point a_α. The present definition of the shear center is a restatement of the *least energy* definition of Trefftz (1935).

The shear strain measure briefly mentioned in Section 4.2.2 is now extended in order to incorporate the warping effect. The shear strain $\epsilon_\alpha(x_\gamma, s)$ is initially assumed to be proportional to $\varepsilon_\alpha(s_0)$ and the St. Venant shear strain $\tilde{\gamma}_\alpha(x_\gamma)\kappa_3(s_0)$

$$\epsilon_\alpha(x_\gamma, s) = \varepsilon_\alpha + \tilde{\gamma}_\alpha\,\kappa_3 \tag{4.25}$$

The two terms on the right side can each be associated with a characteristic type of loading. The first term corresponds to a transverse force on the cross-section and the second one represents the St. Venant solution of a homogeneous torsion problem. While the second term represents an exact solution to a problem of three-dimensional elasticity the first one is an approximation. However the contribution from the tranverse force can be improved by demanding that the corresponding part of the shear strain is proportional to a shear force N_β.

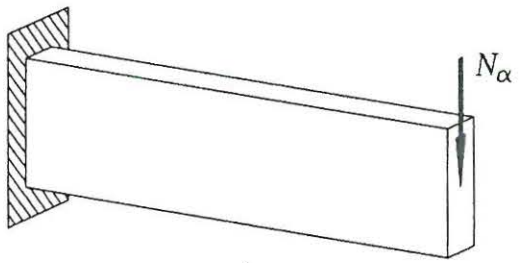

Fig. 4.2: Transverse endforce N_α on cantilever beam.

The shear force problem then consists in finding the shear stress distribution and the shear flexibility for an elastic beam loaded by a transverse force N_α at one end as indicated in Fig. 4.2. When the shear stress distribution is required to be independent of the axial coordinate the solution is unique, see e.g. Love (1944). This unique shear stress distribution can be written in the form

$$\sigma_\alpha(x_\gamma) = \sigma_\alpha^\beta(x_\gamma)\,\frac{N_\beta}{A} \tag{4.26}$$

in which the shear stress distribution functions $\sigma_\alpha^\beta(x_\gamma)$ depend on the cross-section geometry

and material parameters. Returning for a moment to the constant part of the shear strain in (4.25) ε_α, this part must be proportional to the shear force, thus implying a relation of the form

$$\varepsilon_\alpha \;=\; D_{\alpha\beta}\, N_\beta \tag{4.27}$$

where $D_{\alpha\beta}$ is the shear flexibility tensor which incorporates the actual stress distribution over the cross-section. The corresponding shear strain energy as defined in (4.1) is then given by

$$\frac{1}{2}\, N_\alpha\, D_{\alpha\beta}\, N_\beta \;=\; \int_A \frac{1}{2G}\, \sigma_\alpha\, \sigma_\alpha \; dA \tag{4.28}$$

and substitution of (4.26) leads to an expression for the shear flexibility tensor

$$D_{\alpha\beta} \;=\; \frac{1}{A^2} \int_A \frac{1}{G}\, \sigma_\gamma^\alpha\, \sigma_\gamma^\beta \; dA \tag{4.29}$$

This definition of the shear flexibility consistently accounts for tensor properties and a nonhomogeneous shear modulus. The full boundary value problem for the shear stress distribution functions $\sigma_\alpha^\beta(x_\gamma)$ can only be solved explicit in a few simple cases. An approximate solution is given by Krenk (1985) and in another paper Krenk (1989) the relation between the typical shear stiffness GA and the matrix $D_{\alpha\beta}^{-1}$ is compared.

Table 4.2: Cross-section parameters.

F	$=$	$\int_A E \; dA$	weighted area
$I_{\alpha\beta}$	$=$	$\int_A e_{\alpha\gamma}(x_\gamma - c_\gamma) e_{\beta\eta}(x_\eta - c_\eta) \; E \; dA$	weighted moment of inertia
K	$=$	$\int_A \tilde{\gamma}_\alpha(x_\gamma)\, \tilde{\gamma}_\alpha(x_\gamma) \; G \; dA$	weighted torsional stiffness
I_ω	$=$	$\int_A \omega^2(x_\gamma) \; E \; dA$	weighted warping stiffness
r_a^2	$=$	$F^{-1} \int_A (x_\alpha - a_\alpha)(x_\alpha - a_\alpha) \; E \; dA$	radius of gyration
R_a^4	$=$	$F^{-1} \int_A \big((x_\alpha - a_\alpha)(x_\beta - a_\beta)\big)^2 \; E \; dA$	
$I_{\omega r^2}$	$=$	$\int_A \omega(x_\gamma)(x_\alpha - a_\alpha)(x_\alpha - a_\alpha) \; E \; dA$	
β_α	$=$	$\frac{1}{2} I_{\alpha\beta}^{-1} \int_A e_{\beta\eta}(x_\eta - c_\eta)(x_\gamma - a_\gamma)^2 \; E \; dA$	

The strain energy can now be expressed by the generalized deformations by inserting the normal strain (4.15) and the shear strain in (4.1). The shear strain contribution is split into a contribution from the homogeneous torsion and one from the shear force determined directly from (4.27) and (4.28). It follows that

$$W = \frac{1}{2}\varepsilon_\alpha D^{-1}_{\alpha\beta}\varepsilon_\beta + \int_A \left\{ \frac{1}{2}\kappa_3 \tilde{\gamma}_\alpha G \tilde{\gamma}_\alpha \kappa_3 + \frac{1}{2}E\Big(\varepsilon_c - (x_\beta - c_\beta)e_{\beta\alpha}\kappa_\alpha - \omega(x_\gamma)\frac{d\theta}{ds_0} + \frac{1}{2}(x_\alpha - a_\alpha)(x_\alpha - a_\alpha)\kappa_3\kappa_3\Big)^2 \right\} dA \tag{4.30}$$

Performing the area integrations means that the strain energy can be expressed in terms of the cross-section parameters of Table 4.2.

$$W = \frac{1}{2}\Big(\varepsilon_\alpha D^{-1}_{\alpha\beta}\varepsilon_\beta + \varepsilon_c F \varepsilon_c + \kappa_\alpha I_{\alpha\beta}\kappa_\beta + \kappa_3 K \kappa_3 + \frac{d\theta}{ds_0} I_\omega \frac{d\theta}{ds_0}\Big) + \frac{1}{2}\Big(\varepsilon_c r_a^2 F + 2\kappa_\alpha I_{\alpha\eta}\beta_\eta\Big)\kappa_3\kappa_3 - \frac{1}{2} I_{\omega r^2}\kappa_3\kappa_3\frac{d\theta}{ds_0} + \frac{1}{2}R_a^4 F\Big(\tfrac{1}{2}\kappa_3\kappa_3\Big)^2 \tag{4.31}$$

In the present the first variation of (4.31) corresponds to the integrand in (2.10) expanded by the warping contribution, i.e.

$$\delta W = \delta\varepsilon_j \frac{\partial W}{\partial \varepsilon_j} + \delta\kappa_j \frac{\partial W}{\partial \kappa_j} + \delta\theta \frac{\partial W}{\partial\left(\frac{d\theta}{ds_0}\right)} \tag{4.32}$$

and it follows in accordance with (4.5) that

$$N_j = \frac{\partial W}{\partial \varepsilon_j} \quad , \quad M_j = \frac{\partial W}{\partial \kappa_j} \quad , \quad B = \frac{\partial W}{\partial\left(\frac{d\theta}{ds_0}\right)} \tag{4.33}$$

where B is the bimoment.
The internal forces are hereby expressed by the derivatives of the elastic energy with respect to their corresponding deformations. The increments of the internal forces (N_j, M_j, B) can now be expressed in terms of the generalized deformations $(\varepsilon_j, \kappa_j, d\theta/ds_0)$ by use of (4.31) and (4.33). It should be noticed that the generalized strain ε_c is used instead of ε_3 which means that derivatives with respect to ε_c and κ_α lead to the normal force and the bending moments corresponding to the elastic center respectively.

The shear force is given by

$$N_\alpha(s_0) = D^{-1}_{\alpha\beta}\varepsilon_\beta \tag{4.34}$$

and the normal force

$$N_3(s_0) = F\,\varepsilon_c + \tfrac{1}{2}\,r_a^2 F\,\kappa_3\kappa_3 \tag{4.35}$$

The bending moments corresponding to axes through the elastic center (c_1, c_2)

$$M_\alpha^c(s_0) = I_{\alpha\beta}\kappa_\beta + \beta_\eta I_{\eta\alpha}\kappa_3\kappa_3 \tag{4.36}$$

The generalized St. Venant torsional moment is given by

$$M_3(s_0) = K\kappa_3 + r_a^2 F\varepsilon_c\,\kappa_3 + 2\beta_\eta I_{\eta\alpha}\kappa_\alpha\,\kappa_3 - I_{\omega r^2}\,\kappa_3\,\frac{d\theta}{ds_0} + \tfrac{1}{2}\,R_a^4 F\kappa_3\,\kappa_3\,\kappa_3 \tag{4.37}$$

and finally the bimoment

$$B(s_0) = I_\omega\,\frac{d\theta}{ds_0} - \tfrac{1}{2}\,I_{\omega r^2}\,\kappa_3\,\kappa_3 \tag{4.38}$$

Observing equations (4.34-4.38) it follows that if the generalized deformations approach zero the internal forces likewise approach zero. This means fulfilment of a requirement stating that a rigid body motion does not create a change in the internal forces. Further notice that the two relatively unknown cross-sectional parameters $I_{\omega r^2}$ and R_a^4 appears in the equations for the torsional moment and the bimoment. Both parameters are also found in Krenk (1983) where a pretwisted elastic beam is considered. As it appears these new parameters arise as a consequence of the nonlinear contribution from the twist.

The relation in (4.21) which connects the warping displacement θ to the rotation vector can be used to derive an alternative expression for the torsional moment, which incorporates the effect from warping. This is of particular interest because in Chapter 8 an analytical analysis of the buckling and initial postbuckling behavior is performed using only the rotation vector as displacement function.
Substitution of (4.21) into the elastic energy (4.31) and taking the first variation with respect to κ_3 leads to the torsional moment $M_3^*(s_0)$

$$M_3^*(s_0) = K\kappa_3 - \frac{d}{ds_0}\left(I_\omega\,\frac{d\kappa_3}{ds_0}\right) + r_a^2 F\varepsilon_c\,\kappa_3 + 2\beta_\eta I_{\eta\alpha}\kappa_\alpha\,\kappa_3 + \tfrac{1}{2}\,R_a^4 F\kappa_3\,\kappa_3\,\kappa_3 \tag{4.39}$$

whereby it follows that

$$M_3^* = M_3 - \frac{dB}{ds_0} \tag{4.40}$$

It appears that the torsional moment is made up by a contribution from a generalized St. Venant moment and one from nonhomogeneous warping. The analysis of M_3^* is not taken further in this chapter and M_3^* will first be used in Chapter 7.

The internal forces related to the elastic center and the shear center, respectively, are shown in Fig. 4.3.

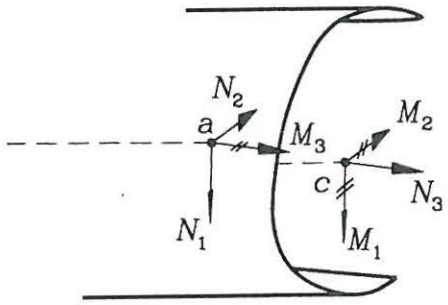

Fig. 4.3: Cross-section with internal forces and moments.

The constitutive equations can be split into three contributions corresponding to a linear, quadratic and a third order dependency on the generalized displacements.

$$\begin{bmatrix} N_\alpha \\ N_3 \\ M_\alpha^c \\ M_3 \\ B \end{bmatrix} = \begin{bmatrix} D_{\alpha\beta}^{-1} & 0 & 0 & 0 & 0 \\ 0 & F & 0 & \frac{1}{2} r_a^2 F \kappa_3 & 0 \\ 0 & 0 & I_{\alpha\beta} & \beta_\eta I_{\eta\alpha} \kappa_3 & 0 \\ 0 & r_a^2 F \kappa_3 & 2\beta_\eta I_{\eta\beta} \kappa_3 & K + \frac{1}{2} R_a^4 F \kappa_3^2 & -I_{\omega r^2} \kappa_3 \\ 0 & 0 & 0 & -\frac{1}{2} I_{\omega r^2} \kappa_3 & I_\omega \end{bmatrix} \begin{bmatrix} \varepsilon_\beta \\ \varepsilon_c \\ \kappa_\beta \\ \kappa_3 \\ \dfrac{d\theta}{ds_0} \end{bmatrix} \tag{4.41}$$

The quadratic terms in (4.41) represent the coupling while the linear and third order terms represent the diagonal terms. The linear terms in the constitutive equations are recognized from the infinitesimal strain theory, Vlasov (1961). The coupling between extension and torsion is expressed by the nonlinear terms in the respective constitutive equations. It follows from (4.35) and (4.36) that the coupling between pure extension and torsion is expressed by the radius of gyration while the coupling between bending and torsion is expressed by the geometric parameter β_α. β_α arises for non-symmetric cross-sections and defines a characteristic length in the plane of the cross-section.

Expressing the constitutive equations in an incremental form leads to

$$\begin{bmatrix} dN_\alpha \\ dN_3 \\ dM_\alpha^c \\ dM_3 \\ dB \end{bmatrix} = \begin{bmatrix} D_{\alpha\beta}^{-1} & 0 & 0 & 0 & 0 \\ & F & 0 & r_a^2 F \kappa_3 & 0 \\ & & I_{\alpha\beta} & 2\beta_\eta I_{\eta\alpha} \kappa_3 & 0 \\ & SYM & & K + r_a^2 F \varepsilon_c + 2\beta_\eta I_{\eta\beta} \kappa_\beta - I_{\omega r^2} \frac{d\theta}{ds_0} + \frac{3}{2} R_a^4 F \kappa_3^2 & -I_{\omega r^2} \kappa_3 \\ & & & & I_\omega \end{bmatrix} \begin{bmatrix} d\varepsilon_\beta \\ d\varepsilon_c \\ d\kappa_\beta \\ d\kappa_3 \\ d\dfrac{d\theta}{ds_0} \end{bmatrix} \tag{4.42}$$

Note that the incremental form is symmetric which insures that internal virtual work can be integrated to yield the elastic part of the potential energy.

4.5 Updated Constitutive Equations

It is pointed out in Section 4.3 that initial deformations and stresses influence the constitutive equations. In this section an updated form of the constitutive equations for thin-walled beams is presented which in a consistent way incorporates effects from the initial state. Due to the transition from the initial state into a buckled state changes in the generalized deformations arise. The increments in the strain $\varepsilon_j^1(s_0)$, curvature $\kappa_j^1(s_0)$ and the warping deformations $d\theta^1/ds_0$ components are defined by

$$\varepsilon_j^1(s_0) = \varepsilon_j - \varepsilon_j^0 \quad , \quad \kappa_j^1(s_0) = \kappa_j - \kappa_j^0 \quad , \quad \frac{d\theta^1(s_0)}{ds_0} = \frac{d\theta}{ds_0} - \frac{d\theta^0}{ds_0} \tag{4.43}$$

The influence from initial curvatures and stresses on the constitutive equations for the prismatic beam has only been discussed briefly in Section 4.1. The warping contribution is also influenced by initial curvatures and therefore some considerations regarding this part have to be performed. At this point it is assumed that only the influence from a pretwist $\kappa_3^0 \neq 0$ is significant. This assumption corresponds to neglecting coupling between bending and torsion caused by warping. When a beam is pretwisted the strain measure has to be modified because the warping function ω rotates with the section, Krenk (1982,1983). The normal strain in (4.17) has to be modified according to this dependency of the warping function on the axial coordinate, i.e

$$\begin{aligned} \epsilon(x_\gamma, s) &= \varepsilon_c - (x_\beta - c_\beta) e_{\beta\alpha}\, \kappa_\alpha - \frac{\partial \omega}{\partial s_0}\,\theta - \omega\,\frac{d\theta}{ds_0} \\ &\quad + \frac{1}{2}\,(x_\alpha - a_\alpha)\,(x_\alpha - a_\alpha)\,\kappa_3\,\kappa_3 \end{aligned} \tag{4.44}$$

Accounting for the pretwist κ_3^0 means that the change of $\omega(x_\gamma, s_0)$ with s_0 is determined by the partial derivative

$$\frac{\partial \omega}{\partial s_0} = -\,\kappa_3^0\,\frac{\partial \omega}{\partial x_\alpha}\, e_{\alpha\gamma}\,(x_\gamma - a_\gamma) \tag{4.45}$$

Substitution of $\partial\omega/\partial x_\alpha$ from (4.22) leads to

$$\frac{\partial \omega}{\partial s_0} = \tilde{\gamma}_\alpha\, e_{\alpha\beta}\,(x_\beta - a_\beta)\,\kappa_3^0 + (x_\alpha - a_\alpha)(x_\alpha - a_\alpha)\,\kappa_3^0 \tag{4.46}$$

The change in distribution of the shear strains and the normal strain can be expressed by the increments of the generalized deformations by inserting (4.43) in (4.25) and (4.44), respectively . It follows that the increment in the shear strain distribution is given by

$$\epsilon_\alpha - \epsilon_\alpha^0 = \varepsilon_\alpha^1 + \tilde{\gamma}_\alpha\,\kappa_3^1 \tag{4.47}$$

where the same considerations as in section 4.4, regarding the first part of the right side, are in place. By substitution of (4.46) into (4.44) the increment in the normal strain is given by

$$\begin{aligned}\epsilon_3 - \epsilon_3^0 &= \varepsilon_c^1 - (x_\beta - c_\beta)\, e_{\beta\alpha}\, \kappa_\alpha^1 - \omega \frac{d\theta^1}{ds_0} + \frac{1}{2}(x_\alpha - a_\alpha)(x_\alpha - a_\alpha)\, \kappa_3^1 \kappa_3^1 \\ &\quad + \kappa_3^0 (x_\alpha - a_\alpha)(x_\alpha - a_\alpha)\, (\kappa_3^1 - \theta^1) - \kappa_3^0 \tilde{\gamma}_\alpha\, e_{\alpha\gamma}\, (x_\gamma - a_\gamma)\, \theta^1 \end{aligned} \tag{4.48}$$

The last term of (4.48) which is proportional to κ_3^0 is for simplicity assumed to be negligible compared to the other terms. Recalling the identity $\kappa_3 = \theta$ from (4.21) it follows that the first term in second line of (4.48) vanishes which means that (4.48) can be simplified into

$$\epsilon_3 - \epsilon_3^0 = \varepsilon_c^1 - (x_\beta - c_\beta)\, e_{\beta\alpha}\, \kappa_\alpha^1 - \omega \frac{d\theta^1}{ds_0} + \frac{1}{2}(x_\alpha - a_\alpha)(x_\alpha - a_\alpha) \kappa_3^1 \kappa_3^1 \tag{4.49}$$

The incremental strain measure is identical to the strain measure if the initial deformations are zero, meaning that requirement regarding rigid body motions is fulfilled. This was accomplished by the modification of the warping contribution. From (4.48) it follows that initial curvatures only appear indirectly through the increments in the generalized deformations, as indicated by the relations in (3.10) and (3.11).

In order to incorporate the initial stress terms some assumptions are made regarding the initial stress distribution $\sigma_j^0(x_\alpha, s_0)$. Assuming that the initial deformations and the initial internal forces are related only through the linear terms of (4.41) means that the shear stress σ_α^0 is given by

$$\sigma_\alpha^0 = \sigma_\alpha^\beta \frac{N_\beta^0}{A} + \tilde{\gamma}_\alpha\, G \frac{M_3^0}{K} \tag{4.50}$$

In case of the normal stress σ_3^0 the contribution from an initial bimoment is neglected which leads to

$$\sigma_3^0 = E\left(\frac{N_3^0}{F} - (x_\beta - c_\beta)\, e_{\beta\alpha}\, I_{\alpha\gamma}^{-1}\, M_\gamma^{c^0}\right) \tag{4.51}$$

The change in elastic energy can now be expressed in terms of the generalized deformations by integration of (4.4).

$$\begin{aligned} W - W^0 &= N_\alpha^0 \varepsilon_\alpha^1 + N_3^0 \varepsilon_c^1 + M_\alpha^{c^0} \kappa_\alpha^1 + M_S^0 \kappa_3^1 \\ &\quad + \frac{1}{2}\Big[\varepsilon_\alpha^1 D_{\alpha\beta}^{-1} \varepsilon_\beta^1 + \varepsilon_c^1 F \varepsilon_c^1 + \kappa_\alpha^1 I_{\alpha\beta} \kappa_\beta^1 + \kappa_3^1 (K + r_a^2 N_3^0 + 2\beta_\alpha M_\alpha^{c^0}) \kappa_3^1 \\ &\quad + \frac{d\theta^1}{ds_0} I_\omega \frac{d\theta^1}{ds_0} + \left(\varepsilon_c^1 F r_a^2 + 2\kappa_\alpha^1 I_{\alpha\eta} \beta_\eta - \frac{d\theta^1}{ds_0} I_{\omega r^2}\right) \kappa_3^1 \kappa_3^1 + R_a^4 F \left(\tfrac{1}{2} \kappa_3^1 \kappa_3^1\right)^2 \Big] \end{aligned}$$

(4.52)

Comparing (4.52) with the corresponding expression without initial stresses (4.31) shows, as expected, that the only change appears in a modified torsional rigidity.

The increments of the internal forces N_j^1, M_j^1 and B^1 can now be expressed by the increments of the generalized deformations by use of the relations in (4.33) together with (4.52).

$$\begin{bmatrix} N_\alpha^1 \\ N_3^1 \\ M_\alpha^{c\,1} \\ M_3^1 \\ \\ B^1 \end{bmatrix} = \begin{bmatrix} D_{\alpha\beta}^{-1} & 0 & 0 & 0 & 0 \\ 0 & F & 0 & \frac{1}{2}r_a^2 F\kappa_3^1 & 0 \\ 0 & 0 & I_{\alpha\beta} & \beta_\eta I_{\eta\gamma}\kappa_3^1 & 0 \\ 0 & r_a^2 F\kappa_3^1 & 2\beta_\eta I_{\eta\beta}\kappa_3^1 & K + r_a^2 N_3^0 + 2\beta_\alpha M_\alpha^{c\,0} & -I_{\omega r^2}\kappa_3^1 \\ & & & + \frac{1}{2}R_a^4 F {\kappa_3^1}^2 & \\ 0 & 0 & 0 & -\frac{1}{2}I_{\omega r^2}\kappa_3^1 & I_\omega \end{bmatrix} \begin{bmatrix} \varepsilon_\beta^1 \\ \varepsilon_c^1 \\ \kappa_\beta^1 \\ \kappa_3^1 \\ \\ \dfrac{d\theta^1}{ds_0} \end{bmatrix}$$

(4.53)

The only direct change caused by initial stresses is concerned with the torsional moment. This additional term is the well-known modification in the torsional rigidity according to coupling between tension and torsion. This means that the constitutive equations from section 4.4 only have to be modified in the torsional stiffness in order to incorporate initial stresses. From (4.53) it is evident that the linear part is symmetric in the total formulation while the nonlinear part adopts the symmetri only in the incremental form as in Section 4.4.

4.6 Conclusions

As it may appear from the previous sections the subject *constitutive equations for beam structures* is a very delicate area if a nonlinear formulation is to be obtained.

It has been shown that by a procedure where a small strain deformation measure and the corresponding Lagrangian strain components are compared a satisfactory deformation measure is obtained by a mixing of those two, whereby a consistent set of constitutive equations for thin-walled beams are derived. The developed constitutive equations are appropriate for the initially straight beam as well as the initially curved beam. In a updated version of the constitutive equations it is found that the torsional stiffness is influenced by the presence of axial stresses.

The updated constitutive equations together with the weak formulation of the stability equation from Section 3.2 form a complete and consistent stability theory usable for thin-walled beams with arbitrary cross-sections.

Chapter 5

Potential Energy

In Section 2.2 the vectorial equilibrium equations were reformulated into a scalar function by the principles of the virtual work. The virtual work equation corresponds to the first variation of the potential energy, i.e. demanding stationarity of the potential energy corresponds to the virtual work, Washizu (1974). This relationship indicates that the potential energy can be found by integration of the virtual work equation.
In the present formulation the integration process from virtual work into potential energy is impeded because in general the virtual rotation $\delta\varphi$ does not correspond to an exact differential, as mentioned in Chapter 2. It turns out that the integration in case of the beam problem, i.e. no initial stress terms, can be performed in a straight-forward way while in case of the stability problem the integration is more complex. In the stability problem the integration can only be performed consistently by fulfilment of the conditions associated with the definition of the rotation tensor.
The subject of Section 5.2 is to identify the necessary relations in order to perform the integration in a consistent way. Finally in Section 5.3 the potential energy is given according to the conditions stated in Section 5.2.

5.1 Energy Principles

Energy principles were briefly touched in Section 4.3 by introducing the strain energy function. The term *energy method* is often used in connections where an energy functional, i.e a scalar function, is used to derive vector equations expressing some kind of equilibrium condition. This relationship is a restatement of a criterion where a stationary value of the potential energy with respect to a set of generalized coordinates is necessary and sufficient for the equilibrium of the system, Budiansky (1974).
In general using the energy methods in structural analysis an assumption is that the potential energy of the structural system is defined by a strain energy potential and a load potential. The strain components appearing in the strain energy are commonly expressed by a set of generalized displacements which means that the state variables to be used in an energy approach are these generalized displacements. The potential energy of the structural system is then considered to be a functional of the generalized displacements, but it is also presumed dependent of the load scalar variable λ, which defines the magnitude of prescribed external loads on the system. By variational principles the equilibrium equations for the system can then be found by demanding stationarity of the potential energy, Washizu (1974).

This procedure gives the possibility of using different displacement fields and strain measures in the energy functional, as mentioned in Section 4.1. In some cases blind use of the energy method may therefore be inconsistent. This is not only because of the different possibilities in kinematical behavior, but also because symmetry assumptions used in the establishment of the energy functional may only be fulfilled in special cases. An example of this is given in Section 5.2 where the necessary conditions allowing integration of the virtual work are examined. Therefore the energy method has to be used in a way which suites the problem at hand in the best possible way.

5.2 Virtual Work/Potential Energy

The virtual work equation (3.17) consists of terms which are associated with internal deformations *shear-extension-bending-torsion* and terms arising from initial stresses and loads. Integration of the first part leads to identification of the elastic energy potential W as already mentioned in Section 4.3 and integration of the stress terms leads to the load potential Π_p. Adding the warping contribution, developed in Section 2.2.1 to (3.17) and substitution of the constitutive equations from Section 4.5 leads to the virtual work equation for thin-walled beams.

$$
\begin{aligned}
\int_0^l \Big\{ & \delta\varepsilon_\alpha D^{-1}_{\alpha\beta}\varepsilon^1_\beta + \delta\varepsilon_c F \varepsilon^1_c + \delta\kappa_\alpha I_{\alpha\beta}\kappa^1_\beta + \delta\kappa_3 \left(K + r_a^2 N_3^0 + 2\beta_\alpha M_\alpha^{c^0}\right)\kappa^1_3 \\
& + \frac{d\delta\theta}{ds_0} I_\omega \frac{d\theta^1}{ds_0} + \frac{1}{2}\delta\varepsilon_c r_a^2 F \kappa^1_3\kappa^1_3 + \delta\kappa_3 r_a^2 F \varepsilon^1_c \kappa^1_3 + \delta\kappa_\alpha \beta_\eta I_{\eta\alpha}\kappa^1_3\kappa^1_3 \\
& + \delta\kappa_3 2\beta_\eta I_{\eta\alpha}\kappa^1_\alpha\kappa^1_3 - \delta\kappa_3 I_{\omega r^2}\kappa^1_3\frac{d\theta^1}{ds_0} - \frac{1}{2}\frac{d\,\delta\theta}{ds_0} I_{\omega r^2}\kappa^1_3\kappa^1_3 + \frac{1}{2}\delta\kappa_3\kappa^1_3 R_a^4 F \kappa^1_3\kappa^1_3 \\
& - \delta\varepsilon_j N^0_l \tilde{A}_{lj} - \delta\kappa_j M^0_l \tilde{A}_{lj} - \delta\varphi_l e_{lnk}\left(\tilde{A}_{n3} + \varepsilon_j A_{nj} - \varepsilon^0_n\right) N^0_k \\
& - \lambda\,\delta r_{a_l} p^0_l - \delta\varphi_l e_{lnk}\left(\tilde{A}_{n\alpha} + \lambda A_{n\alpha}\right) f^0_\alpha p^0_k - \lambda\,\delta\theta\, b^0 \Big\}\, ds_0 \\
& - \left[\delta r_{a_l}\sum_{i=1}^{n}\left(\lambda P^{0i}_l\right) + \delta\varphi_k e_{kln}\sum_{i=1}^{n}\left(P^{0i}_n(\tilde{A}_{l\alpha} + \lambda A_{l\alpha})F^{0i}_\alpha\right)\right]_0^l = 0
\end{aligned}
\tag{5.1}
$$

The virtual work equation (5.1) can be used to examen two kinds of problems, namely the beam problem and the stability problem. The beam problem arises when the initial stress terms are eliminated and the external load is associated with the terms containing λ. Equation (5.1) has been established by introducing a set of virtual displacements $\delta\mathbf{r}_a$, $\delta\boldsymbol{\varphi}$ and $\delta\theta$. In order to perform an integration of (5.1) a relation between the virtual displacements and the increments in the state variables $\mathbf{r}^1_a$, $\boldsymbol{\varphi}^1$ and θ^1 has to be established.

Recalling the definitions of the generalized deformations it is obvious that the nonlinearity

in (5.1) mainly originates from the finite rotation tensor $\mathbf{A}$. The necessary integration conditions must therefore be closely related to the definition of this operator. In the derivation process leading to the generalized displacements the infinitesimal rotation

$$\delta \mathbf{e}_j \;=\; \delta\boldsymbol{\varphi} \times \mathbf{e}_j \tag{5.2}$$

is used. The relation in (5.2) is also used to derive the orthogonal transformation operator $\mathbf{A}$, see e.g. Appendix A, by assuming the direction of the rotation vector $\boldsymbol{\varphi}$ to be fixed as illustrated in Fig. 5.1a.

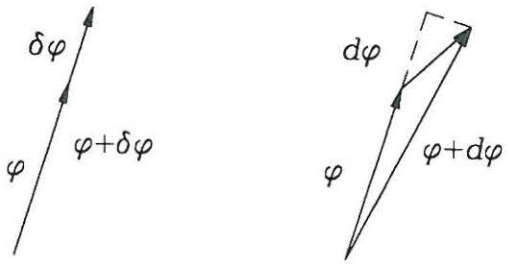

Fig. 5.1: (a) Virtual variation. (b) Increment.

The equivalent change in $\boldsymbol{\varphi}$ without assumption regarding the direction of the change $d\boldsymbol{\varphi}$ is illustrated in Fig. 5.1b. The difference is obvious and it follows that a conversion from $\delta\boldsymbol{\varphi}$ to $d\boldsymbol{\varphi}$ can in general not be performed directly. Only in the special case where the rotation vector indeed is fixed in direction the two variations are similar.

In case of the virtual translation $\delta\mathbf{r}_a$ and the virtual warping displacement $\delta\theta$ no condition was imposed meaning that relations stating that

$$\delta\mathbf{r}_a \;=\; \delta\mathbf{r}_a^1 \qquad ; \qquad \delta\theta \;=\; \delta\theta^1 \tag{5.3}$$

are consistent.

A relation between $\delta\boldsymbol{\varphi}$ and $\delta\boldsymbol{\varphi}^1$ can be obtained by a reformulation of the infinitesimal rotation in (5.2). The orientation of the beam cross-section is described by the unit vectors $\mathbf{e}_j$, i.e.

$$\mathbf{e}_j \;=\; \mathbf{A}(\boldsymbol{\varphi}^1)\cdot\mathbf{e}_j^0 \;=\; A_{lj}(\varphi_k^1\mathbf{e}_k^0)\,\mathbf{e}_l^0 \tag{5.4}$$

Substitution of (5.4) into (5.2) leads to

$$\delta\varphi_k\, e_{knl}\, A_{nj}(\varphi_m^1\mathbf{e}_m^0) \;=\; \delta A_{lj}(\varphi_m^1\mathbf{e}_m^0) \tag{5.5}$$

where the initial unit vectors $\mathbf{e}_j^0$ are considered as known functions and therefore not sensitive to variations. Introducing a new second order tensor $\mathbf{B}(\boldsymbol{\varphi})$ which is closely related to the finite rotation tensor (see e.g. in Appendix A) and rewriting leads to

$$\delta\varphi_k \;=\; \delta\varphi_j^1\, B_{kj}(\varphi_m^1\mathbf{e}_m^0) \quad ; \quad B_{kj}(\varphi_m^1\mathbf{e}_m^0) \;=\; e_{knl}\frac{\partial A_{lm}}{\partial\varphi_j}\,A_{nm} \tag{5.6}$$

Equation (5.6) contains the relation between the virtual rotations $\delta\varphi_k$ and the variations of the rotation increments $\delta\varphi_k^1$. The tensor $\mathbf{B}$ represents the dependency of the higher order terms in the rotation components.

The relations (5.3), (5.5) and (5.6) are in the following used to perform the integration of the virtual work equation. The elastic energy part and the load potential part are treated separately in the following subsections in order to preserve clearness.

5.2.1 Displacement and Deformation Relations

The internal virtual work corresponds to the first variation of the elastic energy. In Section 4.3 the elastic energy is used to obtain constitutive equations by use of energy principles. The derivation is carried out by assuming that the generalized deformations ε_j, κ_j and $d\theta/ds_0$ are the independent variables. In fact the generalized deformations are functions of the generalized displacements $\mathbf{r}_a^1$, $\boldsymbol{\varphi}^1$ and θ^1.

Extracting the internal virtual work δW from (5.1) leads to

$$\begin{aligned}
\delta W \;=\; \int_0^l \Big\{ & \delta\varepsilon_\alpha D^{-1}_{\alpha\beta}\,\varepsilon^1_\beta \;+\; \delta\varepsilon_c\, F\,\varepsilon^1_c \;+\; \delta\kappa_\alpha\, I_{\alpha\beta}\,\kappa^1_\beta \;+\; \frac{d\delta\theta}{ds_0}\, I_\omega\, \frac{d\theta^1}{ds_0} \\
& + \delta\kappa_3 \left(K + r_a^2 N_3^0 + 2\beta_\alpha M_\alpha^{c\,0}\right)\kappa_3^1 \;+\; \frac{1}{2}\,\delta\varepsilon_c\, r_a^2 F\,\kappa_3^1\kappa_3^1 \;+\; \delta\kappa_3\, r_a^2 F\,\varepsilon_c^1\,\kappa_3^1 \\
& + \delta\kappa_\alpha\,\beta_\eta I_{\eta\alpha}\,\kappa_3^1\kappa_3^1 \;+\; \delta\kappa_3\, 2\beta_\eta I_{\eta\alpha}\,\kappa_\alpha^1\,\kappa_3^1 \;-\; \delta\kappa_3\, I_{\omega r^2}\,\kappa_3^1 \frac{d\theta^1}{ds_0} \\
& - \frac{1}{2}\,\frac{d\,\delta\theta}{ds_0}\, I_{\omega r^2}\,\kappa_3^1\kappa_3^1 \;+\; \frac{1}{2}\,\delta\kappa_3\kappa_3^1\, R_a^4 F\,\kappa_3^1\kappa_3^1 \Big\}\, ds_0
\end{aligned} \tag{5.7}$$

Notice that the St. Venant stiffness is modified with the initial stress terms. According to the definitions of the generalized deformations the internal virtual work is nonlinear in the rotation components. Therefore, in order to obtain the potential energy by integration of the virtual work equation the differentability of the generalized deformations expressed by the generalized displacements will be examined in this section.

Strain Increments and Variations :

The strain increment $\varepsilon_j^1(s_0)$ is given by (4.43) and (3.10), i.e.

$$\varepsilon_j^1 \;=\; \left(\frac{dr^1_{a\,k}}{ds_0} + r^1_{a\,l}\, e_{lkn}\,\kappa_n^0\right) A_{kj}(\varphi_m^1) \;+\; \left(\delta_{3k} + \varepsilon_k^0\right)\widetilde{A}_{kj}(\varphi_m^1) \tag{5.8}$$

From (2.11) it follows that if the virtual displacements are decomposed in the initial basis the variation of the strain components can be written in component form as

$$\delta\varepsilon_j = \left(\frac{d\delta r_{a_k}}{ds_0} + \delta r_{a_l}\, e_{lkn}\, \kappa_n^0\right) A_{kj}(\varphi_m^1)$$

$$+ \left(\frac{dr_{ak}^1}{ds_0} + r_{al}^1\, e_{lkn}\, \kappa_n^0 + (\delta_{3k} + \varepsilon_k^0)\right) e_{kmp}\, \delta\varphi_m\, A_{pj}(\varphi_m^1) \tag{5.9}$$

Using the relations (5.5) and (5.3) it follows that

$$\delta\varepsilon_j = \delta\varepsilon_j^1 \tag{5.10}$$

which confirms the relation between virtual and finite variations of the strain components.

Curvature Increments and Variations :
The curvature increment $\kappa_j^1(s_0)$ can be found from (3.11) and (4.43). Using the operator $\mathbf{B}(\boldsymbol{\varphi})$ means that

$$\kappa_j^1(s_0) = \left(\frac{d\varphi_k^1}{ds_0} + \varphi_n^1\, e_{nkm}\, \kappa_m^0\right) B_{kj}(\varphi_l^1) \tag{5.11}$$

From (2.14) it follows that the variation of the curvature components is given by

$$\delta\kappa_j = \left(\frac{d\delta\varphi_k}{ds_0} + \delta\varphi_n\, e_{nkm}\, \kappa_m^0\right) A_{kj}(\varphi_l^1) \tag{5.12}$$

By substitution of (5.6) and some rearranging it can be shown that

$$\delta\kappa_j = \delta\kappa_j^1 \tag{5.13}$$

Equation (5.13) expresses the relation between virtual and finite variations of the curvature components.

Using the considerations and investigations performed above it is now possible to reformulate the internal virtual work (5.7) which allows a direct integration. Substitution of (5.10) and (5.13) leads to

$$\delta W = \delta\Bigg(\int_0^l \frac{1}{2}\Big\{ \varepsilon_\alpha^1\, D_{\alpha\beta}^{-1}\, \varepsilon_\beta^1 + \varepsilon_c^1\, F\, \varepsilon_c^1 + \kappa_\alpha^1\, I_{\alpha\beta}\, \kappa_\beta^1 + \frac{d\theta^1}{ds_0}\, I_\omega\, \frac{d\theta^1}{ds_0}$$

$$+ \kappa_3^1 \left(K + r_a^2 N_3^0 + 2\beta_\alpha M_\alpha^{c^0}\right) \kappa_3^1 + \varepsilon_c^1\, r_a^2 F\, \kappa_3^1 \kappa_3^1 + \kappa_3^1\, 2\beta_\eta I_{\eta\alpha}\, \kappa_\alpha^1 \kappa_3^1$$

$$- \frac{d\theta^1}{ds_0}\, I_{\omega r^2}\, \kappa_3^1 \kappa_3^1 + \frac{1}{4}\, \kappa_3^1 \kappa_3^1\, R_a^4 F\, \kappa_3^1 \kappa_3^1 \Big\}\, ds_0 \Bigg) \tag{5.14}$$

Equation (5.14) expresses the relation between virtual variations and finite variations which

enables integration of the internal virtual work to yield the elastic energy.

5.2.2 Initial Stress Terms and Displacement Increments

The remaining part to be examined in order to be able to perform the integration of the virtual work equation are load increments and the initial stress terms. Identifying the terms of (5.1) consisting of load increments Π_λ and initial stresses Π_σ as $\delta\Pi_P$ leads to

$$\delta\Pi_P = \delta\Pi_\lambda + \delta\Pi_\sigma \tag{5.15}$$

where

$$\begin{aligned}\delta\Pi_\lambda = -\lambda \Bigg(\int_0^l \Big\{ & \delta r_{a_l} p_l^0 + \delta\varphi_l \, e_{lnk} \, A_{n\alpha} \, f_\alpha^0 \, p_k^0 + \delta\theta \, b^0 \Big\} \, ds_0 \\ & - \Big[\delta r_{a_l} \sum_{i=1}^{n} P_l^{0i} + \delta\varphi_k \, e_{kln} \, A_{l\alpha} \sum_{i=1}^{n} \left(F_\alpha^{0i} P_n^{0i} \right) \Big]_0^l \Bigg)\end{aligned} \tag{5.16}$$

and

$$\begin{aligned}\delta\Pi_\sigma = \int_0^l \Big\{ & - \delta\varepsilon_j \, N_l^0 \, \tilde{A}_{lj} - \delta\kappa_j \, M_l^0 \, \tilde{A}_{lj} - \delta\varphi_l \, e_{lnk} \left(\tilde{A}_{n3} + \varepsilon_j A_{nj} - \varepsilon_n^0 \right) N_k^0 \\ & - \delta\varphi_l \, e_{lnk} \tilde{A}_{n\alpha} f_\alpha^0 \, p_k^0 \Big\} \, ds_0 - \Big[\delta\varphi_k \, e_{kln} \sum_{i=1}^{n} \left(P_n^{0i} \tilde{A}_{l\alpha} \, F_\alpha^{0i} \right) \Big]_0^l\end{aligned} \tag{5.17}$$

From (5.16) it follows that Π_λ is proportional to the load increment factor λ. The dependency of Π_λ on the generalized displacement increments can be analysed by use of (5.5) and (5.3). It follows that

$$\begin{aligned}\delta\Pi_\lambda = -\lambda\,\delta \Bigg(\int_0^l \Big\{ & r_{a_l}^1 p_l^0 + p_k^0 \, A_{k\alpha} \, f_\alpha^0 + b^0 \, \theta^1 \Big\} \, ds_0 \\ & - \Big[r_{a_l}^1 \sum_{i=1}^{n} P_l^{0i} + \sum_{i=1}^{n} \left(P_k^{0i} \, \tilde{A}_{k\alpha} \, F_\alpha^{0i} \right) \Big]_0^l \Bigg)\end{aligned} \tag{5.18}$$

The relation in (5.18) implies that Π_λ is linear in $r_{a_l}^1$ and nonlinear in φ_l^1. Further it follows that the integration of Π_λ can be performed in a direct way.

The potential Π_σ is proportional to the initial stresses and it follows that its dependency on $r_{a_l}^1$ is kept in the strain components while the rotation components φ_l^1 appear in different connections. The dependency on the generalized displacements can be given a closer analysis by substitution of (5.5), (5.3), (5.10) and (5.13).

$$\begin{aligned}\delta\Pi_\sigma = \int_0^l \Big\{ & - \delta\left(\varepsilon_j^1 \, N_l^0 \, \tilde{A}_{lj} \right) + \delta\tilde{A}_{kn} \, \tilde{A}_{jn} \left(N_k^0 (\delta_{j3} + \varepsilon_j^0) + p_k^0 \, \delta_{j\alpha} f_\alpha^0 \right)\end{aligned}$$

$$- \delta\kappa_j^1 \, M_l^0 \, \tilde{A}_{lj} \Big\} \, ds_0 \; + \; \Big[\delta\tilde{A}_{kn} \sum_{i=1}^{n} \left(P_k^{0i} \, F_\alpha^{0i} \right) \tilde{A}_{\alpha n} \Big]_0^l \tag{5.19}$$

A closer analysis of (5.19) indicates that the term associated with the strain components can be integrated directly while integration of the remaining part is more complex. Several attempts have been tried but it has not been possible to perform a direct integration of the last term in (5.19). Instead an alternative integration process has to be used where direct integration of the quadratic terms is carried out and integration of higher-order terms is performed by assuming the rotation vector to be fixed in direction.

Introducing the linearized generalized deformations $\tilde{\varepsilon}_j^1$ and $\tilde{\kappa}_j^1$ by

$$\tilde{\varepsilon}_j^1 \;=\; \left(\frac{dr_{aj}^1}{ds_0} + r_{al}^1 \, e_{ljn} \, \kappa_n^0 \right) \; + \; \varphi_n^1 \, e_{njl} \left(\delta_{3l} + \varepsilon_l^0 \right) \tag{5.20}$$

and

$$\tilde{\kappa}_j^1 \;=\; \frac{d\varphi_j^1}{ds_0} \; + \; \varphi_n^1 \, e_{njm} \, \kappa_m^0 \tag{5.21}$$

The linear form in (5.20) arises when the infinitesimal rotation tensor $\boldsymbol{\Omega}(\boldsymbol{\varphi}^1)$ is used instead of the finite rotation tensor $\mathbf{A}(\boldsymbol{\varphi}^1)$.

Extracting the linear part of (5.17) leads to the first variation of the linear load potential Π_σ^{lin}

$$\begin{aligned} \delta\Pi_\sigma^{lin} \;=\; & \int_0^l \Big\{ \delta\left(\tilde{\varepsilon}_j^1 \, e_{jnl} \, N_l^0 \, \varphi_n^1 \right) \; + \; \delta\tilde{\kappa}_j^1 \, e_{jnl} \, M_l^0 \, \varphi_n^1 \\ & + \delta\varphi_l^1 \, e_{lnk} \left(N_k^0 \left(\delta_{j3} + \varepsilon_j^0 \right) \; + \; p_k^0 \, f_\alpha^0 \, \delta_{\alpha j} \right) e_{jmn} \, \varphi_m^1 \Big\} \, ds_0 \\ & - \Big[\delta\varphi_k^1 \, e_{kln} \sum_{i=1}^{n} \left(P_n^{0i} \, F_\alpha^{0i} \right) e_{l\alpha j} \, \varphi_j^1 \Big]_0^l \end{aligned} \tag{5.22}$$

Introducing the permutation rule

$$D_l \, e_{lnk} \left(A_k \, B_m \, e_{mnj} \, C_j \; + \; C_k \, A_m \, e_{mnj} \, B_j \; + \; B_k \, C_m \, e_{mnj} \, A_j \right) \;=\; 0 \tag{5.23}$$

and making use of the initial equilibrium equation, i.e. a component form of (2.2),

$$\frac{dM_l^0}{ds_0} \; + \; e_{jkl} \left(N_k^0 \left(\delta_{3j} \; + \; \varepsilon_3^0 \right) \; + \; \delta_{j\alpha} \, f_\alpha^0 \, p_k^0 \right) \; + \; M_k^0 \, e_{kln} \, \kappa_n^0 \;=\; 0 \tag{5.24}$$

it can be proved that the linear part of the load potential can be written as

$$\Pi_\sigma^{lin} \;=\; \int_0^l \frac{1}{2} \Big\{ 2 \, \tilde{\varepsilon}_j^1 \, e_{jnl} \, N_l^0 \, \varphi_n^1 \; + \; \tilde{\kappa}_j^1 \, e_{jnl} \, M_l^0 \, \varphi_n^1$$

$$+\varphi_l^1\, e_{lnk}\Big(N_k^0\left(\delta_{j3}+\varepsilon_j^0\right)+p_k^0\, f_\alpha^0\,\delta_{\alpha j}\Big)e_{jmn}\,\varphi_m^1\Big\}\,ds_0$$

$$-\frac{1}{2}\Big[\varphi_k^1\, e_{kln}\sum_{i=1}^{n}\left(P_n^{0i}\,F_\alpha^{0i}\right)e_{l\alpha j}\,\varphi_j^1\Big]_0^l \tag{5.25}$$

The validity of (5.25) can be proved by taking the first variation of Π_σ^{lin}.
Returning to the nonlinear form of the potential Π_σ given by (5.17) some assumptions regarding the nonlinear terms have to be made in order to perform an integration. Investigating (5.17) leads to the idea that if the rotation vector is fixed in direction then direct integration is possible.
Introducing a new independent variable ξ means that the rotation vector is fixed when

$$\boldsymbol{\varphi}^1(s_0,\xi) \;=\; \widetilde{\boldsymbol{\varphi}}^1(s_0)\,\xi \qquad , \qquad \delta\widetilde{\boldsymbol{\varphi}}^1(s_0) \;=\; \widetilde{\boldsymbol{\varphi}}^1(s_0)\,\delta\xi \tag{5.26}$$

The scalar ξ may be regarded as the amplitude of the rotation vector.
Assuming as in Section 5.2.1 that the rotation vector $\boldsymbol{\varphi}^1$ is fixed means according to Appendix A that the following relations can be established

$$\delta\kappa_j^1\,\widetilde{A}_{lj} \;=\; \delta\big(\kappa_j^1\,\widetilde{B}_{lj}\big) \qquad ; \qquad \delta\widetilde{A}_{kn}\,\widetilde{A}_{jn} \;=\; \delta\big(\widetilde{A}_{kn}\,\widetilde{B}_{jn}\big) \tag{5.27}$$

when variations are taken with respect to ξ.
Making use of (5.27) means that for a fixed rotation vector the load potential Π_σ^{fix} can be written as

$$\Pi_\sigma^{fix} \;=\; \int_0^l \Big\{ -\varepsilon_j^1\,N_l^0\,\widetilde{A}_{lj} + \widetilde{A}_{kn}\left(N_k^0(\delta_{j3}+\varepsilon_j^0) - p_k^0\,f_\alpha^0\,\delta_{\alpha j}\right)\widetilde{B}_{jn}\Big\}\,ds_0$$

$$-\kappa_j^1\,M_l^0\,\widetilde{B}_{lj} - \Big[\widetilde{A}_{kn}\sum_{i=1}^{n}\left(P_n^{0i}\,F_\alpha^{0i}\right)\widetilde{B}_{\alpha n}\Big]_0^l \tag{5.28}$$

The validity of (5.28) can be proved by taking the first variation with respect to ξ and then comparing it to (5.17).
The investigations performed in this section concerning the load potential Π_P indicate that a consistent and direct integration of the initial stress terms is only possible if the rotation vector is fixed in direction. Existence of a direct integration may still not be denied, but in the present work it has not been possible to prove the existence. The reason for the difficulties in the higher-order terms are meant to be connected to the derivation of the rotation tensor and the partiel integration necessary for the establishment of the stability formulation.

5.3 Virtual Work and Potential Energy

In this section the integration from virtual work to the potential energy is performed according to the conditions and results obtained in Section 5.2. According to the analysis in

Section 5.2 this integration can be performed directly if only the beam problem is considered while in the stability problem the integration has to be performed in accordance with the derivation of the finite rotation tensor, i.e. for the higher-order terms the direction of the rotation vector has to be fixed. This leads to the idea that two versions of the potential energy in the stability formulation are in place. The first is a linearized version, i.e linearized deformations, where no assumptions regarding the generalized displacements are made, and a second one where the direction of the rotation vector has been determined. The connections and possibilities of those two versions are further examined in Chapter 7.

5.3.1 Potential Energy for Beam Problem

The preliminary investigations performed in Section 5.2 enables direct integration of the virtual work equation (5.1) if no initial stress terms are present. Using (5.14) and (5.18) the potential energy describing the beam problem V is given by

$$\begin{aligned} V \;=\; & \int_0^l \frac{1}{2}\Big\{ \varepsilon_\alpha^1 D_{\alpha\beta}^{-1} \varepsilon_\beta^1 + \varepsilon_c^1 F \varepsilon_c^1 + \kappa_\alpha^1 I_{\alpha\beta} \kappa_\beta^1 + \frac{d\theta^1}{ds_0} I_\omega \frac{d\theta^1}{ds_0} \\ & + \kappa_3^1 \left(K + r_a^2 N_3^0 + 2\beta_\alpha M_\alpha^{c^0}\right) \kappa_3^1 + \varepsilon_c^1 r_a^2 F \kappa_3^1 \kappa_3^1 + \kappa_3^1 2\beta_\eta I_{\eta\alpha} \kappa_\alpha^1 \kappa_3^1 \\ & - \frac{d\theta^1}{ds_0} I_{\omega r^2} \kappa_3^1 \kappa_3^1 + \frac{1}{4} \kappa_3^1 \kappa_3^1 R_a^4 F \kappa_3^1 \kappa_3^1 - \lambda r_{a_l}^1 p_l^0 - \lambda p_k^0 \tilde{A}_{k\alpha} f_\alpha^0 - \lambda b^0 \theta^1 \Big\} ds_0 \\ & - \Big[\lambda r_{a_l}^1 \sum_{i=1}^{n} P_l^{0^i} + \sum_{i=1}^{n} \left(\lambda P_k^{0^i} \tilde{A}_{k\alpha} F_\alpha^{0^i} \right) \Big]_0^l \end{aligned} \tag{5.29}$$

Equation (5.29) is a nonlinear version of the potential energy for a thin-walled beam element.

5.3.2 Linearized Potential Energy - Stability Problem

In Section 5.2 it is stated that a *linear* form of the potential energy for an initial stress problem can be achieved from the virtual work (5.1) by direct integration.
The reason for the interest in a linear version of the potential energy arise from the fact that the linear version is sufficient to determine the critical load. In Chapter 7 a brief description of stability theory will be presented.

The linearized form is developed by assuming infinitesimal rotations and thereby achieving linearized deformations. Extracting the quadratic terms of (5.29) and by use of the linear potential Π_σ^{lin} leads to the *linearized potential energy* V_{lin}

$$V_{lin} \;=\; \int_0^l \Big\{ \frac{1}{2} \tilde{\varepsilon}_\alpha^1 D_{\alpha\beta}^{-1} \tilde{\varepsilon}_\beta^1 + \frac{1}{2} \tilde{\varepsilon}_c^1 F \tilde{\varepsilon}_3^1 + \frac{1}{2} \tilde{\kappa}_\alpha^1 I_{\alpha\beta} \tilde{\kappa}_\beta^1 + \frac{1}{2} \frac{d\theta^1}{ds_0} I_\omega \frac{d\theta^1}{ds_0}$$

$$+ \frac{1}{2}\tilde{\kappa}_3^1\left(K + r_a^2 N_3^0 + 2\beta_\alpha M_\alpha^{c0}\right)\tilde{\kappa}_3^1 + 2\,\tilde{\varepsilon}_j^1\, e_{jnl} N_l^0\,\varphi_n^1 + \tilde{\kappa}_j^1\, e_{jnl} M_l^0\,\varphi_n^1 - \lambda\, r_{a\,k}^1\, p_k^0$$

$$- \frac{1}{2}\varphi_l^1\, e_{lnk}\left(N_k^0\,(\delta_{3j} + \varepsilon_j^0) + p_k^0\, f_\alpha^0\,\delta_{\alpha j}\right) e_{jnm}\,\varphi_m^1 - \lambda\, p_k^0 e_{kj\alpha}\, f_\alpha^0\,\varphi_j^1 - \lambda b^0\theta^1\Big\}\, ds_0$$

$$- \left[r_{al}^1 \sum_{i=1}^{n}\left(\lambda\, P_l^{0i}\right) + \frac{1}{2}\varphi_k^1\, e_{kln}\sum_{i=1}^{n}\left(P_n^{0i}\, F_\alpha^{0i}\left(e_{l\alpha j}\,\varphi_j^1 + 2\lambda\,\delta_{l\alpha}\right)\right)\right]_0^l \qquad (5.30)$$

The form given in (5.30) possesses the symmetric properties which insures that a linearized version of the virtual work can be achieved by claiming stationarity of the potential energy.

5.3.3 Potential Energy for Fixed Rotation Vector - Stability Problem

In Section 5.2 it is stated that the nonlinear form of the initial stress terms only can be integrated if the rotation vector is *fixed.*
Interest in a potential energy with such a kinematic constraint arises from the ideas behind an asymptotic postbuckling analysis. The asymptotic postbuckling analysis is mentioned in detail in Chapter 7. The main idea is to determine a buckling form by solving the linear stability problem and then by use of this form to examine the initial postbuckling behavior by inserting the buckling form in the nonlinear potential energy.
The potential energy can be found direct from (5.1) when the rotation vector $\boldsymbol{\varphi}^1(s_0)$ is fixed in direction as given by (5.26). The potential energy then simplifies into a functional determined by six state variables

$$r_{aj}^1 \quad , \quad \theta^1 \quad , \quad \lambda \quad , \quad \xi$$

Integration of (5.1) to yield the potential energy V_{fix} leads to

$$V_{fix} = \int_0^l \Big\{ \frac{1}{2}\varepsilon_\alpha^1\, D_{\alpha\beta}^{-1}\,\varepsilon_\beta^1 + \frac{1}{2}\varepsilon_c^1\, F\,\varepsilon_c^1 + \frac{1}{2}\kappa_\alpha^1\, I_{\alpha\beta}\,\kappa_\beta^1 + \frac{1}{2}\frac{d\theta^1}{ds_0}\, I_\omega\, \frac{d\theta^1}{ds_0}$$

$$+ \frac{1}{2}\kappa_3^1\left(K + r_a^2 N_3^0 + 2\beta_\alpha M^{c0}{}_\alpha\right)\kappa_3^1 + \frac{1}{2}\varepsilon_c^1\, r_a^2 F\,\kappa_3^1\kappa_3^1 + \kappa_\alpha^1\,\beta_\eta I_{\eta\alpha}\,\kappa_3^1\kappa_3^1$$

$$- \frac{1}{2}\frac{d\theta^1}{ds_0}\, I_{\omega r^2}\,\kappa_3^1\kappa_3^1 + \frac{1}{8}\kappa_3^1\kappa_3^1\, R_a^4 F\,\kappa_3^1\kappa_3^1 - \varphi_k^1\, e_{knl}\left(N_l^0\,(\delta_{3j} + \varepsilon_j^0) + p_l^0\, f_\alpha\,\delta_{\alpha j}\right)\tilde{B}_{nj}$$

$$- \varepsilon_k^1 N_l^0\,\tilde{A}_{lk} + \tilde{\kappa}_k^1 M_l^0\,\tilde{B}_{kl} - \lambda\left(r_{al}^1 p_l^0 + p_l^0\,\tilde{A}_{l\alpha}\, f_\alpha^0 - \theta^1 b^0\right)\Big\}\, ds_0$$

$$- \left[r_{al}^1 \sum_{i=1}^{n}\left(\lambda\, P_l^{0i}\right) + \lambda\sum_{i=1}^{n}\left(P_n^{0i}\,\tilde{A}_{n\alpha}\, F_\alpha^{0i}\right) + \tilde{A}_{kn}\sum_{i=1}^{n}\left(P_n^{0i}\, F_\alpha^{0i}\right)\tilde{B}_{l\alpha}\right]_0^l \qquad (5.31)$$

The potential energy functional in (5.31) contains the influence from the initial condition of the beam element in a general way. The initial geometry appears indirect through the increments of the strain and curvature components while the initial stresses appears directly in the functional. The constraint concerning the rotation vector of course in general reduces the applicability of this version of the potential energy, but in buckling and initial postbuckling analysis this is not a major problem. This is further explored in Chapter 7.

5.4 Conclusions

The object of this chapter was to prove that the virtual work equation is the first variation of the potential energy. It was found that this could be achieved for the beam problem while in the stability problem the rotation vector is closely attached to the way in which the finite rotation tensor is developed. This indicates that if a nonlinear stability theory is to be developed from the potential energy the governing equations are limitted to the properties of the displacement field and the validity of the strain measure.
By the virtual work approach performed in this thesis it is insured that the statics is well-described and further by use of the finite rotation tensor enables to account for initial stresses and deformations in a straight forward way. In the present work it is the conviction that an approach where finite rotations are included a nonlinear beam theory as well as stability theory can be developed consistently using the virtual work equation directly.

Chapter 6

Numerical Formulation of the Beam Problem

A static beam theory including finite rotations is presented in Chapter 2 where the nonlinear differential equations as well as the virtual work equation are developed. The warping effect is incorporated in the governing equations in Chapter 5. Only in a few simple cases the differential equations can be solved analytically which immediately demands for an approximative solution method, as e.g. the Finite Element Method. The virtual work equation (5.1) together with the constitutive equations in Chapter 4 are in the present chapter used to develop a numerical model by the principles of the Finite Element Method.

In a finite element analysis the beam structure is replaced with a discrete model consisting of an assembly of finite elements. Within each element a set of shape/trial functions are assumed to model the unknown functions describing the behavior of the beam element. The most popular method of establishing a beam element is the principle of minimum potential energy which is based on the kinematics of the beam. The kinematic derivation makes use of a number of shape functions corresponding to the number of kinematic degrees of freedom. By this approach the primary gain is a well-described kinematical behavior.
The counterpart of minimum potential energy is the principle of stationarity in complementary energy, Washizu (1974). In this method stress-strain relations and equilibrium equations are used to obtain a formulation in terms of the statical functions. Hereby the primary gain is a well-described statical behavior.
Both methods have advantages as well as disadvantages which has led to a mixed formulation, as e.g. the Hellinger-Reissner principle, Washizu (1974). Here the energy functional is constructed by treating all the dependent variables as independent of each other. This means that the number of shape functions corresponds to both the kinematical as well as the statical degrees of freedom. The Hellinger-Reissner principle forms the basis of finite element models, known as the mixed and hybrid models, that are believed to yield better accuracies for stresses than the displacement finite-element models based on the minimum potential energy, Reddy (1984).

Three-dimensional beam elements have been proposed by a number of authors, see e.g. Epstein & Murray (1976), Bathe & Bolourchi (1979), Simo (1985), Elias (1986), Cardona & Geradin (1988), Crisfield (1990) and Hong Chen & Blandford (1991). In the non-linear context, as considered here, the formulation is complicated by the non-vectorial nature of rotational variables, and as a consequence a variety of different formulations exist. For

displacement-based finite elements a usual approach is to represent bending rotational displacements by the derivatives of the transverse displacements thereby achieving a lower number of independent variables. Elias (1986) shows that an inconsistency exists in using the standard bending rotational displacements for geometric, nonlinear, three-dimensional frame analysis. This inconsistency is the basis for the moment imbalance at the corner nodes of frame structures. Elias selected a modified rotation, or Rodriguez vector, as the finite element rotational displacement field. This rotational displacement field maintains corner-node continuity, which eliminates the unbalanced moment problem.

A common method to solve a nonlinear problem by the finite element method is to use an updated Lagrangian formulation. Updated Lagrangian formulations involve expressing the nonlinear equilibrium equations in an incremental form, in terms of the geometry at the start of the incremental step. Such a representation of large-deformation beam response has been shown by Bathe & Bolourchi (1979) to be computationally efficient.

In the present formulation large-deformation behavior is modeled by coupling the small-strain member behavior with finite rotations with-in the framework of an updated Lagrangian scheme. Considering the rotations to be the important displacements in a large-deformation analysis of thin-walled beam structures emphasis is placed on retaining the rotation components as independent variables. In this chapter the development of a numerical beam element is based on a linearized version of the virtual work equation.

The considerations and results of this chapter are in Chapter 8 used to develop an incremental updated Lagrangian beam element where both initial curvatures and initial stresses are incorporated.

6.1 Virtual Work Equation without Initial Stresses

The general expanded form of the virtual work equation is given by (5.1). This form contains the initial stress terms as well as the incremental contributions from three types of generalized deformations corresponding to strain, curvature and warping deformations. In the present chapter a beam element without initial stresses is developed and examined in order to give an impression of the ideas behind the numerical formulation.
For an initially stress free beam element the virtual work (5.1) may be written as

$$\int_0^l \left\{ \delta\varepsilon_j \, N_j^1 + \delta\kappa_j \, M_j^1 + \frac{d\,\delta\theta}{ds_0} B^1 - \delta r_{ak} \, p_k - \delta\varphi_l \, e_{lnk} \, A_{n\alpha} \, f_\alpha p_k - \delta\theta \, b \right\} ds_0$$

$$- \left[\delta \mathbf{r}_a \cdot \mathbf{N}^1 + \delta\boldsymbol{\varphi} \cdot \mathbf{M}^1 + \delta\theta \, B^1 \right]_0^l = 0 \qquad (6.1)$$

where no upper index is used for the external distributed loads because they identify the current loads. The form given in (6.1) is a mixed formulation according to the presence of both kinematical as well as statical variables. A pure kinematical formulation can be obtained by inserting the constitutive equations from Section 4.4, whereby integration, as discussed in Section 5.5, leads to the potential energy for the initially stress free beam element.

Before continuing the development of a finite element modifications of (6.1) are carried out

in order to obtain some simplifications.

6.1.1 Discretisation - Omission of Strain Deformations

A simplified version of the general equation (6.1) is developed by assuming the strain deformations to be insignificant compared to the curvature and warping deformations. Using this assumption leads to a modified virtual work equation given by

$$\int_0^l \left\{ \delta\kappa_j \, M_j^1 + \frac{d\,\delta\theta}{ds_0} B^1 - \delta r_{ak} \, p_k - \delta\varphi_l \, e_{lnk} \, A_{n\alpha} \, f_\alpha p_k - \delta\theta \, b \right\} ds_0$$

$$- \left[\delta\mathbf{r}_a \cdot \mathbf{N}^1 + \delta\boldsymbol{\varphi} \cdot \mathbf{M}^1 + \delta\theta \, B^1 \right]_0^l = 0 \tag{6.2}$$

and a condition stating that

$$\delta\varepsilon_j = \left(\frac{d\,\delta\mathbf{r}_a}{ds_0} - \delta\boldsymbol{\varphi} \times \frac{d\mathbf{r}_a}{ds_0} \right) \cdot \mathbf{e}_j = 0 \tag{6.3}$$

Recalling the constitutive equations from Section 4.4 and examing (6.2) it follows that this form of the virtual work contains no coupling between the three generalized displacements $\mathbf{r}_a^1$, $\boldsymbol{\varphi}^1$ and θ^1. Such a formulation is incomplete because e.g. the rotations of the beam sections have to be related to a position. Further the omission of the generalized axial strain implies that the straight beam element is axial incompressible leading to an internal statical indefiniteness. This lack in completeness can be removed by incorporating the strain condition in (6.2) which states a relationship between translations and rotations. Further the condition (4.21), stating that the warping displacement is equal to the twist, can be used to incorporate a relationship between the warping displacement and the rotations.

The above mentioned conditions can be incorporated in a FE-formulation by use of the Lagrange Multiplier method, see e.g. Reddy (1984). The Lagrange Multiplier method consists of multiplying an appropriate condition, e.g. (6.3), with an arbitrary parameter λ, integrating over the element, and adding the result to the functional in (6.2). A direct use of the condition in (6.3) leads to a similar form as given in (6.1) therefore the condition in (6.3) is converted to a condition in the strain increments ε_j^1, whereby

$$\varepsilon_j^1 = 0 \tag{6.4}$$

Introducing four additional variables λ_j and λ_ω the strain and warping conditions are incorporated in the following way

$$\int_0^l \left\{ \delta\left(\lambda_j \, \varepsilon_j^1\right) + \delta\kappa_j \, M_j^1 + \delta\left(\lambda_\omega \left(\theta^1 - \kappa_3^1\right)\right) + \frac{d\,\delta\theta}{ds_0} B^1 - \delta\varphi_l \, e_{lnk} \, \tilde{A}_{n\alpha} \, f_\alpha p_k \right.$$

$$\left. - \delta r_{ak} \, p_k - \delta\theta \, b \right\} ds_0 - \left[\delta\mathbf{r}_a \cdot \mathbf{N}^1 + \delta\boldsymbol{\varphi} \cdot \mathbf{M}^1 + \delta\theta \, B^1 \right]_0^l = 0 \tag{6.5}$$

It appears from (6.5) that the Lagrange Multipliers λ_j are a replacement for the internal forces while λ_ω represents the torsional moment corresponding to nonhomogeneous torsion. According to this relationship the multipliers inherit the vectorial nature of the internal forces and must therefore be treated accordingly. Equation (6.5) is a mixed formulation where the kinematical variables $\mathbf{r}_a^1$, $\boldsymbol{\varphi}^1$ and θ^1 can be treated independently of the statical variables λ_j and λ_ω. Using a simple example may underline the physical meaning of the multipliers in (6.5).

6.1.2 Plane Example of the Lagrange Multiplier Method

Considering a straight prismatic beam element, see Fig. 6.1, in-plane force and moment equilibrium can be expressed by

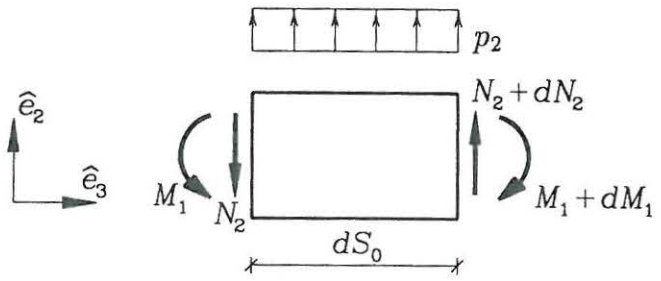

Fig. 6.1: Straight beam element.

$$\frac{dN_2}{ds_0} + p_2 = 0 \quad , \quad \frac{dM_1}{ds_0} - N_2 = 0 \tag{6.6}$$

The corresponding generalized displacements are r_2 and φ_1 whereby the virtual work can be expressed by

$$\int_0^l \left\{ \delta r_2 \left(\frac{dN_2}{ds_0} + p_2 \right) + \delta\varphi_1 \left(\frac{dM_1}{ds_0} - N_2 \right) \right\} ds_0 = 0 \tag{6.7}$$

Integration by parts leads to

$$\int_0^l \left\{ \left(\frac{d\delta r_2}{ds_0} + \delta\varphi_1 \right) N_2 + \frac{d\delta\varphi_1}{ds_0} M_1 - \delta r_2 p_2 \right\} ds_0 - \left[\delta r_2 N_2 + \delta\varphi_1 M_1 \right]_0^l = 0 \tag{6.8}$$

Assuming that the shear strain $\delta\varepsilon_2$ is insignificant, i.e.

$$\delta\varepsilon_2 = \frac{d\delta r_2}{ds_0} + \delta\varphi_1 = 0 \tag{6.9}$$

means that (6.8) simplifies to

$$\int_0^l \left\{ \frac{d\delta\varphi_1}{ds_0} M_1 - \delta r_2 p_2 \right\} ds_0 - \Big[\delta r_2 N_2 + \delta\varphi_1 M_1 \Big]_0^l = 0 \tag{6.10}$$

For linear constitutive equations

$$M_1 = I_{11} \frac{d\varphi_1}{ds_0} \tag{6.11}$$

it is obvious from (6.10) that translations and rotations are uncoupled. Introducing the strain condition back into the virtual work equation via the Lagrange Multiplier Method leads to

$$\int_0^l \left\{ \delta\lambda_2 \Big(\frac{dr_2}{ds_0} + \varphi_1 \Big) + \lambda_2 \Big(\frac{d\delta r_2}{ds_0} + \delta\varphi_1 \Big) + \frac{d\delta\varphi_1}{ds_0} M_1 - \delta r_2 p_2 \right\} ds_0$$

$$- \Big[\delta r_2 N_2 + \delta\varphi_1 M_1 \Big]_0^l = 0 \tag{6.12}$$

Integration by parts leads to

$$\int_0^l \left\{ - \delta\lambda_2 \Big(\frac{dr_2}{ds_0} + \varphi_1 \Big) + \delta r_2 \Big(\frac{d\lambda_2}{ds_0} + p_2 \Big) + \delta\varphi_1 \Big(\frac{dM_1}{ds_0} - \lambda_2 \Big) \right\} ds_0$$

$$- \Big[\delta r_2 \big(\lambda_2 - N_2 \big) \Big]_0^l = 0 \tag{6.13}$$

Comparing (6.7) and (6.13) it is evident that λ_2 appears instead of N_2 in the corresponding terms. The Euler Lagrange equations, i.e. the equilibrium equations, derived from (6.13) are given by

$$\frac{d\lambda_2}{ds_0} + p_2 = 0 \quad , \quad \frac{dM_1}{ds_0} - \lambda_2 = 0 \quad , \quad \frac{dr_2}{ds_0} + \varphi_1 = 0 \tag{6.14}$$

This means that using the Lagrange Multiplier leads to an extra differential equation corresponding to the new variable λ_2. The number of independent variables may be connected with the difficulty in solving the problem. This however is not the case in the present formulation because the Lagrange Multiplier can be treated in the same way as the generalized displacements, giving that the state variables r_2, φ_1 and λ_2 can be approximated by simple shape functions. Hereby a consistent beam element is obtained.

6.1.3 Linear Beam Analysis

The linear problem, which occurs when the infinitesimal rotation operator $\boldsymbol{\Omega}$ is used in the derivation of the virtual work equation, is considered in the present section. The present analysis serves as an introduction to an incremental formulation carried out in Chapter 8.

In Section 6.2 a linear formulation of the straight beam in the plane is presented. Later, in Sections 6.3-4, the element is expanded in order to incorporate initial curvatures and a spatial behavior.

The linear form of the virtual work equation can be obtained by substituting the linearized constitutive equations into the discretized equation (6.5) and further use the linearized form of the generalized deformations (5.20) and (5.21). Performing this and making use of the symmetry properties stated in Section 5.2 leads to

$$\delta \int_0^l \left\{ \lambda_j \left(\frac{dr^1_{a_j}}{ds_0} + r^1_{a_l} e_{ljn} \kappa^0_n + e_{j3n} \varphi^1_n \right) + \lambda_\omega \left(\theta^1 - \frac{d\varphi^1_3}{ds_0} + \varphi^1_\gamma e_{\gamma\eta} \kappa^0_\eta \right) \right.$$

$$+ \frac{1}{2} \left(\frac{d\varphi^1_\alpha}{ds_0} + \varphi^1_n e_{n\alpha m} \kappa^0_m \right) I_{\alpha\beta} \left(\frac{d\varphi^1_\beta}{ds_0} + \varphi^1_k e_{k\beta j} \kappa^0_j \right) + \frac{1}{2} \frac{d\theta^1}{ds_0} I_\omega \frac{d\theta^1}{ds_0}$$

$$\left. + \frac{1}{2} \left(\frac{d\varphi^1_3}{ds_0} - \varphi^1_\alpha e_{\alpha\beta} \kappa^0_\beta \right) K \left(\frac{d\varphi^1_3}{ds_0} - \varphi^1_\gamma e_{\gamma\eta} \kappa^0_\eta \right) - r^1_{a_j} p_j - \varphi^1_l \, e_{l\alpha j} \, f_\alpha p_j - \theta^1 \, b \right\} ds_0$$

$$- \delta \left[r^1_{a_j} N^1_j + \varphi^1_j M^1_j + \theta^1 B^1 \right]_0^l \quad = \quad 0 \tag{6.15}$$

Equation (6.15) is the linear form of the virtual work expressed in terms of the generalized displacements. The initial curvatures are incorporated in a way which preserves the generality in the formulation and thereby the possibility of examing arbitrary curved beams.

In order to develop the FEM-element a three fased procedure is used. First the plane straight element is developed in detail and second an initial curvature is incorporated in this element. Finally the spatial element is derived by use of the same precedures as for the plane element.

6.2 Straight Beam - Plane Formulation

In the plane case only three generalized displacement components occur, namely two translations and one rotation. The plane used in this section is decribed by the two base vectors $\hat{\mathbf{e}}_2$ and $\hat{\mathbf{e}}_3$.

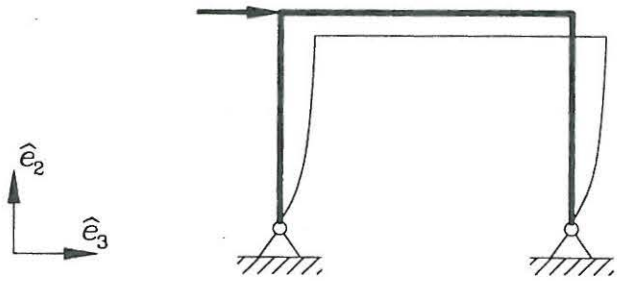

Fig. 6.2: Plane frame structure.

The further development of the beam element is performed in two fases. First the element is analysed in a local coordinate system and at the end the local elements are assembled in a global system.

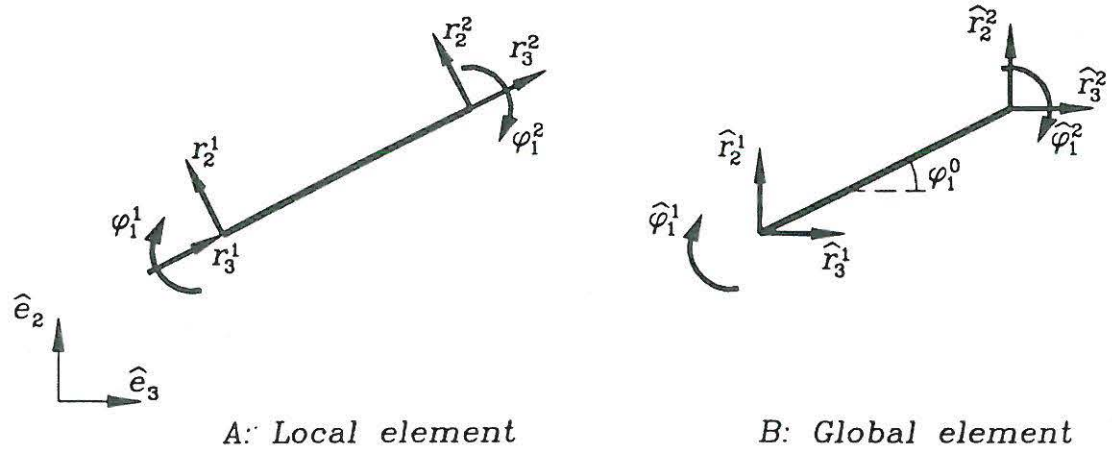

Fig. 6.3: Local and global generalized displacements.

This is indicated in Fig. 6.3 where the generalized displacements in the two fases are shown.

6.2.1 Local Analysis for Straight Beam Element

In case of a straight beam, i.e. $\kappa_j^0 = 0$ the virtual work equation describing the plane element in the local coordinate system is expressed by, see e.g. Fig. 6.3

$$\delta \int_0^l \left\{ \lambda_2 \left(\frac{dr_{a2}^1}{ds_0} + \varphi_1^1 \right) + \lambda_3 \frac{dr_{a3}^1}{ds_0} + \frac{1}{2} \frac{d\varphi_1^1}{ds_0} I_{11} \frac{d\varphi_1^1}{ds_0} - r_{a2}^1 p_2 - r_{a3}^1 p_3 \right\} ds_0$$

$$- \delta \left[r_{a2}^1 N_2^1 + r_{a3}^1 N_3^1 + \varphi_1^1 M_1^1 \right]_0^l = 0 \tag{6.16}$$

In equation (6.16) five state variables appear indicating that the plane straight beam element has five degrees of freedom.
The statical indefiniteness associated with the axial behavior, as mentioned in Section 6.1, is obvious in case of the straight beam element. Analyzing equation (6.16) it follows that the two variables r_{a3}^1 and λ_3 describing the axial behavior are uncoupled with the remaining variables in the local analysis. When the beam structure is identified by a straight line the internal relationship between r_{a3}^1 and λ_3 then leads to incompleteness in the governing equations. This incompleteness only occurs in this particular case and can be removed by either a static condensation where the degrees of freedom related to r_{a3}^1 and λ_3 are modified, or by use of the original linear contribution from axial deformations

$$\delta\varepsilon_3 N_3^1 = \delta \left(\frac{1}{2} \frac{dr_{a3}^1}{ds_0} F \frac{dr_{a3}^1}{ds_0} \right) \tag{6.17}$$

Forcing the static condensation means that axial displacements can not be analysed directly in straight beam structures. This is of minor importance because axial displacements are commonly negligible and the statics of the beam structure is preserved. Therefore in order not to loose the generality in the formulation the static condensation is used in the Finite Element Formulation.

In equation (6.16) five unknown functions appear. Therefore in order to achieve a FE-formulation from (6.16), certain choices have to be made. Observing (6.16) it appears that only first-order derivatives occurs which implies that as approximate functions one could use linear functions and still achieve continuity over the element boundaries. Further the linear functions fulfil the so-called *completeness* requirements, which states that *the approximation must be able to represent an arbitrary constant rigid-body motion* and *the approximation must be able to represent an arbitrary constant strain state.*

Approximate Functions - Shape Functions

In order to achieve a simple and consistent element the shape functions for the state variables are chosen to be linear, i.e. a two node element is used.

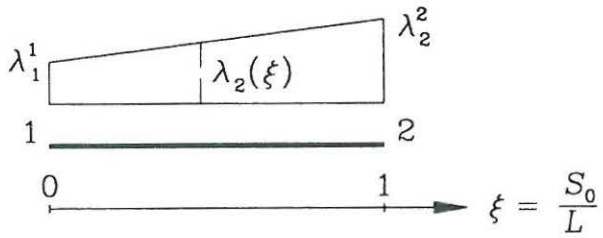

Fig. 6.4: Linear shape functions.

Indicating the two nodes representing the element by upper indices $(^i)$ and $(^j)$ respectively it follows from Fig. 6.4 that

$$
\begin{aligned}
r^1_{a2}(\xi) &= (1-\xi)\, r^i_2 + \xi\, r^j_2 \quad , \quad r^1_{a3}(\xi) = (1-\xi)\, r^i_3 + \xi\, r^j_3 \\
\varphi^1_1(\xi) &= (1-\xi)\, \varphi^i_1 + \xi\, \varphi^j_1 \\
\lambda_2(\xi) &= (1-\xi)\, \lambda^i_2 + \xi\, \lambda^j_2 \quad , \quad \lambda_3(\xi) = (1-\xi)\, \lambda^i_3 + \xi\, \lambda^j_3
\end{aligned}
\tag{6.18}
$$

The dimensionless coefficient ξ is defined by the ratio

$$
\xi = \frac{s_0}{L_e} \quad , \quad ds_0 = L_e\, d\xi \tag{6.19}
$$

where L_e is the length of the beam element.

This choice in shape functions is in contrast with usual FE-formulations for beam elements where in general cubic functions are used to represent the displacement field. The possibility of using only linear functions arise from keeping the rotation components as a state variable

in the final formulation. The usual method is to eliminate the rotation components via a strain condition which leads to higher order derivatives and thereby demands for cubic functions in order to achieve continuity over the element boundaries.
As the transverse displacement only occurs as a first order differential the convergence of r^1_{a2} is expected to be worse than for the rotational field φ^1_1 which occurs as a zero as well as first order differential.

Finite Element Equation

The FE-equation can be developed by introducing the nodal vector $\mathbf{u}^e$ containing the element degrees of freedom

$$\mathbf{u}^{eT} = \left[r^i_2, r^i_3, \varphi^i_1, \lambda^i_2, \lambda^i_3, r^j_2, r^j_3, \varphi^j_1, \lambda^j_2, \lambda^j_3\right] \tag{6.20}$$

The virtual work equation (6.16) can now be expressed in matrix-form, i.e

$$\delta\mathbf{u}^{eT} \cdot \left[\mathbf{K}^e \cdot \mathbf{u}^e - \mathbf{f}^e\right] = 0 \tag{6.21}$$

where $\mathbf{K}^e$ represents the element stiffness matrix and $\mathbf{f}^e$ is the element force vector. The equation (6.21) has to be fulfilled for any variation in $\mathbf{u}^e$ which implies the well-known FE-equation

$$\mathbf{K}^e \cdot \mathbf{u}^e - \mathbf{f}^e = \mathbf{0} \tag{6.22}$$

which expresses the equilibrium equations for the beam element. The containments of $\mathbf{K}^e$ and $\mathbf{f}^e$ are discussed in detail in the following.

Stiffness Matrix for Straight Beam Element

Performing the integrations along the element means that for constant cross-sections parameters the element stiffness matrix is given by

$$\mathbf{K}^e = \begin{bmatrix} \mathbf{K}^e_{ii} & \mathbf{K}^e_{ij} \\ \mathbf{K}^e_{ji} & \mathbf{K}^e_{jj} \end{bmatrix} \qquad i \neq j \tag{6.23}$$

where

$$\mathbf{K}^e_{ii} = \frac{1}{6\,L_e} \begin{bmatrix} 0 & 0 & 0 & -3L_e & 0 \\ 0 & 0 & 0 & 0 & -3L_e \\ 0 & 0 & 6I_{11} & 2L_e^2 & 0 \\ -3L_e & 0 & 2L_e^2 & 0 & 0 \\ 0 & -3L_e & 0 & 0 & 0 \end{bmatrix}$$

$$\mathbf{K}_{ij}^e = \frac{1}{6\,L_e}\begin{bmatrix} 0 & 0 & 0 & -3L_e & 0 \\ 0 & 0 & 0 & 0 & -3L_e \\ 0 & 0 & -6I_{11} & L_e^2 & 0 \\ 3L_e & 0 & L_e^2 & 0 & 0 \\ 0 & 3L_e & 0 & 0 & 0 \end{bmatrix} \quad , \quad \mathbf{K}_{ji}^e = \mathbf{K}_{ij}^{e\,T}$$

$$\mathbf{K}_{jj}^e = \frac{1}{6\,L_e}\begin{bmatrix} 0 & 0 & 0 & 3L_e & 0 \\ 0 & 0 & 0 & 0 & 3L_e \\ 0 & 0 & 6I_{11} & 2L_e^2 & 0 \\ 3L_e & 0 & 2L_e^2 & 0 & 0 \\ 0 & 3L_e & 0 & 0 & 0 \end{bmatrix} \tag{6.24}$$

One will notice that the stiffness matrix contains several diagonal elements which are zero, in fact only the diagonal elements corresponding to the bending contribution are nonzero. Comparing $\mathbf{K}_{ii}^e$ and $\mathbf{K}_{jj}^e$ for $i \neq j$ one major difference appears, namely the sign of the terms representing coupling between the translations and the Lagrange Multipliers corresponding to the vectorial properties of λ_j.

Load Vector

The load vector is divided into a contribution from distributed forces along the element and one from nodal forces, see Fig. 6.5. Only the distributed forces are discussed in detail because the nodal forces can be accounted for in a simple way directly in the global analysis.

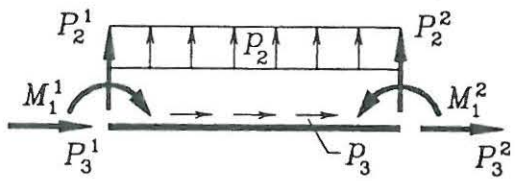

Fig. 6.5: Forces on beam element.

The distributed force is represented by linear interpolation, i.e.

$$p_2(\xi) = (1-\xi)\,p_2^i + \xi\,p_2^j \quad , \quad p_3(\xi) = (1-\xi)\,p_3^i + \xi\,p_3^j \tag{6.25}$$

This representation of the distributed force necessiates an appropriate number of elements

as the distributed force only gets represented by a set of node forces.
Substitution of (6.25) in the last term of (6.16) and finally performing the integrations leads to the load vector $\mathbf{f}_p^e$ representing the distributed forces

$$\mathbf{f}_p^e = \begin{bmatrix} \mathbf{f}_{p_1}^e \\ \mathbf{f}_{p_2}^e \end{bmatrix} \quad , \quad \begin{aligned} \mathbf{f}_{p_1}^e &= \frac{L_e}{6}\left[2p_2^i + p_2^j\,,\, 2p_3^i + p_3^j\,,\, 0\,,\, 0\,,\, 0\right] \\ \mathbf{f}_{p_2}^e &= \frac{L_e}{6}\left[p_2^i + 2p_2^j\,,\, p_3^i + 2p_3^j\,,\, 0\,,\, 0\,,\, 0\right] \end{aligned} \tag{6.26}$$

This completes the investigations of the beam element in the local coordinate system.

6.2.2 Global Analysis for Straight Beam Element

In order to assemble a set of local beam elements a common reference system has to be used. Using the coordinate system described by $\hat{\mathbf{e}}_2$ and $\hat{\mathbf{e}}_3$ as a reference state means that the local components can be related to the global ones via the transformation operator $\mathbf{A}$ defined in Appendix A.

Transformation of Local Components

Observing Fig. 6.3 it is obvious that the rotation component φ_1^1 is independent of the coordinate systems while the two translations $r_{a_2}^1$ and $r_{a_3}^1$ highly depend on the corresponding coordinate system. Finally λ_2 and λ_3 behave in a similar way as $r_{a_2}^1$ and $r_{a_3}^1$ respectively according to the vector property of $\boldsymbol{\lambda}$.
Letting φ_1^0 represent the angle between the unit vector $\hat{\mathbf{e}}_3$ and the local beam axis, as shown in Fig. 6.3, it follows from Appendix A that the transformation operator in the $\hat{\mathbf{e}}_2, \hat{\mathbf{e}}_3$-plane is given by

$$\mathbf{A}(\varphi_e^0 \hat{\mathbf{e}}_1) = \begin{bmatrix} 1 & 0 & 0 \\ 0 & \cos\varphi_e^0 & -\sin\varphi_e^0 \\ 0 & \sin\varphi_e^0 & \cos\varphi_e^0 \end{bmatrix} \tag{6.27}$$

Introducing a reduced form of the transformation operator, i.e.

$$\mathbf{B}_i^R(\varphi_e^{0^i} \hat{\mathbf{e}}_1) = \begin{bmatrix} \cos\varphi_e^{0^i} & -\sin\varphi_e^{0^i} \\ \sin\varphi_e^{0^i} & \cos\varphi_e^{0^i} \end{bmatrix} \quad , \quad \mathbf{B}_i^R \cdot \mathbf{B}_i^{R^T} = \mathbf{0} \tag{6.28}$$

where the index i indicates a particular node, means that the transformation for the nodal values of a beam element can be expressed by

$$\begin{bmatrix} \mathbf{u}_j^e \\ \mathbf{u}_i^e \end{bmatrix} = \begin{bmatrix} \mathbf{B}_i^e & \\ & \mathbf{B}_j^e \end{bmatrix} \cdot \begin{bmatrix} \hat{\mathbf{u}}_i^e \\ \hat{\mathbf{u}}_j^e \end{bmatrix} \quad \text{where} \quad \mathbf{B}_i^e = \begin{bmatrix} \mathbf{B}_i^R & & \\ & 1 & \\ & & \mathbf{B}_i^R \end{bmatrix}^T \tag{6.29}$$

For the straight beam element $\varphi_e^{0^i} = \varphi_e^{0^j}$.
A similar relation is of course valid for the force vector, i.e.

$$\begin{bmatrix} \mathbf{f}_{p_i}^e \\ \mathbf{f}_{p_j}^e \end{bmatrix} = \begin{bmatrix} \mathbf{B}_i^e & \\ & \mathbf{B}_j^e \end{bmatrix} \cdot \begin{bmatrix} \hat{\mathbf{f}}_{p_i}^e \\ \hat{\mathbf{f}}_{p_j}^e \end{bmatrix} \tag{6.30}$$

where $\hat{\mathbf{f}}_{p_j}$ constitutes the force vector in global coordinates.

Global Element Stiffness Matrix

Substitution of (6.29) and (6.30) into the equilibrium equations (6.22) and further multiplication with the full transformation operator leads to the equilibrium equations in the global coordinate system.

$$\hat{\mathbf{K}} \cdot \hat{\mathbf{u}} = \hat{\mathbf{f}}_p + \hat{\mathbf{f}}_P \tag{6.31}$$

The global element stiffness matrix $\hat{\mathbf{K}}$ is defined by

$$\hat{\mathbf{K}} = \begin{bmatrix} \mathbf{B}_i^e & \\ & \mathbf{B}_j^e \end{bmatrix}^T \cdot \begin{bmatrix} \mathbf{K}_{ii}^e & \mathbf{K}_{ij}^e \\ \mathbf{K}_{ji}^e & \mathbf{K}_{jj}^e \end{bmatrix} \cdot \begin{bmatrix} \mathbf{B}_i^e & \\ & \mathbf{B}_j^e \end{bmatrix} \tag{6.32}$$

The transformation in equation (6.32) constitutes the global form of the element stiffness matrix.

Assembling

Assembling the contributions from the elements to the equilibrium equations in each node means that global equilibrium can be expressed by

$$\mathbf{K}_g \cdot \mathbf{u}_g = \mathbf{f}_g \tag{6.33}$$

Equation (6.33) is the final form of the equilibrium equations where the only unknown terms are the components of the global displacement vector $\mathbf{u}_g$. $\mathbf{K}_g$ constitutes the reduced global stiffness matrix and finally $\mathbf{f}_g$ is the global nodal force vector.

6.2.3 Implementation and Examples

The implementation of the foregoing analysis on a computer has been carried out in order to analyse the performance of the developed beam element. The principles of the developed program are illustrated in Fig. 6.6.

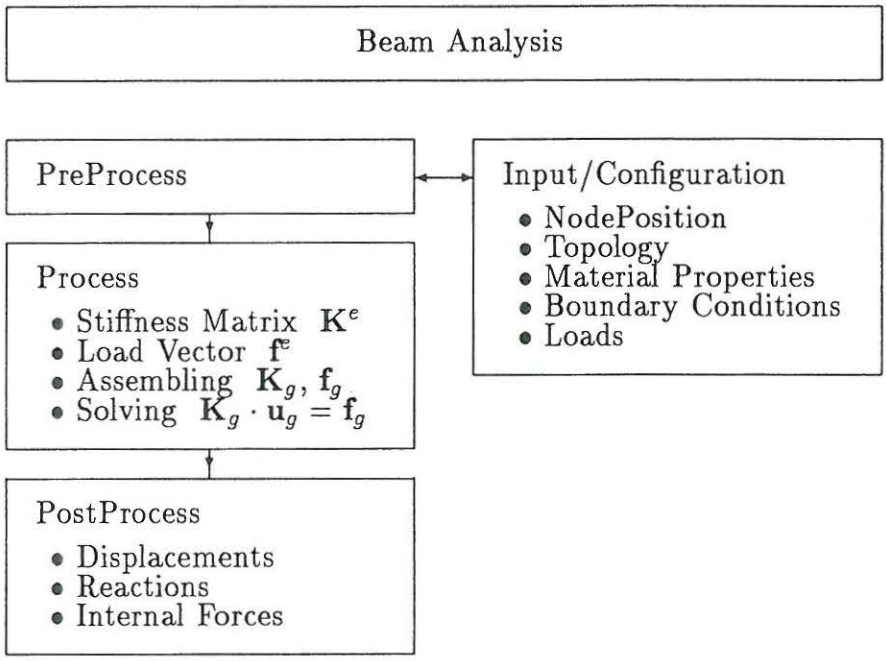

Fig. 6.6: Diagram for a linear beam analysis.

The diagram shown in Fig. 6.6 is the basement for any numerical beam analysis whether it is a linear beam analysis, a linear stability analysis or an incremental beam analysis.

Three examples have been investigated in order to illustrate the performance of the beam element. The numerical results are compared with those of an analysis via the Bernoulli-Euler theory.

Example 1 - Pure Bending

The simply supported beam shown in Fig. 6.7 is investigated.

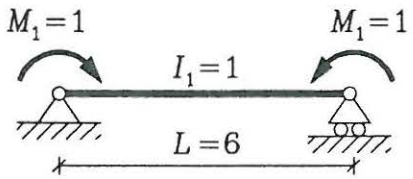

Fig. 6.7: Straight beam in pure bending.

In this example emphasis is placed on the performance of the transverse displacement field. The rotational displacement and the statics are not discussed in detail because of their simple form which can be reproduced at two elements.
The Bernoulli-Euler theory states that the transverse displacement $\hat{r}^1_{a_2}$ is given by

$$\hat{r}^1_{a_2}(\xi) = \frac{1}{2}\frac{M L^2}{I_{11}}\xi\big(1-\xi\big) \tag{6.34}$$

In Fig. 6.8 the results from a numerical analysis with 4 and 5 elements are illustrated together with (6.34).

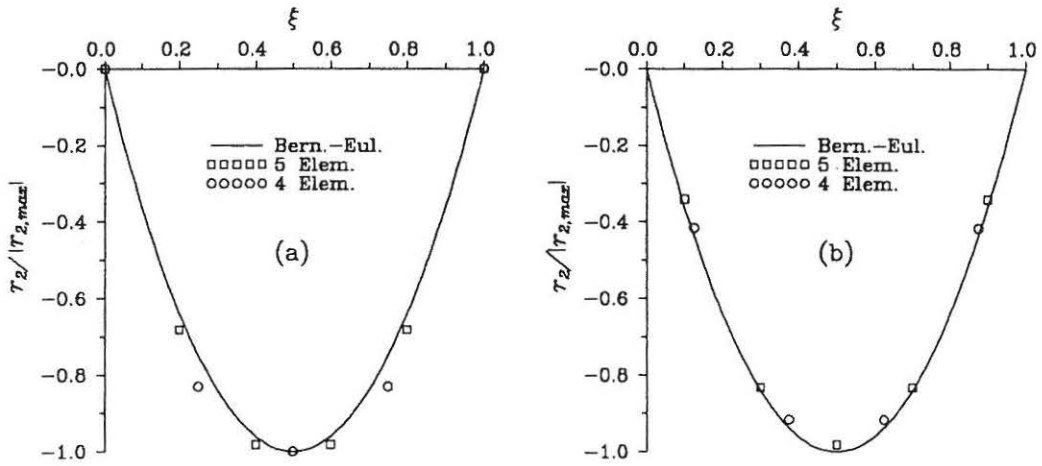

Fig. 6.8: Transverse displacement for beam in pure bending. (a) Node values. (b) Midtpoint values.

As to be expected from a hybrid element with simple shape functions the agreement is not overwhelming at 4-5 elements, as it appears from Fig. 6.8a. Important for this example is to show that the element converges towards the analytical displacement field. It appears from Fig. 6.8b, where the midpoint values are illustrated, that the numerical results are very close to the analytical solution which implies that the element converges.

Example 2 - Midpoint Load

For the simply supported beam with midpoint load, as shown in Fig. 6.9, the kinematical as well as the statical behavior has been examined for different numbers of elements.

The Bernoulli-Euler theory states that the transverse displacement $\hat{r}^1_{a_2}$ and the rotational displacement $\hat{\varphi}^1_1$ are given by

$$\hat{r}^1_{a_2}(\xi) = \frac{1}{16}\frac{P L^3}{I_{11}}\xi\left(1-\frac{4}{3}\xi^2\right) \qquad \text{for} \quad \xi \le \frac{1}{2} \tag{6.35}$$

$$\hat{\varphi}^1_1(\xi) = -\frac{1}{16}\frac{P L^2}{I_{11}}\left(1-4\xi^2\right)$$

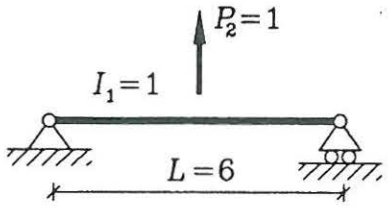

Fig. 6.9: Straight beam with midpoint load.

and the bending moment M_1 by

$$M_1(\xi) = \frac{1}{2} PL\xi \qquad \text{for} \quad \xi \leq \frac{1}{2} \tag{6.36}$$

In Fig. 6.10 selected results from numerical analysis for 2, 4 and 6 elements are given together with the analytical results (6.36) and (6.36).

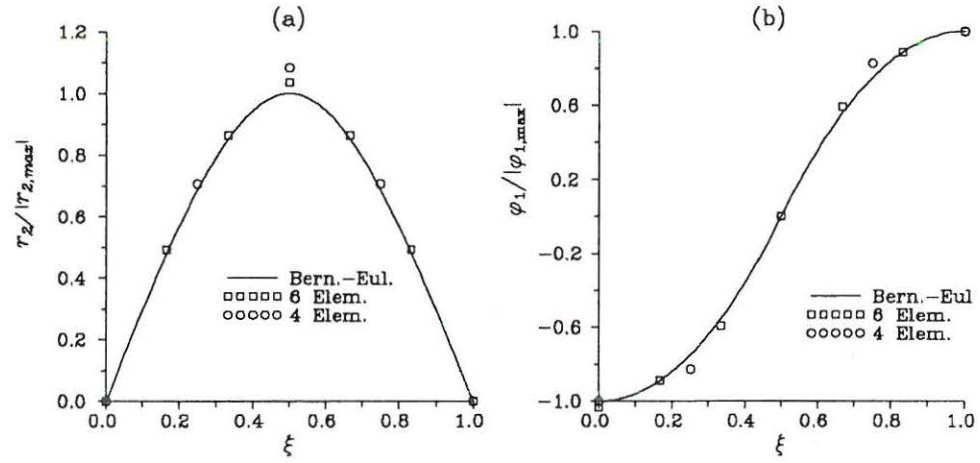

Fig. 6.10: Straight beam with midpoint load. (a) Transverse displacement. (b) Rotational displacement.

From Fig. 6.10 it follows that the rotational field converges faster and better than the transverse displacement, as to be expected from the difference of differential order in the strain condition. Fig. 6.11 illustrates that the bending moment is well-described already at 2 elements. Even though the example is simple the results imply, as it was intended, that for the relatively simple element a satisfacory representation of the rotational field and the statics is obtained for some neglection of the transverse displacement.

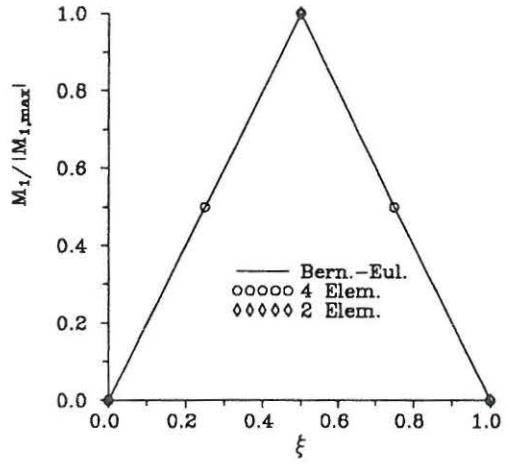

Fig. 6.11: Straight beam with midpoint load. Bending moment.

Example 3 - Clamped Beam with Distributed Load

In this example the clamped beam with transverse load shown in Fig. 6.12 is examined. The Bernoulli-Euler theory states that

$$\begin{aligned} \hat{r}^1_{a2}(\xi) &= \frac{1}{24}\frac{p_2 L^4}{I_{11}}\xi^2\left(1-2\xi+\xi^2\right) \\ \hat{\varphi}^1_1(\xi) &= -\frac{1}{12}\frac{p_2 L^3}{I_{11}}\xi\left(1-3\xi+2\xi^2\right) \end{aligned} \tag{6.37}$$

and the internal forces N_2 and M_1 by

$$\begin{aligned} N_2(\xi) &= -\frac{p_2 L}{2}\left(1-2\xi\right) \\ M_1(\xi) &= \frac{p_2 L^2}{12}\left(1-6\xi+6\xi^2\right) \end{aligned} \tag{6.38}$$

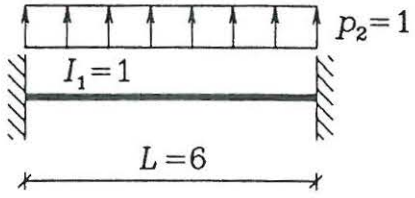

Fig. 6.12: Clamped beam with distributed load.

Numerical models with different numbers of elements have been used and selected results are illustrated together with (6.37) and (6.38) in Fig. 6.13.

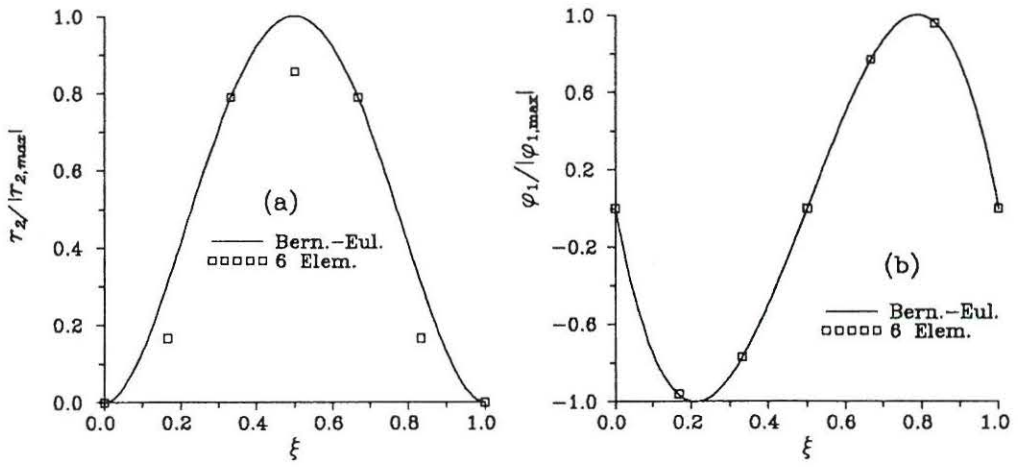

Fig. 6.13: Clamped beam with distributed load. (a) Transverse displacement. (b) Rotational displacement.

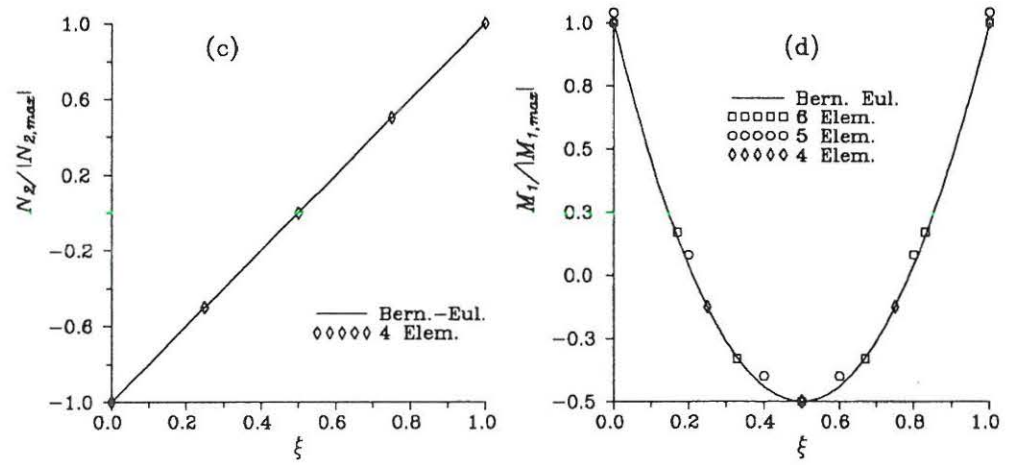

Fig. 6.14: Clamped beam with distributed load. (c) Shear force. (d) Bending moment.

For the kinematical behavior (see Fig. 6.13) the influence from the boundary conditions is obvious for the transverse displacement, while for the rotational degree of freedom the convergence is indeed satisfactory. The results show that the statical behavior is well-described by the developed element. Fig. 6.14 indicate that the statical behavior is well-described for an even number of elements while for an odd number the bending moment shows small discrepancies arising from the simple modelling of the distributed force.

6.2.4 Concluding Remarks for Straight Beam Element

The performance of the in Sections 6.2.1-2 developed two node hybrid element has been examined by analysing three different beam structures. The results show that the element to some extent neglects the kinematical behavior in favour of the statical behavior. This is noticeable for the transverse displacement where a high number of elements is necessary

is noticeable for the transverse displacement where a high number of elements is necessary in order to approximate the analytical solution. The influence on the rotational field is not significantly corresponding to the presence of lower order differentials of the rotational components. Despite some discrepancies it is obvious that the element converges as the midtpoint values are very close to the analytical ones. The rate of convergence is not impressing but one will notice that for different kinds of problems the necessary number of elements in order to obtain a satisfactory rotational field is nearly the same.
The investigations of the statical behavior show that if the numerical model is chosen appropriate the statics are indeed well-described. The necessary number of elements is lower than the corresponding number for the kinematics as to be expected for a hybrid element. Concludingly the hybrid element is suitable for problems where the important parameters are the rotational field and the statics of the beam element.

6.3 Curved Beam - Plane Formulation

The development of a curved beam element is necessary in order to establish an incremental updated Lagrangian element as the curvature represents the initial deformations. The plane formulation of the straight beam element in Section 6.2 is therefore expanded in order to incorporate an initial curvature of the beam. Continuing the analysis in the $(\hat{e}_2, \hat{e}_3)$-plane means that the curvature accepted as nonzero is κ_1^0, as illustrated in Fig. 6.15.

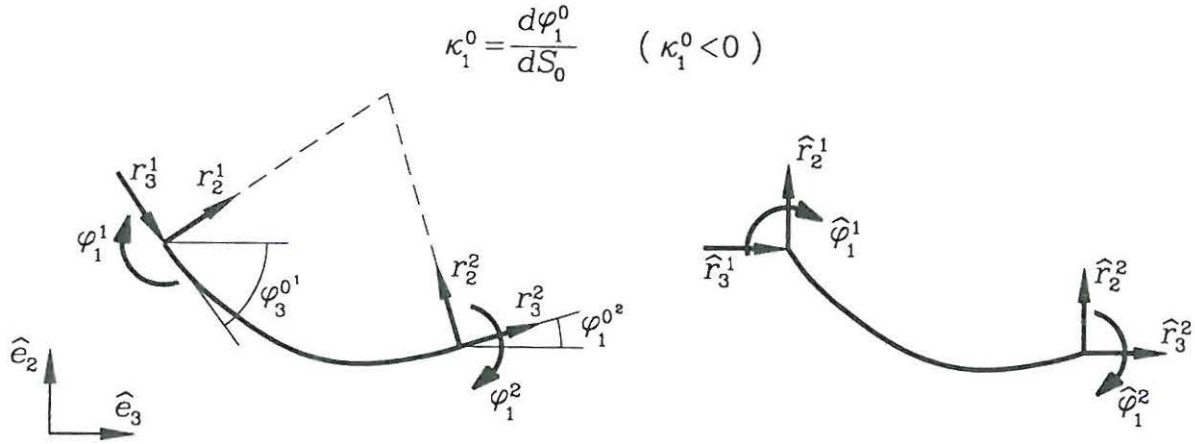

Fig. 6.15: Curved beam element in local and global coordinate system.

The working process is still carried out in two coordinate systems as indicated in Fig. 6.15. In the local system $r_{a_2}^1$ and $r_{a_3}^1$ of course still correspond to a transverse and an axial displacement respectively, but now the directions of the local axes changes along the beam axis. This implies that the beam element is influenced by the curvature in the local as well as the global analysis. These new effects are examined in the following and the considerations serve as a starting point for the spatial element which is a general version of the plane element.

6.3.1 Local Analysis

The virtual work equation for the single curved beam element is given by

$$\delta \int_0^l \left\{ \lambda_2 \left(\frac{dr_{a2}^1}{ds_0} - \kappa_1^0 r_{a3}^1 + \varphi_1^1 \right) + \lambda_3 \left(\frac{dr_{a3}^1}{ds_0} + \kappa_1^0 r_{a2}^1 \right) + \frac{1}{2} \frac{d\varphi_1^1}{ds_0} I_{11} \frac{d\varphi_1^1}{ds_0} \right.$$

$$\left. - r_{a2}^1 p_2 - r_{a3}^1 p_3 \right\} ds_0 - \delta \left[r_{a2}^1 N_2^1 + r_{a3}^1 N_3^1 + \varphi_1^1 M_1^1 \right]_0^l = 0 \tag{6.39}$$

New terms caused by the initial curvature only arise in the strain terms and it follows from (6.39) that the strain conditions are coupled in case of a curved beam. Further still no higher than first order derivatives occur which allows one to use the linear shape functions.

Shape Functions

Using the linear shape functions from (6.19) to model (r_{a2}^1, r_{a3}^1, φ_1^1, λ_2, λ_3) the only function which remains to be given is one which approximates the initial curvature κ_1^0. The initial curvature is defined by (3.4) which for the plane case leads to

$$\kappa_1^0 = \frac{d\varphi_1^0}{ds_0} \tag{6.40}$$

Approximating the initial rotation component φ_1^0 by linear interpolation, i.e.

$$\varphi_1^0(\xi) = (1 - \xi)\varphi_1^{0i} + \xi \varphi_1^{0j} \tag{6.41}$$

and substitution of (6.41) leads to

$$\kappa_1^0 = \frac{1}{L_e}\left(\varphi_1^{0j} - \varphi_1^{0i}\right) \tag{6.42}$$

which means that the initial curvature is assumed to be constant within an element.

FE-Equation

Using the nodal vector $\mathbf{u}^e$ from (6.20) means that the virtual work equation (6.39) can be expressed in matrix-form by

$$\delta \mathbf{u}^{eT} \cdot \left[\left(\mathbf{K}^e + \mathbf{K}^\kappa \right) \cdot \mathbf{u}^e - \mathbf{f}^e \right] = 0 \tag{6.43}$$

where $\mathbf{K}^\kappa$ constitutes the stiffness contribution from an initial curvature. $\mathbf{K}^e$ and $\mathbf{f}^e$ are defined in Section 6.2 which implies that only the initial curvature matrix $\mathbf{K}^\kappa$ needs to be examined.

Initial Curvature Matrix $\mathbf{K}^{\kappa}$

Performing the integrations of (6.39) for the terms containing κ_1^0 along the element leads to the initial curvature matrices $\mathbf{K}_{ij}^{\kappa}$ constituting $\mathbf{K}^{\kappa}$

$$\mathbf{K}^{\kappa} = \begin{bmatrix} \mathbf{K}_{ii}^{\kappa} & \mathbf{K}_{ij}^{\kappa} \\ \mathbf{K}_{ji}^{\kappa} & \mathbf{K}_{jj}^{\kappa} \end{bmatrix} \tag{6.44}$$

where

$$\mathbf{K}_{ii}^{\kappa} = \frac{L_e\,\kappa_1^0}{6} \begin{bmatrix} 0 & 0 & 0 & 0 & 2 \\ 0 & 0 & 0 & -2 & 0 \\ 0 & 0 & 0 & 0 & 0 \\ 0 & -2 & 0 & 0 & 0 \\ 2 & 0 & 0 & 0 & 0 \end{bmatrix}$$

$$\mathbf{K}_{ij}^{\kappa} = \frac{1}{2}\mathbf{K}_{ii}^{\kappa} \quad , \quad \mathbf{K}_{ji}^{\kappa} = \mathbf{K}_{ij}^{\kappa} \quad , \quad \mathbf{K}_{jj}^{\kappa} = \mathbf{K}_{ii}^{\kappa} \tag{6.45}$$

It follows from (6.45) that $\mathbf{K}^{\kappa}$ has a simple form and it can therefore easily be incorporated in the analysis.

6.3.2 Global Analysis

The transformations of the local equations (6.43) into the global form is performed similar as in Section 6.2.

Orientation of Local Unit Vectors

The orientation of the local unit vectors $\mathbf{e}_j^0$ is determined by

$$\mathbf{e}_j^0 = \mathbf{A}(\varphi_1^0 \hat{\mathbf{e}}_1) \cdot \hat{\mathbf{e}}_j \tag{6.46}$$

where φ_1^0 depends on the position along the beam axis. Some modification has to be carried out according to the change in φ_1^0. The two sets of nodal values transform according to the initial rotation component which corresponds to the nodal set in question. From Fig. 6.16 it follows that the node values of φ_1^0 are given by

$$\varphi_1^{0i} = \varphi_1^e + \varphi_1^{\kappa} \quad , \quad \varphi_1^{0j} = \varphi_1^e - \varphi_1^{\kappa} \qquad \varphi_1^{\kappa} = \frac{\beta}{2}$$

$$\sin\varphi_1^{\kappa} = \frac{L_e\,\kappa_1^0}{2} \quad , \quad \varphi_1^{\kappa} \simeq \frac{L_e\,\kappa_1^0}{2} \tag{6.47}$$

The last relation in (6.47) is only an approximation and the validity depends on the factor $\kappa_1^0\,L_e$.

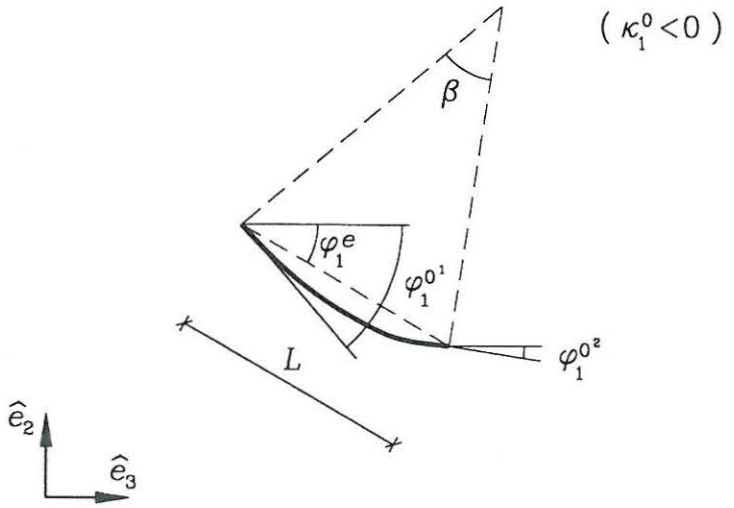

Fig. 6.16: Initial rotation components.

Global Element Stiffness Matrix

The modified global element stiffness matrix $\hat{\mathbf{K}}$ is then given by

$$\hat{\mathbf{K}} = \begin{bmatrix} \mathbf{B}_i^e(\varphi_1^{0^i}\hat{\mathbf{e}}_1) & \\ & \mathbf{B}_j^e(\varphi_1^{0^j}\hat{\mathbf{e}}_1) \end{bmatrix}^T \cdot$$

$$\begin{bmatrix} \mathbf{K}_{ii}^e + \mathbf{K}_{ii}^{\kappa} & \mathbf{K}_{ij}^e + \mathbf{K}_{ij}^{\kappa} \\ \mathbf{K}_{ji}^e + \mathbf{K}_{ji}^{\kappa} & \mathbf{K}_{jj}^e + \mathbf{K}_{jj}^{\kappa} \end{bmatrix} \cdot \begin{bmatrix} \mathbf{B}_i^e(\varphi_1^{0^i}\hat{\mathbf{e}}_1) & \\ & \mathbf{B}_j^e(\varphi_1^{0^j}\hat{\mathbf{e}}_1) \end{bmatrix} \tag{6.48}$$

Comparing with (6.32) the only change is the additional term in the element stiffness matrix.

Assembling

The assembling of the elements is performed in the same way as for the straight beam element leading to the governing equations given in (6.33).

6.3.3 Implementation and Examples

The implementation of the curved beam element has been carried out by expanding the straight beam element with the modifications described in the foregoing.

The principles of the expanded version are illustrated in Fig. 6.17.

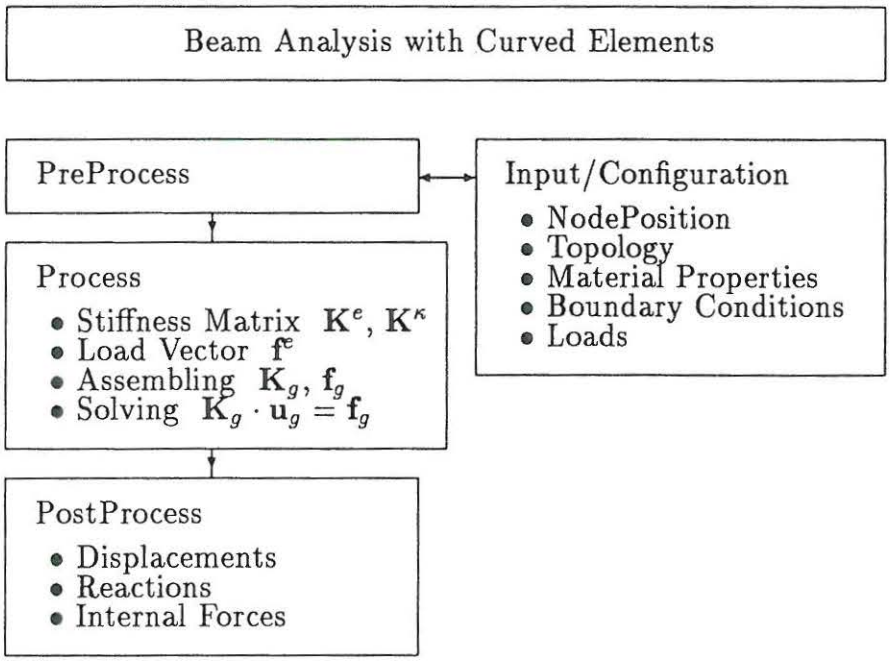

Fig. 6.17: Diagram for linear beam analysis with curved elements.

Comparing with Fig. 6.6 it is evident that only a few modifications of the basement program were necessary.

The performance of the curved beam element is investigated by examing a semi-circle with two endmoments. The results from the present element are compared with an analysis performed with the FEM-program ABAQUS.

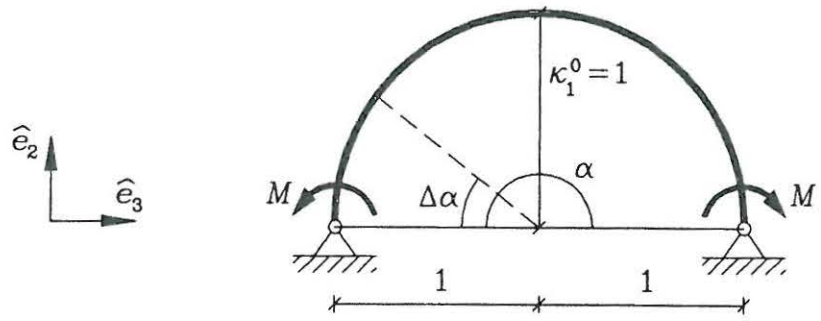

Fig. 6.18: Semi-circular beam with two endmoments.

A FEM-model for the semi-circle can be developed from the entire semi-circle or by symmetry considerations only half of the structure has to be modelled. Both models are considered in the following because of the difference in the boundary conditions.

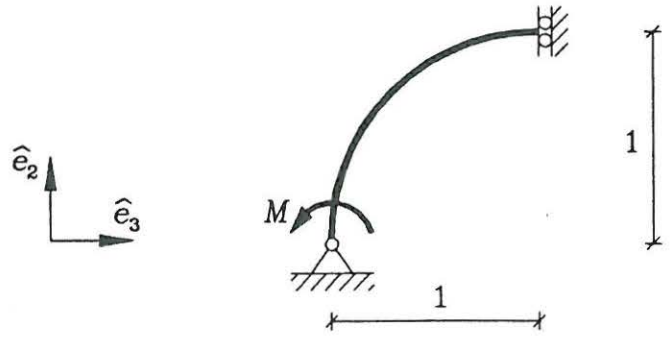

Fig. 6.19: Modified model.

The ABAQUS-model used is illustrated in Fig. 6.20. The model consists of 10 quadratic beam elements *B32* where the single element consists of three equally spaced internal nodes, as illustrated in Fig. 6.20.

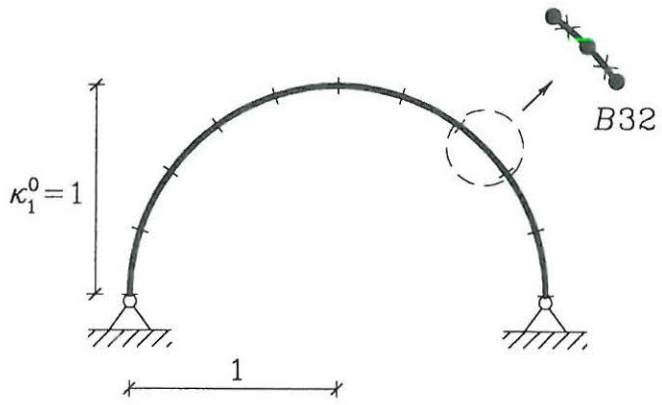

Fig. 6.20: ABAQUS-model for semi-circle.

Both a statical and a geometrical comparison between the ABAQUS-results and the analysis performed with the developed element are presented and discussed in the following. The kinematical results from ABAQUS are given in the nodepoints while the statics are represented by the values of the Gaussian integration points, see e.g Fig. 6.20.

Full Model

Three different meshes for the full model have been analysed by the developed program.

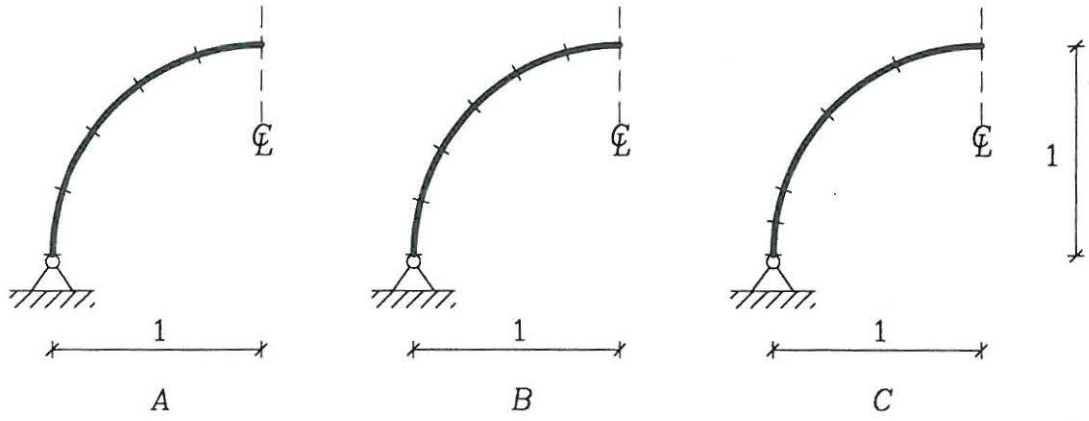

Fig. 6.21: Meshes for full-model.

Kinematics :
The three generalized global displacements ($\hat{r}^1_{a2}$, $\hat{r}^1_{a3}$, $\hat{\varphi}^1_1$) are illustrated in Fig. 6.22-6.23. $\Delta\alpha$ is the angle between the diameter joining the ends and the actual position along the beam axis while $\alpha = \pi$ corresponding to a semi-circle, as illustrated in Fig. 6.18.

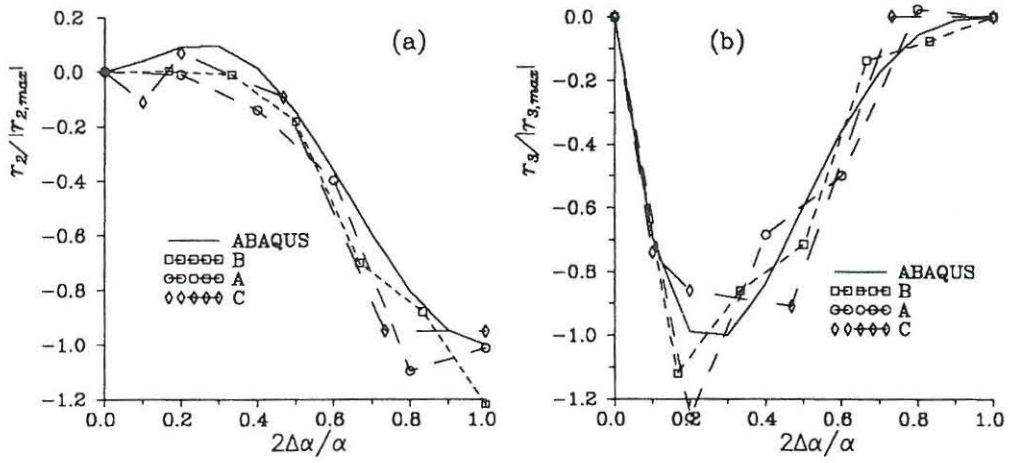

Fig. 6.22: Generalized displacements for semi-circle. (a) Displacement $\hat{r}^1_{a2}$. (b) Displacement $\hat{r}^1_{a3}$.

From Fig. 6.22 it follows that the translations $\hat{r}^1_{a2}$ and $\hat{r}^1_{a3}$, as $\hat{r}^1_{a2}$ for the straight beam, only converge slowly towards the reference values. Nevertheless the convergence of the element is obvious as the midtpoint values are close to the reference values.

The rotational component $\hat{\varphi}_1^1$ in Fig. 6.23 is seen to be close to those from ABAQUS at five elements which is considered as a satisfactory result for the present element, as the semi-circle is a relative complex beam structure.

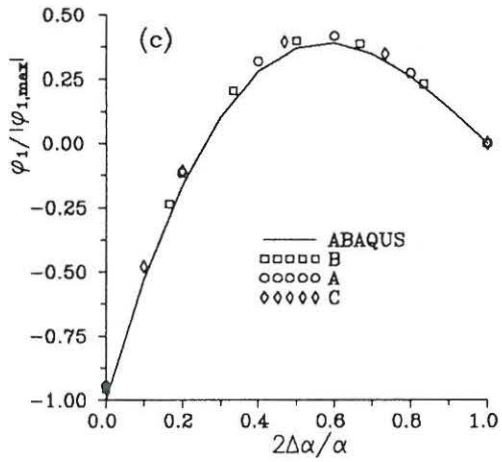

Fig. 6.23: Generalized displacements for semi-circle. (c) Rotation $\hat{\varphi}_1^1$.

Comparing the results from meshes A and B with C it follows that some improvements can be obtained by use of smaller elements locally.

Statics :

In Fig. 6.24-6.25 the shearforce N_2^1, normalforce N_3^1 and bending moment M_1^1 are illustrated.

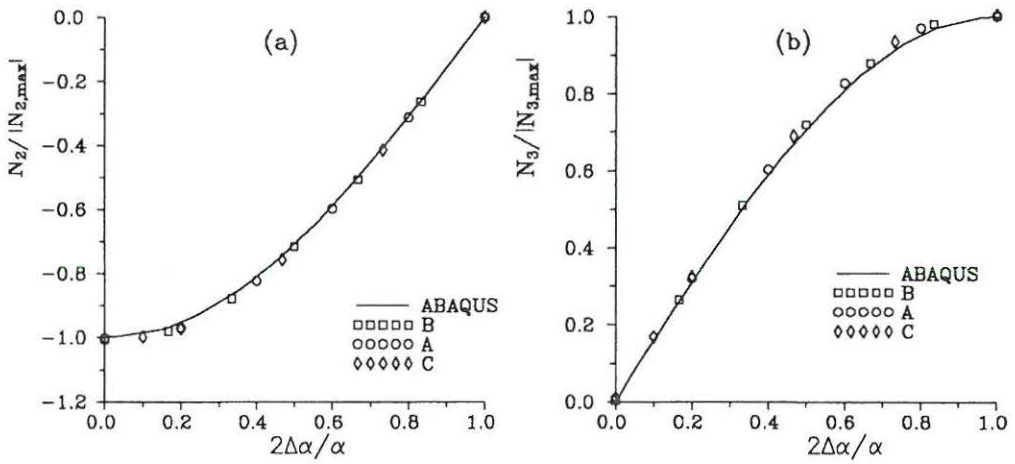

Fig. 6.24: Internal forces for semi-circle. (a) Shear force. (b) Normal force.

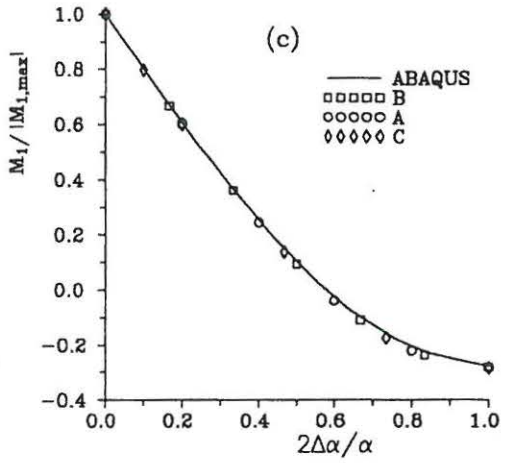

Fig. 6.25: Internal forces for semi-circle. (c) Bending moment.

As for the straight beam the statical behavior of the present element approximates the reference values better than the kinematical. The convergence is satisfactory at 10 elements which is remarkable good for a two node element with linear shape functions even though the element is hybrid.

Modified Model

Using the modified model means that the same number elements can be used to model only half the semi-circle.

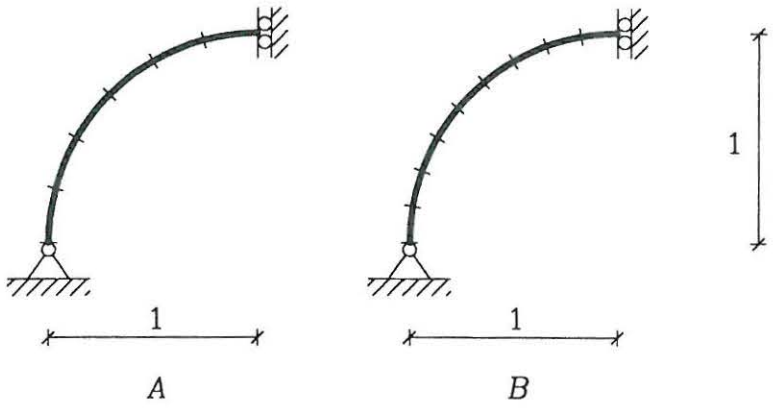

Fig. 6.26: Meshes for modified-model.

Two different meshes for the modified model have been analysed by the developed program. In Fig. 6.27 the two displacements $\hat{r}^1_{a_2}$ and $\hat{r}^1_{a_3}$ are illustrated for the two meshes along with the results from ABAQUS.

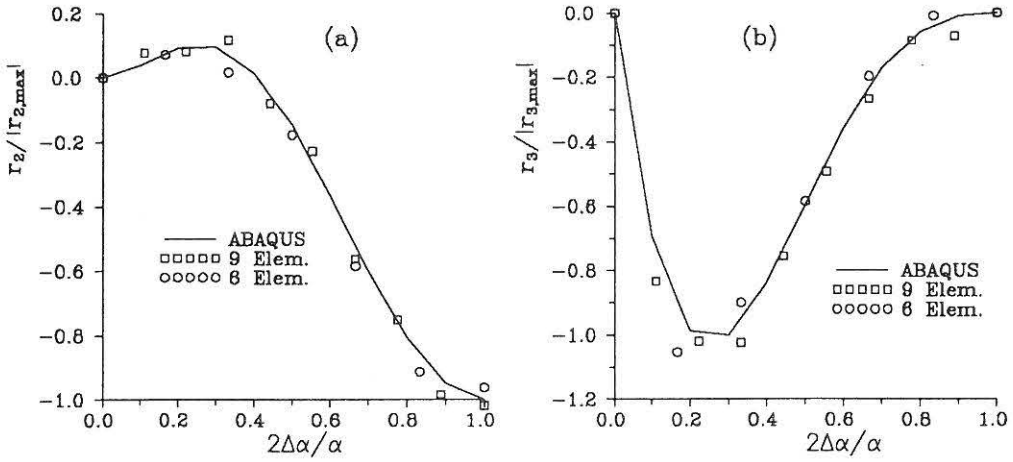

Fig. 6.27: Generalized displacements for semi-circle. (a) Displacement $\hat{r}^1_{a2}$. (b) Displacement $\hat{r}^1_{a3}$.

The results in Fig. 6.27 show that the geometric boundary conditions influence, as to be expected, the kinematical behavior, as the agreement with ABAQUS has been improved. In Fig. 6.28 the internal bending moment is illustrated,

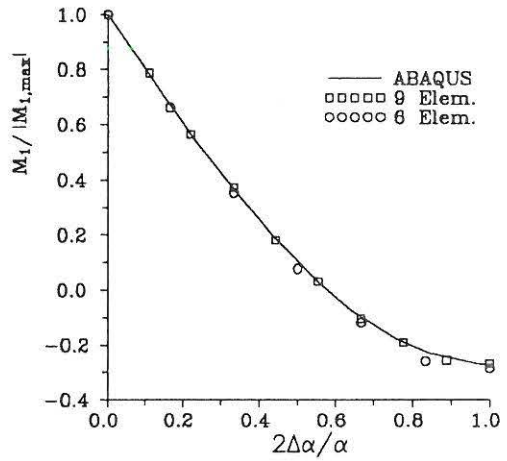

Fig. 6.28: Bending moment for modified-model.

Comparing Fig. 6.28 with Fig. 6.25 the results indicate that no significant improvement or change is obtained by modification of the boundary conditions.

6.3.4 Concluding Remarks for Curved Element

The investigations performed for the semi-circle underlines the results obtained for the straight beam element, i.e. the two node hybrid element reproduces the statics and the rotational field on the expense of the translation field. The presence of an initial curvature is consistently incorporated in the stiffness matrix and the examples show that even though the

semi-circle is a geometric complex structure the necessary number of elements is acceptable. The agreement with results obtained from ABAQUS is very promising towards the development of an incremental element usable for nonlinear analysis.

6.4 Spatial Beam Element

The behavior of thin-walled beams is highly influenced by the possibility of torsion induced by in-plane loads as well as out-of-plane loads. Especially for non-symmetric cross-sections torsion arise. For non-symmetric sections not only torsion may occur but also out-of-plane bending for in-plane loads can occur, e.g. the Z-profile. Therefore in order to describe the behavior of thin-walled beams in general the in-plane behavior has to be expanded to incorporate out-of-plane displacements.

In the present section a spatial element is introduced according to the results and observations from Sections 6.2-3.

6.4.1 Local Analysis for Spatial Element

The virtual work equation in (6.15) constitutes the weak form of the linear equilibrium equations for the spatial element in the local coordinate system described by $\mathbf{e}_j^0$. Investigating (6.15) and recalling the observations from Sections 6.2-3, it appears that only the number of state variables is changed and not the overall form of the weak equation. The spatial element can therefore be developed by expanding the numbers of shape functions according to $\left(r_{al}^1, \varphi_l^1, \theta^1, \lambda_l, \lambda_\omega\right)$ and thereby the dimensions of the connected vectors and matrices.

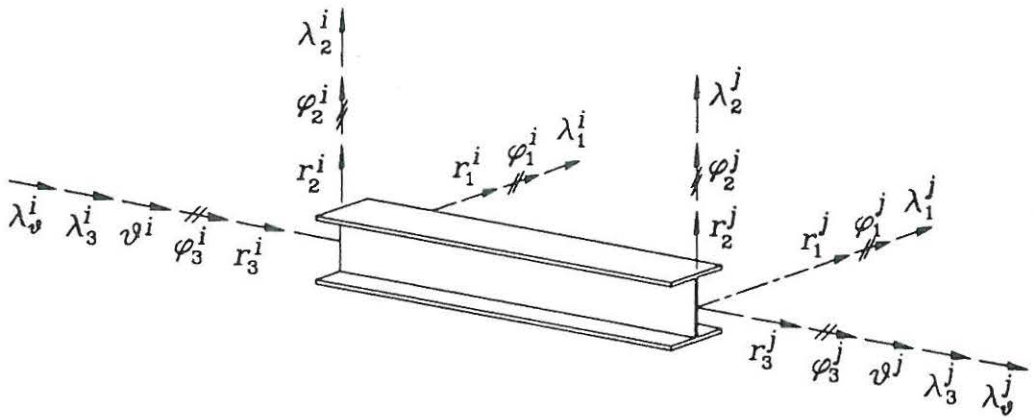

Fig. 6.29: Spatial beam element.

In Fig. 6.29 the two node spatial element is illustrated.

Shape Functions

Indicating the two nodes representing the element by upper indices (^{i}) and (^{j}) the linear shape functions representing the eleven variables, see Fig. 6.29, are given by (6.19) leading

to

$$r^1_{al}(\xi) = (1-\xi)\, r^i_l + \xi\, r^j_l \quad , \quad l = 1,2,3$$

$$\varphi^1_l(\xi) = (1-\xi)\,\varphi^i_l + \xi\,\varphi^j_l \qquad \theta^1(\xi) = (1-\xi)\,\theta^i + \xi\,\theta^j \tag{6.49}$$

$$\lambda_l(\xi) = (1-\xi)\,\lambda^i_l + \xi\,\lambda^j_l \qquad \lambda_\omega(\xi) = (1-\xi)\,\lambda^i_\omega + \xi\,\lambda^j_\omega$$

The dimensionless coefficient ξ is defined in (6.19) and expresses the ratio s_0/L_e.

Finite Element Equation

The finite element equation is again achieved by introducing a displacement vector, now containing the 2×11 degrees of freedom corresponding to an element

$$\mathbf{u}^e = \left[\mathbf{u}^{ei}, \mathbf{u}^{ej}\right] \tag{6.50}$$

where

$$\mathbf{u}^{ei} = \left[r^i_1, r^i_2, r^i_3, \varphi^i_1, \varphi^i_2, \varphi^i_3, \theta^i, \lambda^i_1, \lambda^i_2, \lambda^i_3, \lambda^i_\omega\right] \tag{6.51}$$

The virtual work equation (6.15) can then be expressed in matrix form by

$$\delta\mathbf{u}^{eT} \cdot \left[\left(\mathbf{K}^e + \mathbf{K}^\kappa\right) \cdot \mathbf{u}^e - \mathbf{f}^e\right] = 0 \tag{6.52}$$

which is similar to (6.43) except that now the dimension of the matrices is 22×22.
The stiffness matrices and the load vector are achieved by adding the out-of-plane terms to the matrices given by (6.24) and (6.45). $\mathbf{K}^e$ and $\mathbf{K}^\kappa$ for the spatial element are given in Appendix E.

6.4.2 Global Analysis for Spatial Element

In the global analysis the local form of the finite element equation in (6.52) has to be transformed in order to assemble a set of elements to constitute the beam structure. The procedure for this is the same as for the plane element.

Orientation of Local Unit Vectors

In case of a spatial beam structure all local components except θ^1 and λ_ω have to be transformed according to a global reference.

In the present formulation the position in space relative to the global reference is related to the direction of the beam axis, i.e. the tangent vector is equal to $\mathbf{e}^0_3$. This means that the rotation of the global unit vector $\hat{\mathbf{e}}_3$ into $\mathbf{e}^0_3$ determines the rotation vector $\boldsymbol{\varphi}^0$.

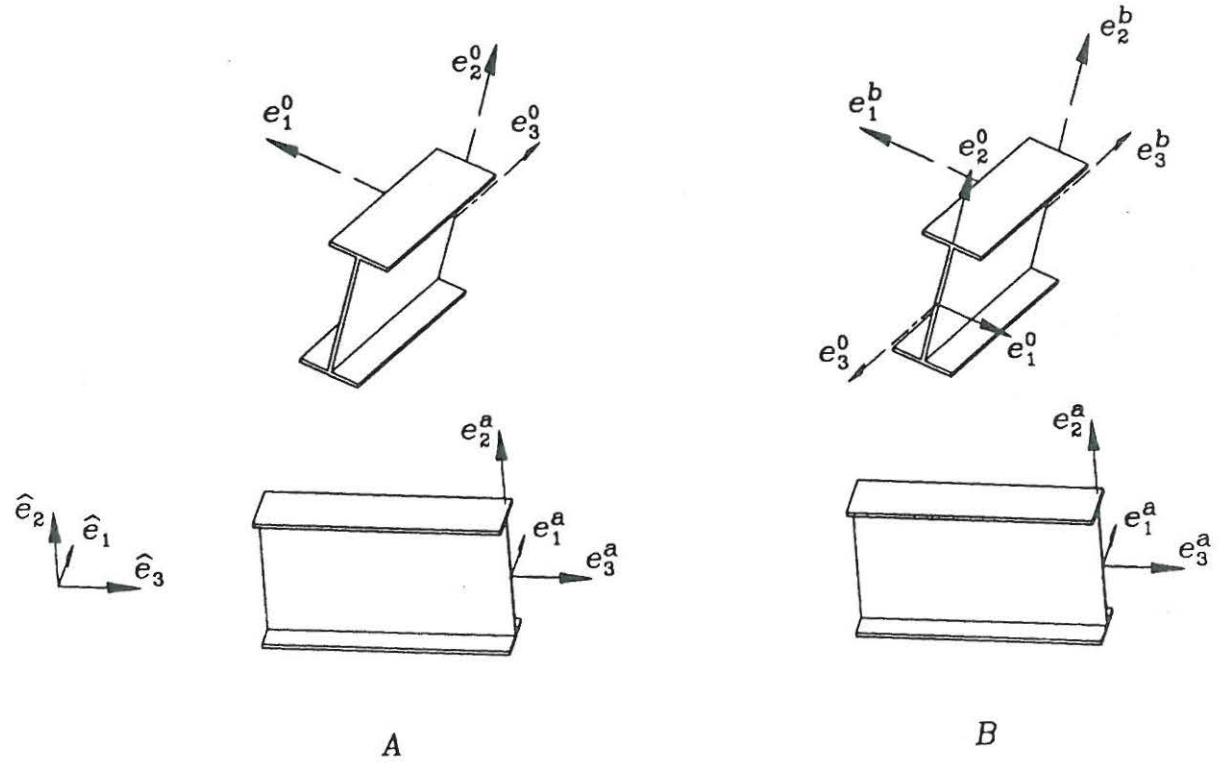

Fig. 6.30: Beam element orientation in space.

Using the orthogonal transformation operator $\mathbf{A}$, $\mathbf{e}_3^0$ is connected to $\hat{\mathbf{e}}_3$ by

$$\mathbf{e}_3^0 = \mathbf{A}(\boldsymbol{\varphi}^0) \cdot \hat{\mathbf{e}}_3 \tag{6.53}$$

Using Appendix A means that the following identities can be established

$$\begin{aligned}
\mathbf{e}_3^0 \cdot \hat{\mathbf{e}}_1 &= A_{13}(\varphi_j^0 \hat{\mathbf{e}}_j) = \frac{\sin\varphi^0}{\varphi^0}\varphi_2^0 + \frac{1-\cos\varphi^0}{\varphi^{0^2}}\varphi_1^0\varphi_3^0 \\
\mathbf{e}_3^0 \cdot \hat{\mathbf{e}}_2 &= A_{23}(\varphi_j^0 \hat{\mathbf{e}}_j) = -\frac{\sin\varphi^0}{\varphi^0}\varphi_1^0 + \frac{1-\cos\varphi^0}{\varphi^{0^2}}\varphi_2^0\varphi_3^0 \\
\mathbf{e}_3^0 \cdot \hat{\mathbf{e}}_3 &= A_{33}(\varphi_j^0 \hat{\mathbf{e}}_j) = 1 - \frac{1-\cos\varphi^0}{\varphi^{0^2}}\left(\varphi_1^{0^2} + \varphi_2^{0^2}\right)
\end{aligned} \tag{6.54}$$

The initial rotation components have to be determined by an iteration procedure. The iteration procedure which can be established from (6.54), with (6.54c) as convergence measure, is only convergent for $\mathbf{e}_3^0 \cdot \hat{\mathbf{e}}_3 > 0$. This means that for $\mathbf{e}_3^0 < 0$ the rotation vector determined via (6.54) has to be expanded by converting the right-hand coordinate system into a left handed system as it is illustrated in Fig. 6.30.

Global Element Stiffness Matrix

Expanding the transformation matrix $\mathbf{A}^e$ from (6.29) into

$$\mathbf{B}^e(\varphi_l^{0^i}\hat{\mathbf{e}}_l) = \begin{bmatrix} \mathbf{A}(\varphi_l^{0^i}\hat{\mathbf{e}}_l) & & & \\ & \mathbf{A}(\varphi_l^{0^i}\hat{\mathbf{e}}_l) & & \\ & & 1 & \\ & & & \mathbf{A}(\varphi_l^{0^i}\hat{\mathbf{e}}_l) \\ & & & & 1 \end{bmatrix}^T . \tag{6.55}$$

means that the transformation of the local stiffness matrix into the global is expressed similar to (6.32), i.e

$$\hat{\mathbf{K}} = \begin{bmatrix} \mathbf{B}_i^e(\varphi_l^{0^i}\hat{\mathbf{e}}_l) & \\ & \mathbf{B}_j^e(\varphi_l^{0^j}\hat{\mathbf{e}}_l) \end{bmatrix}^T \cdot$$

$$\begin{bmatrix} \mathbf{K}_{ii}^e + \mathbf{K}_{ii}^\kappa & \mathbf{K}_{ij}^e + \mathbf{K}_{ij}^\kappa \\ \mathbf{K}_{ji}^e + \mathbf{K}_{ji}^\kappa & \mathbf{K}_{jj}^e + \mathbf{K}_{jj}^\kappa \end{bmatrix} \cdot \begin{bmatrix} \mathbf{B}_i^e(\varphi_l^{0^i}\hat{\mathbf{e}}_l) & \\ & \mathbf{B}_j^e(\varphi_l^{0^j}\hat{\mathbf{e}}_l) \end{bmatrix} \tag{6.56}$$

Assembling

The assembling of the elements is performed in the same way as for the straight beam element leading to the governing equations given in (6.31).

6.5 Conclusions

The purpose of this chapter has been to introduce numerical beam element suitable for an incremental formulation of the stability problem. Based on the linearized version of the virtual work equation a simple but consistent element has been developed. In the development of the beam element the rotation vector is treated as the main variable whereby the differential order is reduced compared with a translation based element.
Assuming the strain deformations to be negligible compared to curvature and warping deformations leads to a simplified formulation where the main variable is the rotation vector. In order to ensure convergence of the element a relationship between rotations and translations has to be incorporated. This is accomplished by incorporating the strain condition $\varepsilon_j = 0$, using the Hellinger-Reissner principle, thereby achieving a mixed formulation. The mixed formulation reduces the quality of the kinematical description but instead the statical behavior is improved which is important in connection with stability analysis. Using this approach, where the rotations are kept in the formulation, linear shape functions can be

used for all involved functions leading to a simple formulation.
The examples performed for the straight and the curved plane element are very promising for especially the statical behavior which means that the element is suitable for stability formulation.

Chapter 7

Analytical Stability Analysis Omitting Strain Deformations

Stability analysis performed in an analytical way is in general very cumbersome and only in a few simple special cases a closed form solution can be obtained. Vlasov (1961) and Timoshenko & Gere (1961) obtained closed form solutions of the critical load for the static determinante beam. Their analyses are only concerned with the determination of the critical load which can be performed by a linear analysis.
The postbuckling behavior of elastic structures has been the subject of research for many years, Koiter (1945). A general theory for buckling and postbuckling behavior of elastic structures was presented by Koiter. The general theory was later developed by for example Thompson & Hunt (1973) and Budiansky (1974). Both obtained an analytical solution for the initial postbuckling behavior of the simply supported column by a perturbation method. During the last twenty years the simply supported column (Euler column) and the cantilever beam have been the subject for postbuckling analysis, see e.g Woolcock & Trahair (1974), Grimaldi & Pignataro (1979) and Szymczak (1980). Further a general treatment giving both theoretical results and experimental verification has been given by Roorda (1980). Despite the difficulties the need for analytical results is obvious because they serve as guidelines for the analysis of more complex structures.

The subject of this chapter is to study the postbuckling behavior of thin-walled beams in analytical sense in order to identify the important parameters and the principal behavior. In order to perform an analytical analysis of some canonical problems in a manageable way some modifications of the general theory presented here have to be made. The general stability equation contains 7 generalized displacements. By assuming negligible strain deformations the stability equation is simplified to be expressed entirely in terms of the rotation vector in Section 7.1. In Section 7.2 the perturbation method is used to describe the bifurcation and initial postbuckling problem in an asymptotic way. Finally examples are given which underline the agreement with the literature and adds new results to the initial postbuckling behavior of thin-walled beams.

7.1 Stability Formulation Neglecting Strain Deformations

The following is used to outline some of the possibilities of the general stability theory developed in the present thesis. It is possible to solve some special problems in an analytical way when some minor assumptions are made. To shown this the starting point is taken in the virtual work equation (3.16). It represents the general formulation, i.e. both strain, bending and torsion deformations are included.

$$\int_0^l \left\{ \left(\frac{d\,\delta\mathbf{r}_a}{ds_0} - \delta\boldsymbol{\varphi} \times \frac{d\mathbf{r}_a}{ds_0} \right) \cdot \mathbf{N}^1 \; + \; \frac{d\,\delta\boldsymbol{\varphi}}{ds_0} \cdot \mathbf{M}^1 \; - \; \delta\boldsymbol{\varphi} \cdot \frac{d\mathbf{r}_a^1}{ds_0} \times \mathbf{N}^0 \right.$$

$$\left. - \; \delta\boldsymbol{\varphi} \cdot \left(\widetilde{\mathbf{A}}(\boldsymbol{\varphi}^1) + \lambda\, \mathbf{A}(\boldsymbol{\varphi}^1) \right) \cdot \mathbf{f}^0 \times \mathbf{p}^0 \; - \; \lambda\, \delta\mathbf{r}_a \cdot \mathbf{p}^0 \right\} ds_0$$

$$- \left[\delta\mathbf{r}_a \cdot \mathbf{N}^1 \; + \; \delta\boldsymbol{\varphi} \cdot \mathbf{M}^1 \right]_0^l \; = \; 0 \tag{7.1}$$

Notice that the warping contribution is not incorporated directly in (7.1). Instead it is the aim to incorporate warping by introducing a warping contribution in the torsional moment M_3^1. This can be accomplished by using the relation between κ_3^1 and θ^1 given in (4.21), which expresses θ^1 in terms of the rotation vector. The reformulation of the torsional moment is carried out because of the simplifications which can be achieved and no major generality is lost.

Solving a stability problem by use of (7.1) in an analytical way is very cumbersome as the general formulation includes 7 state variables ($\mathbf{r}_a^1$, $\boldsymbol{\varphi}^1$ and λ). Instead the virtual work equation can be refomulated by assuming that strain deformations are negligible whereby an unambiguous relation between the translation increment $\mathbf{r}_a^1$ and the rotation increment $\boldsymbol{\varphi}^1$ can be obtained. Assuming that the rotation vector $\boldsymbol{\varphi}^1$ is the main variable in the stability problem the form given in (7.1) is in the following reformulated consistently in order to obtain a formulation which only contains the rotation vector, while the translation vector $\mathbf{r}_a^1$ only appears in connection with the rotation vector in a boundary condition. This procedure leads to a formulation with a reduced order of differentation compared with usual strategies where a strain condition is used to eliminate the bending rotation components.

Force equilibrium in the initial state implies using (2.1) that

$$\mathbf{p}^0 \; = \; -\frac{d\mathbf{N}^0}{ds_0} \tag{7.2}$$

Inserting this relation for $\lambda\delta\mathbf{r}_a \cdot \mathbf{p}^0$ in (7.1) and integration by parts leads to

$$\int_0^l \left\{ \left(\frac{d\,\delta\mathbf{r}_a}{ds_0} - \delta\boldsymbol{\varphi} \times \frac{d\mathbf{r}_a}{ds_0} \right) \cdot \mathbf{N}^1 \; + \; \frac{d\,\delta\boldsymbol{\varphi}}{ds_0} \cdot \mathbf{M}^1 \; - \; \delta\boldsymbol{\varphi} \cdot \frac{d\mathbf{r}_a^1}{ds_0} \times \mathbf{N}^0 \right.$$

$$- \delta\boldsymbol{\varphi} \cdot \left(\widetilde{\mathbf{A}}(\boldsymbol{\varphi}^1) + \lambda\, \mathbf{A}(\boldsymbol{\varphi}^1)\right) \cdot \mathbf{f}^0 \times \mathbf{p}^0 \; - \; \lambda \frac{d\,\delta\mathbf{r}_a}{ds_0} \cdot \mathbf{N}^0 \Bigg\} \, ds_0$$

$$- \left[\delta\mathbf{r}_a \cdot \left(\mathbf{N}^1 - \lambda\, \mathbf{N}^0\right) \; + \; \delta\boldsymbol{\varphi} \cdot \mathbf{M}^1\right]_0^l \; = \; 0 \tag{7.3}$$

The increment in the external load is identified through the load factor λ. From (3.17) it follows that also the boundary term is a function of λ. Considering the force contribution in the boundary term , i.e. the difference between the increment in the internal force $\mathbf{N}^1$ and the increment in the external force $\lambda\, \mathbf{N}^0$ it follows by static considerations that a change in the external force $\lambda\, \mathbf{N}^0$ results in an equivalent change in $\mathbf{N}^1$ as the external force is displacement independent. This means that the force contribution in the boundary term vanishes leaving only the moment contribution. According to this it follows from observing (7.3) that the translation vector only appears as a derivative which implies that a formulation in terms of only the rotation vector is possible.

Often strain deformations are negligible compared to bending and torsional deformations. In the following strain increments are therefore neglected which according to (2.11) implies that

$$\frac{d\delta\mathbf{r}_a}{ds_0} \simeq \delta\boldsymbol{\varphi} \times \frac{d\mathbf{r}_a}{ds_0} \qquad , \qquad \varepsilon_j^1 \simeq 0 \tag{7.4}$$

In addition it follows from Section 4.2 that the relations in (7.4) express an unambiguous relation between the rotation and translation components.

The tangent vectors $d\mathbf{r}_a/ds_0$ and $d\mathbf{r}_a^0/ds_0$ are related to the unit vectors $\mathbf{e}_j$ and $\mathbf{e}_j^0$, respectively by (2.13) which by neglecting strain deformations simplifies to

$$\frac{d\mathbf{r}_a}{ds_0} \simeq \mathbf{e}_3 = \mathbf{A}(\boldsymbol{\varphi}^1) \cdot \mathbf{e}_3^0 \qquad \text{and} \qquad \frac{d\mathbf{r}_a^1}{ds_0} \simeq \mathbf{e}_3 - \mathbf{e}_3^0 = \widetilde{\mathbf{A}}(\boldsymbol{\varphi}^1) \cdot \mathbf{e}_3^0 \tag{7.5}$$

Using these considerations means that the virtual work equation (7.3) now can be expressed solely in terms of the rotation components.

$$\int_0^l \Bigg\{ \frac{d\delta\boldsymbol{\varphi}}{ds_0} \cdot \left(M_j^1 \mathbf{e}_j \; + \; \widetilde{\mathbf{A}}(\boldsymbol{\varphi}^1) \cdot \mathbf{M}^0\right) - \delta\boldsymbol{\varphi} \cdot \left(\widetilde{\mathbf{A}}(\boldsymbol{\varphi}^1) \; + \; \lambda\, \mathbf{A}(\boldsymbol{\varphi}^1)\right) \cdot \mathbf{e}_3^0 \times \mathbf{N}^0$$

$$- \; \delta\boldsymbol{\varphi} \cdot \left(\widetilde{\mathbf{A}}(\boldsymbol{\varphi}^1) \; + \; \lambda\, \mathbf{A}(\boldsymbol{\varphi}^1)\right) \cdot \mathbf{f}^0 \times \mathbf{p}^0 \Bigg\} \, ds_0 \; - \; \left[\delta\boldsymbol{\varphi} \cdot \mathbf{M}^1\right]_0^l \; = \; 0 \tag{7.6}$$

Through the constitutive equations in Section 4.5 the increments M_j^1 are expressed by the rotation vector $\boldsymbol{\varphi}^1$ whereby the virtual work equation is formulated entirely in terms of the increment in the rotation vector.

The form of the virtual work equation in (7.6) can be regarded as an energy formulation as the virtual rotation can be related to the rotation increment via (5.6) as shown in Chapter 5. Hereby the internal work is expressed by $\left(\frac{d\boldsymbol{\varphi}^1}{ds_0} \cdot \mathbf{e}_j\right) M_j^1$ corresponding to a deformation

times the conjugated internal force. Using this approach corresponds to the Galerkin Method and the symmetric properties contained in this formulation makes it in particularly suitable for numerical analysis. Equation (7.6) corresponds to a modification of the weak formulation used in Chapter 6 to develop a numerical beam element.

An alternative form of (7.6), obtainable using integration by parts, would on the other hand be more straight forward for an analytical analysis. The virtual work equation (7.6) contains a term with the derivative of the virtual rotation $\delta\boldsymbol{\varphi}$ and further a boundary term containing $\delta\boldsymbol{\varphi}$. Using integration by parts for these terms a differential formulation can be obtained.

$$\int_0^l \Big\{ -\frac{d}{ds_0}\big(M_j^1 \mathbf{e}_j + \widetilde{\mathbf{A}}(\boldsymbol{\varphi}^1)\cdot\mathbf{M}^0\big) - \big(\widetilde{\mathbf{A}}(\boldsymbol{\varphi}^1) + \lambda\,\mathbf{A}(\boldsymbol{\varphi}^1)\big)\cdot\mathbf{e}_3^0\times\mathbf{N}^0 \\ - \big(\widetilde{\mathbf{A}}(\boldsymbol{\varphi}^1) + \lambda\,\mathbf{A}(\boldsymbol{\varphi}^1)\big)\cdot\mathbf{f}^0\times\mathbf{p}^0\Big\}\cdot\delta\boldsymbol{\varphi}\,ds_0 = 0 \tag{7.7}$$

The form of (7.7) offers the possibility of a straight forward formulation of the nonlinear differential equations as the integrand consists of a scalar product between the virtual rotation $\delta\boldsymbol{\varphi}$ and the modified moment equilibrium equation. The condition $\delta V = 0$ has to be fulfilled for any variation $\delta\boldsymbol{\varphi}$ which means that the term inside the big brackets of the integrand has to vanish identically which leads to a set of differential equations.

In the following a component form of the virtual work equation is presented in two versions corresponding to (7.7) and (7.6) where the first is the weighted form of the differential equations while the second is the energy formulation.

7.1.1 Virtual Work Equation - Differential Formulation

The differential form of the virtual work equation (7.7) can be expressed in terms of components by decomposing the virtual rotation increment in the initial basis, i.e. $\delta\boldsymbol{\varphi} = \delta\varphi_j\,\mathbf{e}_j^0$. It follows that

$$-\int_0^l \Big\{ \frac{d}{ds_0}\big(A_{lj}M_j^1 + \tilde{A}_{lj}M_j^0\big) + e_{lmn}\kappa_m^0\big(A_{nj}M_j^1 + \tilde{A}_{nj}M_j^0\big) \\ + e_{nkl}\big(\tilde{A}_{nm} + \lambda\,A_{nm}\big)\big(\delta_{m3}N_k^0 + \delta_{m\alpha}f_\alpha^0 p_k^0\big)\Big\}\delta\varphi_l\,ds_0 = 0 \tag{7.8}$$

In order to analyse equation (7.8) regarding the components of the rotation vector the expressions for M_j^1 have to be inserted. Substitution of the constitutive equations from Section 4.5 leads to

$$\int_0^l \Big\{ \frac{d}{ds_0}\Big(A_{l\alpha}\big(I_{\alpha\eta}\kappa_\eta^1 + \beta_\eta I_{\eta\alpha}\kappa_3^1\kappa_3^1\big) + \tilde{A}_{l\alpha}M_\alpha^0\Big) \\ + \frac{d}{ds_0}\Big(A_{l3}\Big(\big(K + r_a^2N_3^0 + 2\beta_\alpha M_\alpha^{c0}\big)\kappa_3^1 - \frac{d}{ds_0}\big(I_\omega\frac{d\kappa_3^1}{ds_0}\big)$$

$$+ 2\beta_\eta I_{\eta\alpha}\kappa^1_\alpha\,\kappa^1_3 + \tfrac{1}{2}\,R_a^4 F\kappa^1_3\,\kappa^1_3\,\kappa^1_3\Big) + \tilde{A}_{l3}\,M^0_3\Big)$$

$$+ e_{lmn}\,\kappa^0_m\Big(A_{n\alpha}\Big(I_{\alpha\eta}\kappa^1_\eta + \beta_\eta I_{\eta\alpha}\kappa^1_3\kappa^1_3\Big) + \tilde{A}_{n\alpha}\,M^0_\alpha\Big)$$

$$+ e_{lmn}\,\kappa^0_m\Big(A_{n3}\Big((K + r_a^2 N^0_3 + 2\beta_\alpha M^{c\,0}_\alpha)\,\kappa^1_3 - \frac{d}{ds_0}\Big(I_\omega\frac{d\kappa^1_3}{ds_0}\Big)$$

$$+ 2\beta_\eta I_{\eta\alpha}\kappa^1_\alpha\,\kappa^1_3 + \tfrac{1}{2}\,R_a^4 F\kappa^1_3\,\kappa^1_3\,\kappa^1_3 + \tilde{A}_{l3}\,M^0_3\Big)$$

$$+ e_{nkl}\Big(\tilde{A}_{nm} + \lambda\,A_{nm}\Big)\Big(\delta_{m3}N^0_k + \delta_{m\alpha}f^0_\alpha p^0_k\Big)\Big\}\,\delta\varphi_l\,ds_0 = 0 \tag{7.9}$$

As $\delta V = 0$ has to be fulfilled for any variation $\delta\varphi_l$ equation (7.9) leads to three differential equations corresponding to bending equilibrium ($\delta\varphi_\alpha$) and equilibrium for twisting and warping ($\delta\varphi_3$). Recalling that φ^1_j appears indirectly through the orthogonal transformation operator $A_{lk}(\varphi^1_j)$ and the definition of $\kappa^1_j(\varphi^1_j)$ in (5.11) the term inside the big brackets express a set of non-linear differential equations in terms of φ^1_j.

7.1.2 Virtual Work Equation - Energy Formulation

The energy formulation of the virtual work equation (7.6) can also be written in terms of components if $\delta\boldsymbol{\varphi} = \delta\varphi_j\,\mathbf{e}^0_j$, whereby

$$\int_0^l \Big\{\delta\kappa_j\,M^1_j + \Big(\frac{d\delta\varphi_l}{ds_0} + \delta\varphi_n\,e_{nlm}\,\kappa^0_m\Big)\tilde{A}_{lj}\,M^0_j$$

$$+ e_{lnk}\,\delta\varphi_n\Big(\tilde{A}_{lm} + \lambda\,A_{lm}\Big)\Big(\delta_{m3}N^0_k + \delta_{m\alpha}f^0_\alpha p^0_k\Big)\Big\}\,ds_0$$

$$- \Big[\lambda\sum_{i=1}^{n}\Big(\delta\varphi_n\,e_{nlk}\,P^{0^i}_k\,A_{l\alpha}\,F^{0^i}_\alpha\Big) + \sum_{i=1}^{n}\Big(\delta\varphi_n\,e_{nlk}\,P^{0^i}_k\,\tilde{A}_{l\alpha}\,F^{0^i}_\alpha\Big)\Big]_0^l = 0 \tag{7.10}$$

Notice that the boundary term is expressed by a set of external forces as introduced in Section 2.4. The weak form in (7.10) contains a mixing between virtual variations $\delta\varphi_j$ and increments φ^1_j, and it follows that the virtual quantities can not be extracted in a straight forward way as in (7.9). Instead the relations (5.6) and (5.13) are used to obtain a formulation in terms of φ^1_l solely. Inserting the constitutive equations and by use of the results from Chapter 5 it follows that

$$\int_0^l \Big\{\frac{1}{2}\,\delta\Big(\kappa^1_\alpha\,I_{\alpha\beta}\,\kappa^1_\beta + \kappa^1_3\Big(K + r_a^2 N^0_3 + 2\beta_\alpha M^{c\,0}_\alpha\Big)\kappa^1_3 - \kappa^1_3\,\frac{d}{ds_0}\Big(I_\omega\,\frac{d\kappa^1_3}{ds_0}\Big)$$

$$+\kappa_3^1 2\beta_\eta I_{\eta\alpha}\kappa_\alpha^1\kappa_3^1 + \tfrac{1}{4}\kappa_3^1\kappa_3^1 R_a^4 F\kappa_3^1\kappa_3^1\Big)$$

$$-\delta\kappa_j^1 M_l^0\tilde{A}_{lj} + \delta\tilde{A}_{kn}\left(\delta_{m3}N_k^0 + \delta_{m\alpha}f_\alpha^0 p_k^0\right)\left(\lambda\delta_{jn} + \tilde{A}_{jn}\right)\Big\} ds_0$$

$$-\left[\delta\tilde{A}_{kn}\sum_{i=1}^{n}\left(P_k^{0^i}F_\alpha^{0^i}\right)\left(\lambda\delta_{\alpha n} + \tilde{A}_{\alpha n}\right)\right]_0^l = 0 \tag{7.11}$$

As well as for equation (7.9) in Section 7.1.1 the energy formulation likewise contains a nonlinear problem. The subject of the next section is therefore to introduce a method of solution for this kind of nonlinear problems.

7.2 Perturbation Method

The non-linear problem of the equations (7.9) and (7.11) can be solved by use of a perturbation method. The main idea behind a perturbation method in this connection is to reduce the non-linear differential equations using an expansion technique to a set of sequentially solvable linear differential equations. The asymptotic non-linear solution is then synthesized from the linear ones. This method for postbuckling analysis has been introduced by Koiter (1945) and developed by e.g. Budiansky (1974) with application to continua and finite-dimensional systems in general. In this section the perturbation method is used to derive the governing equations for a postbuckling analysis of thin-walled beams.

Using the expansion technique it is convenient to introduce a small perturbation parameter ξ which is used to represent a measure of progress along the equilibrium curve, i.e. the solution. Thus, it is assumed that the solution can be represented by the following expansions of the rotation vector φ^1 and the load parameter λ

$$\begin{aligned}\varphi_j^1 &= \tilde{\varphi}_j^1\xi + \tilde{\varphi}_j^2\xi^2\ldots\\ \lambda &= \lambda_1\xi + \lambda_2\xi^2\ldots\end{aligned} \tag{7.12}$$

The expansions means that the unknown functions φ_j^1 and λ are expressed by a set of shape functions $\tilde{\varphi}_j^i$ and λ_i, respectively and a new state variable ξ. The order of the perturbation parameter ξ is used as a measure in analysis of the terms contained in the stability equations (7.9) and (7.11).

Arranging the operators of (7.9) and (7.11) according to the order of the new variable ξ is necessary for a closer analysis to be performed. The component form of the orthogonal transformation operator is given by (see e.g. Appendix A)

$$A_{lj}(\tilde{\varphi}_k^i,\xi) \simeq \delta_{lj} + \left[e_{lnj}\tilde{\varphi}_n^1\right]\xi + \left[e_{lnj}\tilde{\varphi}_n^2 + \tfrac{1}{2}e_{lnm}\tilde{\varphi}_n^1\tilde{\varphi}_k^1 e_{mkj}\right]\xi^2$$

$$+ \left[e_{lnj} \left(\widetilde{\varphi}_n^3 - \tfrac{1}{3!} \widetilde{\varphi}_n^1 \widetilde{\varphi}_k^1 \widetilde{\varphi}_k^1 \right) + \tfrac{1}{2} e_{lnm} \left(\widetilde{\varphi}_n^2 \widetilde{\varphi}_k^1 + \widetilde{\varphi}_n^1 \widetilde{\varphi}_k^2 \right) e_{mkj} \right] \xi^3 \ \ldots \quad (7.13)$$

Using (5.11) it follows from Appendix A that the curvature components are given by

$$\kappa_j^1(\widetilde{\varphi}_k^i, \xi) \ \simeq \ \widetilde{\kappa}_j^1 \, \xi \ + \ \left[\widetilde{\kappa}_j^2 + \tfrac{1}{2} e_{knj} \widetilde{\kappa}_k^1 \widetilde{\varphi}_n^1 \right] \xi^2$$

$$+ \left[\widetilde{\kappa}_j^3 + \tfrac{1}{2} e_{knj} (\widetilde{\kappa}_k^2 \widetilde{\varphi}_n^1 + \widetilde{\kappa}_k^1 \widetilde{\varphi}_n^2) \ + \ \tfrac{1}{3!} \widetilde{\kappa}_k^1 \, e_{knm} \, \widetilde{\varphi}_n^1 \, \widetilde{\varphi}_l^1 \, e_{mlj} \right] \xi^3 \ \ldots \quad (7.14)$$

where

$$\widetilde{\kappa}_j^i \ = \ \frac{d\widetilde{\varphi}_j^i}{ds_0} + \widetilde{\varphi}_n^i e_{njm} \kappa_m^0 \quad (7.15)$$

which is consistent with (5.11).

Finally the expanded version of the relation between virtual variations and finite variations of the rotation components is given by (5.6), i.e.

$$\delta\varphi_j \ = \ \delta\varphi_k^1 \, B_{jk}$$

$$= \ \delta\varphi_j^1 \ + \ \tfrac{1}{2} \delta\varphi_k^1 \, e_{knj} \, \varphi_n^1 \ + \ \tfrac{1}{3!} \delta\varphi_k^1 \, e_{kmn} \, \varphi_n^1 \varphi_l^1 \, e_{jlm} \quad \ldots \quad (7.16)$$

Using these expressions in (7.9) and (7.11) it is now possible to solve the non-linear problem in an asymptotic way. The idea is that as long as $\widetilde{\varphi}_j^1$ are unknown functions then ξ is a scaling factor, but if $\widetilde{\varphi}_j^1$ have been determined then ξ represents the state variable. This is the subject of the sections 7.2.1 and 7.2.2. Even though the differential (7.9) and the energy (7.11) formulations of the virtual work are *identical* expressions both formulations are analysed by the perturbation method. This is carried out in order to achieve a complete formulation which in straight forward way enables one to analyse the initial postbuckling behavior of a beam structure.

7.2.1 Stability Analysis by Perturbation - Differential Formulation

Using the expansions of $\boldsymbol{\varphi}^1$ and λ it is now possible to investigate the first version of the virtual work equation in detail. The term inside the big brackets of the integrand in (7.9) can be arranged according to the order of the generalized coordinate ξ

$$\int_0^l \Big\{ \quad \left[F_l(\widetilde{\varphi}_j^1, \lambda_0) + \bar{F}_l(\lambda_1, \lambda_0) \right] \xi \, \delta\varphi_l$$

$$+ \left[F_l(\widetilde{\varphi}_j^2, \lambda_0) + \bar{F}_l(\lambda_2, \lambda_0) - R_l^2(\widetilde{\varphi}_j^1, \lambda_0, \lambda_1) \right] \xi^2 \, \delta\varphi_l$$

$$\ldots .$$

$$+ \left[F_l(\tilde{\varphi}_j^n, \lambda_0) + \bar{F}_l(\lambda_n, \lambda_0) - R_l^n(\tilde{\varphi}_j^{n-1}, \tilde{\varphi}_j^{n-2}, \ldots, \lambda_{n-1}) \right] \xi^n \, \delta\varphi_l \Big\} ds_0 = 0 \quad (7.17)$$

In (7.17) it has been used that the initial stress terms N_j^0, M_j^0 and p_j^0 can be expressed by the single load parameter λ_0 by the identities in (3.15). In each coefficient of ξ, ξ^2, . . , ξ^n in the integrand F_l indicates the part which contains the displacement functions $\tilde{\varphi}_l^i$ and the initial stresses while $\bar{F}_l$ contains the load factor λ_i. Finally R_l^i is the remaining part which is expressed by lower order terms in $\tilde{\varphi}_l^i$ and λ_i than the remaining functions constituting the particular coefficient. It has been indicated that F_l and $\bar{F}_l$ preserves a general format which then remains to be shown.

Inserting the expanded versions of $A_{lj}(\varphi_k^1)$ and $\kappa_j^1(\varphi_k^1)$ in (7.9) and rearranging by use of the equilibrium equations for the initial state leads to the following form of F_l

$$\begin{aligned} F_\alpha(\tilde{\varphi}_j^i, \lambda_0) &= -\frac{d}{ds_0}\left(I_{\alpha\beta} \tilde{\kappa}_\beta^i \right) + \frac{d}{ds_0}\left(e_{\alpha\beta} \kappa_\beta^0 I_\omega \frac{d\tilde{\kappa}_3^i}{ds_0} \right) \\ &\quad - e_{\alpha\beta}\kappa_\beta^0 \left(K + r_a^2 N_3^0 + 2\beta_\eta M_\eta^{c^0} \right) \tilde{\kappa}_3^i + \kappa_3^0 e_{\alpha\gamma} I_{\gamma\beta} \tilde{\kappa}_\beta^i \\ &\quad + e_{\alpha\beta} M_\beta^0 \tilde{\kappa}_3^i - M_3^0 e_{\alpha\beta} \tilde{\kappa}_\beta^i + N_3^0 \tilde{\varphi}_\alpha^i - N_\alpha^0 \tilde{\varphi}_3^i + e_{\alpha\beta} f_\beta^0 p_\gamma^0 e_{\gamma\eta} \tilde{\varphi}_\eta^i \end{aligned} \quad (7.18)$$

$$\begin{aligned} F_3(\tilde{\varphi}_j^i, \lambda_0) &= -\kappa_\gamma^0 e_{\gamma\alpha} I_{\alpha\beta} \tilde{\kappa}_\beta^i - \frac{d}{ds_0}\left(\left(K + r_a^2 N_3^0 + 2\beta_\eta M_\eta^{c^0} \right) \tilde{\kappa}_3^i \right) \\ &\quad + \frac{d^2}{ds_0^2}\left(I_\omega \frac{d\tilde{\kappa}_3^i}{ds_0} \right) + M_\alpha^0 e_{\alpha\beta} \tilde{\kappa}_\beta^i - p_3^0 f_\alpha^0 \tilde{\varphi}_\alpha^i + p_\alpha^0 f_\alpha^0 \tilde{\varphi}_3^i \end{aligned} \quad (7.19)$$

The process leading to the form of (7.18) and (7.19) is further described in Appendix B. It follows that F_α and F_3 are linear functions of the rotation components $\tilde{\varphi}_j^i$. The function F_α may be regarded as the governing differential equations for bending while F_3 is the one for twisting and warping.

The part containing the load factor $\bar{F}_l$ is given by

$$\bar{F}_l(\lambda_i, \lambda_0) = \lambda_i \, e_{mkl} \left(\delta_{m3} \, N_k^0 + \delta_{m\alpha} \, f_\alpha^0 p_k^0 \right) \quad (7.20)$$

Splitting (7.20) into

$$\bar{F}_\alpha(\lambda_i, \lambda_0) = \lambda_i \, e_{\alpha\beta} \left(f_\beta^0 p_3^0 - N_\beta^0 \right) \quad , \quad \bar{F}_3(\lambda_i, \lambda_0) = \lambda_i \, f_\alpha^0 e_{\alpha\beta} p_\beta^0 \quad (7.21)$$

reveals that for lateral loading or if the distributed force acts nonsymmetrically (see e.g. Fig. 7.1) then a direct coupling between λ_i and $\tilde{\varphi}_l^i$ exists.

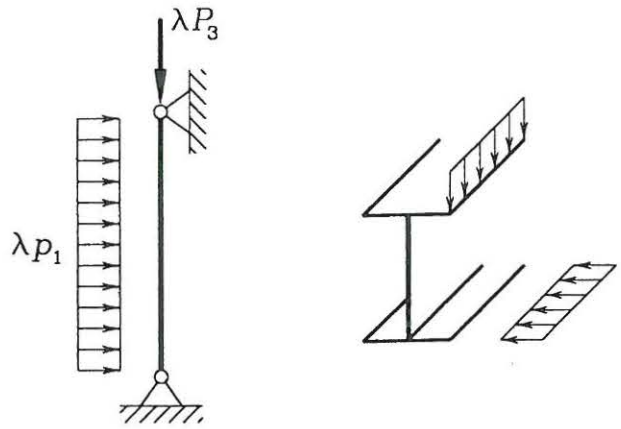

Fig. 7.1: a) Lateral loading. b) Nonsymmetric loading.

This means that for these special loading cases no well-defined eigenvalue problem arises a priori.

Observing (7.18), (7.19) and (7.20) it is obvious that the coefficients of (7.17) preserve a general format, meaning that only the term R_l^i which in each step indicates an effect from a previous state has to be determined for each step in i. The functions R_l^i are further examined in Appendix C.

From (7.17) it follows that the coefficients of ξ, ξ^2,.., ξ^n in the integrand must vanish separately, for all admissible variations in $\delta\varphi_l$. This leaves a set of linear differential equations which can be used successively to determine $\tilde{\varphi}_j^n$.

$$F_l\big(\tilde{\varphi}_j^i, \lambda_0\big) \;=\; R_l^i\big(\tilde{\varphi}_j^{i-1}, \tilde{\varphi}_j^{i-2}, .., \lambda_{i-1}\big) \;-\; \bar{F}_l\big(\lambda_i, \lambda_0\big) \tag{7.22}$$

Observing equation (7.22) it appears that for $i = 1$ and $\bar{F}_l = 0$ an eigenvalue problem arises which determines λ_0 and $\tilde{\varphi}_j^1$ while for $i \geq 2$ (7.22) leads to a set of nonhomogeneous linear differential equations. In most problems the term $\bar{F}_l$ is not coupled with the critical load but in the particular case where $\bar{F}_l \neq 0$ (see e.g. Fig. 7.1) the strategy is to determine the critical load λ_0 by omitting $\bar{F}_l$ leading to an eigenvalue problem and then to use the critical load as an input to the complete expressions in (7.22). From these equations $\tilde{\varphi}_j^i$ may then be determined direct or as a function of λ_i. In case of symmetric lateral loading the effect from $\bar{F}_l$ is only connected with the plane of the loading which leaves the critical load unaffected. None of these problems are considered in a particular example, but their contribution is nevertheless accounted for throughout this chapter.

As indicated above the left-hand side preserves a general format meaning that except for the right-hand side the differential equations (7.22) are self-similar which in general means that the left-hand side corresponds to an eigenvalue problem. In order to obtain an expansion of φ_l^1 which is uniformly convergent the vectors $\tilde{\boldsymbol{\varphi}}^i$ and $\tilde{\boldsymbol{\varphi}}^j$ $(i \neq j)$ have to be chosen as ortogonal whereby the possibility of secular terms can be eliminated, see e.g. Thomson & Hunt (1973). This leads to an orthonormality condition stating that

$$\int_0^l F_l\big(\tilde{\varphi}_j^i, \lambda_0\big)\, \xi^i\, \delta\big(\tilde{\varphi}_l^k \xi^k\big)\, ds_0 \;=\; 0 \qquad \text{for} \qquad i \neq k \tag{7.23}$$

Equation (7.23) implies that the rotation vector $\boldsymbol{\varphi}^1$ is constituted by a set of orthogonal

vectors $\tilde{\varphi}^i$.

Following this procedure leaves a set of equations which can be used to determine the load factor coefficients λ_i. Using the orthonormality condition it follows from (7.17) that

$$\int_0^l R_l^i\left(\tilde{\varphi}_j^{i-1}, .., \lambda_{i-1}\right) \xi^i \, \delta\left(\tilde{\varphi}_l^k \, \xi^k\right) \, ds_0 \; = \; 0 \tag{7.24}$$

can be used successively to determine λ_{i-1}. Inserting the expressions for $\tilde{\varphi}_j^{i-1}$ determined from (7.22) means that the integrations in (7.24) can be performed leading to a functional in ξ. This implies that ξ then represents the state variable meaning that variations in (7.24) are to be taken with respect ξ. This leads to a stepwise solution process where

$$\lambda_0 \quad \rightarrow \quad \tilde{\varphi}_j^1 \quad \rightarrow \quad \lambda_1 \quad \rightarrow \quad \tilde{\varphi}_j^2 \quad \rightarrow \quad \lambda_2 \qquad \text{and so on} \tag{7.25}$$

where λ_0 is determined by solving an eigenvalue problem whereby the following terms can be found by successively use of (7.22) and (7.24).

7.2.2 Stability Analysis by Perturbation - Energy Formulation

In the previos section it was stated that for problems concerning only distributed forces the initial postbuckling behavior can be determined by use of (7.22) and (7.24). In order to handle problems involving concentrated loads in a direct way an alternative to especially (7.24) is derived from (7.11). Inserting the expanded versions of φ_j^1 means that (7.11) can be arranged according to the order of the parameter ξ.

$$\begin{aligned}
0 \; = \; \delta\Big(& \Big[K_{11}^2(\tilde{\varphi}_j^1;\tilde{\varphi}_j^1) + G_{11}^2(\tilde{\varphi}_j^1;\tilde{\varphi}_j^1,\lambda_0) + G_{10}^2(\tilde{\varphi}_j^1;\lambda_1)\Big]\,\xi^2 \\
+ & \Big[K_{21}^3(\tilde{\varphi}_j^1;\tilde{\varphi}_j^2) + K_{11}^3(\tilde{\varphi}_j^1;\tilde{\varphi}_j^1) + G_{20}^3(\tilde{\varphi}_j^2;\lambda_1) + G_{21}^3(\tilde{\varphi}_j^2;\tilde{\varphi}_j^1,\lambda_0) \\
& + G_{10}^3(\tilde{\varphi}_j^1;\lambda_2) + G_{11}^1(\tilde{\varphi}_j^2;\tilde{\varphi}_j^1,\lambda_0,\lambda_1) + G_{21}^3(\tilde{\varphi}_j^1;\tilde{\varphi}_j^2,\lambda_0)\Big]\,\xi^3 \\
+ & \Big[K_{31}^4(\tilde{\varphi}_j^3;\tilde{\varphi}_j^1) + K_{22}^4(\tilde{\varphi}_j^2;\tilde{\varphi}_j^2) + K_{21}^4(\tilde{\varphi}_j^2;\tilde{\varphi}_j^1) + K_{11}^4(\tilde{\varphi}_j^1;\tilde{\varphi}_j^1) \\
& + G_{30}^4(\tilde{\varphi}_j^3;\lambda_1) + G_{31}^4(\tilde{\varphi}_j^3;\tilde{\varphi}_j^1,\lambda_0) + G_{20}^4(\tilde{\varphi}_j^2;\lambda_2) + \\
& + G_{21}^4(\tilde{\varphi}_j^2;\tilde{\varphi}_j^1,\lambda_0,\lambda_1) + G_{22}^4(\tilde{\varphi}_j^2;\tilde{\varphi}_j^2,\lambda_0) + G_{10}^4(\tilde{\varphi}_j^1;\lambda_3) + \\
& + G_{11}^4(\tilde{\varphi}_j^1;\tilde{\varphi}_j^1,\lambda_0,\lambda_1,\lambda_2) + G_{12}^4(\tilde{\varphi}_j^1;\tilde{\varphi}_j^2,\lambda_0,\lambda_1) + G_{13}^4(\tilde{\varphi}_j^1;\tilde{\varphi}_j^3,\lambda_0)\Big]\,\xi^4 \\
& \qquad . \; . \; . \quad . \; . \; . \quad . \; . \; . \quad . \; . \; . \qquad \Big)
\end{aligned} \tag{7.26}$$

In each set of square brackets the terms represent a particular order in ξ, i.e. ξ^2, ξ^3,..., ξ^n which implies that each set represents an equation which has to be identical zero. The functions K and G represent the elastic energy and the load potential, respectively. The splitting into different subterms is performed because of the amount of terms connected to the higher order coefficients in (7.26) and by the decomposition a general format in the functions is partially achieved.

The function K_{ij}^{i+j} is defined by

$$K_{ij}^{i+j}\left(\widetilde{\varphi}_l^i;\widetilde{\varphi}_l^j\right) = \int_0^l \frac{1}{2}\Big\{\widetilde{\kappa}_\alpha^i\, I_{\alpha\beta}\,\widetilde{\kappa}_\beta^j + \frac{d\widetilde{\kappa}_3^i}{ds_0} I_\omega \frac{d\widetilde{\kappa}_3^j}{ds_0} + \widetilde{\kappa}_3^i\left(K + r_a^2 N_3^0 + 2\beta_\alpha M_\alpha^{c\,0}\right)\widetilde{\kappa}_3^j\Big\}\, ds_0 \tag{7.27}$$

The function G_{j0}^i which contains the load increment factors is given by

$$G_{j0}^i\left(\widetilde{\varphi}_l^i;\lambda_{i-j}\right) = \lambda_{i-j}\left(\int_0^l \left\{\widetilde{\varphi}_n^i\, e_{nkm}\left(\delta_{m3}N_k^0 + \delta_{m\alpha}f_\alpha^0 p_k^0\right)\right\} ds_0 - \Big[\sum_{i=1}^{n}\left(P_k^{0i}\,\widetilde{\varphi}_m^i\, e_{km\alpha}\, F_\alpha^{0i}\right)\Big]_0^l\right) \tag{7.28}$$

The function G_{ij}^{i+j} is defined by

$$\delta G_{ij}^{i+j}\left(\widetilde{\varphi}_l^i;\widetilde{\varphi}_l^j,\lambda_0\right) = \int_0^l \Big\{\delta\widetilde{\kappa}_k^i\, e_{knl}\, M_l^0\,\widetilde{\varphi}_n^j + \delta\widetilde{\varphi}_m^i\, e_{mnk}\left(N_k^0(\delta_{3j}-\varepsilon_j^0) + p_k^0 f_\alpha^0\delta_{\alpha j}\right) e_{jpn}\,\widetilde{\varphi}_p^j\Big\}\, ds_0 - \Big[\delta\widetilde{\varphi}_m^i\, e_{mnk}\sum_{i=1}^{n}\left(P_k^{0i}\,F_\alpha^{0i}\right) e_{jpn}\,\widetilde{\varphi}_p^j\Big]_0^l \tag{7.29}$$

Notice that in case of the load terms the finite variation is connected to a particular rotation component while for the elastic terms the symmetry properties are used to avoid this. This is in agreement with the results obtained in Chapter 5 regarding the relation between virtual work and potential energy. The remaining functions are given in Appendix D.

The virtual work equation in (7.26) can be used in two stages. The terms inside each set of square brackets represents a particular order in ξ and therefore they have to be identically zero. This requirement can be used to obtain the energy formulation of (7.22) and (7.24). The displacement functions $\widetilde{\varphi}_l^i$ can be determined due to the assumption that only this particular set is sensitive to variations. This leads to the general form

$$\delta K_{ii}^{2i}\left(\tilde{\varphi}_l^i;\tilde{\varphi}_l^i\right) + \delta K_{ij}^{2i}\left(\tilde{\varphi}_l^i;\tilde{\varphi}_l^j\right) + \delta G_{ii}^{2i}\left(\tilde{\varphi}_l^i;\tilde{\varphi}_l^i,\lambda_0\right) + \delta G_{ij}^{2i}\left(\tilde{\varphi}_l^i;\tilde{\varphi}_l^j,..,\lambda_j\right) = 0$$

$$j = (1,..,i-1) \tag{7.30}$$

from which $\tilde{\varphi}_l^i$ can be determined. It follows from (7.30), as also mentioned in Section 7.2.1, that for some special loading cases no well-defined eigenvalue problem arises directly. The energy form of the orthonormality condition in (7.23) is given by

$$\delta K_{ij}^{i+j}\left(\tilde{\varphi}_l^i;\tilde{\varphi}_l^j\right) + \delta G_{ij}^{i+j}\left(\tilde{\varphi}_l^i;\tilde{\varphi}_l^j,\lambda_0\right) = 0 \qquad i \neq k \tag{7.31}$$

If the displacement functions $\tilde{\varphi}_l^1, \ldots, \tilde{\varphi}_l^i$ have been determined from (7.30) means that the conditions of (7.26) render a set of functionals in ξ which can be used to determine λ_{i-1}. Further using the condition (7.31) in a particular coefficient of (7.26) means that the remaining terms associated with shape functions $\tilde{\varphi}_l^j$ where $j < i$ can be used to determine the load increment factors λ_i as each coefficient has to vanish identically. A general form of these equations is not obtainable from (7.26), but in Section 7.4 the equations necessary for determination of λ_1 and λ_2 are presented.

7.3 Bifurcation Analysis

The buckling load or critical load λ_0 determines the transition point corresponding to the beginning of an instability phenomen. Therefore the buckling load λ_0 has to be found corresponding to $\lambda = 0$. The bifurcation problem is then described by

$$\int_0^l F_l\left(\tilde{\varphi}_j^1,\lambda_0\right)\delta\tilde{\varphi}_l^1 \, ds_0 = 0 \tag{7.32}$$

This problem can be solved in two different ways either by solving the linear differential equations given by $F_l = 0$ directly or by use of numerical methods where the symmetric form given in (7.30) is preferable. The first is referred to as the strong form while the second is the weak form. Only the strong form is analysed in detail in this section dealing with the analytical approach. The weak form for a bifurcation analysis is treated separately in Chapter 8.

7.3.1 Linear Differential Equations

The condition stating that $\delta V = 0$ has to be fulfilled for any variation in φ_j. Using the first set of differential equations in (7.22) and assuming that $\bar{F}_l(\lambda_1,\lambda_0) = 0$ means that λ_0 can be found from a homogeneous set of differential equations expressed by the identity

$$F_l\left(\tilde{\varphi}_j^1,\lambda_0\right) = 0 \tag{7.33}$$

Using the identity of (3.15) the governing differential equation for flexure can be found from (7.18) as

$$
\begin{aligned}
&-\frac{d}{ds_0}\Big(I_{\alpha\beta}\tilde{\kappa}^1_\beta\Big) - e_{\alpha\beta}\kappa^0_\beta K\,\tilde{\kappa}^1_3 + \frac{d}{ds_0}\Big(e_{\alpha\beta}\kappa^0_\beta I_\omega \frac{d\tilde{\kappa}^1_3}{ds_0}\Big) + \kappa^0_3 e_{\alpha\gamma} I_{\gamma\beta}\tilde{\kappa}^1_\beta \\
&+ \lambda_0\Big[e_{\alpha\beta}\bar{M}^0_\beta\tilde{\kappa}^1_3 - \bar{M}^0_3 e_{\alpha\beta}\tilde{\kappa}^1_\beta + \bar{N}^0_3\tilde{\varphi}^1_\alpha - \bar{N}^0_\alpha\tilde{\varphi}^1_3 \\
&\quad + e_{\alpha\beta}f^0_\beta\bar{p}^0_\gamma e_{\gamma\eta}\tilde{\varphi}^1_\eta - e_{\alpha\beta}\kappa^0_\beta\Big(r_a^2\bar{N}^0_3 + 2\beta_\eta\bar{M}^{c^0}_\eta\Big)\tilde{\kappa}^1_3\Big] = 0
\end{aligned}
\tag{7.34}
$$

The governing equation for torsion and warping is given by (7.19), i.e.

$$
\begin{aligned}
&-\kappa^0_\gamma e_{\gamma\alpha} I_{\alpha\beta}\tilde{\kappa}^1_\beta - \frac{d}{ds_0}\Big(K\,\tilde{\kappa}^1_3\Big) + \frac{d^2}{ds_0^2}\Big(I_\omega\frac{d\tilde{\kappa}^1_3}{ds_0}\Big) \\
&+ \lambda_0\Big[\bar{M}^0_\alpha e_{\alpha\beta}\tilde{\kappa}^1_\beta - \frac{d}{ds_0}\Big(\Big(r_a^2\bar{N}^0_3 + 2\beta_\eta\bar{M}^{c^0}_\eta\Big)\tilde{\kappa}^1_3\Big) - \tilde{\varphi}^1_\alpha f^0_\alpha\bar{p}^0_3 + \bar{p}^0_\alpha f^0_\alpha\tilde{\varphi}^1_3\Big] = 0
\end{aligned}
\tag{7.35}
$$

Even if the cross-sectional parameters are constant the coefficients in (7.34) and (7.35) may depend on the arc-length coordinate s_0 through the loads and internal forces. This implies that closed form solutions only can be obtained in special cases.

7.4 Asymptotic Postbuckling Analysis

If the critical load λ_0 and the buckling form $\tilde{\varphi}^1_j$ have been determined from (7.22) the postbuckling behavior can be examined in an asymptotic way. An asymptotic postbuckling analysis can be performed by inserting the buckled form and demanding stationarity in the higher-order terms.

Differential Formulation

It follows from Section 7.2.1 that if λ_0 and $\tilde{\varphi}^1_j$ have been determined then λ_1 can be determined from (7.24), i.e.

$$
\int_0^l R^2_l\big(\tilde{\varphi}^1_j, \lambda_0, \lambda_1\big)\,\tilde{\varphi}^1_l\,ds_0 = 0 \tag{7.36}
$$

Continuing the solution process $\tilde{\varphi}^2_j$ can now be determined from the next set of linear differential equations given by (7.22), i.e.

$$
F_l\big(\tilde{\varphi}^2_j, \lambda_0\big) = R^2_l\big(\tilde{\varphi}^1_j, \lambda_0, \lambda_1\big) - \bar{F}_l\big(\lambda_2, \lambda_0\big) \tag{7.37}
$$

From (7.37) it follows that $\tilde{\varphi}^2_j$ in some cases may not be determined direct but as a function of λ_2. Inserting the expressions for $\tilde{\varphi}^2_j$ in the next term of (7.24) means that λ_2 can be

determined from

$$\int_0^l R_l^3\left(\tilde{\varphi}_j^2, \tilde{\varphi}_j^1, \lambda_0, \lambda_1, \lambda_2\right) \tilde{\varphi}_l^1 \, ds_0 \;=\; 0 \tag{7.38}$$

This completes the postbuckling analysis as λ_1 and λ_2 indicates the initial postbuckling behavior.

Energy Formulation

In general a solution by the energy method follows the same stages as for differential formulation. If λ_0 and $\tilde{\varphi}_j^1$ have been determined from (7.30) it is possible to determine λ_1 from the third order coefficient in (7.26). Using (7.30) and (7.31) means that λ_1 can be found from

$$\delta K_{11}^3\left(\tilde{\varphi}_j^1; \tilde{\varphi}_j^1\right) + \delta G_{11}^3\left(\tilde{\varphi}_j^1; \tilde{\varphi}_j^1, \lambda_0, \lambda_1\right) + \delta G_{20}^3\left(\tilde{\varphi}_j^2; \lambda_1\right) \;=\; 0 \tag{7.39}$$

where variations are performed with respect to ξ and $\tilde{\varphi}_j^2$ has to be determined from (7.37). Equation (7.39) contains the remaining terms of the third order coefficient in (7.26) which have to be zero in order to make this coefficient identical zero.

Finally λ_2 can be found from the remaining terms of the fourth order coefficient in (7.26) leading to the identity

$$\begin{aligned} &\delta K_{11}^4\left(\tilde{\varphi}_j^1; \tilde{\varphi}_j^1\right) + \frac{1}{2}\delta K_{12}^4\left(\tilde{\varphi}_j^1; \tilde{\varphi}_j^2\right) + \delta G_{12}^4\left(\tilde{\varphi}_j^1; \tilde{\varphi}_j^2, \lambda_0, \lambda_1\right) \\ &+ \delta G_{11}^4\left(\tilde{\varphi}_j^1; \tilde{\varphi}_j^1, \lambda_0, \lambda_1, \lambda_2\right) + \delta G_{20}^4\left(\tilde{\varphi}_j^2; \lambda_2\right) \;=\; 0 \end{aligned} \tag{7.40}$$

where $\tilde{\varphi}_j^1$, $\tilde{\varphi}_l^2$ and λ_1 are supposed to be known. This means that (7.40) is a functional in terms of ξ.

This completes the set of equations which is necessary in order to perform an asymptotic analysis of the initial postbuckling behavior.

7.5 Examples - Simply Supported Beam

In order to give an impression on the possibilities of the present theory some specialised examples are given. These examples represent some of the most popular subjects of the

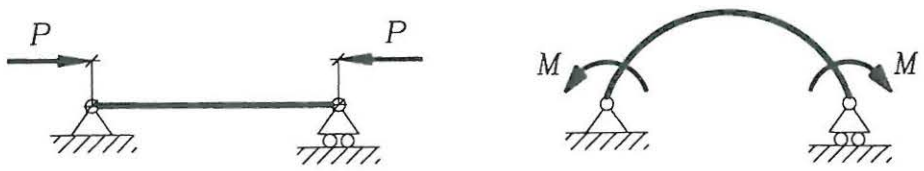

Fig. 7.2: Specialised examples.

buckling and postbuckling studies.
The simply supported beam is a special example where it is possible to solve some *simple* cases in an analytical way. In Fig. 7.2 two examples are given where the statics makes it possible to outline some generalities in a buckling and postbuckling analysis. The first is the simply supported beam subjected to eccentric axial concentrated endloads, sometimes referred to as the Euler column. The second is the curved beam subjected to in-plane pure bending.
Special for the examples shown in Fig. 7.2 is that

$$N_\alpha^0 = M_3^0 = \kappa_3^0 = 0 \quad , \quad N_3^0 = const. \, , \quad M_\alpha^{c\,0} = const. \, , \quad \kappa_\alpha^0 \simeq const. \tag{7.41}$$

The approximation for κ_α^0 is only valid for small deflections. The internal forces N_3^0 and $M_\alpha^{c\,0}$ can be determined by simple statics while the initial curvature may partly be caused by the external loads and partly as an initial *imperfection.*

7.5.1 Buckling Analysis

The buckling analysis of the simply supported beam is performed by use of the strong form given in Section 7.3.1.

Linear Differential Equations for the Specialised Examples

In the determination of the critical load it is assumed that the initial curvature is constant. Inserting the relations of (7.41) in (7.34) leads to the linear differential equations for bending

$$\begin{aligned} &- \frac{d}{ds_0}\Big(I_{\alpha\beta}\tilde{\kappa}_\beta^1\Big) - e_{\alpha\beta}\kappa_\beta^0\Big(K + r_a^2 N_3^0 + 2\beta_\eta M_\eta^{c0}\Big)\tilde{\kappa}_3^1 + e_{\alpha\beta}\kappa_\beta^0 \frac{d}{ds_0}\Big(I_\omega \frac{d\tilde{\kappa}_3^1}{ds_0}\Big) \\ &+ N_3^0\tilde{\varphi}_\alpha^1 + e_{\alpha\beta}\Big(e_{\beta\gamma}(c_\gamma - a_\gamma)N_3^0 + M_\beta^{c0}\Big)\tilde{\kappa}_3^1 + e_{\alpha\beta}f_\beta^0 p_\gamma^0 e_{\gamma\eta}\tilde{\varphi}_\eta^1 = 0 \end{aligned} \tag{7.42}$$

Further inserting in (7.35) leads to the governing equation for torsion and warping

$$\begin{aligned} &- \kappa_\gamma^0 e_{\gamma\alpha} I_{\alpha\beta}\tilde{\kappa}_\beta^1 - \frac{d}{ds_0}\Big(\Big(K + r_a^2 N_3^0 + 2\beta_\eta M_\eta^{c0}\Big)\tilde{\kappa}_3^1\Big) + \frac{d^2}{ds_0^2}\Big(I_\omega \frac{d\tilde{\kappa}_3^1}{ds_0}\Big) \\ &+ \Big(e_{\alpha\beta}(c_\beta - a_\beta)N^0 + M_\alpha^{c0}\Big)e_{\alpha\gamma}\tilde{\kappa}_\gamma^1 + p_\alpha^0 f_\alpha^0 \tilde{\varphi}_3^1 = 0 \end{aligned} \tag{7.43}$$

The governing differential equations in (7.42) and (7.43) are derived according to the assumptions in (7.41) which means that the coefficients are constant and therefore closed form solutions are obtainable.

Determinant Equation

Assuming that the beam has simple supports, so that the ends are free to warp and to rotate about the $\mathbf{e}_\alpha^0$-axes but can't rotate about the $\mathbf{e}_3^0$-axis or deflect in the $\mathbf{e}_\alpha^0$-directions. In this

case it can easily be verified that the buckling mode is given by

$$\tilde{\varphi}_\alpha^1 = \phi_\alpha \cos\alpha s_0 \quad , \quad \tilde{\varphi}_3^1 = \phi_3 \sin\alpha s_0 \quad ; \quad \alpha = \frac{m\pi}{l} \tag{7.44}$$

where the amplitudes ϕ_α and ϕ_3 are constant with respect to s_0. Inserting the general solution (7.44) in the expressions for the linearized curvatures (7.15) leads to

$$\begin{bmatrix} \tilde{\kappa}_\alpha^1 \\ \\ \tilde{\kappa}_3^1 \end{bmatrix} = \begin{bmatrix} \sin\alpha s_0 & 0 \\ \\ 0 & \cos\alpha s_0 \end{bmatrix} \begin{bmatrix} -\alpha\,\delta_{\alpha\beta} & e_{\alpha\gamma}\,\kappa_\gamma^0 \\ \\ \kappa_\gamma^0\, e_{\gamma\beta} & \alpha \end{bmatrix} \begin{bmatrix} \phi_\beta \\ \\ \phi_3 \end{bmatrix} = \begin{bmatrix} C_\alpha \sin\alpha s_0 \\ \\ C_3 \cos\alpha s_0 \end{bmatrix} \tag{7.45}$$

The last relation in (7.45) is introduced as a convenient notation where the combinations of the coefficients α, κ_1^0, ϕ_2 and ϕ_3 are kept in C_2 and C_3.
The coupling between the curvature components $\tilde{\kappa}_j^1$ arising from the initial curvatures κ_α^0 is expressed by the off-diagonal elements in the non-symmetric matrix

$$\mathcal{K} = \begin{bmatrix} -\delta_{\alpha\beta} & e_{\alpha\gamma}\left(\dfrac{\kappa_\gamma^0}{\alpha}\right) \\ \\ \left(\dfrac{\kappa_\gamma^0}{\alpha}\right) e_{\gamma\beta} & 1 \end{bmatrix} \tag{7.46}$$

The matrix $\mathcal{K}$ may be regarded as a transformation operator, indicating a transformation from a reference state to a deformed state.

Inserting (7.45) in the differential equations and assuming that the cross-section is constant leads to a determinant equation of the form

$$\left[\mathbf{K} + \lambda_0 \mathbf{K}_G\right] \cdot \boldsymbol{\phi} = \mathbf{0} \quad , \quad \boldsymbol{\phi}^T = \left[\phi_1\,,\, \phi_2\,,\, \phi_3\right] \tag{7.47}$$

Equation (7.47) is the standard formulation of a linear eigenvalue problem with constant coefficients. $\mathbf{K}$ may be identified as the stiffness matrix while $\mathbf{K}_G$ is the geometrical stiffness matrix. $\mathbf{K}_G$ is given by

$$\mathbf{K}_G = \bar{N}^0 \mathbf{K}_N + \bar{M}_\gamma^{c0} \mathbf{K}_{M_\gamma} + \bar{p}_\gamma^0 \mathbf{K}_{p_\gamma} \tag{7.48}$$

The stiffness matrix is given by

$$\mathbf{K} = \begin{bmatrix} \alpha^2 I_{\alpha\beta} - e_{\alpha\gamma}\kappa_\gamma^0 \left(K + \alpha^2 I_\omega\right) \kappa_\eta^0 e_{\eta\beta} & \alpha\kappa_\gamma^0 e_{\gamma\eta} \left(I_{\alpha\eta} + \delta_{\alpha\eta} \left(K + \alpha^2 I_\omega\right)\right) \\ \\ \alpha\kappa_\gamma^0 e_{\gamma\eta} \left(I_{\beta\eta} + \delta_{\beta\eta} \left(K + \alpha^2 I_\omega\right)\right) & \alpha \left(K + \alpha^2 I_\omega\right) - \kappa_\gamma^0 e_{\gamma\rho} I_{\rho\xi} e_{\xi\eta} \kappa_\eta^0 \end{bmatrix} \tag{7.49}$$

Equation (7.49) expresses the stiffness matrix $\mathbf{K}$ in terms of both the global and the local geometrical parameters. It is possible to separate the two contributions by use of the transformation operator $\mathcal{K}$. Introducing the fundamental stiffness matrix $\mathbf{K}_e$

$$\mathbf{K}_e = \begin{bmatrix} I_{\alpha\beta} & 0 \\ \\ 0 & K + \alpha^2 I_\omega \end{bmatrix} \tag{7.50}$$

means that $\mathbf{K}$ alternatively can be expressed by

$$\mathbf{K} = \alpha^2 \boldsymbol{\mathcal{K}}^T \mathbf{K}_e \boldsymbol{\mathcal{K}} \tag{7.51}$$

The three tensors containing the initial stress contribution are given by

$$\mathbf{K}_N = \begin{bmatrix} \delta_{\alpha\beta} - e_{\alpha\gamma}\kappa^0_\gamma \left(r_a^2 \kappa^0_\eta e_{\eta\beta} - (c_\beta - a_\beta)\right) & -e_{\alpha\gamma}\kappa^0_\gamma r_a^2 \alpha - (c_\alpha - a_\alpha)\alpha \\ -e_{\beta\gamma}\kappa^0_\gamma r_a^2 \alpha - (c_\beta - a_\beta)\alpha & \alpha^2 r_a^2 + \kappa^0_\gamma e_{\gamma\eta}(c_\eta - a_\eta) \end{bmatrix} \tag{7.52}$$

$$\mathbf{K}_{M_\gamma} = \begin{bmatrix} e_{\alpha\eta}\kappa^0_\eta \left(e_{\gamma\beta} - \kappa^0_\rho e_{\rho\beta} 2\beta_\gamma\right) & \alpha e_{\alpha\gamma} - \alpha e_{\alpha\eta}\kappa^0_\eta 2\beta_\gamma \\ \alpha e_{\beta\gamma} - \alpha e_{\beta\eta}\kappa^0_\eta 2\beta_\gamma & -\kappa^0_\gamma + \alpha^2 2\beta_\gamma \end{bmatrix} \tag{7.53}$$

$$\mathbf{K}_{p_\gamma} = \begin{bmatrix} e_{\alpha\eta} f^0_\eta e_{\gamma\beta} & 0 \\ 0 & f^0_\gamma \end{bmatrix} \tag{7.54}$$

The four tensors are symmetric and thus the eigenvalue problem can be solved by use of standard methods.

7.5.2 Straight Beam with Eccentric Axial Load

An important special case of the general stability equations is that of an axially loaded beam. The beam is loaded by 2 endforces as indicated in Fig. 7.3. In this case the beam mainly acts as a column. The simply supported column is the most popular example in case of buckling and postbuckling analysis because it is possible to perform a complete investigation of the initial postbuckling behavior, see e.g. Thomson & Hunt (1973), Budiansky (1974), Grimaldi & Pignataro (1979), Roorda (1980) and Naschie (1990). In the general stability analysis of Thomson, Budiansky and Roorda the double symmetric column is investigated by use of a nonlinear curvature expression, while the theory of Grimaldi & Pignataro is specialised into the nonlinear problem of the central loaded column by use of a linear displacement field in a nonlinear strain measure.

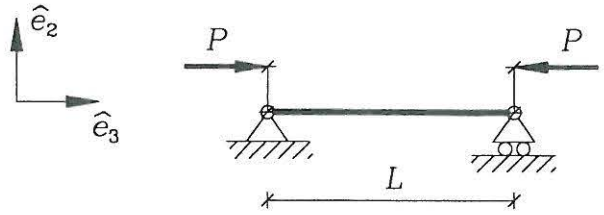

Fig. 7.3: Column with eccentric axial load.

In the present thesis the axially loaded beam is initially considered in a general way and subsequently the specialised examples where the compressive force acts in the shear and elastic centers are considered. Comparisions with some of the above mentioned works are

made. Often the stability equations are of main interest in connection with compressional loads, and it is therefore convenient for the statics in the initial state to introduce the notation

$$N_3^0 = -P^0 = -\lambda_0$$

$$M_\alpha^{c\,0} = -e_{\alpha\beta}(d_\beta - c_\beta)\lambda_0 \tag{7.55}$$

where d_α is the location of the compressive force.

For the straight column the governing differential equations can now be found from (7.42) and (7.43), i.e.

$$-\frac{d}{ds_0}\left(I_{\alpha\beta}\,\tilde{\kappa}_\beta^i\right) - P^0\,\tilde{\varphi}_\alpha^i - (d_\alpha - a_\alpha)\,P^0\,\tilde{\kappa}_3^i = R_\alpha^i \tag{7.56}$$

$$-\frac{d}{ds_0}\left(\left(K - r_a^2\,P^0 + 2\beta_\eta e_{\eta\alpha}(d_\alpha - c_\alpha)\,P^0\right)\tilde{\kappa}_3^i\right) + \frac{d^2}{ds_0^2}\left(I_\omega\,\frac{d\tilde{\kappa}_3^i}{ds_0}\right)$$

$$+ P^0(d_\alpha - a_\alpha)\,\tilde{\kappa}_\alpha^i = R_3^i \tag{7.57}$$

This standard form is in the following used to examine the buckling and postbuckling behavior of the straight column.

Critical Load

The critical load can be found from the eigenvalue problem given in equation (7.47). Using (7.55) it follows from (7.49) and (7.52) that in this particular case

$$\left[\mathbf{K} + \lambda_0\left(\mathbf{K}_N + e_{\alpha\beta}(d_\beta - c_\beta)\,\mathbf{K}_{M_\alpha}\right)\right]\cdot\phi = \mathbf{0} \tag{7.58}$$

where the tensors appearing are defined in Section 7.5.1.

In case of a straight beam, i.e. $\kappa_j^0 = 0$, it follows that λ_0 can be determined from the following determinant equation

$$\left|\alpha^2\begin{bmatrix} I_{\alpha\beta} & 0 \\ 0 & K + \alpha^2 I_\omega \end{bmatrix} - \lambda_0\begin{bmatrix} \delta_{\alpha\beta} & -\alpha(d_\alpha - a_\alpha) \\ -\alpha(d_\beta - a_\beta) & \alpha^2 r_a^2 + \alpha^2\,2\beta_\eta e_{\eta\rho}(d_\rho - c_\rho) \end{bmatrix}\right| = 0 \tag{7.59}$$

It is seen that if the point of attack does not coincide with the shear center, $d_\alpha \neq a_\alpha$, the equations for bending and torsion are coupled. Equation (7.59) is the general form of the determinant equation which determines the critical load for the simply supported column.

In the following examples are given where the load is applied at the shear center and at the elastic center, respectively.

Axial Load Applied at the Shear Center

For an axial load applied at the shear center, $d_\alpha = a_\alpha$, bending and torsion uncouple. Letting $\mathbf{e}^0_\alpha$ represent the direction of the principal axes, i.e. $I_{12} = I_{21} = 0$, the critical loads follow from the determinant equation as

$$P_{cr} = P^0 = \left\{ \begin{array}{c} \alpha^2 I_{11} \\ \\ \alpha^2 I_{22} \\ \\ \dfrac{K + \alpha^2 I_\omega}{r_a^2 + 2\beta_\eta e_{\eta\alpha}(a_\alpha - c_\alpha)} \end{array} \right. \tag{7.60}$$

The critical load is then given by the lowest of the 3 eigenvalues. Note that the ratio expression which corresponds to a torsional buckling load for cross-sections with non coincident shear and elastic centers is influenced by the geometrical parameter β_α. This implies that for an axial load applied at the shear center only the torsional buckling load is influenced by possible unsymmetry of the cross-section.
The buckling modes corresponding to the buckling loads are given by either a bending mode

$$\tilde{\boldsymbol{\varphi}}^1 = \phi_\alpha \cos\alpha s_0 \, \mathbf{e}^0_\alpha \qquad \text{(bending mode)} \quad \text{no } \alpha \text{ summation} \tag{7.61}$$

or a torsional mode

$$\tilde{\boldsymbol{\varphi}}^1 = \phi_3 \sin\alpha s_0 \, \mathbf{e}^0_3 \qquad \text{(torsion mode)} \tag{7.62}$$

The one to occur is determined by the lowest value of P^0 in (7.60).

Postbuckling for Axial Load at the Shear Center

The analysis of the postbuckling behavior is performed by use of the strong formulation presented in the previous sections.
In the following the postbuckling behavior is examined by assuming that the column buckles in a bending mode. The buckling form is given by

$$\tilde{\boldsymbol{\varphi}}^1 = \left[\tilde{\varphi}^1_1, \tilde{\varphi}^1_2, \tilde{\varphi}^1_3\right]^T = \phi_1 \cos\alpha s_0 \, \mathbf{e}^0_1 = \begin{bmatrix} \phi_1 \cos\alpha s_0 \\ \\ 0 \\ \\ 0 \end{bmatrix} \tag{7.63}$$

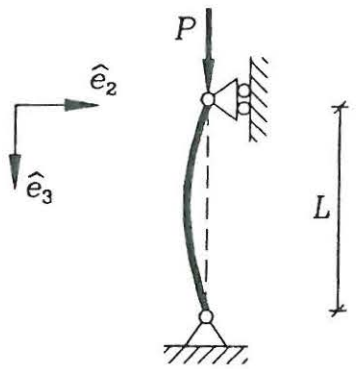

Fig. 7.4: Bending mode.

The load increment factor λ_1 can now be found from equation (7.36). From Appendix C it follows that the right-hand sides of the differential equations determining $\tilde{\varphi}_l^2$ are given by

$$R_1^2 = \lambda_1 \tilde{\varphi}_1^1 P^0 \quad , \quad R_2^2 = R_3^2 = 0 \tag{7.64}$$

Inserting this in (7.36) leads to the identity

$$\int_0^l \lambda_1 \tilde{\varphi}_1^1 \tilde{\varphi}_1^1 P^0 \, ds_0 = 0 \quad , \quad \lambda_1 = 0 \tag{7.65}$$

This means that when the axial load is placed at the shear center then the initial postbuckling behavior is symmetric for all types of cross-sections.

The next step in the postbuckling analysis is to determine $\tilde{\varphi}_j^2$ from equation (7.56) and (7.57). From (7.64) and (7.65) it follows that $R_l^2 = 0$ which means that the homogeneous linear differential equations in (7.42) and (7.43) are recovered, but now in terms of $\tilde{\varphi}_j^2$. The boundary condtions still have to be fulfilled which together with the orthonormality condition implies that $\tilde{\varphi}_j^2$ represents the trivial solution, i.e.

$$\tilde{\varphi}_j^2 = 0 \tag{7.66}$$

Finally λ_2 can now be found from (7.38). Using Appendix C it follows that

$$R_1^3 = P^0\Big(\frac{\tilde{\varphi}_1^{1\,3}}{3!} - \lambda_2 \tilde{\varphi}_1^1\Big) \quad , \quad R_2^3 = R_3^3 = 0 \tag{7.67}$$

Inserting (7.63) and (7.67) in the functional (7.38) means that

$$\int_0^l P^0\Big(\tfrac{1}{3!}\,\phi_1^4 \cos^4\alpha s_0 - \lambda_2\,\phi_1^2 \cos^2\alpha s_0\Big)\, ds_0 = 0 \tag{7.68}$$

and performing the integrations means that λ_2 is given by

$$\lambda_2 = \frac{1}{8}\,\phi_1^2 \tag{7.69}$$

This completes the determination of the parameters describing the initial postbuckling be-

havior, which is described by the first two terms of the expansion in (7.12). The external load P may approximatively be written as

$$P = P^0 \left(1 + \frac{1}{8}\phi_1^2 \xi^2\right) \quad , \quad P^0 = \alpha^2 I_{11} \tag{7.70}$$

Equation (7.70) corresponds to the formula for the postbuckling behavior for the Euler column found by Budiansky (1974) and Naschie (1990).
The change in P is more illustrative if the relation in (7.70) is reformulated in terms of the midpoint deflection. Using the linearized part of ε_2^1 means that the relation between the displacement component $r_{a_2}^1$ and the rotation component φ_1^1 is expressed by

$$\frac{dr_{a2}^1}{ds_0} + \varphi_1^1 = 0 \tag{7.71}$$

Using (7.71) the amplitude $\phi_1 \xi$ can be expressed by the midpoint deflection δ_2. It follows that approximately

$$\phi_1 \xi = -\pi \frac{\delta_2}{L} \tag{7.72}$$

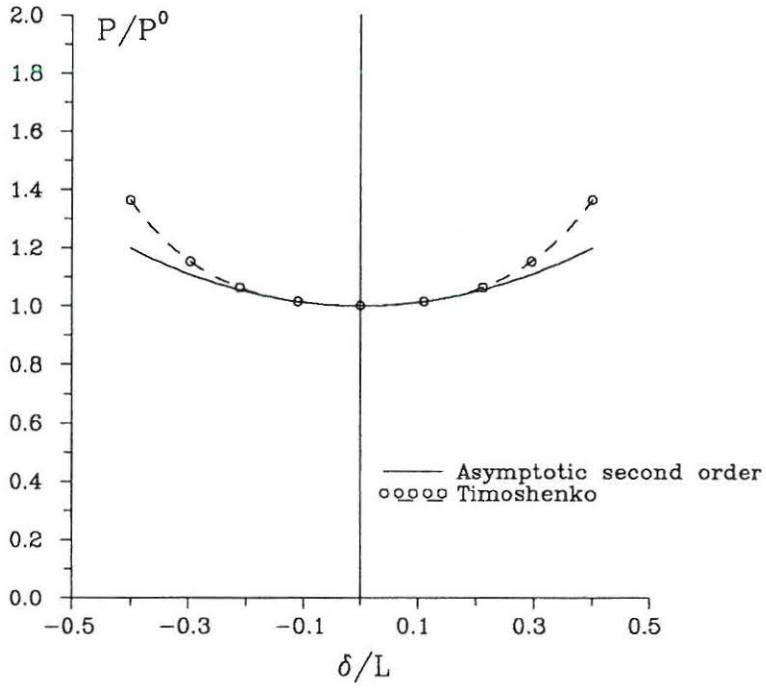

Fig. 7.5: Initial-postbuckling for the straight column.

Substitution of (7.72) into (7.70) leads to

$$\frac{P}{P^0} = 1 + \frac{\pi^2}{8}\left(\frac{\delta}{L}\right)^2 \quad , \quad P^0 = \alpha^2 I_{11} \tag{7.73}$$

which expresses the asymptotic second-order initial postbuckling behavior of the double

symmetric simply supported column. In Fig. 7.5 the load-deflection relation is illustrated together with the complete solution obtained by Timoshenko & Gere (1961). By use of finite rotations thereby achieving the exact expression for the curvature in the buckled state Timoshenko & Gere obtained a closed form solution of the postbuckling behavior.
Fig. 7.5 indicates that the postbuckling curve initially is very flat meaning that the column with axial load applied at the shear center is not sensitive to initial deformations. For most actual columns, as bending increases, the combined axial and bending stress will exceed the proportional limit of the material long before the deviation of the critical load determined by the linearized equations from the nonlinear theory becomes significant. Consequently, within the range of elastic behavior the results obtained from the finite roation analysis show that no significant postbuckling strength exist for the simply supported column.

Buckling for Axial Load at the Elastic Center

The buckling as well as the postbuckling behavior for different types of cross-sections of the central loaded column is analysed in the following. In the postbuckling analysis focus is placed on determination of whether the initial behavior is symmetric or nonsymmetric.

Critical Load :
If the axial load is applied at the elastic center, $d_\alpha = c_\alpha$, bending and torsion may couple if the cross-section is nonsymmetric. The critical load P_{cr} can be determined from (7.59) leading to

$$\left| \begin{bmatrix} \alpha^2 I_{11} - P^0 & 0 & \alpha (c_1 - a_1) P^0 \\ 0 & \alpha^2 I_{22} - P^0 & \alpha (c_2 - a_2) P^0 \\ \alpha (c_1 - a_1) P^0 & \alpha (c_2 - a_2) P^0 & \alpha^2 r_a^2 \left(\frac{1}{r_a^2} (K + \alpha^2 I_\omega) - P^0 \right) \end{bmatrix} \right| = 0 \qquad (7.74)$$

Notice that the effects from a nonsymmetric form now are represented by the difference between the location of the elastic and the shear center, while previously β_α occured in the determinant equation.

Double Symmetric Cross-section :
In case of a double symmetric cross-section, i.e. $c_\alpha = a_\alpha$, the bending and torsion problems uncouple. The critical load then follows directly from (7.74)

$$P_{cr} = P^0 = \begin{cases} P_1 = \alpha^2 I_{11} \\ P_2 = \alpha^2 I_{22} \\ P_3 = \frac{1}{r_a^2} \left(K + \alpha^2 I_\omega \right) \end{cases} \qquad (7.75)$$

The critical load is then given by the lowest of the 3 eigenvalues. As bending and torsion uncouples the buckling modes are similar to those found in the example where the load is applied at the shear center. According to this the postbuckling behavior is also similar and therefore no further analysis is necessary.

Monosymmetric Cross-section :
Examples of monosymmetric cross-sections are the T- and C-profiles. Letting $c_1 = a_1$ and $c_2 \neq a_2$ then the critical load P_{cr} can be determined from

$$P_{cr} = P^0 : \quad P^0 = \begin{cases} \alpha^2 I_{11} \\ r_a^2 \left(1 - \left(\frac{c_2 - a_2}{r_a}\right)^2\right) P^{0\,2} - (P_2 + P_3) P^0 + P_2 P_3 = 0 \end{cases} \tag{7.76}$$

where P_2 and P_3 are defined in (7.75). The buckling load is given by the lowest of the three eigenvalues given in (7.76).

The buckling modes corresponding to the buckling loads are given by either a bending mode

$$\tilde{\boldsymbol{\varphi}}^1 = \phi_1 \cos\alpha s_0 \, \mathbf{e}_1^0 \qquad \text{(bending mode)} \tag{7.77}$$

or a combined bending and torsion mode

$$\tilde{\boldsymbol{\varphi}}^1 = \phi_2 \cos\alpha s_0 \, \mathbf{e}_2^0 + \phi_3 \sin\alpha s_0 \, \mathbf{e}_3^0 \qquad \text{(bending/torsion mode)} \tag{7.78}$$

The bending mode corresponds to the results for the double symmetric cross-section, therefore emphasis is placed on the combined mode in the investigation of the initial postbuckling behavior.

$$\tilde{\boldsymbol{\varphi}}^1 = \left[\tilde{\varphi}_1^1, \tilde{\varphi}_2^1, \tilde{\varphi}_3^1\right]^T = \begin{bmatrix} 0 \\ \phi_2 \cos\alpha s_0 \\ \phi_3 \sin\alpha s_0 \end{bmatrix} \tag{7.79}$$

Using the combined buckling mode (7.79) in (7.36) the first order load increment factor λ_1 can be determined. If $c_1 = a_1$ and $c_2 \neq a_2$ and it follows from Table 4.2 that $\beta_1 \neq 0$ and $\beta_2 = 0$. From Appendix C it follows that the functions R_l^2 necessary for the determination of the first order load increment factor λ_1 are now given by

$$\begin{aligned} R_1^2 &= \frac{d}{ds_0}\Big(- I_{22}\tilde{\kappa}_2^1\tilde{\varphi}_3^1 + \tfrac{1}{2} I_{11}\left(\tilde{\kappa}_2^1\tilde{\varphi}_3^1 - \tilde{\kappa}_3^1\tilde{\varphi}_2^1\right) + \tilde{\varphi}_2^1 K \tilde{\kappa}_3^1 \\ &\qquad - \tilde{\varphi}_2^1 \frac{d}{ds_0}\left(I_\omega \frac{d\tilde{\kappa}_3^1}{ds_0}\right) + \beta_1 I_{11}\tilde{\kappa}_3^1\tilde{\kappa}_3^1 + \tfrac{1}{2}\left(\tilde{\varphi}_2^1\tilde{\varphi}_2^1 + \tilde{\varphi}_3^1\tilde{\varphi}_3^1\right)(c_2 - a_2)P^0\Big) \\ R_2^2 &= \lambda_1 \tilde{\varphi}_2^1 P^0 \\ R_3^2 &= 0 \end{aligned} \tag{7.80}$$

It follows that the right-hand side of the bending equation in (7.56) which determines $\tilde{\varphi}_1^2$ is nonzero. The second order components of $\tilde{\varphi}_j^2$ are not explored further. Inserting (7.80) in

(7.36) together with (7.79) leads to the identity

$$\int_0^l \lambda_1 \, \phi_2^2 \cos^2(\alpha s_0) \, ds_0 \; = \; 0 \tag{7.81}$$

whereby it follows that $\lambda_1 = 0$. This means that if the axial load is placed at the elastic center the initial postbuckling behavior is symmetric for monosymmetric cross-sections.

Cross-sections with no Axis of Symmetry :
The Z- and L-profiles are examples of cross-sections with no axis of symmetry. In case of the Z-profile the elastic and shear center are coincident, i.e. $c_\alpha = a_\alpha$ and $\beta_\alpha = 0$, whereby it from (7.74)follows that no coupling occurs. This means that for the Z-profile the initial postbuckling behavior is similar to that of the double symmetric cross-section.
For the L-profile the elastic and shear center are noncoincident, i.e. $c_\alpha \neq a_\alpha$ and $\beta_\alpha \neq 0$. It follows from (7.74) that linearly independent buckling modes do not occur, i.e $\tilde{\varphi}_l^1 \neq 0$. Based on the experience from the investigations of the double and the monosymmetric cross-section it is evident that $\lambda_1 \neq 0$ whereby it can be concluded that the initial postbuckling behavior is nonsymmetric as it also was found by Grimaldi & Pignataro (1979).
The analysis is not performed in detail because a closed form expression for λ_1 can not be obtained without several rewritings.

7.5.3 Curved Beam in Pure Bending

The stability behavior of a beam in pure bending has been investigated for many years, see e.g. Vlasov (1961) and Timoshenko (1961). During the last decade the interest in the stability behavior of the curved thin-walled beam has been significant see e.g. Yoo (1982), Yang & Kuo (1987) and Papangelis & Trahair (1986). Some differencies occured in the results but the majority seems to agree with the formulations obtained by Vlasov as the beam in pure bending was considered. The analysis performed by the above mentioned authors are all limitted to the buckling behavior.

In this section the buckling as well as initial postbuckling behavior is investigated in order to identify the governing parameters for the thin-walled beam element.

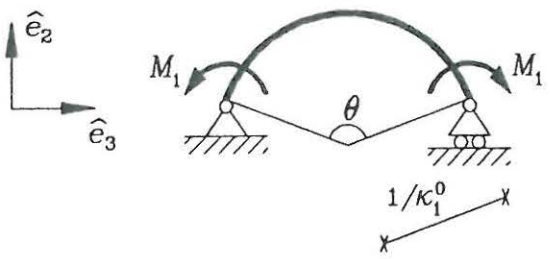

Fig. 7.6: Curved beam with in-plane moment.

The problem *beam in pure bending* is illustrated via the example shown in Fig. 7.6. It follows that the quantities which may differ from zero are

$$M_1(0) \; = \; M_1(L) \; = \; M_1^0\left(1 + \lambda\right) \qquad \text{and} \qquad \kappa_1^0 \; = \; M_1^0/I_{11} + 1/R \tag{7.82}$$

where $1/R$ indicates the possibility of an initial curvature which is present before loading. In the following κ_1^0 is assumed constant and κ_1^0 is considered to be the total curvature at the critical point.

Critical Load

The critical moment M_1^0 can be determined by solving the standard problem

$$\left[\mathbf{K} + M_1^0 \mathbf{K}_{M_1}\right] \cdot \boldsymbol{\phi} = \mathbf{0} \tag{7.83}$$

where $\mathbf{K}$ and $\mathbf{K}_{M_1}$ are defined in Section 7.5.1. First the beam bends in plane of the applied moment, i.e. $\varphi_1^0 \neq 0$ and $\kappa_1^0 \neq 0$. The stability problem then arises when the applied moment reaches the critical value which courses the beam to buckle out of the plane, i.e $\varphi_2^1 \neq 0$ and $\varphi_3^1 \neq 0$. In the following $\mathbf{e}_\alpha^0$ indicates the direction of the principal axes, i.e. $I_{12} = I_{21} = 0$. The eigenvalue problem (7.83) can now be expressed by

$$\left(\alpha^2 \begin{bmatrix} I_{22} + \left(\frac{\kappa_1^0}{\alpha}\right)^2 \left(K + \alpha^2 I_\omega\right) & \left(\frac{\kappa_1^0}{\alpha}\right)\left(I_{22} + \left(K + \alpha^2 I_\omega\right)\right) \\ \left(\frac{\kappa_1^0}{\alpha}\right)\left(I_{22} + \left(K + \alpha^2 I_\omega\right)\right) & K + \alpha^2 I_\omega + \left(\frac{\kappa_1^0}{\alpha}\right)^2 I_{22} \end{bmatrix} \right.$$

$$\left. + M_1^0 \alpha \begin{bmatrix} -\left(\frac{\kappa_1^0}{\alpha}\right)\left(1 - \kappa_1^0 2\beta_1\right) & -\left(1 - \kappa_1^0 2\beta_1\right) \\ -\left(1 - \kappa_1^0 2\beta_1\right) & \alpha 2\beta_1 - \left(\frac{\kappa_1^0}{\alpha}\right) \end{bmatrix} \right) \begin{bmatrix} \phi_2 \\ \phi_3 \end{bmatrix} = \mathbf{0} \tag{7.84}$$

The form of the eigenvalue problem in (7.84) is symmetric and can therefore be solved by use of standard methods. It follows that the critical moment can be found from the quadratic equation

$$A\, M_1^{0\,2} + B\, M_1^0 + C = 0 \tag{7.85}$$

where the coefficients A, B, and C are given by

$$\begin{aligned} A &= \left(1 - \kappa_1^0 2\beta_1\right) \\ B &= -\left(\alpha^2 - \kappa_1^{0\,2}\right) 2\beta_1 I_{22} - \kappa_1^0 \left(I_{22} + \left(K + \alpha^2 I_\omega\right)\right) \\ C &= -\left(\alpha^2 - \kappa_1^{0\,2}\right) I_{22} \left(K + \alpha^2 I_\omega\right) \end{aligned} \tag{7.86}$$

The expressions for the coefficients of (7.85) contains the influence from an initial curvature as well as a possible unsymmetry of the cross-section. These effects are in the following analysed separately.

Straight Beam in Pure Bending :
For the straight beam, i.e. $\kappa_1^0 = 0$, it follows that the coefficients in (7.86) simplifies to

$$A = 1 \quad , \quad B = -2\alpha^2\beta_1 I_{22} \quad , \quad C = -\alpha^2 I_{22}(K + \alpha^2 I_\omega) \tag{7.87}$$

Substitution of (7.87) into (7.85) means that the critical moment for the straight beam with arbitrary cross-section can be determined from

$$M_1^0 = \alpha^2\,\beta_1\,I_{22} \pm \sqrt{\alpha^2\,I_{22}(K + \alpha^2 I_\omega) + (\alpha^2\,\beta_1\,I_{22})^2} \tag{7.88}$$

For the double symmetric cross-section $\beta_1 = 0$ which leads to the introduction of a reference moment M_{str} given by

$$M_{str} = \alpha\sqrt{I_{22}\left(K + \alpha^2 I_\omega\right)} \tag{7.89}$$

Equation (7.89) is the well-known formula for the critical moment of a double symmetric straight beam in pure bending, see e.g. Timoshenko & Gere (1961).

The influence from a possible unsymmetry of the cross-section can be investigated by use of the reference load M_{str}. It follows that (7.88) can be rewritten to yield

$$M_1^0 = \gamma_\beta\,M_{str} \tag{7.90}$$

where the coefficient γ_β is defined by

$$\gamma_\beta = \sqrt{b} \pm \sqrt{1+b} \quad , \quad b = \left(\frac{\pi\,\beta_1}{L}\right)^2 \frac{I_{22}}{K + \alpha^2 I_\omega} \tag{7.91}$$

It follows that the influence from an unsymmetry γ_β is closely connected to the bending/torsion ratio as well as it depends on the beam length. From (7.91) it appears that for cross-sections which are nonsymmetric in the plane of the applied moment a significant difference between the positive and negative critical moment can occur. This is for example the case for a T-beam with ordinary proportions loaded in the plane of the web.

Double Symmetric Curved Beam :
The influence from an initial curvature on the critical moment can be examined by introducing $\kappa_1^0 = M_1^0/I_{11}$ and assuming that $\beta_1 = 0$.
From (7.86) it follows that

$$A = 1 \quad , \quad B = -\frac{M_1^0}{I_{11}}\left(I_{22} + (K + \alpha^2 I_\omega)\right)$$

$$C = -\left(\alpha^2 - \left(\frac{M_1^0}{I_{11}}\right)^2\right) I_{22}\left(K + \alpha^2 I_\omega\right) \tag{7.92}$$

which by substitution into (7.85) leads to

$$M_1^0 = \gamma_\kappa M_{str} \tag{7.93}$$

where

$$\gamma_\kappa^2 = \frac{1}{\left(1 - \frac{I_{22}}{I_{11}}\right)\left(1 - \frac{K + \alpha^2 I_\omega}{I_{11}}\right)} \tag{7.94}$$

A corresponding expression was found by Vacharajittiphan *et. al.* (1974) who analysed the effect of in-plane deformation on lateral buckling for double symmetric cross-sections. As the in-plane bending stiffness in general is significantly larger than the torsional stiffness for cross-sections with ordinary properties (7.94) indicates that γ_κ is independent of the beam length, i.e. only the cross-sectional parameters influence γ_κ. From (7.94) it follows that for a high beam the influence from an initial curvature is insignificant while for stocky beams the influence may become significant.

Examples :
The general expression contained in (7.85)-(7.86) is first used to make some comparisons with the literature. An IPE330 (see e.g. Fig. 7.7) beam with length $L = 6000mm$ has been analysed for different values of a prescribed initial curvature, i.e. $\kappa_1^0 = \Theta/L$.

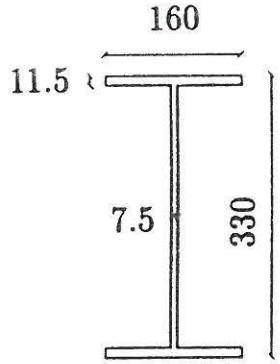

$$F/E = 6260mm^2$$
$$I_{11}/E = 117.7 \cdot 10^6 mm^4$$
$$I_{22}/E = 7.88 \cdot 10^6 mm^4$$
$$K/G = 0.283 \cdot 10^6 mm^4$$
$$I_\omega/E = 199 \cdot 10^9 mm^6$$

Fig. 7.7: IPE330 - Cross-section.

In Fig. 7.8 the critical moment for a double symmetric cross-section determined by (7.85) is illustrated together with results obtained by Vlasov (1961) and Yang & Kuo (1987). These authors developed their formulations by considering the single curved beam directly, thereby loosing the generality achieved in the present formulation. The method of solution for Vlasov was to substitute the generalized deformations of the straight beam with the corresponding for a curved beam in the governing differential equations. Yoo develops the governing differential equations from the potential energy by variational principles. The potential energy for a curved beam is obtained by replacing the straight beam terms with those of a single curved beam. Yang used a linear displacement field in a nonlinear strain measure and identified the initial stress terms through the higher order terms. In his developing process Yang underlines the importance of including special effects as for instance *coupled stress/strain*

relations and radial stresses.

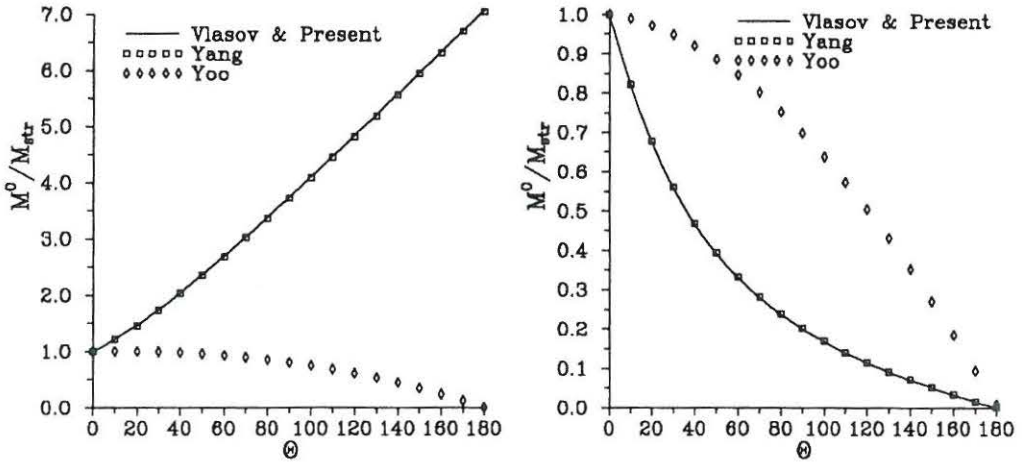

Fig. 7.8: Critical moment for pure bending. a) Positive moment. b) Negative moment.

For the special case of a semicircular beam ($\Theta = \pi$), only the negative critical moment will reduce to zero. Such a result corresponds to the freedom of a pinned semicircular beam to rotate about the diameter joining the ends. In an eigenvalue test each zero root is associated with one rigid body mode. For a pinned semicircular beam, there exists a single rigid body mode, i.e., rotation about the diameter joining the two ends. Therefore, only the applied loads that may result in a buckling deformation involving the rigid body motion will reach the critical value of zero. From Fig. 7.8 it appears that besides of Yoo the different approaches lead to the same critical moment. As Yoo's expressions deviates significantly from the others it seems that an error must have occured in his rewritting of the potential energy from the straight beam case into that of a curved beam. It is believed that the error is associated with the initial stress terms as the elastic terms are in agreement with those of Vlasov and the present formulation. Further Fig. 7.8 indicates that no further information is obtained by Yangs approach which questions the need for additional terms as introduced by Yang.

The last example is a comparison between three different types of cross-sections for a prescribed initial curvature. The cross-sections used are an IPE100, a CNP100 and finally a T(h=100,b=50,t=11) and the length of the beam is $L = 2400mm$. In all three cases the moment is applied in the plane of the largest bending stiffness. The dimensionless cross-

Table 7.1: Cross-sectional parameters for I-, C- and T-profiles.

	$\frac{I_{11}}{I_{22}}$	$\frac{I_{22}}{K+\alpha^2 I_\omega}$	$\frac{\beta_1}{L}$	$\frac{\beta_2}{L}$	γ_β^+	γ_β^-	γ_κ
IPE100	10.8	28.8	0.000	0.000	1.00	-1.00	1.054
CNP100	7.0	24.8	0.000	-0.036	1.00	-1.00	1.082
T(100,50,11)	15.9	4.5	0.026	0.000	1.15	-0.87	1.039

sectional parameters are illustrated in Table 7.1 together with γ_β and γ_κ. The results in Table 7.1 and Fig. 7.9 illustrate that even for standard profiles as the IPE100 and CNP100 the initial curvature influences the critical moment at small values of Θ. For the T(100,50,11) beam the influence from the unsymmetry is more significant than that of the initial curvature for small values of Θ.

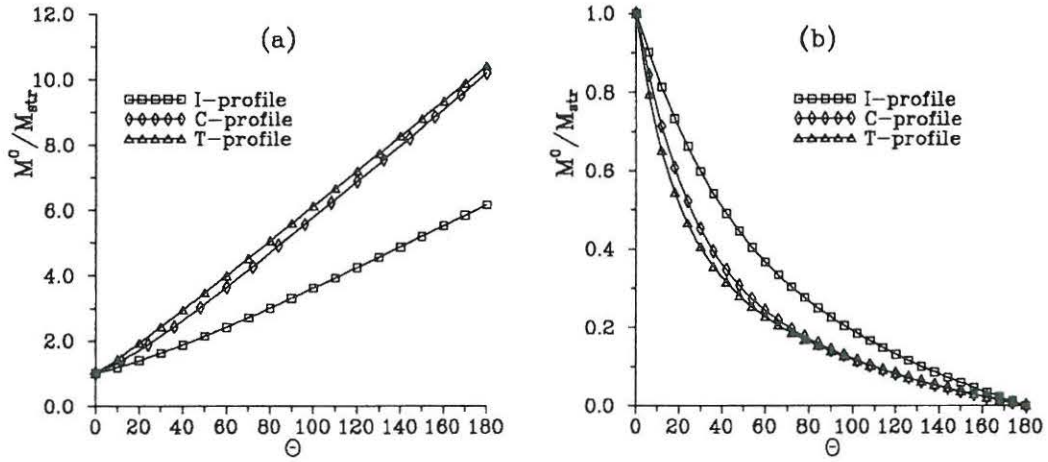

Fig. 7.9: Critical moment for pure bending. a) Positive moment. b) Negative moment.

The results obtained here demands a method which accounts for initial deformations in a buckling analysis. The formulation in the present work enables to perform an analysis where the geometry and statics of the beam structure is updated continuously. A numerical formulation of this is presented in Chapter 8.

Buckling Mode for Straight Beam

If the critical moment M^0 has been determined from (7.85) then the first order term $\tilde{\varphi}^1$ of the buckling mode can be determined. The buckling mode $\tilde{\varphi}^1$ is described by

$$\tilde{\varphi}^1 \;=\; \phi_2 \cos\alpha s_0 \, \mathbf{e}_2^0 \;+\; \phi_3 \sin\alpha s_0 \, \mathbf{e}_3^0 \tag{7.95}$$

where the coefficients ϕ_2^1 and ϕ_3^1 describe the eigenvector of the eigenvalueproblem in (7.84). The buckling modes may be illustrated by neglecting the initial deformations, i.e. $\kappa_1^0 = 0$, and concentrating on cross-sections where $\beta_1 = 0$. The critical moment for the straight beam M_{str} is given by (7.89) and it follows from (7.84) that the corresponding buckling mode is given by

$$\begin{bmatrix} \phi_2 \\ \\ \phi_3 \end{bmatrix} \;=\; \begin{bmatrix} \sqrt{\dfrac{K + \alpha^2 I_\omega}{I_{22}}} \\ \\ -1 \end{bmatrix} \qquad , \qquad M_{str} \;=\; -\,\alpha \phi_2 \phi_3 I_{22} \tag{7.96}$$

Using an I-beam with web height h to illustrate the buckling modes it follows that

$$I_\omega \;=\; \frac{h^2}{4}\, I_{22} \tag{7.97}$$

which leads to

$$\begin{bmatrix} \phi_2 \\ \\ \phi_3 \end{bmatrix} = \begin{bmatrix} \sqrt{\dfrac{K}{I_{22}}\left(1 + \left(\dfrac{\pi\, h}{2\, L}\right)^2 \dfrac{I_{22}}{K}\right)} \\ \\ -1 \end{bmatrix} \tag{7.98}$$

For a high I-beam the bending component ϕ_2 is predominant which means that the bending mode is dominant. In the case of a slender rectangular cross-section $I_\omega \simeq 0$ and the ratio K/I_{22} equals $4G/E$. This means that the buckling mode is given by an equal combination of bending and torsion.

Postbuckling for beam in pure bending

The postbuckling behavior is now examined by use of the buckling mode given in (7.95). The analysis consist of the determination of the postbuckling displacements and the corresponding load increment factors. In this example the second order displacement vector $\tilde{\boldsymbol{\varphi}}^2$ has to be determined before the load increment factors can be found.

Postbuckling Displacements :

The second order term of the rotation vector, $\tilde{\boldsymbol{\varphi}}^2$, can be determined from (7.37) where only the right-hand side is different from the equations used to determine λ_0. From (7.42)-(7.43) it follows that the linear differential equations determining $\tilde{\varphi}_j^2$ are given by

In-plane bending :

$$-\frac{d}{ds_0}\Big(I_{11}\tilde{\kappa}_1^2\Big) = R_1^2\big(\tilde{\varphi}_1^1, \lambda_0, \lambda_1\big) \tag{7.99}$$

Out-of-plane bending :

$$-\frac{d}{ds_0}\Big(I_{22}\tilde{\kappa}_2^2\Big) + \kappa_1^0\big(K + 2\beta_1 M_1^0\big)\tilde{\kappa}_3^2 - \kappa_1^0\frac{d}{ds_0}\Big(I_\omega\frac{d\tilde{\kappa}_3^2}{ds_0}\Big) - M_1^0\tilde{\kappa}_3^2 = R_2^2 \tag{7.100}$$

Torsion and Warping :

$$-\kappa_1^0 I_{22}\tilde{\kappa}_2^2 - \frac{d}{ds_0}\Big(\big(K + 2\beta_1 M_1^0\big)\tilde{\kappa}_3^2\Big) + \frac{d^2}{ds_0^2}\Big(I_\omega\frac{d\tilde{\kappa}_3^2}{ds_0}\Big) + M_1^0\tilde{\kappa}_2^2 = R_3^2 \tag{7.101}$$

From Appendix C it follows that the right-hand sides of the differential equations are given by

$$\begin{aligned} R_1^2 = \frac{d}{ds_0}\Big(& - I_{22}\tilde{\kappa}_2^1\tilde{\varphi}_3^1 + \tfrac{1}{2}\, I_{11}\left(\tilde{\kappa}_2^1\tilde{\varphi}_3^1 - \tilde{\kappa}_3^1\tilde{\varphi}_2^1\right) + \tilde{\varphi}_2^1\big(K + 2\beta_1 M_1^0\big)\tilde{\kappa}_3^1 \\ & - \tilde{\varphi}_2^1\frac{d}{ds_0}\Big(I_\omega\frac{d\tilde{\kappa}_3^1}{ds_0}\Big) + \beta_1 I_{11}\tilde{\kappa}_3^1\tilde{\kappa}_3^1 - \tfrac{1}{2}\left(\tilde{\varphi}_2^1\tilde{\varphi}_2^1 + \tilde{\varphi}_3^1\tilde{\varphi}_3^1\right)M_1^0\Big) \end{aligned}$$

$$R_2^2 = \frac{d}{ds_0}\Big(\beta_2 I_{22}\tilde{\kappa}_3^1\tilde{\kappa}_3^1\Big) + \kappa_1^0\, 2\beta_2 I_{22}\tilde{\kappa}_2^1\tilde{\kappa}_3^1 \tag{7.102}$$

$$R_3^2 = \frac{d}{ds_0}\Big(2\beta_2 I_{22}\tilde{\kappa}_2^1\tilde{\kappa}_3^1\Big) - \kappa_1^0\beta_2 I_{22}\tilde{\kappa}_3^1\tilde{\kappa}_3^1$$

Using (7.45) means that R_l^2 can be expressed by the trigonometric functions

$$\begin{aligned} R_1^2 = -\frac{d}{ds_0}\Big(&\tfrac{1}{2}\,\alpha\, I_{11}\,\phi_2\phi_3 - \beta_1 I_{11} C_3 C_3 \cos^2(\alpha s_0) \\ &+\Big(\tfrac{1}{2}\, I_{11}\,\kappa_1^0\phi_2\phi_2 - \phi_2\Big(K + \alpha^2 I_\omega + 2\beta_1 M_1^0\Big)C_3 + \tfrac{1}{2}\,\phi_2\phi_2 M_1^0\Big)\cos^2(\alpha s_0) \\ &+\Big(I_{22}C_2\phi_3 + \tfrac{1}{2}\, I_{11}\,\kappa_1^0\phi_3\phi_3 + \tfrac{1}{2}\,\phi_3\phi_3\, M_1^0\Big)\sin^2(\alpha s_0)\Big) \end{aligned} \tag{7.103}$$

where C_2 and C_3 are defined in (7.45). The splitting of R_1^2 which is associated with in-plane bending into three groups is performed because the first term is dominant compared with the others. This can be shown by numerical analysis, but such analysis is omitted here. Rewritting using (7.82) leads to

$$\begin{aligned} R_1^2 = -\frac{d}{ds_0}\Big(&\tfrac{1}{2}\,\alpha\, I_{11}\,\phi_2\phi_3 - \beta_1 I_{11} C_3 C_3 \cos^2(\alpha s_0) \\ &-\Big(\phi_2\Big(K + \alpha^2 I_\omega + 2\beta_1 M_1^0\Big)C_3 - \kappa_1^0 I_{11}\,\phi_2\phi_2\Big)\cos^2(\alpha s_0) \\ &+\Big(C_2\, I_{22}\,\phi_3 + \kappa_1^0\, I_{11}\,\phi_3\phi_3\Big)\sin^2(\alpha s_0)\Big) \end{aligned} \tag{7.104}$$

$$R_2^2 = -\beta_2 I_{22}\Big(\alpha C_3 C_3 + \kappa_1^0\, C_2 C_3\Big)\sin(2\alpha s_0) \tag{7.105}$$

$$R_3^2 = \frac{1}{2}\beta_2 I_{22}\Big(\kappa_1^0 C_3 C_3 + \Big(4\alpha C_2 C_3 + \kappa_1^0\, C_3 C_3\Big)\cos(2\alpha s_0)\Big) \tag{7.106}$$

It appears that the right-hand side in general preserves a simple form but for nonsymmetric sections a set of non-homogeneous linear differential equations arise. In order to determine the load increments λ_1 and λ_2 the components $\tilde{\boldsymbol{\varphi}}^2$ are investigated in the following.

In-plane bending :
The differential equation for in-plane bending (7.99) is of course still uncoupled from the others. The next term in the expansion of $\tilde{\varphi}_1^1$, i.e. $\tilde{\varphi}_1^2$, can then be determined directly from from

$$-\frac{d}{ds_0}\Big(I_{11}\,\tilde{\kappa}_1^2\Big) = -\frac{d}{ds_0}\Big(I_{11}\,\frac{d\tilde{\varphi}_1^2}{ds_0}\Big) = R_1^2 \tag{7.107}$$

where R_l^2 is given by (7.104).

Integration leads to the curvature component $\tilde{\kappa}_1^2$

$$\begin{aligned}\tilde{\kappa}_1^2 &= \tfrac{1}{2}\alpha\phi_2\phi_3 - \beta_1 C_3 C_3 \cos^2(\alpha s_0) \\ &\quad - \left(\phi_2 \frac{K + \alpha^2 I_\omega + 2\beta_1 M_1^0}{I_{11}} C_3 - \kappa_1^0 \phi_2 \phi_2\right) \cos^2(\alpha s_0) \\ &\quad + \left(C_2 \frac{I_{22}}{I_{11}} \phi_3 + \kappa_1^0 \phi_3 \phi_3\right) \sin^2(\alpha s_0) \end{aligned} \tag{7.108}$$

It is now possible to examinen the expansion of κ_1^1 from (7.14) in detail. Substitution of (7.95) and (7.108) leads to

$$\begin{aligned}\kappa_1^1 &= -\left(\phi_2 \frac{K + \alpha^2 I_\omega + 2\beta_1 M_1^0}{I_{11}} C_3 + \beta_1 C_3 C_3 - \kappa_1^0 \phi_2 \phi_2\right) \cos^2(\alpha s_0) \\ &\quad + \left(C_2 \frac{I_{22}}{I_{11}} \phi_3 + \kappa_1^0 \phi_3 \phi_3\right) \sin^2(\alpha s_0) \end{aligned} \tag{7.109}$$

Notice that the term which is dominating in (7.108) vanishes in the expression for the in-plane curvature component κ_1^1. This indicates that most of the in-plane displacement is converted into internal forces connected to the out-of-plane problem.

Finally the identity $\tilde{\kappa}_1^2 = d\tilde{\varphi}_1^2/ds_0$ can be used to obtain an expression for the second order rotation component $\tilde{\varphi}_1^2$. Integration of (7.108) leads to

$$\begin{aligned}\tilde{\varphi}_1^2 &= -\frac{1}{2}\alpha\phi_2\phi_3\left(s_0 - \frac{L}{2}\right) \\ &\quad + \left[\phi_2 \frac{K + \alpha^2 I_\omega + 2\beta_1 M_1^0}{I_{11}} C_3 + \beta_1 C_3 C_3 - \kappa_1^0 \phi_2 \phi_2\right] \left(\frac{L}{2} - s_0 + \sin 2\alpha s_0\right) \\ &\quad - \left[C_2 \frac{I_{22}}{I_{11}} \phi_3 + \kappa_1^0 \phi_3 \phi_3\right] \left(\frac{L}{2} - s_0 - \sin 2\alpha s_0\right) \end{aligned} \tag{7.110}$$

where L is the length of the beam.
In the integration process the symmetri of the problem at hand has been used to obtain the form given in (7.110). From (7.110) it follows that the beam continues the deformation in the plane of the applied moment after reaching the critical load.

Out-of-plane Bending and Torsion/Warping:
The differential equations concerned with out-of-plane bending and (7.100) and torsion-warping (7.101) are still coupled. In case of nonsymmetric cross-sections the right-hand sides of (7.100)-(7.101) may differ from zero. The two missing components of the second order rotation vector $\tilde{\varphi}^2$ can then be determined from the linear differential equations

$$-\frac{d}{ds_0}\left(I_{22}\tilde{\kappa}_2^2\right) + \kappa_1^0\left(K + 2\beta_1 M_1^0\right)\tilde{\kappa}_3^2 - \kappa_1^0 \frac{d}{ds_0}\left(I_\omega \frac{d\tilde{\kappa}_3^2}{ds_0}\right) - M_1^0 \tilde{\kappa}_3^2$$

$$= -\beta_2 I_{22}\Big(\alpha C_3 C_3 + \kappa_1^0 C_2 C_3\Big)\sin(2\alpha s_0) \tag{7.111}$$

$$-\kappa_1^0 I_{22}\tilde{\kappa}_2^2 - \frac{d}{ds_0}\Big(\big(K + 2\beta_1 M_1^0\big)\tilde{\kappa}_3^2\Big) + \frac{d^2}{ds_0^2}\Big(I_\omega \frac{d\tilde{\kappa}_3^2}{ds_0}\Big) + M_1^0\tilde{\kappa}_2^2$$

$$= \frac{1}{2}\beta_2 I_{22}\Big(\kappa_1^0 C_3 C_3 + \big(4\alpha C_2 C_3 + \kappa_1^0 C_3 C_3\big)\cos(2\alpha s_0)\Big) \tag{7.112}$$

The linear differential equations are nonhomogeneous if $\beta_2 \neq 0$, which may occur for monosymmetric and nonsymmetric cross-sections. If $\beta_2 \neq 0$ then $\tilde{\varphi}_2^2 = \tilde{\varphi}_3^2 = 0$ according to the orthogonality condition of the eigenforms $\tilde{\boldsymbol{\varphi}}^i$ (7.24).

In Fig. 7.10 an illustration of the load versus displacement of the beam in pure bending is presented.

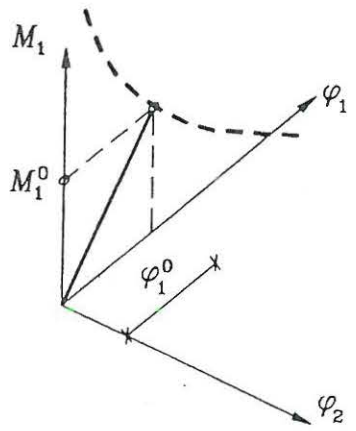

Fig. 7.10: Load-Displacements for beam in pure bending.

The process consists of an initial state where only in-plane deformations occurs followed by deformations out of the plane corresponding to a buckled state.

Load Increment Factors :
In order to determine the load increment λ the alternative version has to be used. The change in the external moment M_1 in the vicinity of the critical point is described by the load increment factors λ_1 and λ_2. λ_1 can be found from (7.39). This means that $\tilde{\varphi}_j^2$ has to be determined.
In this example λ_1 can be determined from (7.39)

$$\delta K_{11}^3\big(\tilde{\varphi}_j^1;\tilde{\varphi}_j^1\big) + \delta G_{20}^3\big(\tilde{\varphi}_j^2;\lambda_1\big) + \delta G_{11}^3\big(\tilde{\varphi}_j^1;\tilde{\varphi}_j^1,\lambda_0,\lambda_1\big) = 0 \tag{7.113}$$

where it follows from Appendix D that in this particular example

$$\delta K_{11}^3\big(\tilde{\varphi}_j^1\,;\,\tilde{\varphi}_j^1,\lambda_0,\lambda_1\big) = \frac{3}{2}\xi^2\delta\xi\int_0^l 2\beta_2 I_{22}\,\tilde{\kappa}_2^1\,\tilde{\kappa}_3^1\,\tilde{\kappa}_3^1\,ds_0 \tag{7.114}$$

and

$$\delta G^3_{11}\left(\tilde{\varphi}^1_j;\tilde{\varphi}^1_j,\lambda_0,\lambda_1\right) \;=\; 0 \tag{7.115}$$

From (7.29) it follows that

$$\delta G^3_{20}\left(\tilde{\varphi}^2_j\,;\,\lambda_1\right) \;=\; -\lambda_1\left[\tilde{\varphi}^2_1\,M^0_1\right]^l_0\,\xi\,\delta\xi^2 \tag{7.116}$$

Notice that if the external moment is applied in the direction of one of the principal axes the coefficient λ_1 is only nonzero if $\beta_2 \neq 0$, i.e. the cross-section has to be non-symmetric in the plane ortogonal to the plane of the applied moment. An example where the parameter β_2 is nonzero is the C-profile if the moment is applied in the plane of the web.

λ_2 can be determined from (7.40)

$$\begin{aligned}&\delta K^4_{11}\left(\tilde{\varphi}^1_j;\tilde{\varphi}^1_j\right) \;+\; \frac{1}{2}\,\delta K^4_{12}\left(\tilde{\varphi}^1_j;\tilde{\varphi}^2_j\right) \;+\; \delta G^4_{12}\left(\tilde{\varphi}^1_j;\tilde{\varphi}^2_j,\lambda_0,\lambda_1\right)\\ &\quad+\delta G^4_{11}\left(\tilde{\varphi}^1_j;\tilde{\varphi}^1_j,\lambda_0,\lambda_1,\lambda_2\right) \;+\; \delta G^4_{20}\left(\tilde{\varphi}^2_j;\lambda_2\right) \;=\; 0\end{aligned} \tag{7.117}$$

From Appendix D it follows that

$$\begin{aligned}\delta K^4_{11}\left(\tilde{\varphi}^1_j\,;\,\tilde{\varphi}^1_j\right) \;=\; &\frac{1}{6}\,\xi^3\,\delta\xi\int_0^l\Big\{\tilde{\kappa}^1_2\tilde{\kappa}^1_2\left(3I_{11}-4I_{22}\right)\tilde{\varphi}^1_3\tilde{\varphi}^1_3\\ &-\tilde{\kappa}^1_2\tilde{\varphi}^1_2\left(6I_{11}-4(I_{22}+K+2\beta_1M^0_1)\right)\tilde{\kappa}^1_3\tilde{\varphi}^1_3 \;+\; \tilde{\kappa}^1_3\frac{d}{ds_0}\left(I_\omega\frac{d}{ds_0}\left(\tilde{\kappa}^1_2\tilde{\varphi}^1_2\tilde{\varphi}^1_3\right)\right)\\ &+\tilde{\varphi}^1_2\tilde{\varphi}^1_2\left(3I_{11}-4K-2\beta_1M^0_1\right)\tilde{\kappa}^1_3\tilde{\kappa}^1_3 \;-\; \tilde{\kappa}^1_3\frac{d}{ds_0}\left(I_\omega\frac{d}{ds_0}\left(\tilde{\varphi}^1_2\tilde{\varphi}^1_2\tilde{\kappa}^1_3\right)\right)\\ &+6\,\tilde{\kappa}^1_3\,2\beta_1I_{11}\left(\tilde{\kappa}^1_2\tilde{\varphi}^1_3-\tilde{\kappa}^1_3\tilde{\varphi}^1_2\right)\tilde{\kappa}^1_3 \;+\; 3\,\tilde{\kappa}^1_3\tilde{\kappa}^1_3\,R^4_a F\,\tilde{\kappa}^1_3\tilde{\kappa}^1_3\Big\}\,ds_0\end{aligned} \tag{7.118}$$

and

$$\begin{aligned}\delta K^4_{12}\left(\tilde{\varphi}^1_j\,;\,\tilde{\varphi}^2_j\right) \;=\; &2\,\xi^3\,\delta\xi\int_0^l\Big\{\tilde{\kappa}^2_1\,I_{11}\left(\tilde{\kappa}^1_2\tilde{\varphi}^1_3\;-\;\tilde{\kappa}^1_3\tilde{\varphi}^1_2\right)\\ &+\tilde{\kappa}^1_2\,I_{22}\left(\tilde{\kappa}^1_3\tilde{\varphi}^2_1\;-\;\tilde{\kappa}^2_1\tilde{\varphi}^1_3\right) \;+\; \tilde{\kappa}^1_3\left(K\;+\;2\beta_1M^0_1\right)\left(\tilde{\kappa}^2_1\tilde{\varphi}^1_2\;-\;\tilde{\kappa}^1_2\tilde{\varphi}^2_1\right)\\ &+\frac{d\tilde{\kappa}^1_3}{ds_0}\,I_\omega\,\frac{d}{ds_0}\left(\tilde{\kappa}^2_1\tilde{\varphi}^1_2\;-\;\tilde{\kappa}^1_2\tilde{\varphi}^2_1\right) \;+\; \tilde{\kappa}^1_3\,2\beta_1I_{11}\,\tilde{\kappa}^2_1\tilde{\kappa}^1_3\Big\}\,ds_0\end{aligned} \tag{7.119}$$

The functions containing the initial stresses and the load increments can be found from

Appendix D, leading to

$$\delta G_{11}^4\left(\widetilde{\varphi}_j^1\,;\,\widetilde{\varphi}_j^1,\lambda_0,\lambda_1,\lambda_2\right) \;=$$

$$\frac{1}{6}\,\xi^3\,\delta\xi\,\int_0^l M_1^0\left(\widetilde{\kappa}_3^1\widetilde{\varphi}_2^{1\,3}-\widetilde{\kappa}_2^1\widetilde{\varphi}_2^{1\,2}\widetilde{\varphi}_3^1+\widetilde{\kappa}_3^1\widetilde{\varphi}_2^1\widetilde{\varphi}_3^{1\,2}-\widetilde{\kappa}_2^1\widetilde{\varphi}_3^{1\,3}\right)\,ds_0 \tag{7.120}$$

$$\delta G_{12}^4\left(\widetilde{\varphi}_j^1\,;\,\widetilde{\varphi}_j^2,\lambda_0,\lambda_1,\right) \;=\; \frac{1}{2}\,\xi^3\,\delta\xi\,\int_0^l M_1^0\left(\widetilde{\varphi}_2^1\widetilde{\varphi}_2^1+\widetilde{\varphi}_3^1\widetilde{\varphi}_3^1\right)\widetilde{\kappa}_1^2\;ds_0$$

$$+\frac{1}{2}\,\xi^3\,\delta\xi\,\left[\widetilde{\varphi}_2^1\widetilde{\varphi}_2^1\,\widetilde{\varphi}_1^2\,M_1^0\right]_0^l \tag{7.121}$$

From (7.29) it follows that

$$\delta G_{20}^4\left(\widetilde{\varphi}_j^2\,;\,\lambda_2\right) \;=\; -\,\lambda_2\left[\widetilde{\varphi}_1^2\,M_1^0\right]_0^l\,\xi^2\,\delta\xi^2 \tag{7.122}$$

In the following the initial postbuckling behavior is analysed in detail for different types of cross-sections.

Double Symmetric Cross-Sections :

In case of a double symmetric cross-section, e.g. I- or H-profiles, the postbuckling rotations are described by

$$\widetilde{\boldsymbol{\varphi}}^1 \;=\; \begin{bmatrix} 0 \\ \phi_2\cos\alpha s_0 \\ \phi_3\sin\alpha s_0 \end{bmatrix}\,,\quad \widetilde{\boldsymbol{\varphi}}^2 \;=\; \frac{1}{2}\begin{bmatrix} \alpha\phi_2\phi_3\,(s_0-L/2)\;\ldots\;\text{see (7.110)} \\ 0 \\ 0 \end{bmatrix} \tag{7.123}$$

In the expression for $\widetilde{\varphi}_1^2$ only the dominant part is written. Nevertheless the remaining part is included in the further investigations, as this contribution is essential for an accurate derivation of the initial postbuckling behavior.

The load increment factor λ_1 was previously found to be zero for double symmetric cross-sections, therefore emphasis can be placed on the determination of λ_2.

Inserting (7.123) in (7.118) and (7.122) and performing the integrations leads to the identity

$$\lambda_2\,\alpha\,\phi_2\,\phi_3\,M_1^0\,L \;=\; -\,\frac{L}{48}\Big[3C_2^2\left(3I_{11}-4I_{22}\right)\phi_3^2\;+\;3\phi_2^2\left(3I_{11}-(K+\alpha^2 I_\omega)\right)C_3^2$$

$$-\,\phi_2 C_2\left(6I_{11}-4(I_{22}+K+\alpha^2 I_\omega)\right)\phi_3 C_3\;+\;C_3^2\,R_a^4\,F\,C_3^2$$

$$+\,12\alpha\phi_2\phi_3\,I_{11}\left(C_2\phi_3\;-\;C_3\phi_2\right)\;+\;6\left(\phi_2^2\;+\;\phi_3^2\right)\kappa_1^0 I_{11}\left(3C_2\phi_3\;-\;C_3\phi_2\right)$$

$$+\,6\left(C_2 I_{22}\phi_3\;-\;\phi_2(K+\alpha^2 I_\omega)\phi_3\right)\left(3C_2\phi_3\;-\;C_3\phi_2\;-\;2\alpha\phi_2\phi_3\right)$$

$$+\frac{6}{\pi}C_2\big(I_{22}-(K+\alpha I_\omega)\big)C_3\alpha\phi_2\phi_3 + 12M_1^0\,\alpha\phi_2^3\phi_3$$

$$+M_1^0\big(3\phi_2^3C_3-\phi_2^2C_2\phi_3+\phi_2\phi_3^2C_3-3C_2\phi_3^3+6\alpha\,\phi_2\phi_3(\phi_2^2+\phi_3^2)\big)\Big] \qquad (7.124)$$

where the effect from the initial curvature κ_1^0 is contained in the coefficients C_2 and C_3 determined by (7.45). The term associated with the fourth-order moment R_a^4 which only depends on the twist $\tilde{\kappa}_3^1$ is also a term which does not possess the same structure as the remaining terms.
If the initial curvature is neglected in (7.124) $C_2 = -\alpha\phi_2$ and $C_3 = \alpha\phi_3$. Performing such an analysis leads to an impression of whether the postbuckling behavior is stable or not. Letting h represent a characteristic length inside the cross-section then the term containing R_a^4 hereby becomes proportional to $(h/L)^2$ compared to the other terms. This indicates that for beams with ordinary proportions the contribution is negligible. Substitution of the expression for the critical moment M_1^0 in terms of the buckling form (ϕ_2, ϕ_3) from (7.96) leads to

$$\lambda_2 \simeq \frac{5}{16}\left(1+\frac{K+\alpha^2 I_\omega}{I_{22}}\right) \qquad (7.125)$$

This means that for the double symmetric beam in pure bending the initial postbuckling behavior is always stable.

The external moment M_1 in the vicinity of the critical point is expressed by

$$M_1 = M_1^0\left(1+\lambda_2\xi^2\right) \qquad (7.126)$$

where λ_2 is given by (7.125). Using a relation between rotation φ_1 and translation r_{a_2} similar to (7.71) the scale factor ξ can be related to the deflection out-of-plane of the elastic center at the middle of the beam

$$\xi\,\phi_2 = \pi\frac{\delta_1}{L} \qquad (7.127)$$

Using the eigenform (7.96) and substitution of (7.127) leads to

$$\frac{M_1}{M_1^0} \simeq 1+\frac{5}{16}\,\pi^2\left(1+\frac{I_{22}}{K+\alpha^2 I_\omega}\right)\left(\frac{\delta_1}{L}\right)^2 \qquad (7.128)$$

Notice that in the vicinity of the critical point the curvature of the initial postbuckling curve depends on the ratio between the out-of-plane bending stiffness and the torsional stiffness. This means that the postbuckling strength is closely related to the tendency of the beam to twist instead of to bend out of the plane as it could be expected. In Fig. 7.11 the initial postbuckling curves are illustrated for IPE100 and HB10 (rectangular profile where the height/depth ratio is 10) profiles with $L = 2400mm$. The important cross-section parameters are for the I-beam $I_{11}/I_{22} = 10.75$ and $I_{22}/(K+\alpha^2 I_\omega) = 28.8$ whereby $\lambda_2 = 0.323$ while for the HB-beam $I_{11}/I_{22} = 100$, $I_{22}/K = 0.655$ and $\lambda_2 = 0.790$.

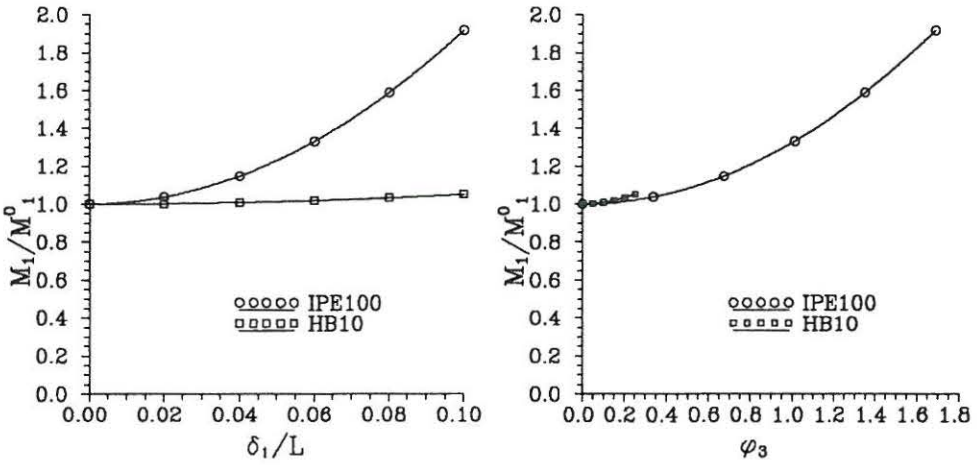

Fig. 7.11: Asymptotic 2nd order postbuckling curve for double symmetric cross-section. a) Out-of-plane deflection. b) Twist.

From Fig. 7.11a it is evident that for a beam with standard proportions some deflection has to occur before the beam regains some strength out-of-plane. An important aspect in the investigation of the postbuckling strength is the twist φ_3 of the cross-section plane at the midpoint of the beam developing during the buckling process, see e.g. Fig. 7.11b. Using (7.127) and (7.96) it follows that approximately

$$\varphi_3 = \pi \frac{\delta_1}{L} \sqrt{\frac{I_{22}}{K + \alpha^2 I_\omega}} \tag{7.129}$$

which indicates that a significant twist has to occur before the beam regains strength. A deflection of $\delta_1/L = 0.05$ means for the IPE100 that $\varphi_3 \simeq \pi/4$ while $\varphi_3 \simeq \pi/80$ for HB10. Finally Fig. 7.11 indicates that slender beams have more reserve strength after buckling commences than do stocky beams.

The asymptotic postbuckling analysis performed for the IPE-profile and the rectangular profile have shown that only an insignificant postbuckling strength is available.

Monosymmetric Cross-Sections - $\beta_1 \neq 0$:

A cross-section where $\beta_1 \neq 0$ is e.g. a T-profile if the moment is applied in the plane of the web. The postbuckling rotations are now given by

$$\tilde{\varphi}^1 = \begin{bmatrix} 0 \\ \\ \phi_2 \cos\alpha s_0 \\ \\ \phi_3 \sin\alpha s_0 \end{bmatrix}, \quad \tilde{\varphi}^2 = \frac{1}{4} \begin{bmatrix} (2\alpha\phi_2\phi_3 + 2\beta_1 C_3 C_3)(s_0 - L/2) \\ + \beta_1 C_3 C_3 \sin 2\alpha s_0 \ \ldots \text{ (see (7.110))} \\ \\ 0 \\ \\ 0 \end{bmatrix} \tag{7.130}$$

From (7.130) it follows that the sign of the second order term $\tilde{\varphi}_1^2$ depends on the influence from the term containing the parameter β_1. It can easily be shown that the first term is dominant meaning that the sign of this term prescribes the sign of $\tilde{\varphi}_1^2$. From the investigations concerned with the double symmetric cross-section it was obvios that the amount of terms

makes it almost impossible to include everything. In the following the author has given his best to obtain a reasonable description for the monosymmetric cross-section.

The load increment factor λ_1 is again found to be zero. Inserting (7.130) in (7.118-7.122) and performing the integrations means that λ_2 can be determined from

$$\begin{aligned}
&\lambda_2 \left[\alpha\, \phi_2\, \phi_3 \,+\, \beta_1 C_3 C_3 \right] M_1^0\, L \;=\; \\
&-\frac{L}{48}\Big[3C_2^2\big(3I_{11}-4I_{22}\big)\phi_3^2 \,+\, 3\phi_2^2\big(3I_{11}-(K+\alpha^2 I_\omega+2\beta_1 M_1^0)\big)C_3^2 \\
&-\phi_2 C_2\big(6I_{11}-4(I_{22}+K+\alpha^2 I_\omega+2\beta_1 M_1^0)\big)\phi_3 C_3 \,+\, C_3^2\, R_a^4 F\, C_3^2 \\
&12\alpha\phi_2\phi_3\, I_{11}\,\big(C_2\phi_3 \,-\, C_3\phi_2\big) \,+\, 6\big(\phi_2^2 \,+\, \phi_3^2\big)\kappa_1^0 I_{11}\,\big(3C_2\phi_3 \,-\, C_3\phi_2\big) \\
&6\big(C_2 I_{22}\phi_3 \,-\, \phi_2(K+\alpha^2 I_\omega+2\beta_1 M_1^0)\phi_3\big)\big(3C_2\phi_3 \,-\, C_3\phi_2 \,-\, 2\alpha\phi_2\phi_3\big) \\
&+\frac{6}{\pi}C_2\big(I_{22}-(K+\alpha I_\omega+2\beta_1 M_1^0)\big)C_3\alpha\phi_2\phi_3 \\
&+\beta_1 C_3 C_3\Big[(3+12/\pi)\,C_2 C_3\,\big(I_{22}-(K+\alpha^2 I_\omega+2\beta_1 M_1^0)\big) \,-\, 12\beta_1 I_{11} C_3 C_3 \\
&\qquad +24\alpha\phi_2\phi_3 I_{11} \,+\, 6\big(3C_2 I_{22}\phi_3-\phi_2(K+\alpha^2 I_\omega+2\beta_1 M_1^0)\big)\,C_3\Big] \\
&+6\big(C_2\phi_3-3\phi_2 C_3\big)\,2\beta_1 I_{11}\,C_3^2 \,+\, 12M_1^0\,\alpha\phi_2^3\phi_3 \,+\, 24\phi_2\phi_2\beta_1 C_3 C_3 \\
&+M_1^0\big(3\phi_2^3 C_3-\phi_2^2 C_2\phi_3+\phi_2\phi_3^2 C_3-3C_2\phi_3^3+6\alpha\,\phi_2\phi_3(\phi_2^2+\phi_3^2)\big)\Big] \qquad (7.131)
\end{aligned}$$

A simple expression for λ_2, as obtained for the double symmetric, can not be achieved for the monosymmetric cross-section because of the influence from β_1 on M_1^0. The sign of λ_2 therefore has to be examined by analysing specific examples. This has not been carried out at this point.

Monosymmetric Cross-Sections - $\beta_2 \neq 0$:

An example of a monosymmetric cross-section where $\beta_2 \neq 0$ is the C-profile if the moment is applied in the plane of the web. The postbuckling rotations can be written as

$$\tilde{\varphi}^1 \;=\; \begin{bmatrix} 0 \\ \phi_2\cos\alpha s_0 \\ \phi_3\sin\alpha s_0 \end{bmatrix},\; \tilde{\varphi}^2 \;=\; \frac{1}{4}\begin{bmatrix} \alpha\phi_2\phi_3(2s_0-L) \\ \tilde{\varphi}_2^2(s_0) \\ \tilde{\varphi}_3^2(s_0) \end{bmatrix} \;\simeq\; \frac{1}{4}\begin{bmatrix} \alpha\phi_2\phi_3(2s_0-L) \\ 0 \\ 0 \end{bmatrix} \qquad (7.132)$$

Notice that the second and third component of $\tilde{\varphi}^2$ are assumed to be negligible.

The load increment factor λ_1 can be found from (7.114) and (7.116) by substitution of (7.132). Performing the integrations it follows that

$$\lambda_1 \, \alpha \phi_2 \phi_3 \, M_1^0 L \;=\; \frac{1}{\alpha} 2\beta_2 \, I_{22} \, C_2 C_3^2 \tag{7.133}$$

whereby

$$\lambda_1 \;=\; \frac{2\beta_2}{L} \frac{\alpha I_{22}}{M_1^0} \frac{C_2 C_3^2}{\alpha^3 \phi_2 \phi_3} \tag{7.134}$$

Equation (7.134) implies that the slope of the postbuckling curve is proportional to the ratio between the cross-sectional parameter β_2 and the length of the beam L.

Analysing the dependency of λ_1 on the the cross-section dimensions can be performed by neglecting the initial curvature κ_1^0. Using the relations obtained for the straight beam case leads to

$$\lambda_1 \;\simeq\; -\frac{2\beta_2}{L} \sqrt{\frac{I_{22}}{K + \alpha^2 I_\omega}} \tag{7.135}$$

Notice that the slope also depends on the ratio between the out-of-plane bending stiffness and the torsional stiffness. Comparing with γ_β in (7.91) it appears that the influence from an unsymmetry on the buckling behavior indeed is decribed by the dimensionless factor γ_β.

Recalling that β_2 doesn't appear in the relation (7.117) which determines λ_2 it follows that λ_2 equals the one found for the double symmetric cross-section in (7.125). The external moment can then be expressed by

$$M_1 \;=\; M_1^0 \left(1 + \lambda_1 \xi + \lambda_2 \xi^2\right) \tag{7.136}$$

Using the identity of (7.127) equation (7.136) can be rewritten to yield

$$\frac{M_1}{M_1^0} \;=\; 1 \,-\, 2\pi \frac{\beta_2}{L} \frac{I_{22}}{K + \alpha^2 I_\omega} \left(\frac{\delta_1}{L}\right) + \frac{5}{16} \pi^2 \left(1 + \frac{I_{22}}{K + \alpha^2 I_\omega}\right) \left(\frac{\delta_1}{L}\right)^2 \tag{7.137}$$

It follows from (7.137) that the ratio between the bending stiffnesses and the torsional stiffness is essential for the postbuckling strength of the beam element in pure bending. The initial postbuckling curve for an CNP100 beam (see e.g. Table 7.1) with length $L = 2400mm$ loaded in the plane of the web is illustrated in Fig. 7.12. The result illustrated in Fig. 7.12 is one example of how skew the bifurcation problem can be. It follows from Fig. 7.12 that the minimum value of the critical moment M_1 is about 10 procent smaller than the critical moment determined from (7.93), i.e. a perfect beam ($\delta_1/l = 0$) and further that this point is displaced by $\delta_1/L \simeq -0.035$. From (7.129) and Table 7.1 it follows that an deflection corresponding to $\delta_1/L = -0.035$ leads to a significant twist. From a practical point of view this means that no postbuckling strength is available in this particular example for a *negative imperfection.*

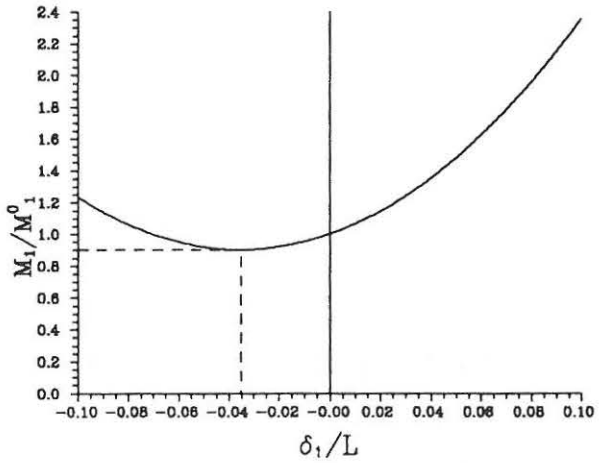

Fig. 7.12: Asymptotic 2nd order postbuckling curve for monosymmetric cross-section. (CNP100)

All this indicates that for the CNP-profile a significant influence from the unsymmetry in the loading plane occurs. The asymptotic analysis has revealed that cross-section which are nonsymmetric in the loading plane are sensitive to imperfections and further it has identified the governing parameters which are describing how sensitive a particular beam is.

7.6 Conclusions

An asymptotic buckling and postbuckling theory has been developed from the virtual work equation (3.16) by use of a perturbation method. The general stability equation which contains seven generalized displacements is, by omitting strain deformations, simplified to be expressed entirely in terms of the rotational components. Both a differential as well as an energy formulation of the asymptotic buckling and postbuckling problem are presented. The solution procedure is to determine a buckling mode from the linearized problem, i.e. bifurcation problem, and then by reinserting the buckling mode in the expanded version of the virtual work equation to identify the first order load increment factor. A successive use of the differential equations where the influence from a previos step are accounted for and the virtual work equation then leads to identification of the load-displacement relation in asymptotic sense.
The simply supported column with arbitrary cross-section and the beam in pure bending have been investigated by use of the developed theory which has led to identification of the governing parameters in the stability problem. The investigations have not revealed any new geometric quantities, as it was expected, but they have identified the relations between the cross-section parameters which determines the postbuckling behavior.

Chapter 8

Numerical Formulation of the Stability Problem

In linear problems the solution is always unique which is no longer the case in many nonlinear situations. Thus, if "a solution" is achieved it may not necessarily be "the solution" sought. Physical insight into the nature of the problem and, usually, small-step incremental approaches are essential to obtain physically significant answers. Nonlinear problems are usually solved by taking a series of linear steps. In a structural analysis the process is to express the equilibrium equations in incremental form $\mathbf{K} \cdot \Delta\mathbf{u} = \Delta\mathbf{f}$. Here the stiffness matrix $\mathbf{K}$ is a function of the displacements $\mathbf{u}$ because the problem is nonlinear. The current $\mathbf{K}$, often referred to as the *tangent stiffness*, is used to compute the next step in $\Delta\mathbf{u}$. Then $\mathbf{u}$ and $\mathbf{K}$ are updated thereby being ready to take another step.
The nonlinear stability problem, as considered in this context, can be solved by use of an updated Lagrangian solution procedure. Updated Lagrangian schemes have been used successfully for the displacement-based finite element beam formulation by Yang & McGuire (1986), Conci & Gattass (1990) and Kouhia (1991). A partially updated Lagrangian formulation has been used by Peterson & Petersson (1985).

The weak formulation derived in Chapter 4 is obtained by considering the beam element in two adjacent states. An updated Lagrangian formulation is therefore the obvious choice as the initial state represents the history of the loading-displacement process and an incremental step can be taken from this state. In this chapter an incremental updated Lagrangian two node hybrid element is developed using the results obtained for the beam element in Chapter 6. Assuming small displacements but finite rotations the updating procedure is focused on the rotation components. The performance of the hybrid element in a nonlinear context is finally tested by analysing canonical problems. Comparisons are made with the literature as well as the asymptotic analysis performed in Chapter 7.

8.1 Incremental Virtual Work Equation

In the general form presented in Chapter 5 the nonlinear stability equation (5.1) contains 7 unknown displacement functions and the load increment factor λ. In both Chapters 6 and 7 the general form was reformulated by neglecting the strain deformations in order to obtain simple but consistent formulations. In the numerical formulation in Chapter 6 the number

of degrees of freedom was raised from 7 to 11 using a mixed formulation. The simple formulation and the statical performance of the element developed from the mixed formulation compensates for the high number of degrees of freedom. In the analytical analysis in Chapter 7 the stability equation was formulated entirely in terms of the rotation components, i.e. 3 displacement degrees of freedom and a load increment factor, which could be used to investigate some canonical problems in an asymptotic way. Based on the experience from both chapters emphasis is placed on developing a two node hybrid element in agreement with the beam element in Chapter 6.

By a mixing of the element formulation in Chapter 6, i.e. (6.5), and the weak formulation in Chapter 8, i.e. (7.11), the weak form describing the stability problem can be obtained.

$$\int_0^l \Big\{ \frac{1}{2}\delta\Big(2\lambda_j\,\varepsilon_j^1 + \kappa_\alpha^1\, I_{\alpha\beta}\,\kappa_\beta^1 + \kappa_3^1\Big(K + r_a^2 N_3^0 + 2\beta_\alpha M_\alpha^{c\,0}\Big)\kappa_3^1 + \frac{d\theta^1}{ds_0}\, I_\omega \frac{d\theta^1}{ds_0}$$

$$+ \lambda_\omega\,(\theta^1 - \kappa_3^1) + \kappa_3^1\, 2\beta_\eta I_{\eta\alpha}\,\kappa_\alpha^1\,\kappa_3^1 + \tfrac{1}{4}\,\kappa_3^1\,\kappa_3^1\, R_a^4 F\,\kappa_3^1\,\kappa_3^1\Big) - \lambda\,\delta r_{a_l}^1\, p_l^0$$

$$- \delta\kappa_j^1\, M_l^0\,\tilde{A}_{lj} + \delta\tilde{A}_{kn}\, f_\alpha^0 p_k^0\,\big(\lambda\,\delta_{\alpha n} + \tilde{A}_{\alpha n}\big) + \delta\tilde{A}_{kn}\, N_k^0\,\tilde{A}_{3n} - \lambda\,\delta\theta^1\, b^0 \Big\}\, ds_0$$

$$- \Big[\lambda\,\delta r_{a_j}^1 \sum_{i=1}^{n} P_j^{0i} + \delta\tilde{A}_{kn} \sum_{i=1}^{n}\big(P_k^{0i}\, F_\alpha^{0i}\big)\big(\lambda\,\delta_{\alpha n} + \tilde{A}_{\alpha n}\big)\Big]_0^l = 0 \qquad (8.1)$$

The functions λ_j and λ_ω are the Lagrange Multipliers as introduced in Chapter 6. Notice that the load increment associated with the internal force N_j^0, i.e. point loads, is accounted for in the boundary term in contrast to the weak formulation in (7.11).

In order to obtain a formulation suitable for the Finite Element method the linearized version of (8.1) is introduced similar to (6.15) but now expanded with the initial stress terms. Using the symmetry obtained in the linearized potential energy V_{lin} given in (5.30) means that the linearized version of (8.1) is given by

$$\int_0^l \Big\{ \delta\Big(\lambda_j\Big(\frac{dr_{a_j}^1}{ds_0} + r_{a_l}^1 e_{ljn}\kappa_n^0 + e_{j3n}\varphi_n^1\Big) + \lambda_\omega\Big(\theta^1 - \frac{d\varphi_3^1}{ds_0} + \varphi_\gamma^1 e_{\gamma\eta}\kappa_\eta^0\Big)$$

$$+ \frac{1}{2}\Big(\frac{d\varphi_\alpha^1}{ds_0} + \varphi_n^1 e_{n\alpha m}\kappa_m^0\Big) I_{\alpha\beta}\Big(\frac{d\varphi_\beta^1}{ds_0} + \varphi_k^1 e_{k\beta j}\kappa_j^0\Big) + \frac{1}{2}\frac{d\theta^1}{ds_0}\, I_\omega \frac{d\theta^1}{ds_0}$$

$$+ \frac{1}{2}\Big(\frac{d\varphi_3^1}{ds_0} - \varphi_\alpha^1 e_{\alpha\beta}\kappa_\beta^0\Big)\Big(K + r_a^2\, N_3^0 + 2\,\beta_\alpha\, M_\alpha^{c\,0}\Big)\Big(\frac{d\varphi_3^1}{ds_0} - \varphi_\gamma^1 e_{\gamma\eta}\kappa_\eta^0\Big)\Big)$$

$$+ \Big(\frac{d\varphi_j^1}{ds_0} + \varphi_k^1 e_{kjm}\kappa_m^0\Big)\, e_{jnl} M_l^0\,\varphi_n^1 - \varphi_l^1\, e_{lnk}\Big(N_k^0\,(\delta_{3j} + \varepsilon_j^0) + p_k^0\, f_\alpha^0\,\delta_{\alpha j}\Big)\, e_{jnm}\,\varphi_m^1$$

$$- \lambda\, r^1_{a\,k}\, p^0_k - \lambda\, p^0_k e_{kj\alpha}\, f^0_\alpha\, \varphi^1_j - \lambda b^0 \theta^1 \Big) \Big\}\, ds_0$$

$$- \delta \Big[r^1_{al} \sum_{i=1}^{n} \left(\lambda\, P^{0i}_l \right) + \frac{1}{2} \varphi^1_k\, e_{kln} \sum_{i=1}^{n} \left(P^{0i}_n\, F^{0i}_\alpha \left(e_{l\alpha j}\, \varphi^1_j + 2\lambda\, \delta_{l\alpha} \right) \right) \Big]_0^l \;=\; 0 \qquad (8.2)$$

Equation (8.1) is a mixed formulation of the stability problem as both kinematical as well as statical functions are present and it follows that the only deviation from (6.5) is the presence of the initial stress terms. The mixed formulation of the incremental equilibrium equations is in the following used to introduce the tangent stiffness.

8.2 Incremental Updated Lagrangian Two Node Hybrid Element

The development of an updated Lagrangian element is performed similar to the development of the static beam element in Chapter 6. This means that linear shape functions are used for all involved functions.

A deviation from Chapter 6 is the presence of the initial forces. Using linear interpolation it follows that

$$N^0_k(\xi) \;=\; (1 - \xi)\, N^{0i}_k + \xi\, N^{0j}_k \quad , \quad M^0_k(\xi) \;=\; (1 - \xi)\, M^{0i}_k + \xi\, M^{0j}_k \qquad (8.3)$$

Equation (8.2) expresses the incremental form of the equilibrium equations at the beginning of an incremental step. This means that the initial terms have to be updated before proceeding with the next load increment. Assuming small displacements but finite rotations it follows from Chapter 3 that updating has to be performed corresponding to

$$\boldsymbol{\varphi}^0_u \;=\; \boldsymbol{\varphi}^0 + \boldsymbol{\varphi}^1 \quad , \quad \mathbf{N}^0_u \;=\; \left(N^0_j + N^1_j \right) \mathbf{e}_j \quad , \quad \mathbf{M}^0_u \;=\; \left(M^0_j + M^1_j \right) \mathbf{e}_j \qquad (8.4)$$

i.e. the increments in the rotation vector are added in a vector relation while the internal force components are updated according to the convected basis described by $\mathbf{e}_j$.

The Finite Element formulation can be obtained by assembling the degrees of freedom in a node vector $\mathbf{u}$. For an assembly of elements the equilibrium equation then takes the form

$$\delta \mathbf{u}^T \cdot \Big[\left(\mathbf{K} + \mathbf{K}^\kappa + \lambda_0\, \mathbf{K}^\sigma \right) \cdot \mathbf{u} \;-\; \lambda \mathbf{f} \Big] \;=\; 0 \qquad (8.5)$$

where the conventional stiffness matrix $\mathbf{K}$, the initial displacement matrix $\mathbf{K}^\kappa$ and the load increment vector $\mathbf{f}$ are developed in Chapter 6 and the complete form of the matrices is given in Appendix E. The initial stress matrix $\mathbf{K}^\sigma$ is developed in a similar way as $\mathbf{K}$ and is also given in Appendix E. The investigations performed in Chapter 6 indicated a very simple formulation of $\mathbf{K}$ and $\mathbf{K}^\kappa$. Further it follows from (8.2) and Appendix E that $\mathbf{K}^\sigma$ may only have nonzero elements in connection with the rotation components indicating a simple and compact form. λ_0 is the proportional constant of the initial stress distribution and the matrix inside the parenthesis is the *tangent stiffness* for an incremental load step.

Equation (8.5) has to be fulfilled for any variation in $\mathbf{u}$ which leads to

$$\left(\mathbf{K} + \mathbf{K}^{\kappa} + \lambda_0 \mathbf{K}^{\sigma}\right) \cdot \mathbf{u} - \lambda \mathbf{f} = \mathbf{0} \tag{8.6}$$

The transition point from the initial state into the buckled state is identified by $\lambda = 0$ and

$$\det \left| \mathbf{K} + \mathbf{K}^{\kappa} + \lambda_0 \mathbf{K}^{\sigma} \right| = 0 \tag{8.7}$$

As both $\mathbf{K}^{\kappa}$ and $\mathbf{K}^{\sigma}$ depend on the precritical displacements $\mathbf{u}^0$ (8.7) is not to be solved directly as a generalized eigenvalue problem instead the matrices and λ_0 are updated successively until (8.7) is fulfilled, i.e. $\lambda_0 = \lambda_{cr}$. The solution procedure is illustrated in Fig. 8.1.

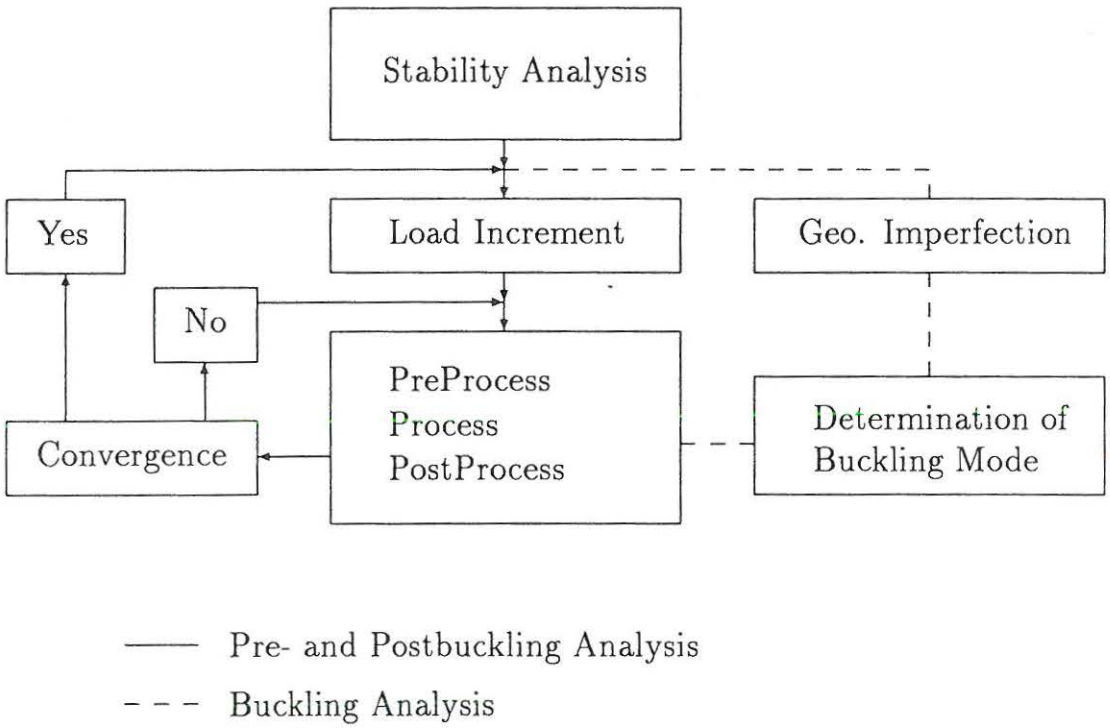

Fig. 8.1: Principles of a stability analysis.

During each load step a Newton-Raphson procedure is used to obtain the solution. In a stability analysis where both the pre- and post-buckling load-displacement are sought an iterative procedure as the Newton-Raphson method may fail to give a satisfactory solution for the postbuckling problem. This is due to that reaching the critical point may imply that the structural system has only insignificant stiffness in a plane ortogonal to the loading plane. The continuation of the loading process therefore becomes very sensitive and the possibility of different equilibrium paths, i.e. a bifurcation point, may force a nonconvergent solution. In this context this problem is avoided by introducing an imperfection which forces the beam structure to begin a deformation according to the buckling form corresponding to the critical load. Determination of how to impose the imperfection can be performed by solving the generalized eigenvalue problem in (8.7). If λ_{cr} has been determined the buckling

mode $\mathbf{u}_{buck}$ can be found from

$$\left(\mathbf{K} + \mathbf{K}^{\kappa} + \lambda_{cr}\,\mathbf{K}^{\sigma}\right) \cdot \mathbf{u}_{buck} \;=\; \mathbf{0} \tag{8.8}$$

Restarting the stability analysis with an imperfection corresponding to (8.8) means that the pre- and post-buckling behavior can be examined by successive use of (8.6).

8.3 Numerical Examples

Four examples have been analysed with the developed element in order to test the performance compared with the literature and further to investigate some canonical problems thereby achieving general information about the buckling and postbuckling behavior of thin-walled beams.

8.3.1 Cantilever Subjected to an End-Moment

The first example does not test the full three-dimensional behavior but, in two-dimensions, it is a severe test of the performance of the two node hybrid element exposed to large rotations. This example has been used by a number of authors, see e.g. Surana & Sorem (1987) and Crisfield (1990), to illustrate the nonlinear performance.

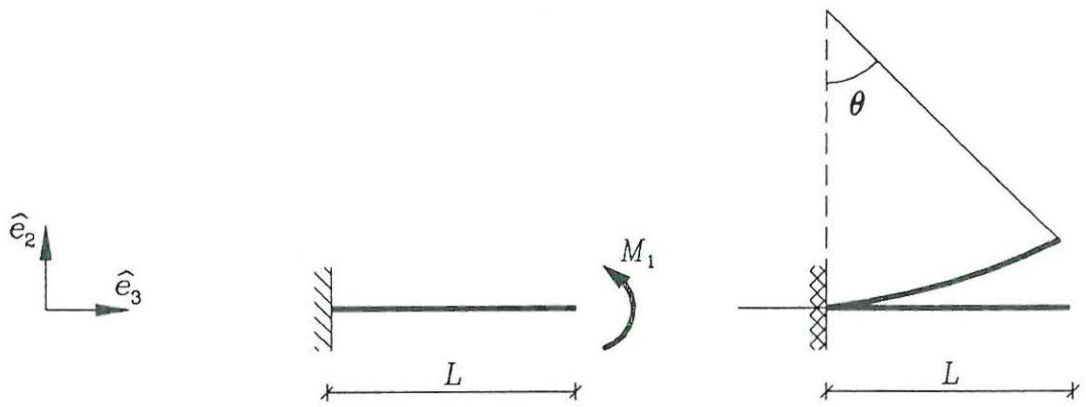

Fig. 8.2: Cantilever subjected to an end-moment.

An initially-straight cantilever is subjected to an end-moment, as shown in Fig. 8.2 whereby

$$M_1 \;=\; I\,\frac{\theta}{L} \qquad , \qquad M_{ref} \;=\; I\,\frac{2\pi}{L} \tag{8.9}$$

Fig. 8.3a illustrates the deformation of the cantilever, using the curved two node hybrid element, during the loading process. Increasing the moment until $M_1 = M_{ref}$ forces the beam to curl into a complete circular ring as shown in Fig. 8.3a. The deformed configurations are in Fig. 8.3 illustrated with straight lines between the element nodes.

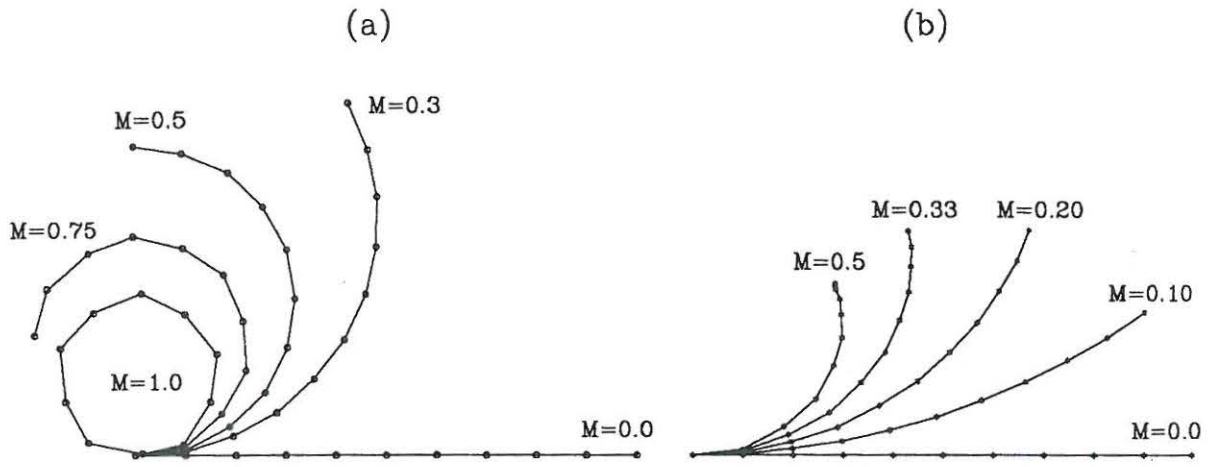

Fig. 8.3: Initial and deformed geometries for cantilever subjected to an end-moment (10 elements). a) curved elements. b) straight elements.

The analytical position of the endpoint during the loading process is given by

$$\begin{bmatrix} r_2 \\ \\ r_3 \end{bmatrix} = \frac{L}{\theta} \begin{bmatrix} 1 - \cos\theta \\ \\ \sin\theta \end{bmatrix} \tag{8.10}$$

Using ten identical elements the numerical results for the two node hybrid element using straight as well as curved elements are illustrated together with (8.10) in Fig. 8.4.

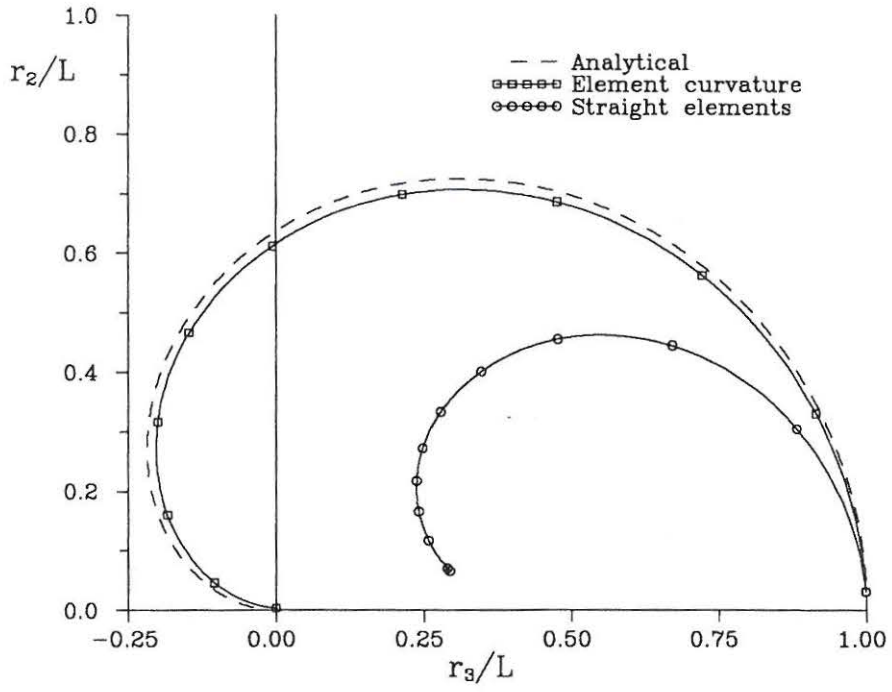

Fig. 8.4: Endpoint position for cantilever (10 elements).

Fig. 8.4 shows that using straight beam elements leads to a totally different load-displacement

path already at small values of M while the curved element is close to the analytical during all the loading process. The behavior of the straight elements are also shown in Fig. 8.3b and it strongly indicates the lack of validity for large displacements. This result indicates that using straight beam elements in a large-rotation analysis may lead to a qualitatively wrong behavior of the beam structure.

8.3.2 Simply Supported Column

The next example is presented in order to illustrate the performance of the developed element in a pre- and post-buckling analysis. The postbuckling behavior of the simply supported column has been known for many years Koiter (1945) and the example serves as a guideline for the possibilities of tracing the equilibrium path in a postbuckling analysis with the developed element.

In Fig. 8.5 the numerical results using 6 identical elements are shown together with the analytical solution from Timoshenko & Gere (1961) and the asymptotic fourth-order solution taken from Thompson & Hunt (1973). The postbuckling curve has been initiated by a small imperfection $\epsilon = r_2/L = 4.17 \cdot 10^{-5}$ at the midpoint of the beam.

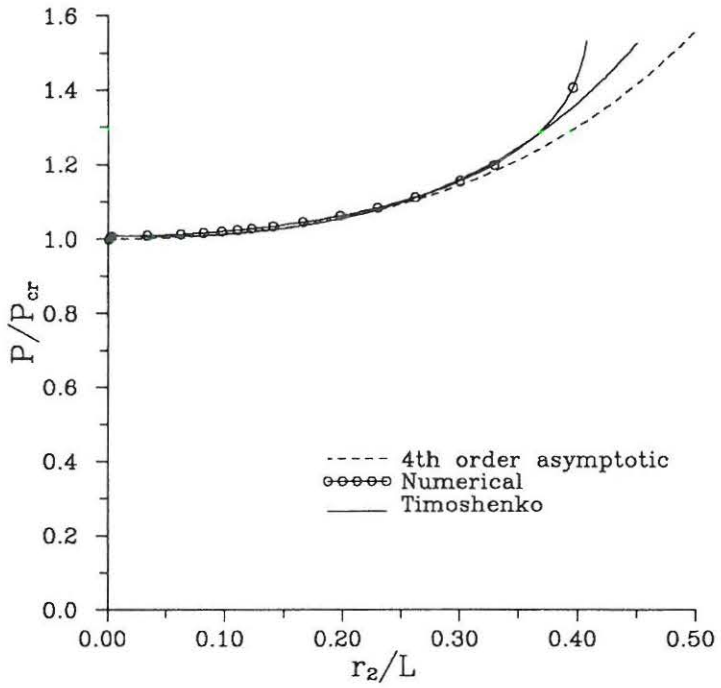

Fig. 8.5: Midpoint deflection for simply supported column.

The results indicate that the two node hybrid element is capable of reproducing the nonlinear behavior of the simply supported column as given by Timoshenko & Gere (1961). The numerical postbuckling curve lies a small part above the analytical ones which indicates as to be expected that the numerical model in a small degree is to stiff. The error is insignificant and the results for this plane problem are regarded as very promising for the spatial behavior as to be considered in the following examples.

8.3.3 Beam in Pure Bending

The next example which has been considered is lateral buckling of the beam in pure bending. This example has been analysed in order to make some comparisons with the asymptotic solution for the initial postbuckling behavior obtained in Chapter 7.
Assuming that the ends are free to warp the critical moment for the straight beam case is given by (7.89), i.e.

$$M_{cr}^{str} = \alpha\sqrt{I_{22}\left(K + \alpha^2 I_\omega\right)} \quad , \quad \alpha = \frac{\pi}{L} \tag{8.11}$$

In Fig. 8.6-8.8 the out-of-plane deflection at the midpoint for a rectangular-, IPE20- and CNP100-section is illustrated together with the asymptotic second-order solution from (7.125). The asymptotic solutions are weighted with γ_κ from (7.94) in order to incorporate the influence from an initial curvature. For the rectangular section a ratio height/depth of $h/b = 10$ has been used. The dimensionless section properties for the IPE20-section are $I_{11}/I_{22} = 13.7$, $I_{22}/(K + \alpha^2 I_\omega) = 28.4$. For the rectangular- and the IPE- beams the length of the beam is $L = 240mm$. The properties of the CNP100 beam are those given in Section 7.5.3, i.e $I_{11}/I_{22} = 7.0$, $I_{22}/(K + \alpha^2 I_\omega) = 24.8$ and $L = 2400mm$. The numerical models consists of ten identical elements and the postbuckling curves are initiated by a small imperfection $\epsilon = 4 \cdot 10^{-4}$ at the midpoint of the beam.

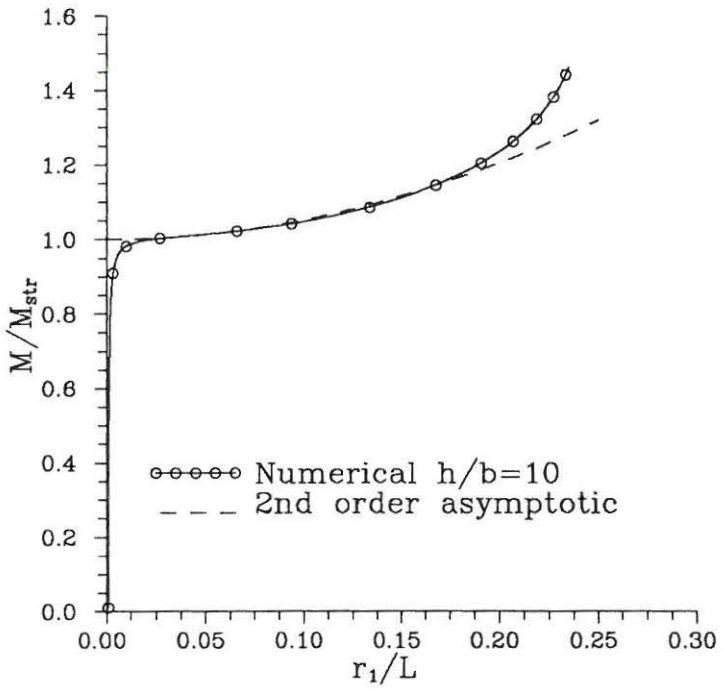

Fig. 8.6: Postbuckling curve for rectangular beam in pure bending.

From Fig. 8.6 it appears that the critical load for a rectangular section is well-determined by (7.128). For the rectangular section the postbuckling curve is very flat corresponding to that the torsional stiffness is comparable with the out-of-plane stiffness (see Tab. 8.1) whereby it follows from (7.96) that the buckling mode becomes an equal distribution of twist and deflection. Notice that a significant deflection has to arise before the beam regains some

strength. The numerical and the asymptotic solutions are close in the vicinity of the critical point implying that for a rectangular section (7.128) reveals the initial postbuckling behavior for a beam in pure bending.

In Fig. 8.7 the numerical result for the IPE20 section is illustrated together with the asymptotic result from Section 7.5.3.

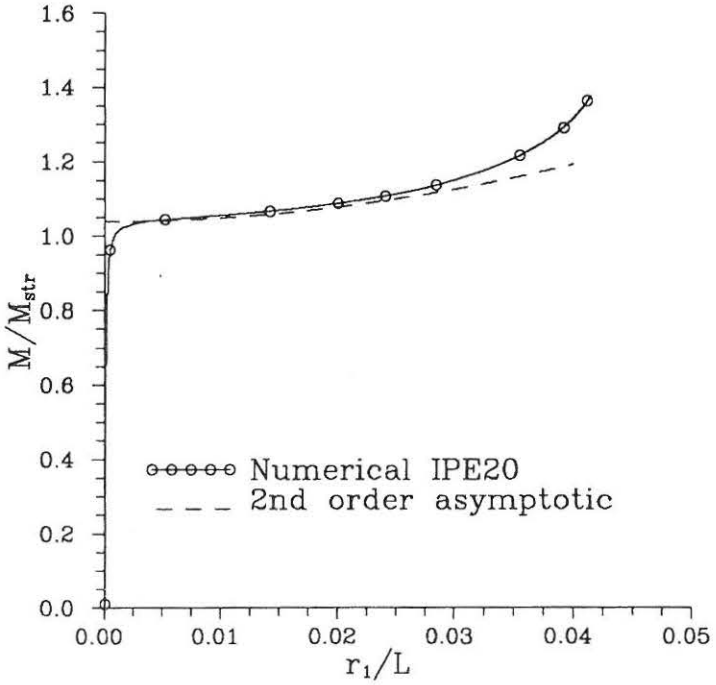

Fig. 8.7: Postbuckling curve for IPE-beam in pure bending.

Continuing with the I-section it is evident from Fig. 8.7 that prebuckling deformation influences the value of the critical load as it also is found in Chapter 7. Analysing Fig. 8.7 in detail it follows that the numerical solution possesses a curvature in the vicinity of the critical point which is close to the one given by (7.128). As the load increases and thereby the deformations the difference between the asymptotic and the numerical solution becomes conspicuous implying that the actual configuration of the beam influences the postbuckling behavior. Further one should notice that the IPE-beam regains strength at a relative small out-of-plane deflection compared with the rectangular section. This is because the small torsional stiffness forces the IPE-beam to twist whereby the in-plane bending stiffness contribute to the out-of-plane stiffness.
The IPE-profile is a standard profile where the dimensionless cross-sectional ratios are nearly constant. It can therefore be concluded from Fig. 8.7 that only a small postbuckling strength is available for the standard version.

A concluding remark is that for double symmetric cross-sections the initial postbuckling behavior is stable but the gain in strength is insignificant for practical purpose.

The numerical results for the CNP100 section are illustrated in Fig. 8.8 together with the asymptotic result (7.125). Two different ratios of β_2/L have been used because the CNP-profile twists significant implying that the effect from the unsymmetry may be erased in the postbuckling behavior as the deformation increases.

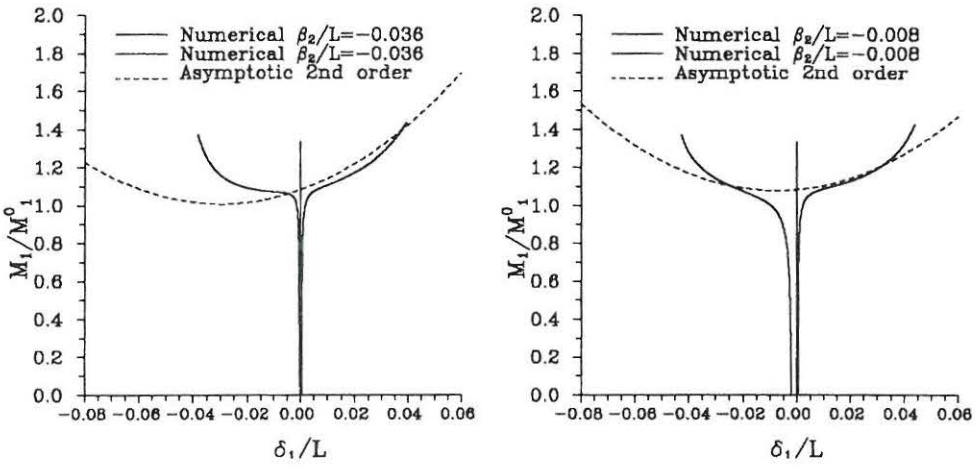

Fig. 8.8: Postbuckling curve for a CNP-beam in pure bending.

The numerical results obtained by the hybrid element confirms that a skew symmetric bifurcation behavior occurs as found by the asymptotic approach in Section 7.5.3. The two solutions are not as close as for the double symmetric cross-section. This is surely caused by the significant twist which was found to be present allready at small lateral deflections, see e.g. 7.5.3. Nevertheless it seems that the asymptotic result can be used as a guideline for the postbuckling behavior.
Concludingly the numerical analysis confirms that beams with cross-sections which are non-symmetric in the loading plane are sensitive to imperfections.

8.3.4 Lateral Buckling of Cantilever Beam

The lateral buckling behavior of a cantilever beam is a three-dimensional problem which has been given some interest by modern researchers (see e.g. Fig. 8.9). Especially the rectangular cantilever has been studied intensively, see e.g. Timoshenko & Gere (1961), Zamost & Johnston (1971) and Woolcock & Trahair (1974). Timoshenko analysed the effect of in-plane displacements on the critical load and found a severe influence if the height/depth ratio h/b (see e.g. Fig. 8.9) is a small quantity. Both Zamost and Woolcock analysed the post lateral behavior by solving a set of nonlinear differential equations and further Woolcock gave some experimental data. Woolcock extended the analysis with the post lateral buckling behavior of an I-beam. For small values of h/b Zamost found that the influence from precritical deformations are significantly different from those found by Timoshenko. Regarding the postbuckling behavior it was found that the out-of-plane deflection, see e.g. Fig. 8.9, rise as slowly as column buckling.
Later Attard (1986) performed lateral buckling analysis of the cantilever by the finite element method and found similar to Zamost that in-plane displacements are insignificant for slender beams. Recently Kouhia (1991) published a numerical study of the large elastic deformations of buckled rectangular cantilevers. In his approach he used a displacement based two node straight beam element in an updated Lagrangian formulation. He found an influence from precritical deformations similar to the one found by Timoshenko and further he also found that the postbuckling curves rise slowly.

Based on the disagreements of the literature the analysis of the lateral buckling of a cantilever is an obvios example in order to illustrate the performance of the developed two node hybrid element in a pre- as well as post-buckling analysis. The purpose of this section is to make some comparisons with the literature and further to add some new results for the lateral buckling behavior of a rectangular and I-beam cantilever regarding the governing parameters. The cantilever beam is initially straight and is subjected to a single load P at the elastic center at its free end as shown in Fig. 8.9.

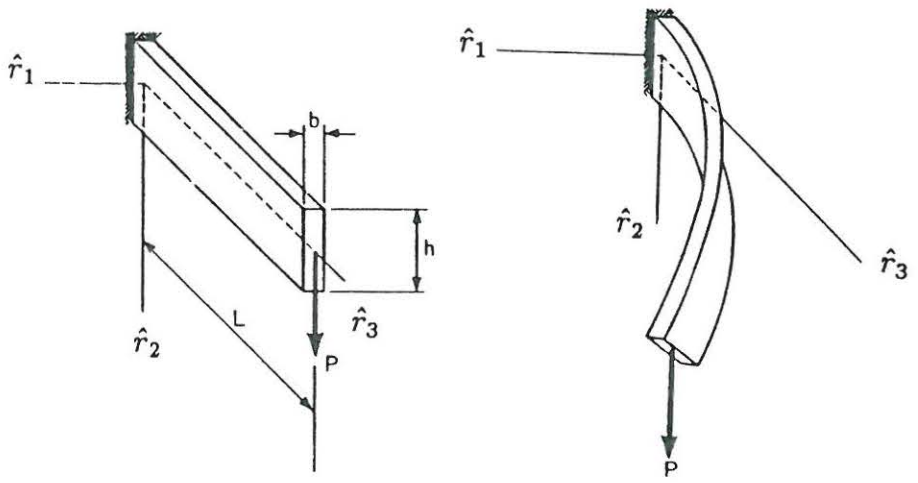

Fig. 8.9: Cantilever beam with end load. a) Undeformed beam. b) Deformed beam.

The critical load found by solving the linearized problem is given by (see e.g. Timoshenko & Gere (1961))

$$P_{cr} = \gamma P_{ref} \tag{8.12}$$

where the reference load P_{ref} is defined by

$$P_{ref} = \frac{\sqrt{I_{22}\, K}}{L^2} \tag{8.13}$$

and the factor γ is for large values of the ratio $L^2\, K/I_\omega$ approximatively given by (see e.g. Timoshenko & Gere (1961))

$$\gamma = \frac{4.013}{\left(1 - \sqrt{\frac{1}{(kL)^2}}\right)^2} \quad , \quad k^2 = \frac{K}{I_\omega} \tag{8.14}$$

The rectangular and the I-beam cantilevers are analysed separately in the following.

Rectangular Cantilever :
For a rectangular cross-section the warping stiffness is negligible, i.e. $I_\omega \simeq 0$, which means that $\gamma = 4.013$ whereby the critical load P_{cr} is given by

$$P_{cr} = 4.013\, \frac{\sqrt{I_{22}\, K}}{L^2} \tag{8.15}$$

Different proportions (h/b) of the cross-section have been examined. In all cases the moment of inertia in the primary bending plane I_{11} has been constant. The length of the beam L is $240mm$ and the material constants are $E = 71.24GPa$ and $G = 27.19GPa$. In Tab. 8.1 the reference loads P_{ref}, as given by (8.13), the cross-section dimensions, the principal moments of inertia and the torsion constants are given. A similar example has been investigated by Kouhia (1991) and some comparisons are made.

Table 8.1: Cross-section properties and the reference loads

$\frac{h}{b}$	$h\ (mm)$	$b\ (mm)$	$\frac{I_{11}}{E}\ (mm^4)$	$\frac{I_{22}}{E}\ (mm^4)$	$\frac{K}{G}\ (mm^4)$	$P_{ref}\ (N)$
50	30.000	0.600	1350	0.540	2.133	0.82
5	16.870	3.374	1350	54.000	188.895	77.17
3	14.848	4.949	1350	150.000	474.538	203.86

The ratio between the out-of-plane stiffness I_{22} and the torsional stiffness K is almost constant for a rectangular profile which implies that neither twist nor deflection is dominant in the buckling mode. In contrast the ratio between the bending stiffnesses varies significantly, but it should be noticed that the in-plane stiffness is much higher than the one out-of-plane. All this implies that the in-plane deformations, *prebuckling curvatures*, are expected to influence the critical load similar as for the *beam in pure bending*. Further no significant differences are to be expected in the overall buckling behavior corresponding to the constant ratio between the out-of-plane stiffnesses.

In Fig. 8.10-8.12 the pre- and postbuckling behavior is illustrated via the deflection and *twist* at the endpoint for the 3 different ratios. The numerical models consist of ten identical elements and the postbuckling curves have been initiated by introducing a small lateral imperfection $(\epsilon = r_1/L = 2.083 \cdot 10^{-4})$ at the free end.

Fig. 8.10 which illustrates the in-plane deflection reveals that a sudden change in the in-plane stiffness occurs as the critical point is reached indicating that the beam redistributes the action as expected.

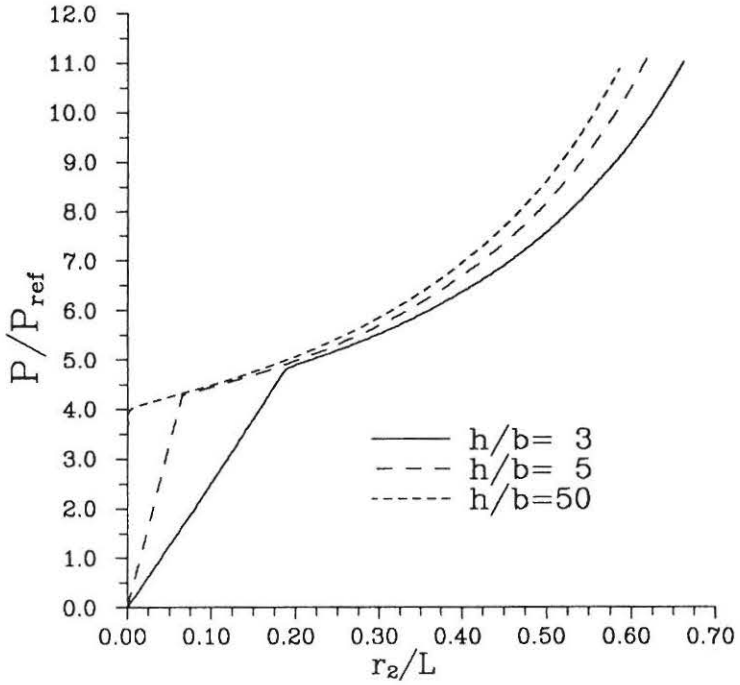

Fig. 8.10: In-plane deflection of elastic center at endpoint of rectangular cantilever.

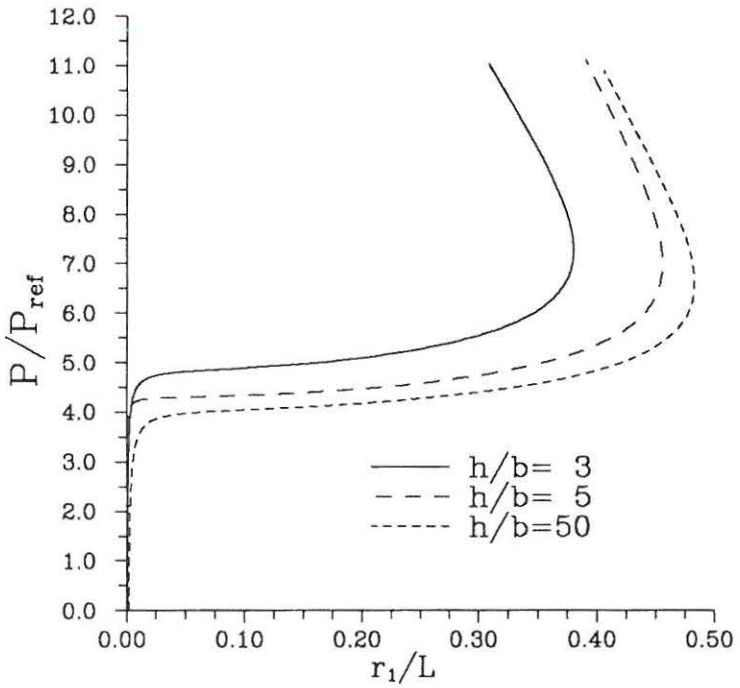

Fig. 8.11: Out-of-plane deflection of elastic center at endpoint of rectangular cantilever.

From Fig. 8.11 it appears that a significant out-of-plane deflection is necessary for a rectangular beam to obtain some postbuckling strength. This implies that for a rectangular cantilever with ordinary proportions the postbuckling strength is insignificant and may be neglected.

The *twist* at the endpoint can only be related directly to φ_3 as carried out here as long as φ_1 or φ_2 are small. The twist of the cross-section plane as illustrated in Fig. 8.12 is therefore to be used with care.

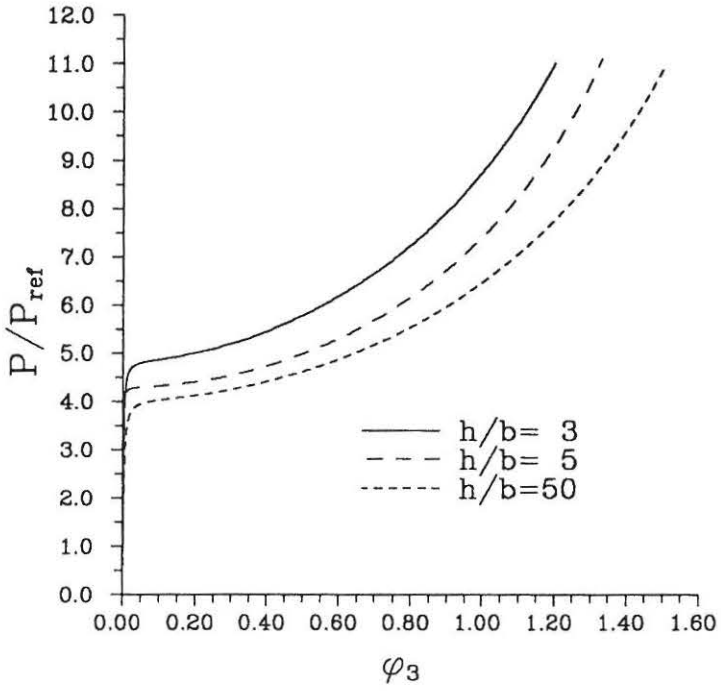

Fig. 8.12: Twist of cross-section plane at endpoint of rectangular cantilever.

Comparing Fig. 8.11 and Fig. 8.12 it is obvious that the out-of-plane displacement is dominant compared with twisting. This was also found for the *beam in pure bending* and is a consequence of the relative large torsional stiffness. The postbuckling behavior for the three different ratios is similar implying that the postbuckling behavior is closely related to the ratio between the out-of-plane stiffnesses. Further Fig. 8.10-8.12 shows that the in-plane displacements increases the buckling load as the ratio is changed from $h/b = 50$ downto $h/b = 3$. This reveals that (8.15) is a minimum value and further it confirms the results obtained by Timoshenko & Gere (1961).

In a similar example Kouhia (1991) investigated the pre- and postbuckling behavior using straight linear beam elements and found likewise that despite the differences in the bending ratios the postbuckling curves were similar while γ was highly influenced by in-plane deflections. In order to compare the present formulation with the one performed by Kouhia analysis with straight and curved elements have been performed for $h/b = 3$. The results for the out-of-plane deflection are illustrated in Fig. 8.13 together with the corresponding results from Kouhia (1991).

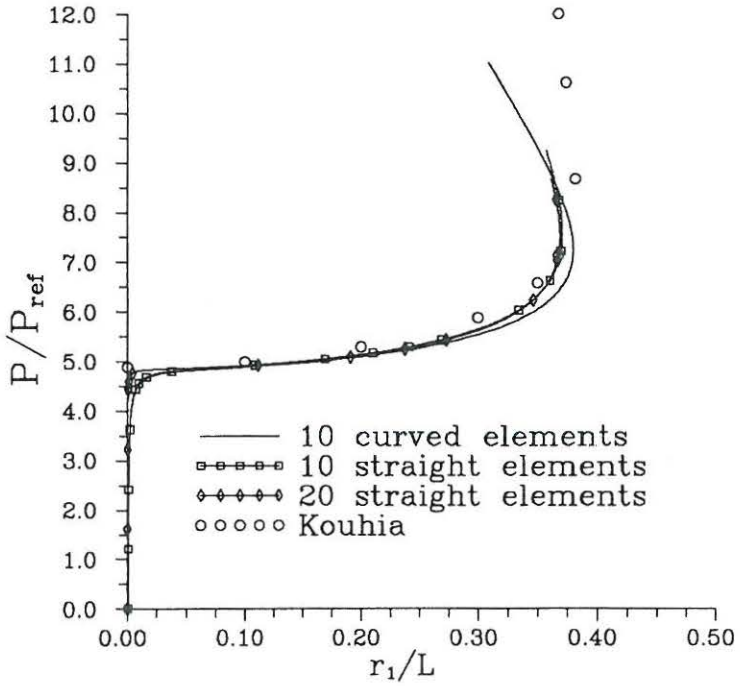

Fig. 8.13: Out-of-plane deflection of elastic center at endpoint of rectangular cantilever (h/b = 3).

As shown in Fig. 8.13 the critical load remains almost unaffected by the two kinds of elements, but the postbuckling behavior is influenced as the displacements become large. It appears that using straight elements locks the out-of-plane displacement at a certain level, meaning that no change occurs even though the load is increased. The form of the curve for straight elements is almost similar to the one found by Kouhia. Based on the experiences from *Cantilever subjected to an endmoment* in Section 8.3.1. and the results in Fig. 8.13 implies that straight beam elements are to be used with care in a large displacement analysis.

I-Section Cantilever :

The influence from warping has been studied by numerical analysis of an I-section cantilever with different lengths. As a reference profile an IPE20 has been used, i.e. $I_{11}/E = 1940mm^4$, $I_{22}/E = 142mm^4$, $K/G = 7.2mm^4$ and $I_\omega/E = 13000mm^6$. The material constants used in this example are $E = 210kN/mm^2$ and $G = 81kN/mm^2$. Restraining the beam from warping at the clamped end the critical load can be found from (8.14) and (8.12).

In Table 8.2 the reference loads for different beam lengths are presented together with the values of γ obtained from (8.14). Comparing with the rectangular cantilever differencies are to be expected as the out-of-plane bending stiffness is significantly larger than the *torsional stiffness*, which implies that the I-section cantilever tends to twist significantly in the postbuckling fase.

Table 8.2: Cross-section properties and the reference loads.

$L\ (mm)$	$(k\,L)^2$	$P_{ref}\ (N)$	$P_{cr}(N)$	γ	γ^{num}	γ^{num}/γ
180	6.90	128.5	1344	10.46	8.77	0.84
240	12.27	72.3	568	7.86	7.66	0.97
300	19.17	46.3	312	6.74	6.98	1.04

In Fig. 8.14-8.16 the pre- and postbuckling behavior is illustrated via the endpoint deflection and the *twist* of the cross-section plane. The numerical models consist of ten identical elements and the postbuckling curves have been initiated by introducing a small lateral imperfection ($\epsilon = r_1/L = 2.083 \cdot 10^{-4}$) at the free end.

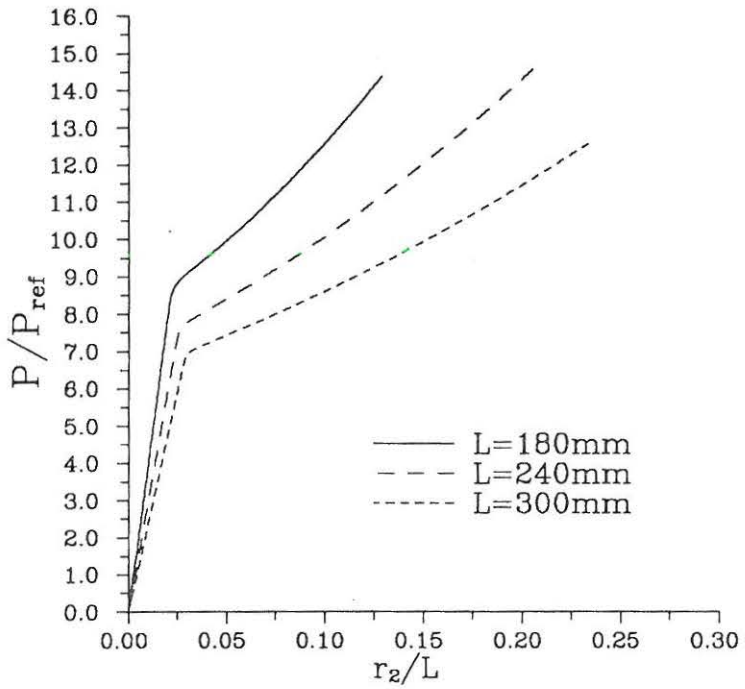

Fig. 8.14: In-plane deflection of elastic center at endpoint of I-section cantilever.

It appears that for the I-section cantilever the postbuckling behavior is similar for different lengths which was to be expected as the out-of-plane bending stiffness is dominant. Further the dependency of γ on L is evident from the displaced form of the curves. In Table 8.2 the values of γ obtained in the numerical analysis are given. These values have been determined by use of a best fit line (quadratic function) of the out-of-plane displacement in the vicinity of the critical point. As to be expected a great difference between the analytical values of γ is obtained for $(kL)^2 \to 0$ while a small deviation occurs as the length of the beam increases beyond $300mm$. The latter implies that the critical load is influenced as it also was found for the rectangular cantilever.

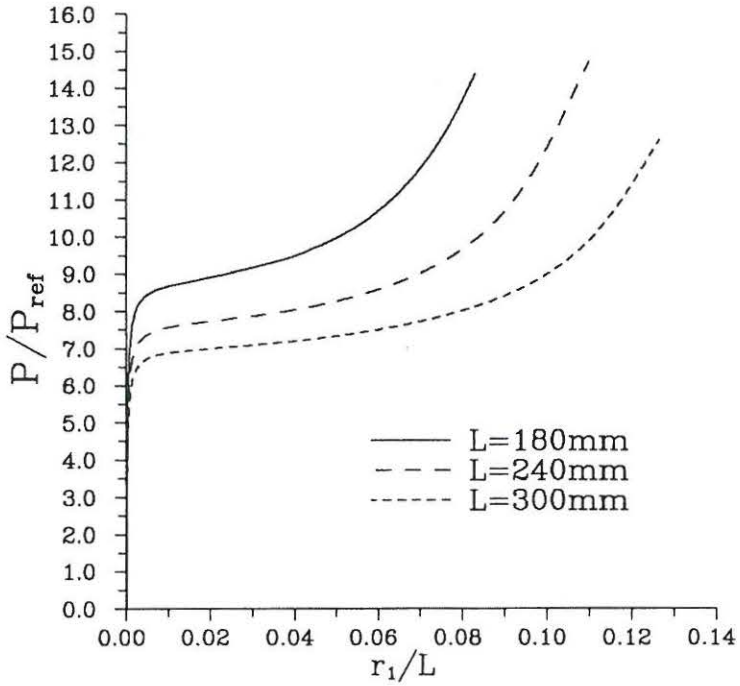

Fig. 8.15: Out-of-plane deflection of elastic center at endpoint of I-section cantilever.

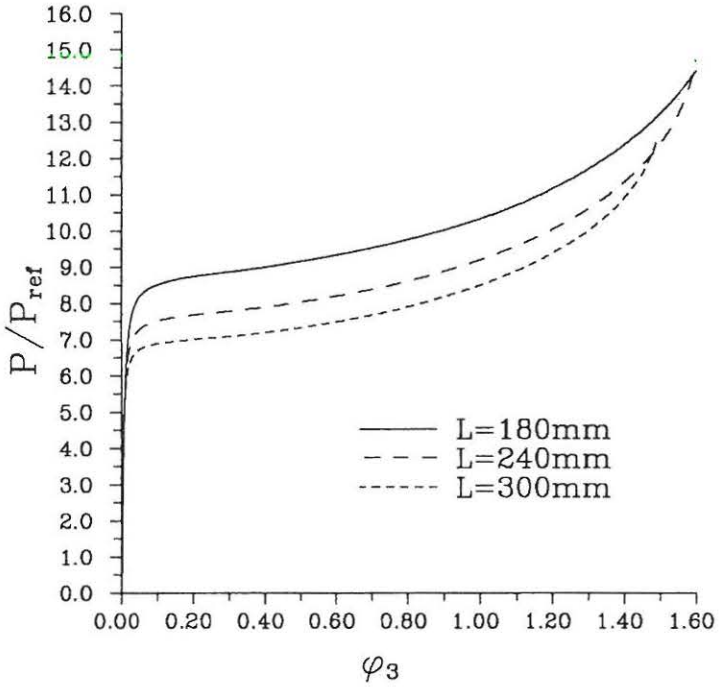

Fig. 8.16: Twist of cross-section plane at endpoint of I-section cantilever.

Comparing Fig. 8.10-8.12 with Fig. 8.14-8.16 it is evident that the postbuckling deflections are significantly smaller for the I-section as for the rectangular section while the opposite occurs for the twist.

In order to analyse the initial postbuckling behavior of an I-section in detail additional information has been obtained by investigating the influence from changing I_{11}, I_{22} and K.

A parameter identification has been carried out by assuming that the initial postbuckling behavior, as a function of the out-of-plane displacement, is approximatively given by

$$\frac{P}{P_{ref}} \simeq \gamma \left(1 + f\left[I_{11}, I_{22}, K, \alpha^2 I_\omega\right] \left(\frac{r_1}{L}\right)^2\right) \tag{8.16}$$

The cross-section parameters used are given in Table 8.3 together with the coefficients of the second-order polynomial $\left(g(x) = a + cx^2\right)$ obtained by a best fit method in the vicinity of the critical point, see e.g. Fig. 8.17.

Observing Table 8.3 it is evident that the initial postbuckling behavior of the I-section is

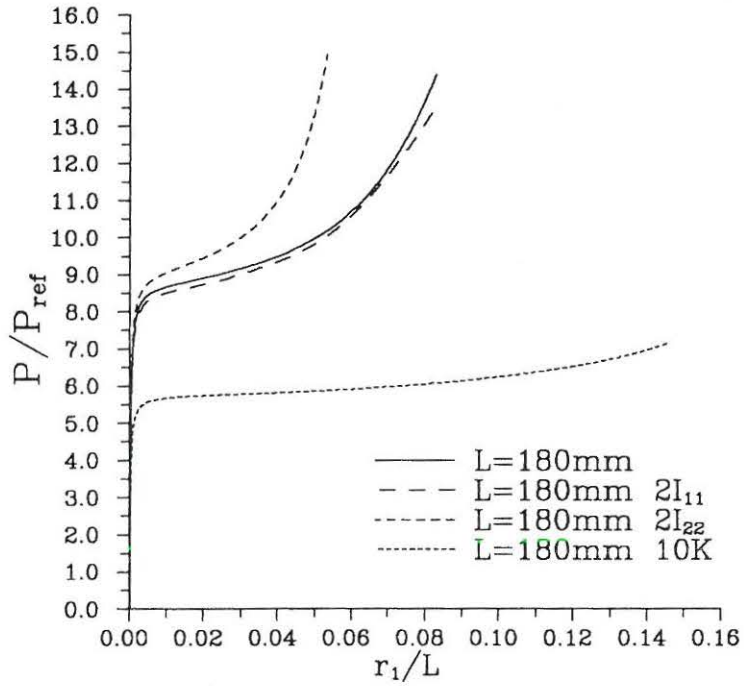

Fig. 8.17: Postbuckling curves of I-section cantilever for different cross-section parameters.

influenced by the ratio between the out-of-plane bending stiffness and the torsional rigidity.

Table 8.3: Cross-section properties and coefficients.

$(k\,L)^2$	$\frac{I_{11}}{E}\ (mm^4)$	$\frac{I_{22}}{E}\ (mm^4)$	$\frac{K + \alpha^2 I_\omega}{E}\ (mm^4)$	a	c
6.90	1940	142	3.75	8.75	478
6.90	3880	142	3.75	8.54	502
6.90	1940	284	3.75	9.00	1091
69.00	1940	142	28.50	5.71	48

Based on the values of Table 8.3 it is found that (8.16) approximately can be written as

$$\frac{P}{P_{ref}} = \gamma \left(1 + \frac{\pi}{2} \left(1 + \frac{I_{22}}{K + \alpha^2 I_\omega} \right) \left(\frac{r_1}{L} \right)^2 \right) \tag{8.17}$$

where the effective length in the expression for $(K + \alpha^2 I_\omega)$ is $2\,L$. In the determination of the bending/torsional relation in (8.17) the author has been guided by the asymptotic analysis of the *beam in pure bending* performed in Section 7.5.3. The relation in (8.17) is an approximation and therefore additional computations would be necessary in order to check the validity. Nevertheless it is evident from the results obtained for the I-section as well as for the rectangular cantilever that the initial postbuckling behavior is closely related to the ratio between the out-of-plane bending stiffness and the torsional stiffness.

Based on the results obtained with the present theory a concluding remark for the cantilever beam is that for slender beams in-plane deflections are insignificant for the critical load $P_{cr.}$ and further that the post lateral deflection rise as slowly as for column buckling. The coefficients in (8.17) are related to the I-section profile IPE20 and might therefore lead to totally wrong results if it is used for analysing other types of cross-sections. Equation (8.17) should therefore only be used as a guideline for the important parameters regarding an estimation of an eventual postbuckling strength for the cantilever beam.

8.4 Conclusions

An incremental updated Lagrangian two node element has been developed by expanding the beam element developed in Chapter 6 with the initial stress terms. The updating procedure accounts for both initial deformations and initial stresses. Impossing a small imperfection and thereby forcing a deformation process ortogonal to the deformation which develops as a direct consequence of the loading means that the equilibrium path can be traced in the prebuckling as well as in the postbuckling fase.

The performance of the hybrid element in a large displacement context is verified by analyses of the cantilever subjected to an endmoment which forces the beam to bend into a complete circular ring. Further this example indicates that using straight elements in large displacement analysis may lead to qualitatively wrong results. Comparing the present element with results from the literature where straight elements have been used confirms this and underlines that straight elements should be avoided in large displacement analysis.

The buckling behavior of the beam in pure bending has been analysed in detail and the numerical results have confirmed that the asymptotic analysis of the *perfect structure* reveals the postbuckling behavior in the vicinity of the critical point. The results are very close if the asymptotic solution is weighted according to the influence from in-plane deformations as found in Section 7.5.3.

The investigation of the monosymmetric beam in pure bending has revealed the information regarding the influence from a possible imperfection ortogonal to the loading deformation. The particular example which has been analysed indicates that the critical load determined for a *real* structure may differ significant from the critical load determined for the perfect structure.

A concluding remark is that a simple numerical formulation has been obtained whereby a wide range of stability problems can be analysed.

Chapter 9

Summary and Conclusions

A general stability theory for beams with arbitrary shape has been developed. A basic assumption in the derivation is that a beam can be regarded as a one-dimensional structure described in terms of cross-sections and a length coordinate. The beam is then represented by a curve with a local set of base vectors fixed to the beam cross-section at each point of the curve. A main point is to describe the rotation of the cross-section in a consistent way. This has been accomplished by describing the current unit vectors by a finite rotation vector via an ortogonal transformation of a set of reference vectors. The governing generalized displacements are hereby the position vector for the curve and the rotation vector for the cross-sections.

Introducing the internal force and moment vectors means that expressing equilibrium along the characteristic line leads to the governing equations. The equilibrium equations are reformulated as a virtual work equation, and this defines three generalized strain components and three generalized curvature components. The strain components are functions of both the position and rotation vector while the curvature components are expressed entirely in terms of the rotation vector. All three rotation components are kept as independent displacement parameters in order to preserve a formulation where the ortogonal transformation operator can be retained in the nonlinear equations leading to a compact formulation. If desired the Bernoulli hypothesis concerning the normality of the cross-sections can be introduced in the final equations. Treating the warping effect, characteristic of thin-walled beams, in a similar way means that the warping contribution easily can be superimposed into the virtual work equation.

The beam is considered in two adjacent states, an initial/prebuckled state with prebuckling curvatures and stresses, and a neighbouring buckled state. Subtracting the equilibrium equations for these two states means that the nonlinear beam theory specialises to a stability formulation. Using the equilibrium equations for the initial state means that the effect of prebuckling deformations is considered consistently via the generalized strains and curvatures. A weakness of the line approach in the establishment of a stability theory is the omission of a finite extent in the plane of the cross-section which means that additional initial stress terms occurs. This weakness is removed by a proper choice of the constitutive equations. In nonlinear formulations of beam equations different constitutive equations for the internal forces in terms of the generalized strains have been used. It is found that if the small strain deformation measure is expanded with the effect of twist a set of constitutive equations is obtained which is consistent for the thin-walled beam in a nonlinear formulation. This is

confirmed in an example where the critical load for a single curved beam is investigated using the present formulation and then comparing with some of the literature where a main point is to include additional *new* terms in the constitutive equations. No differencies were found which indicates that there is no need for complex constitutive equations.

The nonlinear stability formulation is obtained via the principle of virtual work. The virtual work equation for the beam problem corresponds to the first variation of the potential energy. In the stability formulation this connection can not be established directly because the variation of the initial stress term is not always an exact differential.

A numerical formulation is obtained by use of an updated Lagrangian procedure corresponding to the formulation with two adjacent states. This means that the current state is found by small increments from the initial state. The rotational components are considered as the main variables and are therefore retained as independent variables in the formulation. When invoking the Bernoulli hypothesis the weak formulation simplifies to a formulation entirely in terms of the rotation components. As the rotation components have to be connected with a position relative to the beam a relation between rotations and translations has to be reincorporated in order to achieve convergence. This is accomplished by incorporating the strain condition via the principle of Lagrange Multipliers. This leads to a mixed/hybrid formulation where linear shape functions can be used for all involved functions thereby achieving a simple formulation. Examples indicate that the developed element to some extent favours the statical behavior on the expense of the kinematical behavior. No significant influence on the rotational field is found corresponding to the presence of lower order differentials of the rotational components.

By means of a perturbation method the general nonlinear formulation is reformulated into an asymptotic buckling and postbuckling theory. Using the rotation components as the governing state variables a set of differential equations is developed from a corresponding functional (the virtual work equation). A successive use of the differential equations and the functional leads to identification of the asymptotic buckling and postbuckling behavior in a mangeable way. Analyses of the simply supported column reveals that the buckling behavior is stable for arbitrary cross-sections if the axial force is placed at the shear center. If the load is placed at the elastic center a nonsymmetric bifurcation arises if the cross-section has no axis of symmetry. Further the analysis of the beam in pure bending indicates that the initial postbuckling behavior is closely related to a possible unsymmetry of the cross-section.

Finally the two node hybrid beam element is expanded with the initial stress terms thereby leading to a numerical element suitable for stability analysis. A finite element program has been developed which is capable of tracing the equilibrium path in a buckling as well as postbuckling fase for arbitrary cross-sections and large displacements. The element has been compared with the literature and the agreement is satisfactory. Investigations of the successive bending of a cantilever beam into a circular ring has illustrated that significant errors occurs if straight elements are used in a large displacement analysis. This has been confirmed by analysing the post lateral buckling of a rectangular cantilever and comparing with the literature where straight elements have been used. The postbuckling analyses of the beam in pure bending confirms that the asymptotic results obtained for the *perfect structure* illustrate the postbuckling behavior in the vicinty of the critical point. The influence from in-plane deformations is found to be contained in a scaling factor expressing the slenderness of the cross-section. Finally investigations of the monosymmetric beam has led to identification of the effect from a possible unsymmetry of the cross-section in the loading plane. The results

underlines that in case of imperfections the critical load for a nonsymmetric cross-section may deviate significant from the one which is found for the perfect structure. Some of the influence is described by the dimensionless parameters derived in Chapter 7, but additional tests are necessary in order to obtain a complete description.

It can be concluded that a fundamental basis for the stability analysis of the thin-walled beam has been obtained. The validity of the formulation is verified by analyses of canonical problems.

Future Perspectives

The future perspectives are

- Development and optimizing of program.
- Additional examples.
    1. distributed load
    2. frame structures
    3. . . .
- Design criterias for practice.

Bibliography

[1] Argyris, J.H., Dunne, P.C., Malejannakis, G.A. and Scharpf, D.W. On Large Displacement - Small Strain Analysis of Structures with Rotational Degrees of Freedom, *Computer Methods in Apllied Mechanics and Engineering*, Vol. 14, pp. 401-451 and Vol. 15, pp. 99-135, 1978.

[2] Attard, D. Lateral Buckling Analysis of Beams by the FEM, *Computers and Structures*, Vol. 23 No. 2 pp. 217-231, 1986.

[3] Barsoum, R.S. and Gallagher, R.H. Finite Element Analysis of Torsional-Flexural Stability Problems, *International Journal for Numerical Methods in Engineering*, Vol. 2, pp. 335-352, 1970

[4] Bathe, K.-J. and Bolourchi, S. Large Displacement Analysis of Three Dimensional Beam Structures, *International Journal for Numerical Methods in Engineering*, Vol. 14, pp. 961-986, 1979.

[5] Bazant, Z.P. and Nimeiri, M.E. Large-Deflection Spatial Buckling of Thin-Walled Beams and Frames, *Journal of the Engineering Mechanics Division*, Vol. 99, No. EM6, pp. 1259-1281, December 1973.

[6] Budiansky, B. Theory of Buckling and Postbuckling Behavior of Elastic Structures, *Advances in Applied Mechanics*, Vol. 14, pp. 1-74, 1974.

[7] Cardona, A. and Geradin, M. A Beam Finite Element Non-Linear Theory with Finite Rotations, *International Journal for Numerical Methods in Engineering*, Vol. 26, pp. 2403-2438, 1988.

[8] Chajes, A. Post-Buckling Behavior, *Journal of Structural Engineering*, Vol. 109, No. 10, pp. 2450-2462, October 1983.

[9] Chajes, A. *Principles of Structural Stability Theory*, Prentice-Hall, New Jersey 1974.

[10] Chajes, A. and Winter, G. Torsional-Flexural Buckling of Thin-Walled Members, *Journal of the Structural Division*, **91**, No. ST4, 1965.

[11] Chan, S.L. and Kitipornchai, S. Geometric Nonlinear Analysis of Asymmetric Thin-Walled Beam-Columns, *Engineering Structures*, Vol. 9, 1987.

[12] Cheney, J.A. Bending and Buckling of Thin-Walled Open-Section Rings, *Journal of the Engineering Mechanics Division*, Vol. 89, EM5, pp. 17-44, May 1963.

[13] Conci, A and Gattass, M. Natural Approach for Geometric Non-Linear Analysis of Thin-Walled Frames, *International Journal for Numerical Methods in Engineering*, Vol. 30, pp. 207-231, 1990.

[14] Connor, J.J., Logcher, R.D. and Chen, S.C. Nonlinear Analysis of Elastic Framed Structures, *Journal of the Structural Division*, Vol. 94, No. ST6, pp. 1525-1547, June 1968.

[15] Crisfield, M.A. A Consistent Co-Rotational Formulation for Non-Linear, Three-Dimensional, Beam-Elements, *Computer Methods in Applied Mechanics and Engineering*, Vol. 81, pp. 131-150, 1990.

[16] Dupuis, G. Stabilite elastique des structures unidimensionelles, *ZAMP*, Vol. 20, pp. 94-106, 1969.

[17] Elias, Z.M. *Theory and Methods of Structural Analysis*, John Wiley and Sons, New York, 1986.

[18] Epstein, M. and Murray, D.W. Three-Dimensional Large Deformation Analysis of Thin-Walled Beams, *International Journal of Solids and Structures*, Vol. 12, pp. 867-876, 1976.

[19] Gattass, M. and Abel, J.F. Equilibrium Considerations of the Updated Lagrangian Formulation of Beam Columns with Natural Concepts, *International Journal for Numerical Methods in Engineering*, Vol. 24, pp. 2119-2143, 1987.

[20] Gendy, A.S. and Saleeb, A.F. On the Finite Element Analysis of the Spatial Response of Curved Beams with Arbitrary Thin-Walled Sections, *Computers and Structures*, Vol. 44, No. 3, pp. 639-652, 1992.

[21] Ghobarah, A.A. and Tso, W.K. A Non-linear Thin-Walled Beam Theory, *International Journal of Mechanical Science*, Vol. 13, pp. 1025-1038, 1971.

[22] Goldstein, H. *Classical Mechanics*, Reading, London, 1950.

[23] Grimaldi, A. and Pignataro, M. Postbuckling Behavior of Thin-Walled Open Cross-section Compression Members, *Journal of Structural Mechanics*, Vol. 7, pp. 143-159.

[24] Hong Chen and Blandford, G. E. Thin-Walled Space Frames. I-II: Large-Deformation Analysis Theory - Algorithmic Details and Applications, *Journal of Structural Engineering*, Vol. 117, No. 8, pp. 2499-2539, August 1991.

[25] Hsiao, K.-M. A Co-Rotational Procedure that Handles Large Rotations of Spatial Beam Structures. *Computers and Structures.* Vol. 27, No. 6, pp. 769-781, 1987.

[26] Koiter, W.T. *On the Stability of Elastic Equilibrium*, National Aeronautics and Space Administration (English Translation), Washington D.C. 1945.

[27] Kollbrunner, C.F. and Hajdin, N. *Dunnwandige Stabe I*, Springer-Verlag, Berlin 1972.

[28] Kouhia, R. On Kinematical Relations of Spatial Framed Structures. *Computers and Structures.* Vol. 40, No. 5, pp. 1185-1191, 1991.

[29] Krenk, S. The Torsion-Extension Coupling In Pretwisted Elastic Beams, *Internaional Journal of Solids and Structures*, Vol. 19, No. 1, pp. 67-72, 1983.

[30] Krenk, S. A Linear Theory for Pretwisted Elastic Beams, *Journal of Applied Mechanics*, Vol. 105, March 1983.

[31] Krenk, S. and Gunneskov, O. Pretwist and Shear Flexibility in the Vibrations of Turbine Blades, *Journal of Applied Mechanics*, Vol. 52, pp. 409-415, 1985.

[32] Krenk, S. *Three-Dimensional Elastic Beam Theory (part 1-2, chapter 2-8)*, Department of Structural Engineering, Technical University of Denmark, Lyngby 1989.

[33] Krenk, S. and Jeppesen, B. Finite Elements for Beam Cross-Sections of Moderate Wall Thickness, *Computers and Structures*, Vol. 32, No. 5, pp.1035-1043, 1989.

[34] Malvern, L.E. *Introduction to the Mechanics of a Continuous Medium chapter 4-6*, Prentice-Hall, Englewood Cliffs, New Jersey 1969.

[35] Mathiesen, F. *En teori for tyndvæggede bjælker med forhåndsdeformationer og initialspændinger* (in danish), University of Aalborg, Aalborg, Report 9023, August 1990.

[36] Mathiesen, F. *En teori for bjælker med store deformationer og initialspændinger* (in danish), University of Aalborg, Aalborg, Report 9124, Maj 1991.

[37] Meek, J.L. and Loganathan, S. Large-Displacement Analysis of Space-Frame Structures, *Computer Methods in Applied Mechanics and Engineering*, **72**, pp.75-75, 1989.

[38] Naschie, El M.S. *Stress, Stability and Chaos - In Structural Engineering : An Energy Approach*, McGraw-Hill, London 1990.

[39] Papangelis, J.P. and Trahair, N.S. Flexural-Torsional Buckling of Arches, *Journal of Structural Engineering*, Vol. 112, No. 11, pp. 2494-2511, November 1986.

[40] Peterson, A. and Petersson, H. Finite Element Analysis of Geometrically Nonlinear Problems, *Computer Methods in Applied Mechanics and Engineering*, **51**, pp.277-286, 1985.

[41] Reddy, J.N. *Energy and Variational Methods in Applied Mechanics*, John Wiley & Sons, New York 1984.

[42] Reissner, E. Lateral Buckling of Beams, *Computers and Structures*, Vol. 33, No. 5, pp.1289-1306, 1989.

[43] Roorda, J. Buckling of Elastic Structures, *Solid Mechanics Division University of Waterloo*, Ontario Canada, 1980.

[44] Rosen, A. and Friedmann, P. The Nonlinear Behavior of Slender Straight Beams Undergoing Small Strains and Moderate Rotations, *Journal of Applied Mechanics*, Vol. 46, pp. 161-168, 1979.

[45] Saleeb, A.F., Chang, T.Y.P. and Gendy, A.S. Effective Modelling of Spatial Buckling of Beam Assemblages, Accounting for Warping Constraints and Rotation-Dependency of Moments, *International Journal for Numerical Methods in Engineering*, Vol. 33, pp. 469-502, 1992.

[46] Simo, J.C. A Finite Strain Beam Formulation. The Three-Dimensional Dynamic Problem. Part I, *Computer Methods in Applied Mechanics and Engineering*, **49**, pp. 55-70, 1985.

[47] Simo, J.C. and Vu-Quoc, L. A Geometrically-Exact Rod Model Incorporating Shear and Torsion-Warping Deformation, *International Journal of Solids and Structures*, Vol. 27, No. 3, pp.371-393, 1991.

[48] Surana, K.S. and Sorem, R.M. Geometrically Non-Linear Formulation for Three Dimensional Curved Beam Elements with Large Rotations. *International Journal for Numerical Methods in Engineering*, Vol. 28, pp. 43-73, 1989.

[49] Szymczak, C. Buckling and Initial Post-Buckling Behavior of Thin-Walled I Columns, *Computers and Structures*, Vol. 11, No. 6, pp. 481-487, 1980.

[50] Thompson, J.M.T. and Hunt, G.W. *A General Theory of Elastic Stability*, John Wiley & Sons, London 1973.

[51] Timoshenko, S.T. and Gere, J.M. *Theory of Elastic Stability*, Second Edition, McGraw-Hill, New York 1961.

[52] Trahair, N.S. and Woolcock, S.T. Effect of Major Axis Curvature on I-Beam Stability, *Journal of the Engineering Mechanics Division*, Vol. 99, No. EM1, pp. 85-98, Feb. 1973.

[53] Trefftz, E. Uber den Schubmittelpunkt in einem durch eine Einzellast gebogenen Balken, *Zeitschrift fur Angewandte Mathematik und Mechanik*, Vol. 15, pp. 220-225, 1935.

[54] Vacharajittiphan, P., Woolcock, S.T. and Trahair, N.S. Effect of In-Plane Deformation on Lateral Buckling, *Journal of Structural Mechanics*, No. **3**, pp. 29-60, 1974.

[55] Vlasov, V.Z. *Thin-Walled Elastic Beams*, translated from Russian by the Israel Program for Scientific Translations. US Department of Commerce, National Information Service, TT-61-11400, 1961.

[56] Washizu, K. *Variational Methods in Elasticity and Plasticity*, Second Edition, Pergamon Press, Oxford 1974.

[57] Wempner, G. *Mechanics of Solids With Application to Thin Bodies* , McGraw-Hill, New York 1973.

[58] Woolcock, S.T. and Trahair, N.S. Post-Buckling Behavior of Determinate Beams. *Journal of the Engineering Mechanics Division*, Vol. 100, EM2, pp. 151-171, April 1974.

[59] Woolcock, S.T. and Trahair, N.S. Post-Buckling of Redundant Rectangular Beams. *Journal of the Engineering Mechanics Division*, Vol. 101, EM4, pp. 301-316, August 1975.

[60] Yang, Yeong-Bin and McGuire, W. Joint Rotation and Geometric Nonlinear Analysis, *Journal of Structural Engineering*, Vol. 112, No.4, April 1986.

[61] Yang, Yeong-Bin and McGuire, W. Stiffness Matrix for Geometric Nonlinear Analysis, *Journal of Structural Engineering*, Vol. 112, No.4, April 1986.

[62] Yang, Yeong-Bin and Kuo, Shyh-Rong Effect of Curvature on Stability of Curved Beams, *Journal of Structural Engineering*, Vol. 113, No. 6, pp. 1185-1203, June 1987.

[63] Yoo, C.H. Bimoment Contribution to Stability of Thin-Walled Assemblages, *Computers and Structures*, Vol. 11, pp. 465-471, 1980.

[64] Yoo, C.H. Flexural-Torsional Stability of Curved Beams, *Journal of the Engineering Mechanics Division*, Vol. 108, No. EM6, December 1982.

[65] Zamost, G. and Johnston, E.R. Post Lateral Buckling Behavior of Beams, *Journal of the Engineering Mechanics Division*, Vol. 97, No. EM4, pp. 1133-1143, August 1971.

Appendix A

Orthogonal Transformation Operator

The orientation of the beam cross-section is described by a set of unit vectors rotating with the beam. The current unit vectors $\mathbf{e}_j$ are described by an orthogonal transformation of a set of reference vectors $\hat{\mathbf{e}}_j$. A finite rotation tensor $\mathbf{A}(\boldsymbol{\varphi})$, i.e. an orthogonal transformation operator, can be regarded as the integrated version of the infinitesimal rotation operator $d\boldsymbol{\varphi}\times$.

Considering the increment of a vector $\mathbf{e}_j$ corresponding to an infinitesimal rotation $d\boldsymbol{\varphi}$

$$d\mathbf{e}_j \;=\; d\boldsymbol{\varphi} \times \mathbf{e}_j \;=\; \Omega(d\boldsymbol{\varphi}) \cdot \mathbf{e}_j \tag{A.1}$$

In (A.1) the second order tensor $\boldsymbol{\Omega}$ is used to obtain an alternative form of writing the vector product. A decomposition of $d\boldsymbol{\varphi}$ in the basis of $\{\mathbf{e}_j\}$ indicates that $\boldsymbol{\Omega}$ is a skew symmetric matrix

$$\boldsymbol{\Omega}(\boldsymbol{\varphi}) \;=\; \begin{bmatrix} 0 & -\varphi_3 & \varphi_2 \\ \varphi_3 & 0 & -\varphi_1 \\ -\varphi_2 & \varphi_1 & 0 \end{bmatrix} \quad , \qquad \Omega_{lj} \;=\; e_{lnj}\,\varphi_n \tag{A.2}$$

If φ is the length of the rotation vector $\boldsymbol{\varphi}$ then (A.1) can be formulated as an ordinary differential equation

$$\frac{d\mathbf{e}_j}{d\varphi} \;=\; \boldsymbol{\Omega}\left(\frac{d\boldsymbol{\varphi}}{d\varphi}\right) \cdot \mathbf{e}_j \tag{A.3}$$

The unit vector $d\boldsymbol{\varphi}/d\varphi$ indicates the direction of the rotation vector. Retaining this direction, (A.3) can be integrated leading to an expression for the finite rotation of a vector. It follows that a unit vector $\mathbf{e}_j$ can be expressed by the rotation of a global unit vector $\hat{\mathbf{e}}_j$ in the following way

$$\mathbf{e}_j \;=\; e^{\boldsymbol{\Omega}(\boldsymbol{\varphi})} \cdot \hat{\mathbf{e}}_j \;=\; \mathbf{A}(\boldsymbol{\varphi}) \cdot \hat{\mathbf{e}}_j \tag{A.4}$$

From (A.4) it follows that the orthogonal transformation operator is the exponential of a skew symmetric matrix. This transformation is often referred to as the *exponential mapping*

or the *Rodrigues formula*, Argyris *et. al.* (1978).
The exponential function in (A.4) may be regarded as defined by its Taylor series expansion, i.e.

$$\mathbf{A}(\boldsymbol{\varphi}) = \sum_{n=0}^{\infty} \frac{1}{n!} \Big[\boldsymbol{\Omega}(\boldsymbol{\varphi}) \Big]^n \tag{A.5}$$

A reformulation of (A.5) can be performed by a closer analysis of the quadratic term in the Taylor series expansion

$$\boldsymbol{\Omega}(\boldsymbol{\varphi}) \cdot \boldsymbol{\Omega}(\boldsymbol{\varphi}) \cdot \hat{\mathbf{e}}_j = \boldsymbol{\varphi} \times \big(\boldsymbol{\varphi} \times \hat{\mathbf{e}}_j \big) \tag{A.6}$$

The triple vector product in (A.6) can be decomposed into a vector parallell to the plane described by $\hat{\mathbf{e}}_j$ and $\boldsymbol{\varphi}$, as shown in Fig. A.1.

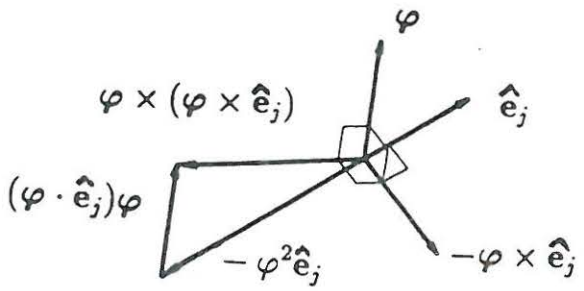

Fig. A.1: Triple vector product.

It follows that

$$\boldsymbol{\varphi} \times \big(\boldsymbol{\varphi} \times \hat{\mathbf{e}}_j \big) = \big(\boldsymbol{\varphi} \cdot \hat{\mathbf{e}}_j \big) \boldsymbol{\varphi} - \big(\boldsymbol{\varphi} \cdot \boldsymbol{\varphi} \big) \hat{\mathbf{e}}_j = \big(\boldsymbol{\varphi} \cdot \hat{\mathbf{e}}_j \big) \boldsymbol{\varphi} - \varphi^2 \, \hat{\mathbf{e}}_j \tag{A.7}$$

Equation (A.7) implies that the transformation in (A.4) is described in a vector space corresponding to the three vectors

$$\hat{\mathbf{e}}_j \qquad \boldsymbol{\varphi} \qquad \boldsymbol{\varphi} \times \hat{\mathbf{e}}_j$$

The Taylor series expansion in (A.5) can then be expressed by a combination of the three first terms of the expansion. Substitution of (A.7) into (A.5) leads to

$$\mathbf{A}(\boldsymbol{\varphi}) \cdot \hat{\mathbf{e}}_j = \left(\mathbf{I} + \boldsymbol{\Omega}(\boldsymbol{\varphi}) + \frac{1}{2} \boldsymbol{\Omega}(\boldsymbol{\varphi}) \cdot \boldsymbol{\Omega}(\boldsymbol{\varphi}) - \varphi^2 \Big[\sum_{n=3}^{\infty} \frac{1}{n!} \Big[\boldsymbol{\Omega}(\boldsymbol{\varphi}) \Big]^{n-2} \Big] \right) \cdot \hat{\mathbf{e}}_j \tag{A.8}$$

The term inside the big parenthesis corresponds to the transformation operator. Decomposing the summation further by use of (A.7) and making use of trigonometric functions the expansions in (A.8) can be reformulated to yield

$$\mathbf{A}(\boldsymbol{\varphi}) = \mathbf{I} + \frac{sin\varphi}{\varphi} \boldsymbol{\Omega}(\boldsymbol{\varphi}) + \frac{1 - cos\varphi}{\varphi^2} \boldsymbol{\Omega}(\boldsymbol{\varphi}) \cdot \boldsymbol{\Omega}(\boldsymbol{\varphi}) \tag{A.9}$$

A closed form expression for the orthogonal transformation operator is hereby obtained. A decomposition of the rotation vector in a basis described by $\hat{\mathbf{e}}_j$, whereby $\boldsymbol{\varphi} = \varphi_j \hat{\mathbf{e}}_j$ leads to the vector relation

$$\mathbf{e}_j \;=\; A_{lj}(\varphi_m)\,\hat{\mathbf{e}}_l \tag{A.10}$$

where

$$\begin{aligned} A_{lj}(\varphi_m) \;&=\; \delta_{lj} \;+\; \frac{sin\varphi}{\varphi}\,\Omega_{lj} \;+\; \frac{1-cos\varphi}{\varphi^2}\,\Omega_{ln}\,\Omega_{nj} \\ &\simeq\; \delta_{lj} \;+\; \Omega_{lj} \;+\; \frac{1}{2!}\Omega_{ln}\,\Omega_{nj} \;-\; \frac{1}{3!}\,\Omega_{lj}\,\varphi^2 \qquad \ldots \qquad +\; 0(\varphi^n) \end{aligned} \tag{A.11}$$

The finite rotation tensor is derived according to the assumption that the direction of the rotation vector is fixed. In the establishment of the deformation measures the relative change between two cross-sections are considered. A convenient notation can be obtained for the expansion of the curvature components in Chapter 5 by introducing the second order tensor $\mathbf{B}$ defined by relation

$$\mathbf{B}(\boldsymbol{\varphi}) \;=\; \mathbf{I} \;+\; \frac{1-cos\varphi}{\varphi^2}\,\boldsymbol{\Omega}(\boldsymbol{\varphi}) \;+\; \frac{\varphi - sin\varphi}{\varphi^3}\,\boldsymbol{\Omega}(\boldsymbol{\varphi})\cdot\boldsymbol{\Omega}(\boldsymbol{\varphi}) \tag{A.12}$$

The tensor $\mathbf{B}$ is connected to the orthogonal transformation operator $\mathbf{A}$ by the following relation

$$\mathbf{A}(\boldsymbol{\varphi}) - \mathbf{I} \;=\; \sum_{n=1}^{\infty} \frac{1}{n!}\left[\boldsymbol{\Omega}(\boldsymbol{\varphi})\right]^{n-1}\boldsymbol{\Omega}(\boldsymbol{\varphi}) \;=\; \mathbf{B}(\boldsymbol{\varphi})\cdot\boldsymbol{\Omega}(\boldsymbol{\varphi}) \tag{A.13}$$

A component form of $\mathbf{B}$ is obtained by decomposing $\boldsymbol{\varphi}$ in the basis $\hat{\mathbf{e}}_j$, i.e.

$$\begin{aligned} B_{lj}(\varphi_m) \;&=\; \delta_{lj} \;+\; \frac{1-cos\varphi}{\varphi^2}\,\Omega_{lj} \;+\; \frac{\varphi - sin\varphi}{\varphi^3}\,\Omega_{ln}\,\Omega_{nj} \\ &\simeq\; \delta_{lj} \;+\; \frac{1}{2!}\,\Omega_{lj} \;+\; \frac{1}{3!}\Omega_{ln}\,\Omega_{nj} \;-\; \frac{1}{4!}\,\Omega_{lj}\,\varphi^2 \qquad \ldots \qquad +\; 0(\varphi^n) \end{aligned} \tag{A.14}$$

Notice the resemblance with (A.11), where the only difference is the shifting of the scalar factors.

Appendix B

Linear Differential Equations

In this appendix the differential equations from (7.22) are reformulated to a more informative form. From [7.9) it follows that the virtual work equation in terms of components is given by (multiplication with -1)

$$\int_0^l \Big\{ \frac{d}{ds_0}\big(A_{lj}M_j^1 + \tilde{A}_{lj}M_j^0\big) + e_{lmn}\kappa_m^0\big(A_{nj}M_j^1 + \tilde{A}_{nj}M_j^0\big) + e_{nkl}\big(\tilde{A}_{nm} + \lambda\, A_{nm}\big)\big(\delta_{m3}N_k^0 + \delta_{m\alpha}f_\alpha^0 p_k^0\big)\Big\}\,\delta\varphi_l\, ds_0 \;=\; 0 \tag{B.1}$$

Expanding the rotation vector $\boldsymbol{\varphi}^1$ in terms of a generalized perturbation parameter ξ, i.e.

$$\varphi_j^1 \;=\; \tilde{\varphi}_j^1\,\xi \;+\; \tilde{\varphi}_j^2\,\xi^2 \ldots \tag{B.2}$$

Setting $\lambda = 0$ and observing only the first-order terms in $\tilde{\varphi}_j^i$ of the part in-side the big brackets leads to

$$\int_0^l F_l(\tilde{\varphi}_j^i)\,\delta\varphi_l\; ds_0 \;=\; \int_0^l \Big\{ \frac{d}{ds_0}\big(M_l^1 + e_{lnj}\,\tilde{\varphi}_n^i M_j^0\big) + e_{lmn}\kappa_m^0\big(M_n^1 + e_{nkj}\,\tilde{\varphi}_k^i M_j^0\big) + e_{njm}\,\tilde{\varphi}_j^i\big(\delta_{m3}N_k^0 + \delta_{m\alpha}f_\alpha^0 p_k^0\big)e_{nkl}\Big\}\,\delta\varphi_l\, ds_0 \;=\; 0 \tag{B.3}$$

Inserting the constitutive equations from section 4.1, making use of (7.15) and rearranging according to $\delta\varphi_\alpha$ and $\delta\varphi_3$ leads to

$$\int_0^l \Big\{F_\alpha(\tilde{\varphi}_j^i)\,\delta\varphi_\alpha + F_3(\tilde{\varphi}_j^i)\,\delta\varphi_3\Big\}\, ds_0 \;=$$

$$\int_0^l \Big\{\Big[\frac{d}{ds_0}\big(I_{\alpha\beta}\tilde{\kappa}_\beta^i\big) - \kappa_3^0 e_{\alpha\gamma}I_{\gamma\beta}\tilde{\kappa}_\beta^i - e_{\alpha\beta}\kappa_\beta^0\frac{d}{ds_0}\Big(I_\omega\Big(\frac{d\tilde{\kappa}_3^i}{ds_0}\Big)\Big)$$

$$
\begin{aligned}
&+ e_{\alpha\beta}\kappa^0_\beta\Big(K + r_a^2 N_3^0 + 2\beta_\alpha M_\alpha^{c\,0}\Big)\widetilde{\kappa}^i_3 \\
&+ e_{\alpha\beta}M_3^0\Big(\frac{d\widetilde{\varphi}^i_\beta}{ds_0} - \kappa_3^0 e_{\beta\gamma}\widetilde{\varphi}^i_\gamma\Big) - e_{\alpha\beta}M_\beta^0\frac{d\widetilde{\varphi}^i_3}{ds_0} + e_{\alpha\beta}\widetilde{\varphi}^i_\beta\frac{dM_3^0}{ds_0} \\
&+ e_{\alpha\beta}\kappa^0_\beta e_{\gamma\eta}\widetilde{\varphi}^i_\gamma M_\eta^0 - e_{\alpha\beta}\widetilde{\varphi}^i_3\Big(\frac{dM_\beta^0}{ds_0} - \kappa_3^0 e_{\beta\gamma}M_\gamma^0 + e_{\beta\gamma}f_\gamma^0 p_3^0\Big) \\
&- \widetilde{\varphi}^i_\alpha N_3^0 - e_{\alpha\beta}e_{\gamma\eta}\widetilde{\varphi}^i_\gamma f_\eta^0 p_\beta^0\Big]\,\delta\varphi_\alpha \\
&+ \Big[\frac{d}{ds_0}\Big(\Big(K + r_a^2 N_3^0 + 2\beta_\alpha M_\alpha^{c\,0}\Big)\widetilde{\kappa}^i_3\Big) - \frac{d^2}{ds_0^2}\Big(I_\omega\Big(\frac{d\widetilde{\kappa}^i_3}{ds_0}\Big)\Big) \\
&+ \kappa_\gamma^0 e_{\gamma\alpha}I_{\alpha\beta}\widetilde{\kappa}^i_\beta + e_{\alpha\beta}\widetilde{\varphi}^i_\alpha\Big(\frac{dM_\beta^0}{ds_0} - e_{\beta\gamma}N_\gamma^0 + M_3^0\kappa_\gamma^0 e_{\gamma\beta}\Big) \\
&+ e_{\alpha\beta}M_\beta^0\Big(\frac{d\widetilde{\varphi}^i_\alpha}{ds_0} - \widetilde{\varphi}^i_3\kappa_\gamma^0 e_{\gamma\alpha}\Big) - p_\alpha^0 f_\alpha^0\widetilde{\varphi}^i_3\Big]\,\delta\varphi_l\Big\}\,ds_0
\end{aligned}
\tag{B.4}
$$

The expressions for $F_\alpha(\widetilde{\varphi}^i_j)$ and $F_3(\widetilde{\varphi}^i_j)$ can be reformulated by use of the equilibrium equations for the initial state.

$$
\begin{aligned}
&\int_0^l \Big\{F_\alpha(\widetilde{\varphi}^i_j)\,\delta\varphi_\alpha + F_3(\widetilde{\varphi}^i_j)\,\delta\varphi_3\Big\}\,ds_0 = \\
&\int_0^l \Big\{\Big[\frac{d}{ds_0}\Big(I_{\alpha\beta}\widetilde{\kappa}^i_\beta\Big) - \kappa_3^0 e_{\alpha\gamma}I_{\gamma\beta}\widetilde{\kappa}^i_\beta - e_{\alpha\beta}\kappa_\beta^0\frac{d}{ds_0}\Big(I_\omega\Big(\frac{d\widetilde{\kappa}^i_3}{ds_0}\Big)\Big) \\
&\quad + e_{\alpha\beta}\kappa^0_\beta\Big(K + r_a^2 N_3^0 + 2\beta_\alpha M_\alpha^{c\,0}\Big)\widetilde{\kappa}^i_3 + e_{\alpha\beta}M_3^0\Big(\frac{d\widetilde{\varphi}^i_\beta}{ds_0} - \kappa_3^0 e_{\beta\gamma}\widetilde{\varphi}^i_\gamma\Big) \\
&\quad - e_{\alpha\beta}M_\beta^0\frac{d\widetilde{\varphi}^i_3}{ds_0} - e_{\alpha\beta}\,e_{\beta\gamma}\Big(N_\gamma^0 - M_3^0\kappa_\gamma^0\Big)\widetilde{\varphi}^i_3 - \widetilde{\varphi}^i_\alpha N_3^0 \\
&\quad + e_{\alpha\beta}\Big(\kappa_\beta^0 M_\eta^0 - p_\beta^0 f_\eta^0\Big)\widetilde{\varphi}^i_\gamma e_{\gamma\eta} + e_{\alpha\beta}\widetilde{\varphi}^i_\beta\Big(f_\eta^0 p_\gamma^0 + \kappa_\eta^0 M_\gamma^0\Big)e_{\gamma\eta}\Big]\,\delta\varphi_\alpha \\
&+ \Big[\frac{d}{ds_0}\Big(\Big(K + r_a^2 N_3^0 + 2\beta_\alpha M_\alpha^{c\,0}\Big)\widetilde{\kappa}^i_3\Big) - \frac{d^2}{ds_0^2}\Big(I_\omega\Big(\frac{d\widetilde{\kappa}^i_3}{ds_0}\Big)\Big) \\
&\quad + \kappa_\gamma^0 e_{\gamma\alpha}I_{\alpha\beta}\widetilde{\kappa}^i_\beta + \widetilde{\varphi}^i_\alpha e_{\alpha\beta}e_{\beta\gamma}\Big(M_\gamma^0\kappa_3^0 - f_\gamma^0 p_3^0\Big)
\end{aligned}
$$

$$+ e_{\alpha\beta} M^0_\beta \Big(\frac{d\tilde{\varphi}^i_\alpha}{ds_0} - \tilde{\varphi}^i_3 \kappa^0_\gamma e_{\gamma\alpha} \Big) - p^0_\alpha f^0_\alpha \tilde{\varphi}^i_3 \Big] \delta\varphi_l \Big\} \, ds_0 \tag{B.5}$$

Investigating the coefficient of $\delta\varphi_\alpha$ it appears that making use of the permutation rule

$$e_{\alpha\beta} A_\beta B_\gamma e_{\gamma\eta} C_\eta + e_{\alpha\beta} B_\beta C_\gamma e_{\gamma\eta} A_\eta + e_{\alpha\beta} C_\beta A_\gamma e_{\gamma\eta} B_\eta = 0 \tag{B.6}$$

leads to a simple form of the initial stress terms.

$$\begin{aligned}
&\int_0^l \Big\{ F_\alpha(\tilde{\varphi}^i_j)\, \delta\varphi_\alpha + F_3(\tilde{\varphi}^i_j)\, \delta\varphi_3 \Big\} \, ds_0 = \\
&\quad \int_0^l \Big\{ \Big[\frac{d}{ds_0}\Big(I_{\alpha\beta} \tilde{\kappa}^i_\beta \Big) - \kappa^0_3 e_{\alpha\gamma} I_{\gamma\beta} \tilde{\kappa}^i_\beta \\
&\qquad + e_{\alpha\beta} \kappa^0_\beta \Big(K + r_a^2 N^0_3 + 2\beta_\alpha M^{c\,0}_\alpha - \frac{d}{ds_0}\Big(I_\omega \Big(\frac{d\tilde{\kappa}^i_3}{ds_0} \Big) \Big) \Big) \tilde{\kappa}^i_3 \\
&\qquad + M^0_3 e_{\alpha\beta} \tilde{\kappa}^i_\beta - e_{\alpha\beta} M^0_\beta \tilde{\kappa}^i_3 + N^0_\alpha \tilde{\varphi}^i_3 - N^0_3 \tilde{\varphi}^i_\alpha + e_{\alpha\beta} f^0_\beta p^0_\gamma e_{\gamma\eta} \tilde{\varphi}^i_\eta \Big] \delta\varphi_\alpha \\
&\quad + \Big[\frac{d}{ds_0} \Big(\Big(K + r_a^2 N^0_3 + 2\beta_\alpha M^{c\,0}_\alpha \Big) \tilde{\kappa}^i_3 \Big) - \frac{d^2}{ds_0^2} \Big(I_\omega \Big(\frac{d\tilde{\kappa}^i_3}{ds_0} \Big) \Big) \\
&\qquad + \kappa^0_\gamma e_{\gamma\alpha} I_{\alpha\beta} \tilde{\kappa}^i_\beta + e_{\alpha\beta} M^0_\beta \tilde{\kappa}^i_\alpha - p^0_\alpha f^0_\alpha \tilde{\varphi}^i_3 + p^0_3 f^0_\alpha \tilde{\varphi}^i_\alpha \Big] \delta\varphi_l \Big\} \, ds_0
\end{aligned} \tag{B.7}$$

This completes the reformulation of the differential equation as it follows that $F_\alpha(\tilde{\varphi}^i_j)$ and $F_3(\tilde{\varphi}^i_j)$ corresponds to the coefficients in (B.7) and are thereby defined by respectively (7.18) and (7.19).

Appendix C

Higher Order Terms - Differential Formulation

$$R_l^2(\widetilde{\varphi}_j^1, \lambda_0, \lambda_1) \;=\; -\left[\frac{d}{ds_0}\Big(Q_l^2(\widetilde{\varphi}_j^1, \lambda_0)\Big) \;+\; e_{lmn}\kappa_m^0\, Q_n^2(\widetilde{\varphi}_j^1, \lambda_0) \;+\; P_l^2(\widetilde{\varphi}_j^1, \lambda_1)\right] \tag{C.1}$$

where

$$\begin{aligned} Q_\alpha^2\big(\widetilde{\varphi}_j^1, \lambda_1\big) \;=\; & -e_{\alpha\beta}I_{\beta\eta}\widetilde{\kappa}_\eta^1\widetilde{\varphi}_3^1 \;+\; \tfrac{1}{2}I_{\alpha\beta}e_{\beta\eta}\big(\widetilde{\kappa}_\eta^1\widetilde{\varphi}_3^1 - \widetilde{\kappa}_3^1\widetilde{\varphi}_\eta^1\big) \;+\; \beta_\eta I_{\eta\alpha}\widetilde{\kappa}_3^1\widetilde{\kappa}_3^1 \\ & + e_{\alpha\beta}\widetilde{\varphi}_\beta^1\left(\Big(K + r_a^2N_3^0 + 2\beta_\gamma M_\gamma^{c^0}\Big)\widetilde{\kappa}_3^1 \;-\; \frac{d}{ds_0}\Big(I_\omega\frac{d\widetilde{\kappa}_3^1}{ds_0}\Big)\right) \\ & + \tfrac{1}{2}e_{\alpha\beta}\big(\widetilde{\varphi}_\beta^1\widetilde{\varphi}_\gamma^1 e_{\gamma\eta}M_\eta^0 \;+\; e_{\beta\gamma}M_\gamma^0\widetilde{\varphi}_3^1\widetilde{\varphi}_3^1 \;-\; e_{\beta\gamma}\widetilde{\varphi}_\gamma^1\widetilde{\varphi}_3^1M_3^0\big) \end{aligned} \tag{C.2}$$

$$\begin{aligned} Q_3^2\big(\widetilde{\varphi}_j^1, \lambda_1\big) \;=\; & \widetilde{\varphi}_\gamma^1 e_{\gamma\alpha}I_{\alpha\beta}\widetilde{\kappa}_\beta^1 \;-\; \frac{d}{ds_0}\Big(I_\omega\frac{d}{ds_0}\big(\widetilde{\kappa}_\beta^1 e_{\beta\gamma}\widetilde{\varphi}_\gamma^1\big)\Big) \\ & + \tfrac{1}{2}\Big(K + r_a^2N_3^0 + 2\beta_\gamma M_\gamma^{c^0}\Big)\widetilde{\kappa}_\beta^1 e_{\beta\gamma}\widetilde{\varphi}_\gamma^1 \;+\; 2\beta_\eta I_{\eta\alpha}\widetilde{\kappa}_\alpha^1\widetilde{\kappa}_3^1 \\ & + \tfrac{1}{2}\frac{d}{ds_0}\big(\widetilde{\varphi}_\alpha^1\widetilde{\varphi}_3^1M_\alpha^0 \;-\; \widetilde{\varphi}_\alpha^1\widetilde{\varphi}_\alpha^1M_3^0\big) \end{aligned} \tag{C.3}$$

and

$$P_l^2(\widetilde{\varphi}_j^1, \lambda_1) \;=\; e_{nkl}\Big(\tfrac{1}{2}e_{npr}\widetilde{\varphi}_p^1\widetilde{\varphi}_s^1e_{rsm} \;+\; \lambda_1\, e_{npm}\widetilde{\varphi}_p^1\Big)\big(\delta_{m3}N_k^0 \;+\; \delta_{m\alpha}f_\alpha^0p_k^0\big) \tag{C.4}$$

$$R_l^3(\widetilde{\varphi}_j^2, \widetilde{\varphi}_j^1, \lambda_0, \lambda_1, \lambda_2) \;=$$

$$\frac{d}{ds_0}\Big(Q_l^3(\widetilde{\varphi}_j^1, \lambda_0, \lambda_1)\Big) \;+\; e_{lmn}\kappa_m^0\, Q_n^3(\widetilde{\varphi}_j^1, \lambda_0, \lambda_1) \;+\; P_l^3(\widetilde{\varphi}_j^1, \lambda_1, \lambda_2) \tag{C.5}$$

$$Q_\alpha^3\Big(\widetilde{\varphi}_j^2, \widetilde{\varphi}_j^1, \lambda_0, \lambda_1\Big) \;=$$

$$\tfrac{1}{2} I_{\alpha\beta} e_{\beta\eta}\Big(\widetilde{\kappa}_\eta^2\widetilde{\varphi}_3^1 \;+\; \widetilde{\varphi}_\eta^2\widetilde{\kappa}_3^1\Big) \;+\; \tfrac{1}{3!} I_{\alpha\beta} e_{\beta mp}\widetilde{\varphi}_p^1\widetilde{\varphi}_n^1 e_{nmk}\widetilde{\kappa}_k^1 \;+\; \beta_\eta I_{\eta\alpha}\widetilde{\kappa}_3^1\widetilde{\kappa}_\beta^1 e_{\beta\gamma}\widetilde{\varphi}_\gamma^1$$

$$-\,\widetilde{\varphi}_3^1 e_{\alpha\beta}\Big(\tfrac{1}{2} I_{\beta\eta} e_{\eta\gamma}\Big(\widetilde{\kappa}_\gamma^1\widetilde{\varphi}_3^1 - \widetilde{\kappa}_3^1\widetilde{\varphi}_\gamma^1\Big) \;+\; \beta_\eta I_{\eta\beta}\widetilde{\kappa}_3^1\widetilde{\kappa}_3^1\Big)$$

$$+\,\tfrac{1}{2} e_{\alpha mn}\widetilde{\varphi}_m^1\widetilde{\varphi}_k^1 e_{nk\gamma} I_{\gamma\eta}\widetilde{\kappa}_\eta^1 \;+\; e_{\alpha\beta}\widetilde{\varphi}_\beta^1 2\beta_\eta I_{\eta\gamma}\widetilde{\kappa}_\gamma^1\widetilde{\kappa}_3^1$$

$$+\,\tfrac{1}{2} e_{\alpha\beta}\widetilde{\varphi}_\beta^1\Big(\Big(K + r_a^2 N_3^0 + 2\beta_\gamma M_\gamma^{c0}\Big)\widetilde{\kappa}_\eta^1 e_{\eta\gamma}\widetilde{\varphi}_\gamma^1 \;-\; I_\omega\frac{d^2}{ds_0^2}\Big(\widetilde{\kappa}_\eta^1 e_{\eta\gamma}\widetilde{\varphi}_\gamma^1\Big)\Big)$$

$$+\,\tfrac{1}{2}\widetilde{\varphi}_\alpha^1\widetilde{\varphi}_3^1\Big(\Big(K + r_a^2 N_3^0 + 2\beta_\gamma M_\gamma^{c0}\Big)\widetilde{\kappa}_3^1 \;-\; \tfrac{1}{2}\frac{d}{ds_0}\Big(I_\omega\frac{d\widetilde{\kappa}_3^1}{ds_0}\Big)\Big)$$

$$-\,\tfrac{1}{3!} e_{\alpha\beta} M_\beta^0\widetilde{\varphi}_3^1\widetilde{\varphi}_j^1\widetilde{\varphi}_j^1 \;+\; \tfrac{1}{2!} e_{\alpha nm}\Big(\widetilde{\varphi}_n^2\widetilde{\varphi}_k^1 + \widetilde{\varphi}_n^1\widetilde{\varphi}_k^2\Big) e_{mk\gamma} M_\gamma^0$$

$$+\,\tfrac{1}{3!} e_{\alpha\beta}\widetilde{\varphi}_\beta^1\widetilde{\varphi}_j^1\widetilde{\varphi}_j^1 M_3^0 \;+\; \Big(\widetilde{\varphi}_3^2\widetilde{\varphi}_\alpha^1 + \widetilde{\varphi}_3^1\widetilde{\varphi}_\alpha^2\Big) M_3^0 \tag{C.6}$$

$$Q_3^3\Big(\widetilde{\varphi}_j^2, \widetilde{\varphi}_j^1, \lambda_0, \lambda_1, \lambda_2\Big) \;=$$

$$\tfrac{1}{2}\widetilde{\varphi}_\beta^1 e_{\beta\alpha}\Big(I_{\alpha\eta} e_{\eta\gamma}\Big(\widetilde{\kappa}_\gamma^1\widetilde{\varphi}_3^1 - \widetilde{\kappa}_3^1\widetilde{\varphi}_\gamma^1\Big) \;+\; 2\beta_\eta I_{\eta\alpha}\widetilde{\kappa}_3^1\widetilde{\kappa}_3^1\Big) \;+\; \tfrac{1}{2}\widetilde{\varphi}_\alpha^1\widetilde{\varphi}_3^1 I_{\alpha\eta}\widetilde{\kappa}_\eta^1$$

$$+\,\tfrac{1}{2}\Big(K + r_a^2 N_3^0 + 2\beta_\gamma M_\gamma^{c0}\Big)\Big(e_{\alpha\beta}(\widetilde{\kappa}_\alpha^2\widetilde{\varphi}_\beta^1 + \widetilde{\kappa}_\alpha^1\widetilde{\varphi}_\beta^2) + (\widetilde{\kappa}_\alpha^1\widetilde{\varphi}_3^1 - \widetilde{\kappa}_3^1\widetilde{\varphi}_\alpha^1)\widetilde{\varphi}_\alpha^1\Big)$$

$$-\,\tfrac{1}{2}\frac{d}{ds_0}\Big(I_\omega\frac{d}{ds_0}\Big(e_{\alpha\beta}(\widetilde{\kappa}_\alpha^2\widetilde{\varphi}_\beta^1 + \widetilde{\kappa}_\alpha^1\widetilde{\varphi}_\beta^2) + (\widetilde{\kappa}_\alpha^1\widetilde{\varphi}_3^1 - \widetilde{\kappa}_3^1\widetilde{\varphi}_\alpha^1)\widetilde{\varphi}_\alpha^1\Big)\Big) \;+\; \tfrac{1}{2} R_a^4 F\widetilde{\kappa}_3^1\widetilde{\kappa}_3^1\widetilde{\kappa}_3^1$$

$$-\,\tfrac{1}{2}\widetilde{\varphi}_\alpha^1\widetilde{\varphi}_\alpha^1\Big(\Big(K + r_a^2 N_3^0 + 2\beta_\gamma M_\gamma^{c0}\Big)\widetilde{\kappa}_3^1 \;-\; \frac{d}{ds_0}\Big(I_\omega\frac{d\widetilde{\kappa}_3^1}{ds_0}\Big)\Big)$$

$$+\,\tfrac{1}{3!}\widetilde{\varphi}_j^1\widetilde{\varphi}_j^1\widetilde{\varphi}_\beta^1 e_{\beta\alpha} M_\alpha^0 \;+\; \tfrac{1}{2!}\Big(\widetilde{\varphi}_\alpha^2\widetilde{\varphi}_3^1 + \widetilde{\varphi}_\alpha^1\widetilde{\varphi}_3^2\Big) M_\alpha^0 \;-\; \widetilde{\varphi}_\alpha^1\widetilde{\varphi}_\alpha^2 M_3^0 \tag{C.7}$$

$$P_l^3(\tilde{\varphi}_j^2, \tilde{\varphi}_j^1, \lambda_1, \lambda_2) = e_{nkl}\Big(\delta_{m3}N_k^0 + \delta_{m\alpha}f_\alpha^0 p_k^0\Big)$$

$$\Big(\tfrac{1}{3!}e_{njm}\tilde{\varphi}_j^1\tilde{\varphi}_r^1\tilde{\varphi}_r^1 + \tfrac{1}{2}e_{nrs}\Big(\tilde{\varphi}_r^2\tilde{\varphi}_j^1 + \tilde{\varphi}_r^1\tilde{\varphi}_j^2\Big)e_{sjm} + \lambda_1\Big(e_{npm}\tilde{\varphi}_p^2 + \tfrac{1}{2}e_{npr}\tilde{\varphi}_r^1\tilde{\varphi}_s^2 e_{rsm}\Big)$$

$$+ \lambda_2 e_{npm}\tilde{\varphi}_p^1\Big) \tag{C.8}$$

Appendix D

Higher Order Terms - Energy Formulation

$$K_{11}^{3}\left(\widetilde{\varphi}_{l}^{1};\widetilde{\varphi}_{l}^{1}\right) = \int_{0}^{l}\frac{1}{2}\xi^{3}\Big\{\widetilde{\kappa}_{\alpha}^{1}\,I_{\alpha\beta}e_{\beta\gamma}\left(\widetilde{\kappa}_{\gamma}^{1}\widetilde{\varphi}_{3}^{1}-\widetilde{\kappa}_{3}^{1}\widetilde{\varphi}_{\gamma}^{1}\right) + \widetilde{\kappa}_{3}^{1}\left(K+r_{a}^{2}N_{3}^{0}+2\beta_{\gamma}M_{\gamma}^{c^{0}}\right)\widetilde{\kappa}_{\alpha}^{1}e_{\alpha\beta}\widetilde{\varphi}_{\beta}^{1} + \frac{d\widetilde{\kappa}_{3}^{1}}{ds_{0}}\,I_{\omega}\,\frac{d}{ds_{0}}\left(\widetilde{\kappa}_{\alpha}^{1}e_{\alpha\beta}\widetilde{\varphi}_{\beta}^{1}\right) + \widetilde{\kappa}_{3}^{1}\,2\beta_{\eta}I_{\eta\alpha}\widetilde{\kappa}_{\alpha}^{1}\widetilde{\kappa}_{3}^{1}\Big\}\,ds_{0} \tag{D.1}$$

$$K_{21}^{4}\left(\widetilde{\varphi}_{l}^{2};\widetilde{\varphi}_{l}^{1}\right) = \int_{0}^{l}\frac{1}{2}\xi^{4}\Big\{\widetilde{\kappa}_{\alpha}^{2}\,I_{\alpha\beta}e_{\beta kn}\widetilde{\kappa}_{k}^{1}\widetilde{\varphi}_{n}^{1} + \widetilde{\kappa}_{\alpha}^{1}\,I_{\alpha\beta}\,e_{\beta kn}\left(\widetilde{\kappa}_{k}^{2}\widetilde{\varphi}_{n}^{1}+\widetilde{\kappa}_{k}^{1}\widetilde{\varphi}_{n}^{2}\right) + \widetilde{\kappa}_{3}^{1}\left(K+r_{a}^{2}N_{3}^{0}+2\beta_{\gamma}M_{\gamma}^{c^{0}}\right)e_{\alpha\beta}\left(\widetilde{\kappa}_{\alpha}^{2}\widetilde{\varphi}_{\beta}^{1}+\widetilde{\kappa}_{\alpha}^{1}\widetilde{\varphi}_{\beta}^{2}\right) + \widetilde{\kappa}_{3}^{2}\left(K+r_{a}^{2}N_{3}^{0}+2\beta_{\gamma}M_{\gamma}^{c^{0}}\right)\widetilde{\kappa}_{\alpha}^{1}e_{\alpha\beta}\widetilde{\varphi}_{\beta}^{1} + \frac{d\widetilde{\kappa}_{3}^{2}}{ds_{0}}\,I_{\omega}\,\frac{d}{ds_{0}}\left(\widetilde{\kappa}_{\alpha}^{1}e_{\alpha\beta}\widetilde{\varphi}_{\beta}^{1}\right) + \frac{d\widetilde{\kappa}_{3}^{1}}{ds_{0}}\,I_{\omega}\,e_{\alpha\beta}\frac{d}{ds_{0}}\left(\widetilde{\kappa}_{\alpha}^{2}\widetilde{\varphi}_{\beta}^{1}+\widetilde{\kappa}_{\alpha}^{1}\widetilde{\varphi}_{\beta}^{2}\right) + 2\widetilde{\kappa}_{3}^{2}\,2\beta_{\eta}I_{\eta\alpha}\widetilde{\kappa}_{\alpha}^{1}\widetilde{\kappa}_{3}^{1} + \widetilde{\kappa}_{3}^{1}\,2\beta_{\eta}I_{\eta\alpha}\widetilde{\kappa}_{\alpha}^{2}\widetilde{\kappa}_{3}^{1}\Big\}\,ds_{0} \tag{D.2}$$

$$K_{11}^{4}\left(\widetilde{\varphi}_{l}^{1};\widetilde{\varphi}_{l}^{1}\right) = \int_{0}^{l}\frac{1}{2}\xi^{4}\Big\{\tfrac{1}{4}\,\widetilde{\kappa}_{k}^{1}\widetilde{\varphi}_{n}^{1}e_{kn\alpha}\,I_{\alpha\beta}\,e_{\beta lj}\widetilde{\kappa}_{l}^{1}\widetilde{\varphi}_{j}^{1} + \tfrac{1}{3}\,\widetilde{\kappa}_{\alpha}^{1}\,I_{\alpha\beta}\,\widetilde{\kappa}_{k}^{1}e_{knm}\widetilde{\varphi}_{n}^{1}\widetilde{\varphi}_{l}^{1}e_{ml\beta} + \tfrac{1}{4}\,\widetilde{\kappa}_{\alpha}^{1}e_{\alpha\beta}\widetilde{\varphi}_{\beta}^{1}\left(K+r_{a}^{2}N_{3}^{0}+2\beta_{\gamma}M_{\gamma}^{c^{0}}\right)\widetilde{\kappa}_{\eta}^{1}e_{\eta\gamma}\widetilde{\varphi}_{\gamma}^{1} + \tfrac{1}{3}\,\widetilde{\kappa}_{3}^{1}\left(K+r_{a}^{2}N_{3}^{0}+2\beta_{\gamma}M_{\gamma}^{c^{0}}\right)\widetilde{\kappa}_{k}^{1}e_{knm}\widetilde{\varphi}_{n}^{1}\widetilde{\varphi}_{l}^{1}e_{ml3}$$

$$+\tfrac{1}{4}\frac{d}{ds_0}\Big(\widetilde{\kappa}^1_\alpha e_{\alpha\beta}\widetilde{\varphi}^1_\beta\Big)\,I_\omega\,\frac{d}{ds_0}\Big(\widetilde{\kappa}^1_\eta e_{\eta\gamma}\widetilde{\varphi}^1_\gamma\Big)\;+\;\tfrac{1}{3}\frac{d\widetilde{\kappa}^1_3}{ds_0}\,I_\omega\,\frac{d}{ds_0}\Big(\widetilde{\kappa}^1_k e_{knm}\widetilde{\varphi}^1_n\widetilde{\varphi}^1_l e_{ml3}\Big)$$

$$+\widetilde{\kappa}^1_\gamma e_{\gamma\beta}\widetilde{\varphi}^1_\beta\,2\beta_\eta I_{\eta\alpha}\,\widetilde{\kappa}^1_\alpha\widetilde{\kappa}^1_3\;+\;\tfrac{1}{2}\,\widetilde{\kappa}^1_3\,2\beta_\eta I_{\eta\alpha}\,e_{\alpha kn}\widetilde{\kappa}^1_k\widetilde{\varphi}^1_n\widetilde{\kappa}^1_3\;+\;\tfrac{1}{4}\,\widetilde{\kappa}^1_3\widetilde{\kappa}^1_3\,R^4_a F\,\widetilde{\kappa}^1_3\widetilde{\kappa}^1_3\;\Big\}\;ds_0 \quad \text{(D.3)}$$

$$\delta G^3_{11}\big(\widetilde{\varphi}^1_l;\widetilde{\varphi}^1_l,\lambda_0,\lambda_1\big)\;=\;\int_0^l\Big\{\tfrac{1}{4}\,\delta\Big(\widetilde{\varphi}^1_n\xi\Big)e_{njk}\widetilde{\kappa}^1_k\,M^0_l\,e_{ljm}\widetilde{\varphi}^1_m\,\xi^2$$

$$+\tfrac{1}{2}\,\delta\Big(\widetilde{\varphi}^1_p\xi\Big)e_{pnm}e_{mks}\widetilde{\varphi}^1_s\,\Big(N^0_k(\delta_{3j}+\varepsilon^0_j)+p^0_k f^0_\alpha\delta_{\alpha j}\Big)\,e_{jrn}\widetilde{\varphi}^1_r\,\xi^2$$

$$-\tfrac{1}{2}\,\lambda_1\xi\,\delta\Big(e_{knp}\widetilde{\varphi}^1_n\,\widetilde{\varphi}^1_l e_{plj}\,\xi^2\Big)\,\Big(N^0_k(\delta_{3j}+\varepsilon^0_j)+p^0_k f^0_\alpha\delta_{\alpha j}\Big)\;\Big\}\;ds_0$$

$$-\Big[\;\tfrac{1}{2}\,\lambda_1\xi\,\sum_{i=1}^{n}P^{0i}_k\,\delta\Big(e_{kmn}\widetilde{\varphi}^1_m\,\widetilde{\varphi}^1_p e_{np\alpha}\,\xi^2\Big)\,F^{0i}_\alpha$$

$$+\tfrac{1}{2}\,\delta\Big(\widetilde{\varphi}^1_p\xi\Big)e_{pnm}e_{mks}\widetilde{\varphi}^1_s\,\widetilde{\varphi}^1_l e_{ln\alpha}\,\xi^2\sum_{i=1}^{n}F^{0i}_\alpha\,P^{0i}_k\;\Big]_0^l \qquad \text{(D.4)}$$

$$\delta G^4_{21}\big(\delta\widetilde{\varphi}^2_l;\widetilde{\varphi}^1_l,\lambda_0,\lambda_1\big)\;=\;\int_0^l\Big\{\tfrac{1}{2}\,\delta\Big(\widetilde{\varphi}^2_n\xi^2\Big)e_{njk}\widetilde{\kappa}^1_k\,M^0_l\,e_{ljm}\widetilde{\varphi}^1_m\,\xi^2$$

$$+\tfrac{1}{2}\,\delta\Big(\widetilde{\varphi}^2_p\xi^2\Big)e_{pnm}e_{mks}\widetilde{\varphi}^1_s\,\Big(N^0_k(\delta_{3j}+\varepsilon^0_j)+p^0_k f^0_\alpha\delta_{\alpha j}\Big)\,e_{jln}\widetilde{\varphi}^1_l\,\xi^2$$

$$-\tfrac{1}{2}\,\lambda_1\xi\,e_{kpr}\Big(\delta(\widetilde{\varphi}^2_p\xi^2)\widetilde{\varphi}^1_l+\widetilde{\varphi}^1_p\delta(\widetilde{\varphi}^2_l\xi^2)\Big)e_{rlj}\,\xi\,\Big(N^0_k(\delta_{3j}+\varepsilon^0_j)+p^0_k f^0_\alpha\delta_{\alpha j}\Big)\;\Big\}\;ds_0$$

$$-\Big[\;\tfrac{1}{2}\,\lambda_1\xi\,\sum_{i=1}^{n}P^{0i}_k\,e_{kpm}\Big(\delta(\widetilde{\varphi}^2_p\xi^2)\,\widetilde{\varphi}^1_l+\widetilde{\varphi}^1_p\,\delta(\widetilde{\varphi}^2_l\xi^2)\Big)e_{ml\alpha}\,F^{0i}_\alpha\,\xi$$

$$+\tfrac{1}{2}\,\delta\Big(\widetilde{\varphi}^1_p\xi\Big)e_{pnm}e_{mks}\widetilde{\varphi}^1_s\,\widetilde{\varphi}^1_l e_{ln\alpha}\,\xi^2\sum_{i=1}^{n}F^{0i}_\alpha\,P^{0i}_k\;\Big]_0^l \qquad \text{(D.5)}$$

$$\delta G^4_{12}\big(\widetilde{\varphi}^1_l;\widetilde{\varphi}^2_l,\lambda_0,\lambda_1\big)\;=\;\int_0^l\Big\{\tfrac{1}{2}\,\delta\Big(\widetilde{\varphi}^1_n\xi\Big)e_{njk}\Big(\widetilde{\kappa}^2_k\,\widetilde{\varphi}^1_m+\widetilde{\kappa}^1_k\,\widetilde{\varphi}^2_m\Big)\,e_{mlj}\,M^0_l\,\xi^3$$

$$+\tfrac{1}{2}\,\delta\Big(\widetilde{\varphi}^1_p\xi\Big)e_{pnm}e_{mks}\Big(\widetilde{\varphi}^2_s\,\widetilde{\varphi}^1_l+\widetilde{\varphi}_s\,\widetilde{\varphi}^2_l\Big)e_{jln}\Big(N^0_k(\delta_{3j}+\varepsilon^0_j)+p^0_k f^0_\alpha\delta_{\alpha j}\Big)\,\xi^3$$

$$-\tfrac{1}{2}\,\lambda_1\xi\,e_{kpr}\Big(\delta(\widetilde{\varphi}^1_p\xi)\,\widetilde{\varphi}^2_l+\widetilde{\varphi}^2_p\,\delta(\widetilde{\varphi}_l\xi)\Big)e_{rlj}\Big)\,\xi^2\,\Big(N^0_k(\delta_{3j}+\varepsilon^0_j)+p^0_k f^0_\alpha\delta_{\alpha j}\Big)\;\Big\}\;ds_0$$

$$
\begin{aligned}
&- \Big[\tfrac{1}{2}\,\lambda_1 \xi \sum_{i=1}^{n} P_k^{0i}\, e_{kpm} \Big(\delta(\widetilde{\varphi}_p^1 \xi)\, \widetilde{\varphi}_l^2 + \widetilde{\varphi}_p^2\, \delta(\widetilde{\varphi}_l^1 \xi) \Big) e_{ml\alpha} \Big)\, F_\alpha^{0i}\, \xi^2 \\
&+ \tfrac{1}{2}\, \delta\Big(\widetilde{\varphi}_p^1 \xi\Big) e_{pnm} e_{mks} \Big(\widetilde{\varphi}_s^1\, \widetilde{\varphi}_l^2 + \widetilde{\varphi}_s^1\, \widetilde{\varphi}_l^2 \Big) e_{ln\alpha}\, \xi^3 \sum_{i=1}^{n} F_\alpha^{0i}\, P_k^{0i} \Big]_0^l
\end{aligned} \tag{D.6}
$$

$$
\begin{aligned}
\delta G_{11}^4 \big(\widetilde{\varphi}_l^1; \widetilde{\varphi}_l^1, \lambda_0, \lambda_1, \lambda_2\big) \;=\; & \int_0^l \Big\{ \tfrac{1}{3!}\, \delta\Big(\widetilde{\kappa}_j^1 \xi\Big)\, e_{jln}\, M_l^0 \widetilde{\varphi}_n^1 \widetilde{\varphi}_k^1 \widetilde{\kappa}_k^1\, \xi^3 \\
&- \delta\Big(\tfrac{1}{2}\, e_{knj} \widetilde{\kappa}_k^1 \widetilde{\varphi}_n^1\, \xi^2\Big)\, M_l^0\, \tfrac{1}{2}\, e_{lrm} \widetilde{\varphi}_r^1 \widetilde{\varphi}_s^1 e_{smj}\, \xi^2 \;-\; \tfrac{1}{3!}\, \delta\Big(\widetilde{\kappa}_k^1 e_{knm} \widetilde{\varphi}_n^1 \widetilde{\varphi}_p^1 e_{mpj} \xi^3\Big)\, e_{jlr}\, M_l^0 \widetilde{\varphi}_r^1\, \xi \\
&- \tfrac{1}{3!}\, \delta\Big(\widetilde{\kappa}_p^1 \xi\Big) e_{pnk} \Big(N_k^0 (\delta_{3j} + \varepsilon_j^0) + p_k^0 f_\alpha^0 \delta_{\alpha j} \Big) e_{jln} \widetilde{\varphi}_l^1 \widetilde{\varphi}_s^1 \widetilde{\varphi}_s^1\, \xi^3 \\
&- \tfrac{1}{3!}\, \delta\Big(\widetilde{\varphi}_s^1 \widetilde{\varphi}_s^1 \widetilde{\varphi}_p^1 e_{pmk}\, \xi^3\Big) \Big(N_k^0 (\delta_{3j} + \varepsilon_j^0) + p_k^0 f_\alpha^0 \delta_{\alpha j} \Big) e_{jln} \widetilde{\varphi}_l^1\, \xi \\
&+ \delta\Big(\tfrac{1}{2}\, e_{kpm} \widetilde{\varphi}_p^1\, \widetilde{\varphi}_l^1 e_{mln}\, \xi^2\Big) \Big(N_k^0 (\delta_{3j} + \varepsilon_j^0) + p_k^0 f_\alpha^0 \delta_{\alpha j} \Big)\, \tfrac{1}{2}\, e_{jrs} \widetilde{\varphi}_r^1 \widetilde{\varphi}_q^1 e_{sqn}\, \xi^2 \\
&- \Big(N_k^0 (\delta_{3j} + \varepsilon_j^0) + p_k^0 f_\alpha^0 \delta_{\alpha j} \Big) e_{kpn} \Big(\lambda_1 \xi\, \delta(\tfrac{1}{3!}\, \widetilde{\varphi}_p^1 \widetilde{\varphi}_s^1 \widetilde{\varphi}_2^1\, \delta_{nm} \xi^3) + \tfrac{1}{2}\, \lambda_2 \xi^2\, \delta(\widetilde{\varphi}_p^1 \widetilde{\varphi}_l^1 e_{nlj}\, \xi^2) \Big) \\
&- \Big[\lambda_1 \xi \sum_{i=1}^{n} P_k^{0i}\, \delta\Big(- \tfrac{1}{3!} e_{kp\alpha} \widetilde{\varphi}_p^1 \widetilde{\varphi}_l^1 \widetilde{\varphi}_l^1\, \xi^3\Big) F_\alpha^{0i} \;+\; \lambda_2 \xi^2 \sum_{i=1}^{n} P_k^{0i}\, \delta\Big(\tfrac{1}{2} e_{kpn} \widetilde{\varphi}_p^1 \widetilde{\varphi}_l^1 e_{nl\alpha}\, \xi^2\Big) F_\alpha^{0i} \\
&- \delta\Big(\widetilde{\varphi}_p^1 \xi\Big) e_{pnk} \sum_{i=1}^{n} P_k^{0i}\, F_\alpha^{0i}\, \tfrac{1}{3!}\, e_{\alpha ln} \widetilde{\varphi}_l^1 \widetilde{\varphi}_j^1 \widetilde{\varphi}_j^1\, \xi^3 \;-\; \delta\Big(\tfrac{1}{3!}\, e_{kpn} \widetilde{\varphi}_p^1 \widetilde{\varphi}_j^1 \widetilde{\varphi}_j^1\, \xi^3\Big) \sum_{i=1}^{n} P_k^{0i}\, F_\alpha^{0i} e_{\alpha ln} \widetilde{\varphi}_l^1\, \xi \\
&+ \delta\Big(\tfrac{1}{2}\, e_{kpm} \widetilde{\varphi}_p^1\, \widetilde{\varphi}_s^1 e_{msn}\, \xi^2\Big) \sum_{i=1}^{n} P_k^{0i}\, F_\alpha^{0i}\, \tfrac{1}{2}\, e_{\alpha rj} \widetilde{\varphi}_r^1\, \widetilde{\varphi}_q^1 e_{jqn}\, \xi^2 \Big]_0^l
\end{aligned} \tag{D.7}
$$

Appendix E

Matrices for Nonlinear Numerical Stability Analysis

Elastic Stiffness Matrix K :

$$\mathbf{K_{11}} = \begin{bmatrix} \mathbf{0} & & & \mathbf{K}_{r\lambda} & \\ & \mathbf{K}_{\varphi\varphi} & & \mathbf{K}_{\varphi\lambda} & \mathbf{k}_{\varphi\lambda_\omega} \\ & & K_{\theta\theta} & & K_{\theta\lambda_\omega} \\ & sym & & \mathbf{0} & \\ & & & & 0 \end{bmatrix}$$

$$\mathbf{K_{12}} = \begin{bmatrix} \mathbf{0} & & & \mathbf{K}_{r\lambda} & \\ & -\mathbf{K}_{\varphi\varphi} & & \frac{1}{2}\mathbf{K}_{\varphi\lambda} & \mathbf{k}_{\varphi\lambda_\omega} \\ & & -K_{\theta\theta} & & \frac{1}{2}K^{\theta\lambda_\omega} \\ -\mathbf{K}_{r\lambda} & \frac{1}{2}\mathbf{K}_{\varphi\lambda} & & \mathbf{0} & \\ & -\mathbf{k}_{\varphi\lambda_\omega} & \frac{1}{2}K^{\theta\lambda_\omega} & & 0 \end{bmatrix} = \mathbf{K_{21}}^T$$

$$\mathbf{K_{22}} = \begin{bmatrix} \mathbf{0} & & -\mathbf{K}_{r\lambda} & \\ & \mathbf{K}_{\varphi\varphi} & \mathbf{K}_{\varphi\lambda} & -\mathbf{k}_{\varphi\lambda_\omega} \\ & & K_{\theta\theta} & K_{\theta\lambda_\omega} \\ & sym & \mathbf{0} & \\ & & & 0 \end{bmatrix}$$

$$\mathbf{K}_{r\lambda} = -\frac{1}{2}\,\mathbf{I} \qquad \mathbf{K}_{\varphi\varphi} = \frac{1}{L_e}\begin{bmatrix} I_{11} & I_{12} & \\ I_{21} & I_{22} & \\ & & K \end{bmatrix} \qquad K_{\theta\theta} = \frac{I_\omega}{L_e}$$

$$\mathbf{K}_{\varphi\lambda} = \frac{L_e}{3}\begin{bmatrix} 0 & 1 & \\ -1 & 0 & \\ & & 0 \end{bmatrix} \qquad \mathbf{k}_{\varphi\lambda_\omega} = \frac{1}{2}\begin{bmatrix} 0 \\ 0 \\ 1 \end{bmatrix} \qquad K_{\theta\lambda_\omega} = \frac{L_e}{3}$$

Initial Displacement Matrix :

$$\mathbf{K}_{\mathbf{11}}^{\kappa} = \begin{bmatrix} \mathbf{0} & & \mathbf{K}_{11}^{\kappa,r\lambda} & \\ & \mathbf{K}_{11}^{\kappa,\varphi\varphi} & & \mathbf{k}_{11}^{\kappa,\varphi\lambda_\omega} \\ & & 0 & \\ & sym & \mathbf{0} & \\ & & & 0 \end{bmatrix} = \mathbf{K_{22}}$$

$$\mathbf{K}_{\mathbf{12}}^{\kappa} = \begin{bmatrix} \mathbf{0} & & \mathbf{K}_{12}^{\kappa,r\lambda} & \\ & \mathbf{K}_{12}^{\kappa,\varphi\varphi} & & \mathbf{k}_{12}^{\kappa,\varphi\lambda_\omega} \\ & & 0 & \\ & sym & \mathbf{0} & \\ & & & 0 \end{bmatrix} = \mathbf{K}_{\mathbf{21}}^{\kappa\ T}$$

$$\mathbf{K}_{11}^{\kappa,\varphi\varphi} = \frac{1}{2}\begin{bmatrix} 0 & \kappa_3^0(I_{11}-I_{22}) & -\kappa_2^0(I_{11}-K) \\ & 0 & \kappa_1^0(I_{22}-K) \\ sym & & 0 \end{bmatrix} = -\mathbf{K}_{22}^{\kappa,\varphi\varphi}$$

$$\mathbf{K}_{12}^{\kappa,\varphi\varphi} = \frac{1}{2}\begin{bmatrix} 0 & \kappa_3^0(I_{11}+I_{22}) & -\kappa_2^0(I_{11}+K) \\ -\kappa_3^0\,(I_{11}+I_{22}) & 0 & 3\kappa_1^0(I_{22}+K) \\ \kappa_2^0(I_{11}+K) & -\kappa_1^0(I_{22}+K) & 0 \end{bmatrix} = \mathbf{K}_{21}^{\kappa,\varphi\varphi^T}$$

$$\mathbf{K}_{11}^{\kappa,\tau\lambda} = \mathbf{K}_{22}^{\kappa,\tau\lambda} = \frac{1}{2}\mathbf{K}_{12}^{\kappa,\tau\lambda} = -\frac{L_e}{3}\,\boldsymbol{\Omega}(\boldsymbol{\kappa}^0)$$

$$\mathrm{k}_{11}^{\kappa,\varphi\lambda_\omega} = \mathrm{k}_{22}^{\kappa,\varphi\lambda_\omega} = \frac{1}{2}\mathrm{k}_{22}^{\kappa,\varphi\lambda_\omega} = \frac{L_e}{3}\begin{bmatrix} \kappa_2^0 \\ -\kappa_1^0 \\ 0 \end{bmatrix}$$

Initial Stress Matrix :

$$\mathbf{K}_{11}^{\sigma} = \begin{bmatrix} \mathbf{0} & & \\ & \mathbf{K}_{11,\mathrm{N}}^{\sigma} + \mathbf{K}_{11,\mathrm{M}}^{\sigma} + \mathbf{K}_{11,\mathrm{p}}^{\sigma} & \\ & & \mathbf{0} \end{bmatrix}$$

$$\mathbf{K}_{11,\mathrm{N}}^{\sigma} = \frac{L_e}{12}\begin{bmatrix} 3N_3^1+N_3^2 & 0 & 0 \\ 0 & 3N_3^1+N_3^2 & 0 \\ -3N_1^1+N_1^2 & -3N_2^1+N_2^2 & 6\left(\dfrac{r_a}{L_e}\right)^2(N_3^1+N_3^2) \end{bmatrix}$$

$$\mathbf{K}_{11,\mathrm{N}}^{\sigma} = \frac{1}{6}\begin{bmatrix} 0 & -2M_3^1-M_3^2 & 2M_2^1+M_2^2 \\ 2M_3^1+M_3^2 & 0 & -2M_1^1-M_1^2 \\ -2M_2^1-M_2^2 & 2M_1^1+M_1^2 & 3\dfrac{2\beta_\alpha}{L_e}(M_\alpha^1+M_\alpha^2) \end{bmatrix}$$

$$\mathbf{K}^{\sigma}_{\mathbf{12}} = \begin{bmatrix} \mathbf{0} & & \\ & \mathbf{K}^{\sigma}_{\mathbf{12,N}} + \mathbf{K}^{\sigma}_{\mathbf{12,M}} + \mathbf{K}^{\sigma}_{\mathbf{12,p}} & \\ & & \mathbf{0} \end{bmatrix}$$

$$\mathbf{K}^{\sigma}_{\mathbf{12,N}} = \frac{L_e}{12} \begin{bmatrix} N_3^1 + N_3^2 & 0 & 0 \\ 0 & N_3^1 + N_3^2 & 0 \\ -N_1^1 - N_1^2 & -N_2^1 - N_2^2 & -6\left(\frac{r_a}{L_e}\right)^2 (N_3^1 + N_3^2) \end{bmatrix}$$

$$\mathbf{K}^{\sigma}_{\mathbf{12,M}} = \frac{1}{6} \begin{bmatrix} 0 & -M_3^1 - 2M_3^2 & M_2^1 + 2M_2^2 \\ M_3^1 + 2M_3^2 & 0 & -M_1^1 - 2M_1^2 \\ -M_2^1 - 2M_2^2 & M_1^1 + 2M_1^2 & -3\frac{2\beta_\alpha}{L_e}(M_\alpha^1 + M_\alpha^2) \end{bmatrix}$$

$$\mathbf{K}^{\sigma}_{\mathbf{21}} = \begin{bmatrix} \mathbf{0} & & \\ & \mathbf{K}^{\sigma}_{\mathbf{21,N}} + \mathbf{K}^{\sigma}_{\mathbf{21,M}} + \mathbf{K}^{\sigma}_{\mathbf{21,p}} & \\ & & \mathbf{0} \end{bmatrix}$$

$$\mathbf{K}^{\sigma}_{\mathbf{21,N}} = \frac{L_e}{12} \begin{bmatrix} N_3^1 + N_3^2 & 0 & 0 \\ 0 & N_3^1 + N_3^2 & 0 \\ -3N_1^1 - N_1^2 & -3N_2^1 - N_2^2 & -6\left(\frac{r_a}{L_e}\right)^2 (N_3^1 + N_3^2) \end{bmatrix}$$

$$\mathbf{K}^{\sigma}_{\mathbf{21,M}} = \frac{1}{6} \begin{bmatrix} 0 & 2M_3^1 + M_3^2 & -2M_2^1 - M_2^2 \\ -2M_3^1 - M_3^2 & 0 & 2M_1^1 + M_1^2 \\ 2M_2^1 + M_2^2 & -2M_1^1 - M_1^2 & -3\frac{2\beta_\alpha}{L_e}(M_\alpha^1 + M_\alpha^2) \end{bmatrix}$$

$$\mathbf{K}^{\sigma}_{\mathbf{22}} = \begin{bmatrix} \mathbf{0} & & \\ & \mathbf{K}^{\sigma}_{\mathbf{22,N}} + \mathbf{K}^{\sigma}_{\mathbf{22,M}} + \mathbf{K}^{\sigma}_{\mathbf{22,p}} & \\ & & \mathbf{0} \end{bmatrix}$$

$$\mathbf{K}^{\sigma}_{\mathbf{22,N}} = \frac{L_e}{12}\begin{bmatrix} N_3^1+3N_3^2 & 0 & 0 \\ 0 & N_3^1+3N_3^2 & 0 \\ -N_1^1-3N_1^2 & -N_2^1-3N_2^2 & 6\left(\frac{r_a}{L_e}\right)^2(N_3^1+N_3^2) \end{bmatrix}$$

$$\mathbf{K}^{\sigma}_{\mathbf{22,M}} = \frac{1}{6}\begin{bmatrix} 0 & M_3^1+2M_3^2 & -M_2^1-2M_2^2 \\ -M_3^1-2M_3^2 & 0 & M_1^1+2M_1^2 \\ M_2^1+2M_2^2 & -M_1^1-2M_1^2 & 3\frac{2\beta_\alpha}{L_e}(M_\alpha^1+M_\alpha^2) \end{bmatrix}$$

$$\mathbf{K}^{\sigma}_{\mathbf{11,p}} = \frac{L_e}{12}\begin{bmatrix} f_2^0(3p_2^1+p_2^2) & -f_1^0(3p_2^1+p_2^2) & -f_1^0(3p_3^1+p_3^2) \\ -f_2^0(3p_1^1+p_1^2) & f_1^0(3p_1^1+p_1^2) & -f_2^0(3p_3^1+p_3^2) \\ 0 & 0 & f_1^0(3p_1^1+p_1^2)+f_2^0(3p_2^1+p_2^2) \end{bmatrix}$$

$$\mathbf{K}^{\sigma}_{\mathbf{12,p}} = \mathbf{K}^{\sigma}_{\mathbf{21,p}}{}^{T} =$$

$$\frac{L_e}{12}\begin{bmatrix} f_2^0(p_2^1+p_2^2) & -f_1^0(p_2^1+p_2^2) & -f_1^0(p_3^1+p_3^2) \\ -f_2^0(p_1^1+p_1^2) & f_1^0(p_1^1+p_1^2) & -f_2^0(p_3^1+p_3^2) \\ 0 & 0 & f_1^0(p_1^1+p_1^2)+f_2^0(p_2^1+p_2^2) \end{bmatrix}$$

$$\mathbf{K}^{\sigma}_{\mathbf{22,p}} = \frac{L_e}{12}\begin{bmatrix} f_2^0(p_2^1+3p_2^2) & -f_1^0(p_2^1+3p_2^2) & -f_1^0(p_3^1+3p_3^2) \\ -f_2^0(p_1^1+3p_1^2) & f_1^0(p_1^1+3p_1^2) & -f_2^0(p_3^1+3p_3^2) \\ 0 & 0 & f_1^0(p_1^1+3p_1^2)+f_2^0(p_2^1+3p_2^2) \end{bmatrix}$$

Coupling of Initial Stresses and Displacements :

$$\mathbf{K}^{\kappa\sigma}_{\mathbf{11}} = \begin{bmatrix} \mathbf{0} & & \\ & \mathbf{K}^{\kappa\sigma}_{\mathbf{11,M}} & \\ & & \mathbf{0} \end{bmatrix} \qquad \mathbf{K}^{\kappa\sigma}_{\mathbf{12}} = \mathbf{K}^{\kappa\sigma T}_{\mathbf{21}} = \begin{bmatrix} \mathbf{0} & & \\ & \mathbf{K}^{\kappa\sigma}_{\mathbf{12,M}} & \\ & & \mathbf{0} \end{bmatrix}$$

$$\mathbf{K}_{\mathbf{22}}^{\kappa\sigma} = \begin{bmatrix} \mathbf{0} & & \\ & \mathbf{K}_{\mathbf{22,M}}^{\kappa\sigma} & \\ & & \mathbf{0} \end{bmatrix}$$

$$\mathbf{K}_{\mathbf{11,M}}^{\kappa\sigma} = \text{Factor} \quad \frac{L_e}{12} \begin{bmatrix} -\kappa_2^0(3M_2^1 + M_2^2) & \kappa_2^0(3M_1^1 + M_1^2) & \kappa_3^0(3M_1^1 + M_1^2) \\ -\kappa_3^0(3M_3^1 + M_3^2) & & \\ \kappa_1^0(3M_2^1 + M_2^2) & -\kappa_1^0(3M_1^1 + M_1^2) & \kappa_3^0(3M_2^1 + M_2^2) \\ & -\kappa_3^0(3M_3^1 + M_3^2) & \\ \kappa_1^0(3M_3^1 + M_3^2) & \kappa_2^0(3M_3^1 + M_3^2) & -\kappa_1^0(3M_1^1 + M_1^2) \\ & & -\kappa_2^0(3M_2^1 + M_2^2) \end{bmatrix}$$

$$\mathbf{K}_{\mathbf{12,M}}^{\kappa\sigma} = \text{Factor} \quad \frac{L_e}{12} \begin{bmatrix} -\kappa_2^0(M_2^1 + M_2^2) & \kappa_2^0(M_1^1 + M_1^2) & \kappa_3^0(M_1^1 + M_1^2) \\ -\kappa_3^0(M_3^1 + M_3^2) & & \\ \kappa_1^0(M_2^1 + M_2^2) & -\kappa_1^0(M_1^1 + M_1^2) & \kappa_3^0(M_2^1 + M_2^2) \\ & -\kappa_3^0(M_3^1 + M_3^2) & \\ \kappa_1^0(M_3^1 + M_3^2) & \kappa_2^0(M_3^1 + M_3^2) & -\kappa_1^0(M_1^1 + M_1^2) \\ & & -\kappa_2^0(M_2^1 + M_2^2) \end{bmatrix}$$

$$\mathbf{K}_{\mathbf{22,M}}^{\kappa\sigma} = \text{Factor} \quad \frac{L_e}{12} \begin{bmatrix} -\kappa_2^0(M_2^1 + 3M_2^2) & \kappa_2^0(M_1^1 + 3M_1^2) & \kappa_3^0(M_1^1 + 3M_1^2) \\ -\kappa_3^0(M_3^1 + 3M_3^2) & & \\ \kappa_1^0(M_2^1 + 3M_2^2) & -\kappa_1^0(M_1^1 + 3M_1^2) & \kappa_3^0(M_2^1 + 3M_2^2) \\ & -\kappa_3^0(M_3^1 + 3M_3^2) & \\ \kappa_1^0(M_3^1 + 3M_3^2) & \kappa_2^0(M_3^1 + 3M_3^2) & -\kappa_1^0(M_1^1 + 3M_1^2) \\ & & -\kappa_2^0(M_2^1 + 3M_2^2) \end{bmatrix}$$

Appendix F

Resumé

Formålet med den foreliggende afhandling "Stabilitet af tyndvæggede usymmetriske stålbjælker" har været at opstille en generel ulineær stabilitetsteori. Baggrunden for dette er, at der i de senere år har der været en udvikling hen imod slankere stålkonstruktioner og øget brug af koldvalsede profiler. Dette har ført til, at stabilitetsproblemer indtager en stadig mere central plads ved projektering af stålkonstruktioner. De mest benyttede klassiske stålprofiler til bjælke- og rammekonstruktioner er symmetriske. Dette indebærer, at stabilitetssvigt kan vurderes ved at betragte en ideel konstruktion, der ved et vist lastniveau kan blive ustabil, uden at der forinden er indtrådt nævneværdige deformationer. Dette forenkler stabilitetsberegningerne betydeligt, da de kan baseres på den udeformerede konstruktions geometri. I modsætning hertil er koldvalsede profiler oftest usymmetriske. Dette skyldes dels hensyn til transport og samlingsdetailler, men har også forbindelse med fremstillingsteknikken. For bjælker og rammer af sådanne profiler vil stabilitetsproblemet ofte have en anden karakter, idet selv en ideel konstruktion gradvis vil deformeres mere og mere. Der er således ikke tale om en enkelt veldefineret stabilitetslast, men snarere om en større og større fleksibilitet af konstruktionen med voksende last. En rationel udnyttelse af de koldvalsede profiler, der gradvis overtager en stadig større del af markedet, forudsætter derfor en mere detailleret behandling af stabilitetsproblemet.

Projektets formål er gennem en detailleret analyse af den gradvise instabilitet af tyndvæggede usymmetriske stålbjælker at fremskaffe en forbedret beskrivelse af stabilitetsproblemet, samt at opstille en simplificeret beskrivelse med henblik på dimensioneringsberegninger i praksis. Da der findes et stort antal profiltyper og der valses specialprofiler til større opgaver, er det vigtigt at projektet sigter mod en betydelig generalitet. En forudsætning for at denne generalitet kan bibeholdes er, at der foreligger en ulineær bjælketeori, som på en konsistent måde inkluderer forhåndsdeformationer og initialspændinger for bjælker med vilkårlig tværsnit.

I kapitel 2 formuleres en generel bjælketeori ved at betragte bjælken som et en-dimensionalt legeme som beskrives ved tværsnittene og en længdekoordinat. Bjælken kan herved repræsenteres ved en kurve og et sæt af lokale basisvektorer som fastholdes i tværsnittet. Orientering af de lokale basisvektorer beskrives via en endelig rotationsvektor gennem en orthogonal transformation (længdebevarende drejning) af et sæt referencevektorer. De generaliserede flytningsstørrelser er således en stedvektor for kurven og en rotationsvektor for tværsnittene.

Ved at udtrykke ligevægt for et deformeret bjælkeelement gennem snitkræfterne opstilles de ulineære ligevægtsligninger. Disse ligevægtsligninger optræder på vektorform og omformuleres til det virtuelle arbejde, hvorved de generaliserede deformationsmål, henholdsvis 3

tøjninger og 3 krumninger, kan fastlægges. De generaliserede tøjninger indeholder en kobling imellem stedvektoren og rotationsvektoren mens krumningerne udelukkende udtrykkes ved rotationskomponenterne. Det er vigtigt for systematikken at bibeholde de tre rotationskomponenter således, at den orthogonale transformationsoperator kan udnyttes til at opnå en kompakt formulering. Hvælvningsbidraget, som er karakteristisk for tyndvæggede bjælker, behandles tilsvarende, hvilket betyder, at dette bidrag direkte kan adderes til det oprindelige virtuelle arbejde.

En stabilitetsformulering udledes i kapitel 3 ved at betragte bjælkeelementet i to tætliggende tilstande svarende til en initial- og en sluttilstand. Initialtilstanden indeholder forhåndsdeformationer og initialspændinger, og udtrykker at bjælken er i ligevægt i denne tilstand. Sluttilstanden fremkommer ved at betragte småændringer fra initialtilstanden. Ved at subtrahere den initialle tilstand fra sluttilstanden fremkommer stabilitetsligningerne. Gennem denne fremgangsmåde opnås det, at forhåndsdeformationer medtages på en konsistent måde. I en fremstilling, hvor bjæken betragtes som en kurve med tilhørende basisvektorer skal der i en stabilitetsformulering tages højde for, at en endelig udstrækning af tværsnittet medfører at aksielle spændinger influerer på vridningsstivheden. Dette opnås i kapitel 4 gennem de konstitutive ligninger for sammenhængen mellem snitkræfter og de generaliserede deformationer. Ved at indføre denne *vridningseffekt* i deformationsmålet svarende til små tøjninger fremkommer et sæt konsistente konstitutive ligninger, som også er velegnet ved ulineære formuleringer. Det vises i en sammenligning med en del af litteraturen, hvor komplekse konstitutive ligninger benyttes, at der ikke er behov for yderligere bidrag udover de her anvendte.

I kapitel 5 diskuteres sammenhængen mellem det virtuelle arbejde og den potentielle energi. Den velkendte sammenhæng som udtrykker, at det virtuelle arbejde er den første variation af den potentielle energi genfindes for den initielt spændingsfri bjælke, mens den kun genfindes i de kvadratiske led for en bjælke med initialspændinger. Dette indikerer, at en undersøgelse med højere ordens led bør gennemføres med passende forsigtighed.

En grundlæggende analyse vedrørende muligheden for at etablere en numerisk model, som muliggør en inkremental formulering af det generelle ulineære stabilitetsproblem, gennemføres i kapitel 6 ved at betragte et initielt spændingsfrit element. Med udgangspunkt i den ulineære formulering af det virtuelle arbejde og en negligering af tøjningsdeformationerne fremkommer en inkremental formulering, hvor rotationsvektoren fremhæves som den primære variabel. En konsistent formulering opnås ved at inddrage stedvektoren gennem tøjningsbetingelsen via Lagrange Multiplier metoden. Dette fører til en blandet formulering, hvor både kinematiske som statiske størrelser indgår som uafhængige variable. Fremgangsmåden betyder, at der kan benyttes lineære formfunktioner for alle implicerede variable hvilket fører til en simpel formulering. Eksempler viser, at specielt flytningsbestemmelsen mærkes af det simple funktionsvalg, mens de statiske størrelser derimod opnår en meget tilfredsstillende beskrivelse.

Ved anvendelse af perturbationsmetoden opstilles i kapitel 7 en asymptotisk bifurkations- og efterbulings-teori udfra det ulineære virtuelle arbejde. I formuleringen betragtes rotationsvektoren igen som den primære variabel, hvilket fører til at differentationsordenen holdes nede. Et sæt differentialligninger benyttes til at bestemme udviklingen i rotationsvektoren mens et tilhørende funktional (det virtuelle arbejde) benyttes til at fastlægge ændringen i den ydre last. Analyser af enkelte grundtilfælde har ført til bestemmelse af de parametre, som har afgørende indflydelse på stabilitetsproblemets karakter.

Afslutningsvis er der med udgangspunkt i bjælkeelementet fra kapitel 6 udviklet et inkrementalt opdateret Lagrange element i kapitel 8. Dette element indeholder en opdatering af forhåndsdeformationer og initialspændinger, hvilket gør det anvendeligt i stabilitetsanalyser. Ved at påføre imperfektioner på de undersøgte konstruktioner er det muligt at følge ligevægtskurven i pre-bulingsfasen såvel som i post-bulingsfasen. Ved sammenligninger med litteraturen er det verificeret, at det udviklede element er brugbart ved analyser af problemer indeholdende store flytninger. En sammenligning med de asymptotiske løsninger indikerer, at de rigtige parametre er identificeret, og endvidere at den asymptotiske løsning er anvendelig for begyndende efterbuling. En analyse af det enkeltsymmetriske profil viser, at imperfektioner har en betydelig indflydelse på den kritiske last. Denne indflydelse findes at kunne identificeres gennem de i kapitel 7 udledte faktorer. De gennemførte analyser understreger således nødvendigheden af faktorer, som tager hensyn til at den kritiske last bestemt for en ideel retlinet konstruktion, influeres af imperfektioner i den praktiske anvendelse.

ENGINEERING MECHANICS PAPERS

PAPER NO. 18: S. Krenk: *An Orthogonal Residual Procedure for Nonlinear Finite Element Equations.* ISSN 0902-7513 R9325.

PAPER NO. 19: F. Mathiesen: *Stability Analysis of Thin-Walled Non-Symmetric Steel Beams.* Ph.D.-Thesis. ISSN 0902-7513 R9327.

Department of Building Technology and Structural Engineering
The University of Aalborg, Sohngaardsholmsvej 57, DK 9000 Aalborg
Telephone: 45 98 15 85 22 Telefax: 45 98 14 82 43

ENGINEERING MECHANICS PAPERS

PAPER NO. 1: S. Krenk: *Constrained Lateral Buckling of I-Beam Gable Frames.* ISSN 0902-7513 R8923.

PAPER NO. 2: S. Krenk & H. Gluver: *Markov Models and Range Counting in Random Fatigue.* ISSN 0902-7513 R9010.

PAPER NO. 3: S. Krenk & L. Damkilde: *Models of Thin-Walled Beam Connections.* ISSN 0902-7513 R9022.

PAPER NO. 4: S. Krenk & L. Damkilde: *Warping of Joints in I-Beam Assemblages.* ISSN 0902-7513 R9038.

PAPER NO. 5: S. Krenk: *Energy Release Rate of Adhesive Joints.* ISSN 0902-7513 R9111.

PAPER NO. 6: J. Jönsson, S. Krenk & L. Damkilde: *The Semi-Loof Element for Plate Instability.* ISSN 0902-7513 R9122.

PAPER NO. 7: S. Krenk: *A General Format for Curved and Nonhomogeneous Beam Elements.* ISSN 0902-7513 R9125.

PAPER NO. 8: S. Krenk: *A Calibration Formula for Clip-Gauge Measurement of Crack Growth in Adhesive Joints.* ISSN 0902-7513 R9127.

PAPER NO. 9: J. Jönsson, S. Krenk & L. Damkilde: *A Hybrid Displacement Plate Element for Bending and Stability Analysis.* ISSN 0902-7513 R9208.

PAPER NO. 10: S. Krenk, S. Vissing & C. Vissing-Jørgensen: *A Finite Step Updating Method for Elasto-Plastic Analysis of Frames.* ISSN 0902-7513 R9224.

PAPER NO. 11: Z. Zembaty & S. Krenk: *On the Spatial Seismic Excitations and Response Spectra.* ISSN 0902-7513 R9236.

PAPER NO. 12: J. Mann & S. Krenk: *Fourier Simulation of a Non-Isotropic Wind Field Model.* ISSN 0902-7513 R9248.

PAPER NO. 13: O. Hededal & S. Krenk: *A Profile Solver in C for Finite Element Equations.* ISSN 0902-7513 R9301.

PAPER NO. 14: L. Damkilde, O. Høyer & S. Krenk: *A Direct Linear Programming Solver in C for Structural Applications.* ISSN 0902-7513 R9304.

PAPER NO. 15: S. Vissing & S. Krenk: *A Generalized Jacobi Algorithm.* ISSN 0902-7513 R9316.

PAPER NO. 16: S. Krenk, L. Damkilde & O. Høyer: *Limit Analysis and Optimal Design of Plates with Triangular Equilibrium Elements.* ISSN 0902-7513 R9321.

PAPER NO. 17: S. Vissing & O. Hededal: *A Subspace Algorithm.* ISSN 0902-7513 R9322.